THE TRANSCRIPTIONAL REGULATION OF MEMORY

EDITED BY: Benedict C. Albensi and Jelena Djordjevic
PUBLISHED IN: Frontiers in Molecular Neuroscience

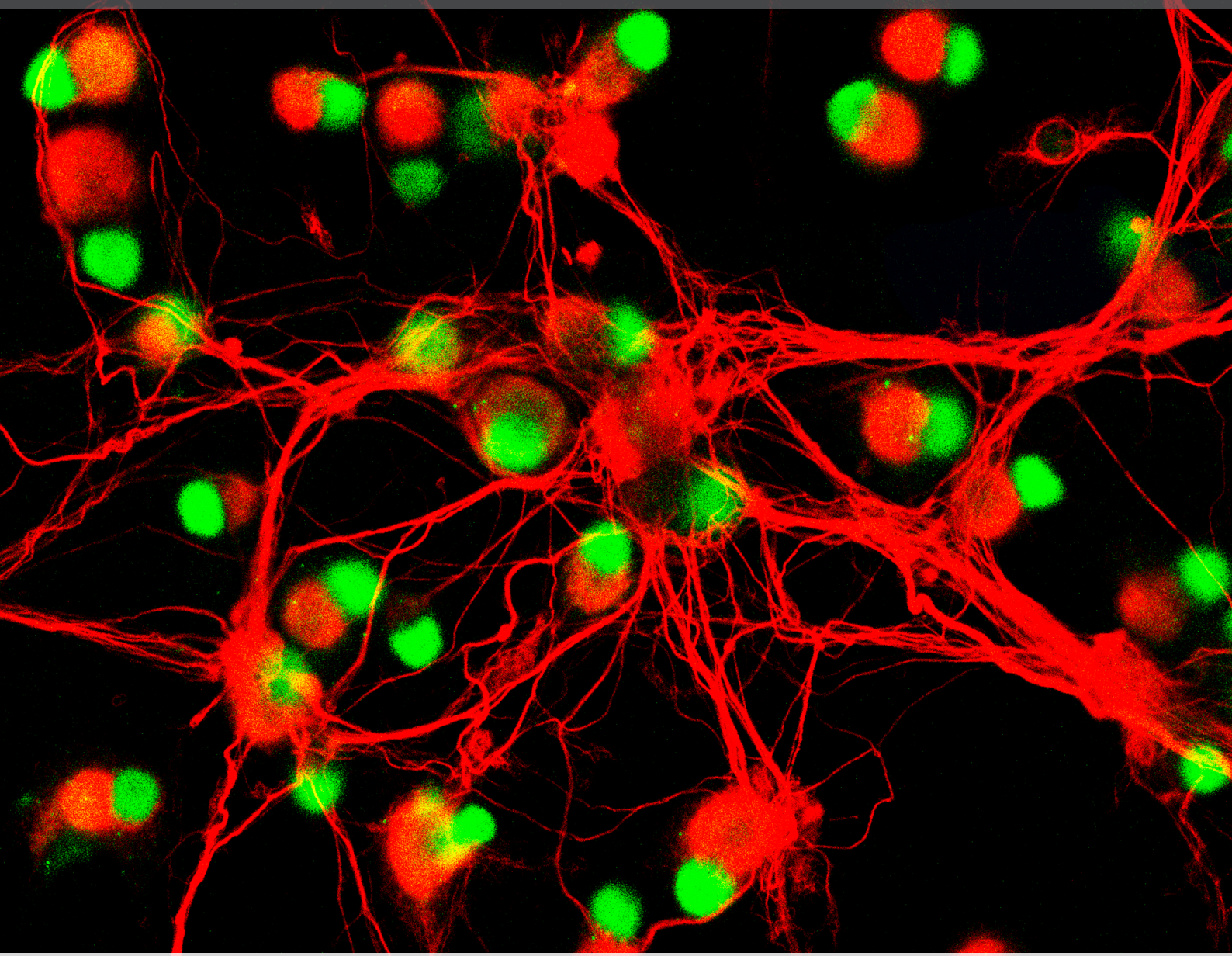

frontiers Research Topics

frontiers

ISSN 1664-8714
ISBN 978-2-88919-865-8
DOI 10.3389/978-2-88919-865-8

About Frontiers

Frontiers is more than just an open-access publisher of scholarly articles: it is a pioneering approach to the world of academia, radically improving the way scholarly research is managed. The grand vision of Frontiers is a world where all people have an equal opportunity to seek, share and generate knowledge. Frontiers provides immediate and permanent online open access to all its publications, but this alone is not enough to realize our grand goals.

Frontiers Journal Series

The Frontiers Journal Series is a multi-tier and interdisciplinary set of open-access, online journals, promising a paradigm shift from the current review, selection and dissemination processes in academic publishing. All Frontiers journals are driven by researchers for researchers; therefore, they constitute a service to the scholarly community. At the same time, the Frontiers Journal Series operates on a revolutionary invention, the tiered publishing system, initially addressing specific communities of scholars, and gradually climbing up to broader public understanding, thus serving the interests of the lay society, too.

Dedication to Quality

Each Frontiers article is a landmark of the highest quality, thanks to genuinely collaborative interactions between authors and review editors, who include some of the world's best academicians. Research must be certified by peers before entering a stream of knowledge that may eventually reach the public - and shape society; therefore, Frontiers only applies the most rigorous and unbiased reviews.
Frontiers revolutionizes research publishing by freely delivering the most outstanding research, evaluated with no bias from both the academic and social point of view.
By applying the most advanced information technologies, Frontiers is catapulting scholarly publishing into a new generation.

What are Frontiers Research Topics?

Frontiers Research Topics are very popular trademarks of the Frontiers Journals Series: they are collections of at least ten articles, all centered on a particular subject. With their unique mix of varied contributions from Original Research to Review Articles, Frontiers Research Topics unify the most influential researchers, the latest key findings and historical advances in a hot research area! Find out more on how to host your own Frontiers Research Topic or contribute to one as an author by contacting the Frontiers Editorial Office: **researchtopics@frontiersin.org**

THE TRANSCRIPTIONAL REGULATION OF MEMORY

Topic Editors:
Benedict C. Albensi, University of Manitoba, Canada
Jelena Djordjevic, University of Manitoba, Canada

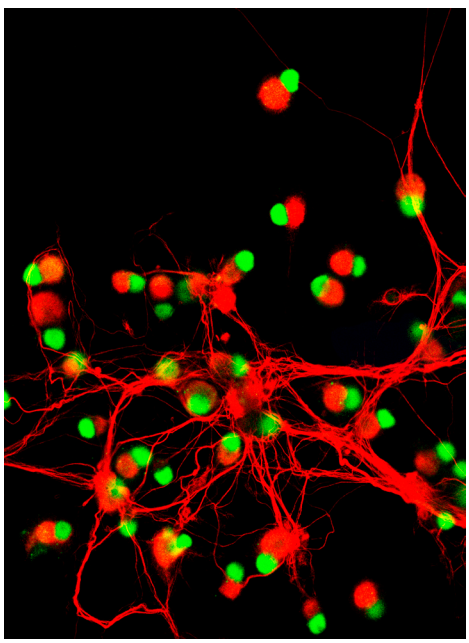

Dissociated adult rat sensory neurons, maintained in culture and immunostained, showing beta-tubilin III associated cytoskeleton (red) and cAMP Responsive Element Binding Protein 1 (CREB1) in the nucleus(green).
Image courtesy of Mohammad Golam Sabbir, PhD, St. Boniface Hospital Research Centre, University of Manitoba, Canada.

The formation of various forms of memory involves a series of distinct cellular and molecular mechanisms, many of which are not fully understood. There are highly conserved pathways that are involved in learning, memory, and synaptic plasticity, which is the primary substrate for memory storage. The formation of short-term (across minutes) memory is mediated by local changes in synapses, while long-term (across hours to days) memory storage is associated with activation of transcription and synthesis of proteins that modify synaptic function. Transcription factors, which can either repress or activate transcription, play a vital role in driving protein synthesis underlying synaptic plasticity and memory, whereby protein synthesis provides the necessary building blocks to accommodate structural changes at the synapse that foster memory formation. Recent data implicate several families of transcription factors that appear critically

important in the regulation of memory. In this Topic we will focus on the families of transcription factors thus far found to be critically involved in synaptic plasticity and memory formation. These include cAMP response element binding protein (CREB), Rel/nuclear factor B (Rel/NFB), CCAAT enhancer binding protein (C/EBP), and early growth response factor (Egr).

In recent years, numerous studies have implicated epigenetic mechanisms, changes in gene activity and expression that occur without alteration in gene sequence, in the memory consolidation process. DNA methylation and chromatin remodeling are critically involved in learning and memory, supporting a role of epigenetic mechanisms. Here we provide more evidence of the importance of DNA methylation, histone posttranslational modifications and the role of histone acetylation and HDAC inhibitors in above mentioned processes.

Citation: Albensi, B. C., Djordjevic, J., eds. (2016). The Transcriptional Regulation of Memory. Lausanne: Frontiers Media. doi: 10.3389/978-2-88919-865-8

Table of Contents

frontiers in Molecular Neuroscience

EDITORIAL
published: 19 April 2016
doi: 10.3389/fnmol.2016.00024

Editorial: Transcriptional Regulation of Memory

Benedict C. Albensi and Jelena Djordjevic*

Laboratory of Synaptic Plasticity and Memory Dysfunction, Division of Neurodegenerative Disorders, Department of Pharmacology and Therapeutics, University of Manitoba, Winnipeg, MB, Canada

Keywords: molecular, memory, transcription, epigenetic, synaptic plasticity (LTP/LTD)

The Editorial on the Research Topic

Transcriptional Regulation of Memory

Memory is the capacity for retaining and reviving information, facts, events, impressions, etc., and of recalling or recognizing previous experiences (Kandel et al., 2013). The formation of human memories involves a series of complicated biochemical processes, many of which are not fully understood. Short-term, intermediate-term, and long-term memories have different biological and molecular substrates and therefore represent distinct forms of memory. A short-term memory is the retention of information for a brief time (seconds to minutes) without creation of the neural changes for later recall. In contrast, a long-term memory (hours to weeks to years) occurs when changes in neural pathways result in the storage of information that can be recalled weeks, months, or even years later. There are thousands of molecules presumably involved in memory. However, recent data implicate several families of transcription factors and epigenetic processes that appear critical in the regulation of memory. Transcription factors are already well-known to regulate the basal process of transcription, the selective activation of genes, and/or the repression of genes. Albeit, we further acknowledge the importance of transcriptional processes for both memory consolidation and reconsolidation, and recognize there are still a lot of unanswered questions: For example, what are the key transcription factors involved in the regulation of memory? What are their gene targets and how do they mediate memory formation? How is transcription regulated over time? How does epigenetics contribute to memory? Can the context or our experience influence the pattern of transcription and regulate the formation of memory?

To this end, emerging from the literature are examples of transcription factors, transcriptional processes, mechanisms of epigenetics that appear to be critically involved in synaptic plasticity and long term memory. Some of these include histone variant H3.3, nuclear factor kappa B (NF-kB) protein, nuclear factor (erythroid-derived 2)-like 2 (Nrf2) protein, histone deacetylase inhibitors, Gadd45beta expression, CREB-regulated transcriptional coactivator (CRTC1), CREB, and early growth response (Egr) factor protein. The existence of genetic interactions, epigenetic processes, and non-genetic mechanisms that transfer unique environmental context to the memory formation is of growing interest.

This *Frontiers in Molecular Neuroscience* Research Topic-Special Issue on the *Transcriptional Regulation of Memory* includes both reviews and experimental studies focused on transcription factors and epigenetic processes that regulate various forms of memory, sometimes in unique ways. Dr. Ted Abel and colleagues (McNally, et al.) developed a transgenic mouse line that expresses a tetO-regulated, hemagglutin (HA)-tagged histone H3.3, which they demonstrate has control over transgene expression. In this study, they characterize this mouse line during memory consolidation and evaluate the contribution of H3.3 to fear memory and motor learning. Drs. Barbra Kaltschmidt and Christian Kaltschmidt (Kaltschmidt and Kaltschmidt) discuss roles for NF-kB in structural plasticity and long-term memory. In this review, they also discuss differences in NF-kB activity in

OPEN ACCESS

Edited and reviewed by:
Jochen C. Meier, Technical University Braunschweig, Germany

****Correspondence:***
Benedict C. Albensi
balbensi@sbrc.ca

Received: *22 February 2016*
Accepted: *24 March 2016*
Published: *19 April 2016*

Citation:
Albensi BC and Djordjevic J (2016) Editorial: Transcriptional Regulation of Memory. Front. Mol. Neurosci. 9:24. doi: 10.3389/fnmol.2016.00024

neurons versus glia related to NF-kB homeostasis and whether NF-kB activation is a *friend* or *foe*. Data from my laboratory is also presented by Dr. Snow (Snow et al.) that demonstrates training in the Morris water maze (MWM) is associated with the upregulation of the NF-kB p65 subunit, correlations with CREB, increases in the factor Nrf2, and elevations of actin protein. These data show that the MWM is associated with transcriptional changes in the hippocampus, including those related to redox regulation. Dr. Feng and colleagues (Jia et al.) go on to discuss epigenetic regulation and how the dysregulation of histone acetylation contributes to postoperative cognitive dysfunction. In this study, the HDAC inhibitor, suberoylanilide hydroxamic acid (SAHA) was shown to attenuate long term memory impairments in aging mice. Dr. Farah Lubin and colleagues (Jarome et al.) also present a study on epigenetic regulation in memory consolidation. In this case, they demonstrate a novel role for NF-kB in the regulation of Gadd45beta expression and DNA methylation during fear memory formation. Dr. Arturo Romano and his colleagues (de la Fuente et al.) also focus on NF-kB activity in their review and specifically address consolidation and reconsolidation memory phases. In addition, there is a discussion on the regulation of immediate-early and late genes by epigenetic mechanisms that determine enduring forms of memories. Moving on to a more classically recognized transcription factor pathway, Dr. Kelsey Martin and colleagues (Ch'ng et al.) present a study on the CREB-regulated transcriptional coactivator (CRTC1) in regulating learning and memory. Here they provide evidence for the sources of calcium required for the nuclear import of CRTC1 and show CRTC1 undergoes dynein-mediated and nuclear localization signal (NLS)-dependent transport along microtubules to reach the nucleus. Dr. Sylvia Ortega-Martínez also presents a paper on CREB that reviews various members of the CREB family. The review also highlights the role of CREB as a modulator of adult hippocampal neurogenesis (AHN) during memory consolidation. Finally, Dr. Joanna Williams and her colleagues (Nido et al.) present a study on the genomic response following long-term potentiation (LTP), an experimental paradigm associated with memory encoding. These data present the view that a new homeostatic state is created 24 h post LTP, by which the stability of neural networks regulated at different times parallel properties observed at the synapse.

From reading these papers, it becomes obvious that the formation of human memories involves a series of complicated biochemical processes many of which are not fully understood. The studies and reviews presented here implicate several families of transcription factors and epigenetic mechanisms that highlight the complexity associated with the transcriptional regulation of memory.

Finally we wish to thank the *Frontiers* family of open access journals for their excellent support in putting this series of reviews and studies together for this Research Topic.

AUTHOR CONTRIBUTIONS

All authors listed, have made substantial, direct and intellectual contribution to the work, and approved it for publication.

FUNDING

St. Boniface Hospital Research Foundation, Alzheimer Society of Manitoba, Natural Sciences and Engineering Council of Canada (NSERC), and Research Manitoba.

ACKNOWLEDGMENTS

BA is the Manitoba Dementia Research Chair and the Honourable Douglas and Patricia Everett and Royal Canadian Properties Limited Endowment Fund Chair. He is also a Research Affiliate of the Centre on Aging at the University of Manitoba and a Scientist at the Children's Hospital Research Institute of Manitoba.

REFERENCES

Kandel, E. R., Schwartz, J. H., Jessell, T. M., Siegelbaum, S. A., and Hudspeth, A. J., (2013). *Principles of Neural Science, 5th Edn.* McGraw-Hill Companies.

Conflict of Interest Statement: The authors declare that the research was conducted in the absence of any commercial or financial relationships that could be construed as a potential conflict of interest.

frontiers in Molecular Neuroscience

REVIEW
published: 09 September 2015
doi: 10.3389/fnmol.2015.00050

NF-κB transcription factor role in consolidation and reconsolidation of persistent memories

*Verónica de la Fuente, Noel Federman, Gisela Zalcman, Angeles Salles, Ramiro Freudenthal and Arturo Romano**

Laboratorio de Neurobiología de la Memoria, Departamento de Fisiología, Biología Molecular y Celular, Facultad de Ciencias Exactas y Naturales, Instituto de Fisiología, Biología Molecular y Neurociencias (IFIBYNE, UBA-CONICET), Universidad de Buenos Aires, Ciudad Universitaria, Buenos Aires, Argentina

Transcriptional regulation is an important molecular process required for long-term neural plasticity and long-term memory (LTM) formation. Thus, one main interest in molecular neuroscience in the last decades has been the identification of transcription factors that are involved in memory processes. Among them, the nuclear factor κB (NF-κB) family of transcription factors has gained interest due to a significant body of evidence that supports a key role of these proteins in synaptic plasticity and memory. In recent years, the interest was particularly reinforced because NF-κB was characterized as an important regulator of synaptogenesis. This function may be explained by its participation in synapse to nucleus communication, as well as a possible local role at the synapse. This review provides an overview of experimental work obtained in the last years, showing the essential role of this transcription factor in memory processes in different learning tasks in mammals. We focus the review on the consolidation and reconsolidation memory phases as well as on the regulation of immediate-early and late genes by epigenetic mechanisms that determine enduring forms of memories.

Keywords: NF-κB, transcription factors, consolidation, reconsolidation, memory

OPEN ACCESS

Edited by:
Benedict C. Albensi, University of Manitoba, Canada

Reviewed by:
Hansjürgen Volkmer, NMI an der Universität Tübingen, Germany
Lan Ma, Fudan University, China

****Correspondence:***
Arturo Romano, Laboratorio de Neurobiología de la Memoria, Departamento de Fisiología, Biología Molecular y Celular, Facultad de Ciencias Exactas y Naturales, Instituto de Fisiología, Biología Molecular y Neurociencias (IFIBYNE, UBA-CONICET), Universidad de Buenos Aires, Ciudad Universitaria, Pab. II, 2do Piso, 1428EGA Buenos Aires, Argentina
aromano@fbmc.fcen.uba.ar

Received: *29 May 2015*
Accepted: *24 August 2015*
Published: *09 September 2015*

Citation:
de la Fuente V, Federman N, Zalcman G, Salles A, Freudenthal R and Romano A (2015) NF-κB transcription factor role in consolidation and reconsolidation of persistent memories. Front. Mol. Neurosci. 8:50. doi: 10.3389/fnmol.2015.00050

Transcription Factors and Memory

Early in the research on the molecular basis of memory it was proposed that memory consolidation is a period during which new proteins must be synthesized (Davis and Squire, 1984; Goelet et al., 1986). The first evidence came from the use of antibiotics like puromycin and cycloheximide (Flexner et al., 1963; Agranoff and Klinger, 1964; Barondes and Cohen, 1966, 1967), which are protein synthesis inhibitors. These inhibitors were effective when administered shortly before or after acquisition, and induced memory impairment only when tested at long-term but not at short-term periods. Almost at the same time of these findings with protein synthesis inhibitors, the role of mRNA synthesis in memory formation was initially evidenced by the use of the antibiotic actinomycin D, which interferes with transcription (Barondes and Jarvik, 1964; Appel, 1965; Cohen and Barondes, 1966). Like the other antibiotics, actinomycin D impaired long-term memory (LTM) only when administered around training session, and the amnesic effect was manifested when tested at long-term periods. Many years later, the first transcription factors involved in synaptic plasticity, cAMP response element binding protein (CREB; Dash et al., 1990) and in memory consolidation, c-Fos (a member of the activated protein 1-AP-1-family; Anokhin and Rose, 1991) were identified. Subsequent work on CREB, from a series

of studies in *Aplysia*, *Drosophila* and rodents, supported that this transcription factor takes part in an evolutionarily conserved molecular mechanism involved in neural plasticity associated with memory formation (Kaang et al., 1993; Bourtchuladze et al., 1994; Yin et al., 1994).

The identification of other transcription factors involved in neural plasticity and memory was achieved in the following years, such as CAAT enhancer binding protein (C/EBP; Alberini et al., 1994), zinc finger inducing factor 268 (Zif268; Okuno and Miyashita, 1996; Jones et al., 2001) and nuclear factor κB (NF-κB; Freudenthal et al., 1998; Freudenthal and Romano, 2000). For these five transcription factors, strong evidence is now available supporting their essential function in memory processes (Alberini, 2009).

NF-κB Transcription Factor in the Nervous System

NF-κB was first characterized in lymphocytes but is ubiquitously expressed in different tissues. In mammals, the Rel/NF-κB family of transcription factors consists of five members: p50, a product of the NF-κB1 gene; p52, a product of the NF-κB2 gene; p65 or RelA; c-Rel; and RelB. The Rel/NF-κB family also shares the Rel homology domain containing the following structural regions: DNA binding, dimerization, nuclear localization, and inhibitor κB (IκB) interaction sites. Members of the Rel/NF-κB family bind to DNA, recognizing the consensus decameric sequence 5′-GGGPuNNPyPyCC-3′, designated as the κB site. Different dimers bind with diverse affinities to the distinct κB sites. In addition, gene transcription can be activated or repressed depending on the dimer composition. For example, heterodimers between Rel and NF-κB 1 or NF-κB 2 are activators while homodimers of NF-κB 1 and NF-κB 2 are repressors. Evidence for the existence of Rel/NF-κB members has been found in different species such as humans, rats, mice, chicks, *Xenopus*, *Drosophila*, *Anopheles*, honeybees, crabs, oysters and *Aplysia*, indicating that this transcription factor family is evolutionarily conserved. At variance with most of the transcription factors that are normally found in the nucleus, inactive NF-κB dimers are usually retained in the cytoplasm by binding to IκB inhibitory protein. IκB occludes the nuclear localization signal (NLS) of NF-κB subunits (Hayden and Ghosh, 2008). Upon stimulation, the IκB kinase complex becomes activated and phosphorylates IκB, leading to its ubiquitination and subsequent degradation. In the canonical pathways for NF-κB activation, this degradation allows NF-κB to translocate to the nucleus and regulate the expression of its target genes. NF-κB is expressed in the nervous system both in neurons and non neuronal cells such as glia. The subunits most commonly expressed in neurons are p50-p65 heterodimers and p50 homodimers. NF-κB has been found in pre- and postsynaptic sites (Kaltschmidt et al., 1993; Guerrini et al., 1995; Meberg et al., 1996; Freudenthal and Romano, 2000). The presence of inducible NF-κB in synapses led to the hypothesis that NF-κB is locally activated by synaptic activity and then, in this activated state, is retrogradely transported to the nucleus to regulate gene expression. This fact would confer to this transcription factor a dual function as synaptic activity detector and as transcriptional regulator.

Until now, a number of NF-κB target genes have been found in neurons, and many of them are related to neural plasticity and memory. These include the genes that codify for the following proteins: calcium/calmodulin protein kinase II delta (CaMKIIδ) (see below, Federman et al., 2013), insulin-like growth factor 2 (IGF2; Schmeisser et al., 2012), Zif268 immediate-early gene (Zhou et al., 2003), C/EBP delta (Liu et al., 2007), brain-derived neurotrophic factor (Saha et al., 2006), neural cell adhesion molecule (NCAM; Simpson and Morris, 2000), inducible and neural nitric oxide synthetase (NOS; Morris et al., 2003), cAMP dependent protein kinase A (PKA) α catalytic subunit (Kaltschmidt et al., 2006), protein kinase C (PKC) δ (Suh et al., 2003), and amyloid precursor protein (APP; Song and Lahiri, 1998). NF-κB is widely distributed in the central nervous system (CNS) in regions such as the hippocampus, cerebral cortex, and cerebellum. It is activated upon glutamatergic excitatory synaptic transmission by signals involved in neural plasticity such as depolarization and transient increment of intracellular Ca^{2+} through the Ca^{2+}-dependent signaling and the activation of CaMKII (Meffert et al., 2003). NF-κB is also activated in response to dopamine and by neuropetides such as angiotensin II (Frenkel et al., 2002) and by NCAM (Krushel et al., 1999).

NF-κB in Neural Plasticity and Memory

Long-term potentiation (LTP) and long-term depression (LTD) are models of synaptic plasticity that increase or decrease, respectively, the synaptic efficacy. The induction of *in vivo* LTP in hippocampus increased the expression and the activation of NF-κB (Meberg et al., 1996; Freudenthal et al., 2004). Accordingly, the inhibition of NF-κB reduced LTP and impaired LTD (Albensi and Mattson, 2000). Thus, NF-κB is required in these experimental processes of synaptic plasticity which are considered good models of the synaptic changes occurring during memory storage.

The first evidence of the involvement of NF-κB in memory was obtained in invertebrates, in the context-signal memory of the crab *Chasmagnathus*. In this model, in which contextual cues are associated with a danger stimulus, the activation of NF-κB highly correlates with LTM formation (Freudenthal et al., 1998; Freudenthal and Romano, 2000) while inhibition of this transcription factor impairs memory formation (Merlo et al., 2002). Further studies found NF-κB involved in memory processes in rodents, in different learning tasks such as fear startle potentiation (Yeh et al., 2002), Inhibitory Avoidance (IA; Freudenthal et al., 2005), radial arms maze (Meffert et al., 2003), contextual fear conditioning (FC; Lubin and Sweatt, 2007), conditioned place preference (Yang et al., 2011) and novel object recognition (NOR; Federman et al., 2013).

In the following sections, we will review a series of recent studies in rodents describing the involvement of NF-κB, not only in the memory formation, but also in the different phases of memory, its persistence and its role at the synapse.

NF-κB in Memory Consolidation

Initially, evidence for the role of Rel/NF-κB in rodents was obtained studying fear-potentiated startle conditioning in rats (Yeh et al., 2002). In this task, trained animals received 10 light stimuli paired with a footshock, and controls received a pseudorandom presentation of the same number of light stimuli and footshocks. In a testing session, the conditioned stimulus was presented together with a white noise and the fear-potentiated startle was evaluated. Using this model, an increment of NF-κB DNA-binding activity was found by electrophoretic mobility shift assay at 2–6 h after training in amygdala but not in hippocampus or cerebellum. IKK activation was also found at 10 and 30 min after training, decreasing to basal levels at 90 min. The intra-amygdala inhibition of NF-κB before training significantly reduced potentiated startle at LTM testing, supporting the idea that NF-κB activation in amygdala is required for memory storage. A further study in this model revealed that FC induced an association between NF-κB and the acetyl transferase CREB binding protein (CBP), resulting in an increase in acetylated p65. The administration of general deacetylase inhibitors prolonged the acetylation state of p65 in amygdala and facilitated LTM (Yeh et al., 2004).

The first evidence for the role of Rel/NF-κB in hippocampus was found in an IA task in mice (**Figure 1A**). The hippocampal formation is a key structure for contextual memories because it is involved in processing and identification of contextual characteristics of different places and in the coding of the unconditioned stimulus associated with a particular place. In this task, animals were placed on an illuminated platform in front of the entrance to a dark compartment. Once the animals entered the dark compartment, they received a mild footshock while controls did not. At LTM testing, trained animals typically showed high latencies to step-through or avoided entering the compartment. Conversely, control animals showed very low latencies to enter. Moreover, we found that the inhibition of this transcription factor by immediate post-training i.c.v. administration of the IKK inhibitor sulfasalazine (SSZ) induced retention deficit in a dose-dependent manner when tested 48 h later (Freudenthal et al., 2005). On the contrary, delayed injections of SSZ at 3 or 24 h post-training did not affect retention. In order to study the effect of direct NF-κB inhibition, we used the κB decoy strategy. The κB decoy consists of a double-stranded DNA oligodeoxinucleotide (ODN) containing a κB consensus sequence that binds to the transcription factor, impeding its action. The κB decoy was administered i.c.v. 2 h pretraining, showing memory impairment. Conversely, injection of the κB decoy with a single base mutation did not affect LTM. Hippocampal NF-κB activity after training increased in shocked animals at 45 min, having returned to basal levels at 2 h post training. These results support the idea that NF-κB activation in the hippocampus is required for the consolidation of contextual features that constitute the conditioned stimulus representation (Freudenthal et al., 2005).

We also studied the dynamics of hippocampal NF-κB activation in the consolidation of contextual fear memory (**Figure 1A**). In this task, mice associate contextual characteristics of the training chamber with a mild footshock. During testing, the percentage of freezing response is determined. Similar to the results obtained in IA, an activation of hippocampal NF-κB at 45 min was observed after the three-trials training (de la Fuente et al., 2014). The intra-hippocampal administration of SSZ induced amnesic effects, which were revealed by further testing sessions at 24 h and 2 weeks after training (de la Fuente et al., 2014), suggesting a permanent amnesic effect. These findings support that NF-κB is involved in contextual fear memory consolidation in the hippocampus.

IA and FC both entail the presence of an aversive reinforcement, the mild footshock that acts as unconditioned stimulus. At this point, one possible interpretation that could be formulated is that NF-κB is specifically involved in memories associated with aversive and stressful stimuli. NOR is a widely investigated form of declarative memory. It refers to the ability of determining whether a newly found item or object has been previously encountered (Squire et al., 2007). In the classical variant of the task, the animal is exposed during training to two identical objects and is allowed to explore them for a defined time period. During testing, animals are exposed to two different objects, one of them is identical to the training objects and the other is a novel object. The time of exploration of the two objects is then determined to obtain a discrimination index, taking advantage of the rodent's natural predisposition to explore novel objects more thoroughly. In the NOR, on the one hand, aversive stimuli are absent but on the other hand, the involvement of the hippocampus in this task is a matter of debate (Warburton and Brown, 2010). We then tested whether NF-κB is activated in hippocampus during NOR memory consolidation and found that this transcription factor is active in the nucleus of hippocampal cells at both 45 and 60 min. In other experiment, the infusion of κB decoy in the dorsal hippocampus after training drastically impaired object discrimination when tested 24 h post training (Federman et al., 2013; Zalcman et al., 2015; **Figure 1C**). All in all, these experiments support both the participation of NF-κB in NOR memory consolidation and the involvement of the hippocampus in this task.

Transcription factors such as NF-κB are involved in the first step of gene expression regulation. These factors are already present at the moment of neuronal activity induced by training. The activation of this kind of transcription factors allows for a second step in gene regulation by induction of immediate-early genes (IEGs) whose protein products are, in turn, transcription factors. Among these IEGs, *zif268* has been found to play a critical role in LTM formation and reprocessing after retrieval. NF-κB binding to the *zif268* promoter region has been identified (Thyss et al., 2005), supporting that NF-κB is involved in its expression. We recently found that Zif268 protein expression was induced 45 min after NOR training in the hippocampus and that the post-training intrahippocampal administration of ODN antisense of the Zif268 mRNA impaired recognition memory. In addition, we found that NF-κB inhibition by κB decoy ODN significantly reduced the training-induced Zif268 increment, indicating that NF-κB is involved in the regulation of Zif268 expression in the hippocampus

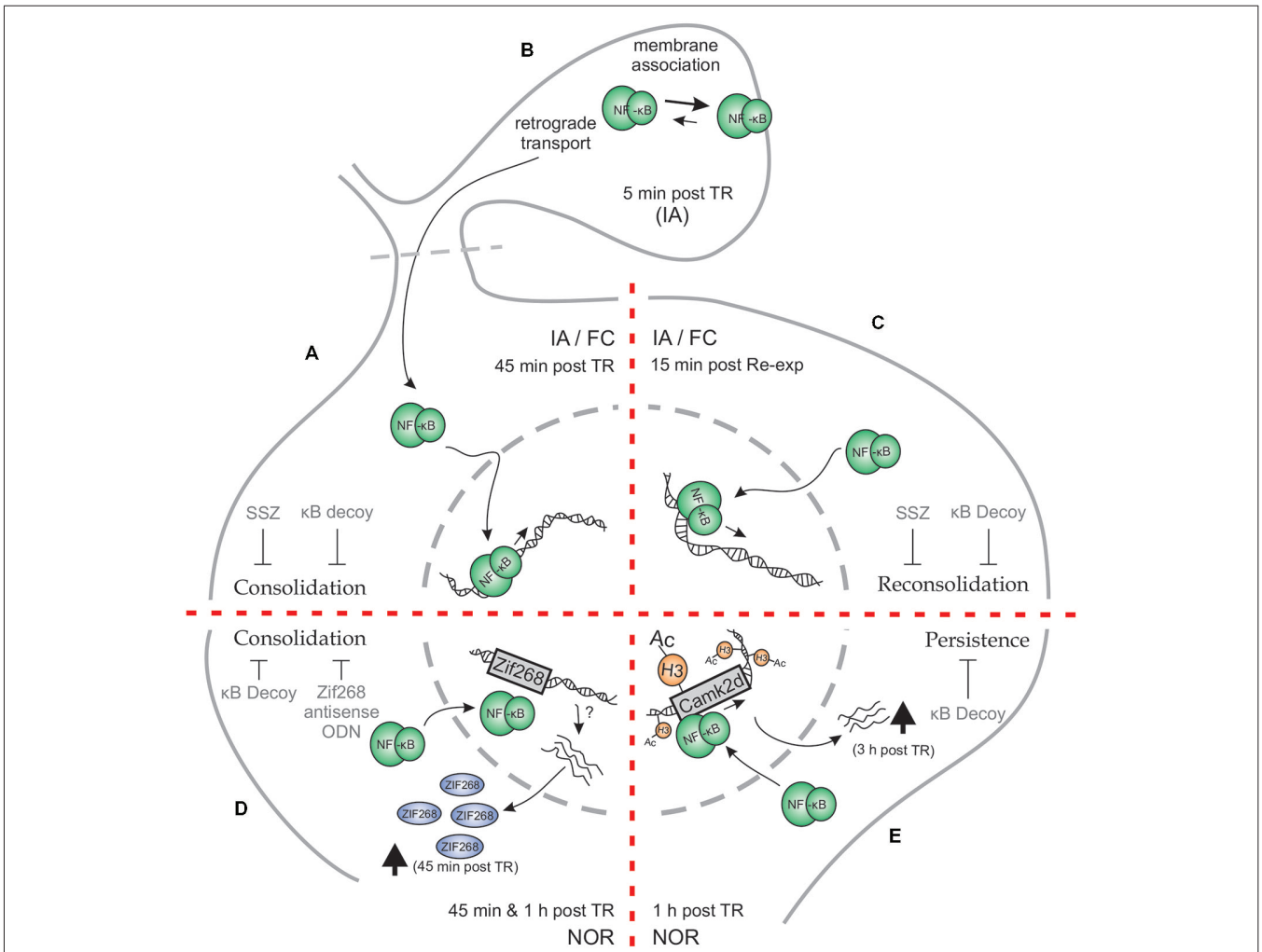

FIGURE 1 | Schematic representation of Hippocampal NF-κB involvement in different phases of memory for different memory tasks. (A–C) Inhibitory Avoidance (IA) and Fear Conditioning (FC). **(A)** Both in IA and in FC, training (TR) induces an increase in hippocampal NF-κB activity 45 min after TR. Administration of NF-κB inhibitory drugs—κB decoy or sulfasalazine (SSZ)—in hippocampus disrupts long-term memory (LTM) consolidation. **(B)** When hippocampal synaptosmal preparations were analyzed, a membrane association of NF-κB was observed 5 min post TR in IA paradigm, postulating that synaptic NF-κB not only acts as a retrograde messenger but also has a localized function as well. **(C)** Memory reactivation induces an increase in hippocampal NF-κB activity 15 min after re-exposure to the TR context (Re-exp), both in IA and FC. Hippocampal κB decoy or SSZ administration also impairs LTM reconsolidation in both tasks. **(D–E)** Novel Object Recognition (NOR). **(D)** Training in a NOR paradigm elicits an increment in hippocampal NF-κB activity both at 45 min and 1 h after TR. Moreover, NOR training induces an increment in hippocampal Zif268 protein, which is prevented by κB decoy administration. Both κB decoy and Zif268 antisense oligodeoxinucleotide (ODN) administration in hippocampus impair long-term recognition memory. **(E)** Strong TR elicits a persistent form of NOR memory which involves an increment in histone (H3) acetylation 1 h after TR, that is not observed after weaker trainings. This H3 acetylation is dependent on NF-κB activity, as κB decoy administration prevents it. In particular, CamkIIδ gene was found to be acetylated in its promoter at an NF-κB consensus sequence, which was concomitantly reversed by NF-κB inhibition. CamkIIδ mRNA levels were found to be augmented 3 h post TR. Hippocampal κB decoy administration impaired memory persistence.

during recognition memory consolidation (Zalcman et al., 2015; **Figure 1C**).

NF-κB in Memory Reconsolidation

In the classical postulation, memory is stored in its definitive long-term form once consolidated few hours after acquisition. During this process, memory becomes resistant to different disruption treatments. However, an important body of evidence has challenged this assumption, supporting the view that memory is more dynamic and can be modified when reactivated by a reminder during retrieval. Under these circumstances, a new period of lability followed by a consolidation-like process takes place. This phenomenon, known in literature as reconsolidation, has been under intense research for the last 15 years (Dudai, 2012).

In an initial report in mammals on the role of NF-κB in memory reconsolidation, we found that NF-κB inhibition in the hippocampus by SSZ or κB decoy after memory reactivation impaired retention of IA memory in mice (**Figure 1D**). In contrast, mutated κB decoy had no effect. Furthermore, we found NF-κB activation in the hippocampus, with a peak 15 min

after memory retrieval (Boccia et al., 2007). This activation was faster than the one previously found in the hippocampus during consolidation of the same task, with a peak at 45 min (Freudenthal et al., 2005), suggesting a temporal signature for both processes. In contextual FC, when animals are re-exposed for 5 min to the training context 1 day after training (once memory consolidation is fully achieved), a labilization-reconsolidation process takes place. During this process, we found that after an initial inhibition, NF-κB showed a peak of activation in mice hippocampus 15 min after the animal was removed from the context (**Figure 1D**), which is the same time point at which NF-κB was activated after retrieval in the IA task. The infusion of κB decoy immediately after a brief re-exposure caused memory impairment when animals were tested a day after re-exposure, but not 4 h after re-exposure or when mice were not re-exposed. The memory deficit was present even when the mice were tested 2 weeks later, supporting a permanent impairment of memory (de la Fuente et al., 2011). All these findings led us to postulate that NF-κB is activated after memory reactivation as part of the molecular mechanisms involved in memory reconsolidation. Furthermore, the intra-hippocampal administration of the calcineurin phosphatase inhibitor FK506 previous to the re-exposure session induced NF-κB activation and a concomitant memory enhancement that was reverted by the administration of SSZ. Calcineurin actually acts constraining memory in both consolidation and reconsolidation by NF-κB inhibition (de la Fuente et al., 2014).

Lubin and Sweatt (2007) also found evidence on the role of the hippocampal NF-κB pathway in FC reconsolidation in rats, supporting the direct involvement of IKK, the protein kinase that activates NF-κB, in histone phosphorilation in the nucleus. In a recent study, Si et al. (2012) demonstrated that inhibition of NF-κB after memory reactivation in the basolateral amygdala impairs the retention of cued auditory FC. This latter finding supports that NF-κB is not only acting in reconsolidation in the hippocampus but also in amygdala for hippocampal independent tasks. Memory impairment by NF-κB inhibition in reconsolidation was also found in the morphine-induced conditioned place preference task (Yang et al., 2011). Thus, the role of NF-κB in memory reconsolidation is supported in different tasks and different areas of the brain.

Knock-Out Mice for NF-κB Pathway

The use of gene-targeting strategies in mice gave further support to the role of NF-κB in learning and memory. Mice with a null mutation of p50 showed acquisition deficits in an active avoidance task (Kassed et al., 2002) but, strikingly, normal LTM 24 h after training. Similarly, in another report short-term but not LTM deficits were found in p50 deficient mice (Denis-Donini et al., 2008). Although these results would suggest that p50 is not required for LTM formation, the general effect of the p50 knock-out on κB-dependent transcription is not easy to predict, as this subunit is a component of both a transcriptional activator (p65/p50 heterodimer) and a repressor (p50/p50 homodimer). However, more recent studies of p50 knock-out mice showed that the absence of this NF-κB subunit produced late phase LTP impairment but not early phase LTP impairment, and deficits in long-term spatial memory in the Morris water maze. These results support the hypothesis that the p50 subunit is required in long-term plasticity and spatial memory in the hippocampus (Oikawa et al., 2012).

Baltimore and colleagues have systematically deleted individual NF-κB subunits in transgenic mice. Deletion of the p65 subunit is lethal during embryogenesis (Beg et al., 1995) but the knock-out can be rescued by concurrent deletion of type 1 TNF receptors (Alcamo et al., 2001). The brains of p65/TNFR1 double knock-out mice appear normal under general examination and no obvious behavioral abnormalities were described. With this mutant, Meffert et al. (2003) analyzed memory performance using the radial-arm maze with both the spatial and non-spatial (cued) version. In the spatial version of the task, the external end of all the eight arms had food pellets and spatial clues external to the maze were available. In order to optimize food rewards mice had to remember and to avoid the already visited arms. p65/TNFR1 KO mutants made more errors than $p65^{+/+}/TNFR1^{-/-}$ siblings during the first sessions, but in the last sessions no differences in the level of errors were found. In the non-spatial cued version of the task, no external clues were available and only the arms that were illuminated had food pellets. No performance deficit was found in the cued version. The spatial version of this paradigm depends on hippocampus whereas this area is not involved in the non-spatial version. Thus, this result suggests that p65 is required in the hippocampus for neural plasticity necessary in spatial information storage.

Levenson et al. (2004) studied the effect of genetic deletion of c-Rel, a member of the NF-κB family, in FC. In the cued version, animals received a white noise paired with a foot-shock in the training chamber. During testing, freezing response to the noise was evaluated in a different chamber. No differences between c-Rel knock-out and wild type mice were found. However, in the contextual version of the task, in which the training chamber was paired with foot-shock, and the testing was performed in the same chamber, the c-Rel knock-out mice showed impaired LTM. Therefore, c-Rel protein seemed to be necessary for the contextual FC, which is hippocampal dependent, and not required for the cued version in which the hippocampus is not necessary. In a more recent work, the same laboratory found that $c\text{-}rel^{-/-}$ mice displayed significant deficits in freezing behavior 24 h after training for contextual FC, but showed normal freezing behavior in cued FC and in short-term contextual FC. Moreover, $c\text{-}rel^{-/-}$ mice showed impairment in NOR task. These results indicate that $c\text{-}rel^{-/-}$ mice have impaired hippocampus-dependent memory formation (Ahn et al., 2008).

In another study, Kaltschmidt et al. (2006) generated a double transgenic mouse with the expression of tetracycline transactivator (tTA) under the CamKIIa promoter, which confers postnatal expression restricted to the forebrain. The second transgene includes a TetO promoter, regulated by tTA, which allows expression of an IκB super-repressor (non-phosphorylatable form of IκBα). This genetic manipulation caused a general inhibition of NF-κB in forebrain neurons. Treatment with doxycyline rescues the NF-κB deficiency.

The performance of this double transgenic mouse without doxycycline (NF-κB deficient) was tested in the hippocampal dependent Morris water maze. The double transgenic animals showed higher latencies during training to reach to the platform than controls, and a deficit in the transfer test without the platform, in which the time spent searching in the correct quadrant was determined. However, no differences were found between these NF-κB-deficient animals and doxycycline-treated animals (NF-κB-rescued), probably due to a nonspecific influence of the drug on memory formation. Besides the behavioral experiments, authors also showed that LTP and LTD were reduced in the Schaffer-collaterals hippocampal path. Notably, they found a down-regulation of the junD gene and the N-CAM gene in these double transgenic mice. In this same study, gene profiling experiments and analysis of regulatory regions identified the α catalytic subunit of PKA as a NF-κB target gene (Kaltschmidt et al., 2006).

In conclusion, most of the studies on genetic manipulation of the NF-κB pathway reviewed here point to an important role of this transcription factor in memory, particularly in hippocampal-dependent tasks.

Epigenetic Regulation of Persistent Memories

Epigenetic mechanisms regulate the magnitude and the extent of the gene expression pattern induced by learning. The genome of all cells is packaged in the chromatin, a structure comprising DNA and associated proteins, the histones, which determine the different degrees of DNA compaction in its basic structure, the nucleosome. Epigenetic marks consist of modifications of the chromatin structure, which affects transcription of genes. These marks may be post-translational modifications of histones, such as acetylation, phosphorylation, ubiquitination and methylation, as well as changes in the methylation patterns of DNA cytosine residues. Other epigenetic mechanisms include histone variants incorporation to nucleosomes, nucleosome remodeling, and changes in the position of the chromosome in relation to pores in the nuclear envelope (Raisner and Madhani, 2006; Draker and Cheung, 2009; Kundu and Peterson, 2009). All these epigenetic processes occur in an interdependent and coordinated manner, in order to regulate the expression of different parts of the genome (Mehler, 2008).

Previous studies showed that epigenetic mechanisms are involved in memory formation and in particular, in recognition memory. The histone acetyl transferase (HAT) CREB-binding protein (CBP)/p300 is involved in recognition memory consolidation (Oliveira et al., 2011). For instance, the HAT activity domain of CBP is required for NOR memory consolidation (Korzus et al., 2004; Wood et al., 2005) and knock-out mice of the cbp gene show deficits in the NOR task (Alarcón et al., 2004). Furthermore, by the use of specific drugs, it has been found that p300 activity is required for memory formation (Marek et al., 2011; Oliveira et al., 2011; Federman et al., 2013). As was previously mentioned, NF-κB is able to recruit CBP/p300 and to induce histone acetylation in promoter regions containing κB sites (Pradhan et al., 2012).

We hypothesized that NF-κB-dependent histone acetylation during memory consolidation is a molecular feature particularly required for the formation of enduring memories. To test this hypothesis we used three different training protocols: one group of animals received a weak training (3 min of object exploration) which did not induce LTM; another group received a standard training (10 min) that induced LTM which lasts for 24 h but not for 1 week; and the last group received a strong training (15 min) that induced LTM that lasts for 7 days. We found an induction of general histone H3 acetylation of the chromatin in the hippocampus only in animals trained with the strong training protocol. Therefore, these data suggest that the consolidation of more persistent memories differ at the molecular level from the less enduring memories by the induction of this epigenetic mechanism. Next, we explored if the increment in histone acetylation is dependent on NF-κB (**Figure 1E**). We found that NF-κB inhibition by κB decoy impaired memory persistence and concomitantly, prevented the induction of general H3 acetylation (Federman et al., 2013).

Following up on these findings, we investigated if specific genes involved in memory consolidation showed histone acetylation changes. In particular, we studied the promoters of *zif268* as an instance of immediate-early gene (Davis et al., 2003; Soulé et al., 2008) and calcium/calmodulin kinase II δ (*camk2d*) as an instance of late gene (Sirri et al., 2010; Lucchesi et al., 2011). We found a significant increase in histone H3 acetylation at a specific NF-κB-regulated promoter region of the *camk2d* gene, which was reversed by NF-κB inhibition (**Figure 1E**). This H3 acetylation increment led to CaMKIIδ mRNA induction 3 h after strong training, but not after weaker training protocols (Federman et al., 2013). No changes in histone acetylation were found in the promoter of the immediate-early gene *zif268*. This work presents a molecular link between NF-κB transcription factor activation, epigenetic mechanisms, and late gene expression in the regulation of memory persistence.

NF-κB in Neural Synaptic Plasticity

In the last years, important experimental results point to a key role of NF-κB in the determination of synaptogenesis (Boersma et al., 2011; Schmeisser et al., 2012), a basic structural process in the formation of the memory trace. In relation with these findings, the IGF2 gene has been recently identified as a novel IKK/NF-κB target. In IKK/NF-κB signaling-deficient neurons, synapse density is reduced and exogenous IGF2 is able to restore synapse density and promote spine maturation within 24 h. This process depends on IGF2 receptor via MEK/ERK activation. These findings illustrate a fundamental role of IKK/NF-κB–IGF2–IGF2R signaling in synapse formation and maturation in adult mice (Schmeisser et al., 2012). In fact, IGF2 has been previously identified as a memory enhancement factor (Chen et al., 2011).

Several results show that NF-κB is present at the synapses (Kaltschmidt et al., 1993; Guerrini et al., 1995; Meberg et al., 1996; Suzuki et al., 1997; Heckscher et al., 2007) and more recently, the role of the transcription factor during memory consolidation at this neuronal compartment has been explored.

There is evidence supporting two major hypotheses regarding the transcription factor at this localization. The first one being that the transcription factor plays a role in the synapse-to-nucleus communication, ultimately regulating gene expression (Wellmann et al., 2001). This synapse to nucleus transport is initiated by an increase in calcium that follows the N-Methyl-D-aspartate (NMDA) receptor activation at the synapse (Wellmann et al., 2001; Meffert et al., 2003). A different hypothesis that could work simultaneously with the previous one, is that NF-κB may modulate synaptic function locally (Heckscher et al., 2007; Salles et al., 2014). On the one hand, it has been reported that the dynein/dynactin motor complex mediates the transport of NF-κB to the nucleus along microtubules and that this transport is dependent on an intact NLS (Mikenberg et al., 2007). It was also observed that NLSs from p50 and p65 are recognized by α importins and that such interaction is necessary for the translocation of the transcription factor to the nucleus (Fagerlund et al., 2005). It would be interesting to study the relation of importins with the dynein/dynactin motor complex in the transport/translocation of NF-κB to nucleus. On the other hand, and supporting the second hypothesis, we found that there are two pools of the transcription factor at this site, one free in the synaptoplasm and another one strongly bound to synaptic membranes (Salles et al., 2015; **Figure 1B**). The quantities of NF-κB for each pool change after training, decreasing in the synaptosomal content and increasing at the membranes 5 min post-training. This supports the idea that the free NF-κB may be either retrogradely transported to the nucleus or be translocated to synaptic membranes. Furthermore, we found that synaptosomal NF-κB activation occurs 5 min post-training during consolidation (Salles et al., 2015). Therefore synaptosomal activation has a different time course than nuclear activation (**Figure 1B**). This local activation and membrane dynamics support the idea that NF-κB may be important in the synaptic environment during consolidation. As outlined before, NF-κB may be involved in post-translational modifications of other proteins such as acetylation. There is at least one acetyl-transferase that has been described in dendrites and has been reported to interact with NF-κB, ADP-ribosylation factor domain protein 1 (ARD1; Ohkawa et al., 2008). It has been proposed that this protein is implicated in the microtubule dynamics during spine remodeling, suggesting an involvement of NF-κB in this process. Moreover, in the fruit fly neuromuscular junction, NF-κB homolog Dorsal mediates the membrane insertion of glutamate receptors locally at a post-translational level (Heckscher et al., 2007). All this evidence points towards the idea that parallel to the retrograde transport of NF-κB to the nucleus, the transcription factor may play a key role at the synapses during memory consolidation.

Concluding Remarks

More than a decade after the initial descriptions of NF-κB's involvement in memory both in invertebrates (Freudenthal et al., 1998; Freudenthal and Romano, 2000) and vertebrates (Yeh et al., 2002, 2004; Freudenthal et al., 2005), an important body of evidence supports now the participation of NF-κB as a key regulator of gene transcription for long-term storage of information in the nervous system. Furthermore, the presence of NF-κB at the synapses and local activation during memory consolidation may directly influence this process through post-translational modifications of other proteins (Salles et al., 2014). The results reviewed here support that the activity of this family of transcription factors is necessary in the hippocampus for the storage and the persistence of memory in different learning tasks, and both in consolidation and reconsolidation. One of the future directions in the research of the NF-κB role in memory should be the precise characterization of the NF-κB function at the synapse. Another direction for future work is to elucidate the effector genes that are regulated by this transcription factor and the specific role of their protein products. Among the target genes of NF-κB, brain derived neurotrophic factor (bdnf), *zif268* and *camk2d* are candidates for future research efforts in the elucidation of the NF-κB-dependent gene regulation of key proteins that allow memory formation and particularly in the case of the latter gene, in the determination of more persistent memories.

Acknowledgments

We thank Dr. Liliana Orelli for helpful comments on the manuscript. The work reviewed here was supported by research grants from the National Agency of Scientific and Technological Promotion of Argentina (ANPCyT) PICT1482 and PICT2369, National Council of Research (CONICET) PIP5466 and University of Buenos Aires grant X198.

References

Agranoff, B. W., and Klinger, P. D. (1964). Puromycin effect on memory fixation in the goldfish. *Science* 146, 952–953. doi: 10.1126/science.146.3646.952

Ahn, H. J., Hernandez, C. M., Levenson, J. M., Lubin, F. D., Liou, H. C., and Sweatt, J. D. (2008). c-Rel, an NF-κB family transcription factor, is required for hippocampal long-term synaptic plasticity and memory formation. *Learn. Mem.* 15, 539–549. doi: 10.1101/lm.866408

Alarcón, J. M., Malleret, G., Touzani, K., Vronskaya, S., Ishii, S., Kandel, E. R., et al. (2004). Chromatin acetylation, memory and LTP are impaired in $CBP^{+/-}$ mice: a model for the cognitive deficit in Rubinstein-Taybi syndrome and its amelioration. *Neuron* 42, 947–959. doi: 10.1016/j.neuron.2004.05.021

Albensi, B. C., and Mattson, M. P. (2000). Evidence for the involvement of TNF and NF-κB in hippocampal synaptic plasticity. *Synapse* 35, 151–159. doi: 10.1002/(sici)1098-2396(200002)35:2<151::aid-syn8>3.3.co;2-g

Alberini, C. M. (2009). Transcription factors in long-term memory and synaptic plasticity. *Physiol. Rev* 89, 121–145. doi: 10.1152/physrev.00017.2008

Alberini, C. M., Ghirardi, M., Metz, R., and Kandel, E. R. (1994). C/EBP is an immediate-early gene required for the consolidation of long-term facilitation in *aplysia*. *Cell* 76, 1099–1114. doi: 10.1016/0092-8674(94)90386-7

Alcamo, E., Mizgerd, J. P., Horwitz, B. H., Bronson, R., Beg, A. A., Scott, M., et al. (2001). Targeted mutation of TNF receptor I rescues the RelA-deficient mouse and reveals a critical role for NF-jB in leukocyte recruitment. *J. Immunol.* 167, 1592–1600. doi: 10.4049/jimmunol.167.3.1592

Anokhin, K. V., and Rose, S. P. (1991). Learning-induced increase of immediate early gene messenger RNA in the chick forebrain. *Eur. J. Neurosci.* 3, 162–167. doi: 10.1111/j.1460-9568.1991.tb00076.x

Appel, S. H. (1965). Effect of inhibition of RNA synthesis on neural information storage. *Nature* 207, 1163–1166. doi: 10.1038/2071163a0

Barondes, S. H., and Cohen, H. D. (1966). Puromycin effect on successive phases of memory storage. *Science* 151, 594–595. doi: 10.1126/science.151.3710.594

Barondes, S. H., and Cohen, H. D. (1967). Comparative effects of cycloheximide and puromycin on cerebral protein synthesis and consolidation of memory in mice. *Brain Res.* 4, 44–51. doi: 10.1016/0006-8993(67)90147-3

Barondes, S. H., and Jarvik, M. E. (1964). The influence of actinomycin-D on brain RNA synthesis and on memory. *J. Neurochem* 11, 187–195. doi: 10.1111/j.1471-4159.1964.tb06128.x

Beg, A. A., Sha, W. C., Bronson, R. T., Ghosh, S., and Baltimore, D. (1995). Embryonic lethality and liver degeneration in mice lacking the RelA component of NF-kappa B. *Nature* 376, 167–170. doi: 10.1038/376167a0

Boccia, M., Freudenthal, R., Blake, M., de la Fuente, V., Acosta, G., Baratti, C., et al. (2007). Activation of hippocampal nuclear factor-kappa B by retrieval is required for memory reconsolidation. *J. Neurosci.* 27, 13436–13445. doi: 10.1523/jneurosci.4430-07.2007

Boersma, M. C., Dresselhaus, E. C., De Biase, L. M., Mihalas, A. B., Bergles, D. E., and Meffert, M. K. (2011). A requirement for nuclear factor-κB in developmental and plasticity-associated synaptogenesis. *J. Neurosci.* 31, 5414–5425. doi: 10.1523/jneurosci.2456-10.2011

Bourtchuladze, R., Frenguelli, B., Blendy, J., Cioffi, D., Schutz, G., and Silva, A. J. (1994). Deficient long-term memory in mice with a targeted mutation of the cAMP-responsive element-binding protein. *Cell* 79, 59–68. doi: 10.1016/0092-8674(94)90400-6

Chen, D. Y., Stern, S. A., Garcia-Osta, A., Saunier-Rebori, B., Pollonini, G., Bambah-Mukku, D., et al. (2011). A critical role for IGF-II in memory consolidation and enhancement. *Nature* 469, 491–497. doi: 10.1038/nature09667

Cohen, H. D., and Barondes, S. H. (1966). Further studies of learning and memory after intracerebral actinomycin-D. *J. Neurochem* 13, 207–211. doi: 10.1111/j.1471-4159.1966.tb06793.x

Dash, P. K., Hochner, B., and Kandel, E. R. (1990). Injection of the cAMP-responsive element into the nucleus of *aplysia* sensory neurons blocks long-term facilitation. *Nature* 345, 718–721. doi: 10.1038/345718a0

Davis, H. P., and Squire, L. R. (1984). Protein synthesis and memory: a review. *Psychol. Bull.* 96, 518–559. doi: 10.1037/0033-2909.96.3.518

Davis, S., Bozon, B., and Laroche, S. (2003). How necessary is the activation of the immediate early gene zif268 in synaptic plasticity and learning?. *Behav. Brain Res.* 142, 17–30. doi: 10.1016/s0166-4328(02)00421-7

de la Fuente, V., Federman, N., Fustiñana, M. S., Zalcman, G., and Romano, A. (2014). Calcineurin phosphatase as a negative regulator of fear memory: control on nuclear factor-κB signaling in consolidation and reconsolidation. *Hippocampus* 24, 1549–1561. doi: 10.1002/hipo.22334

de la Fuente, V., Freudenthal, R., and Romano, A. (2011). Reconsolidation or extinction: transcription factor switch in the determination of memory course after retrieval. *J. Neurosci.* 31, 5562–5573. doi: 10.1523/JNEUROSCI.6066-10.2011

Denis-Donini, S., Dellarole, A., Crociara, P., Francese, M. T., Bortolotto, V., Quadrato, G., et al. (2008). Impaired adult neurogenesis associated with short-term memory defects in NF-κB p50-deficient mice. *J. Neurosci.* 28, 3911–3919. doi: 10.1523/jneurosci.0148-08.2008

Draker, R., and Cheung, P. (2009). Transcriptional and epigenetic functions of histone variant H2A.Z. *Biochem. Cell Biol.* 87, 19–25. doi: 10.1139/o08-117

Dudai, Y. (2012). The restless engram: consolidations never end. *Annu. Rev. Neurosci* 35, 227–247. doi: 10.1146/annurev-neuro-062111-150500

Fagerlund, R., Kinnunen, L., Köhler, M., Julkunen, I., and Melén, K. (2005). NF-kappaB is transported into the nucleus by importin alpha3 and importin alpha4. *J. Biol. Chem.* 280, 15942–15951. doi: 10.1074/jbc.m500814200

Federman, N., de la Fuente, V., Zalcman, G. P., Corbi, N., Onori, A., Passananti, C., et al. (2013). Nuclear factor κB-dependent histone acetylation is specifically involved in persistent forms of memory. *J. Neurosci.* 33, 7603–7614. doi: 10.1523/JNEUROSCI.4181-12.2013

Flexner, J. B., Flexner, L. B., and Stellar, E. (1963). Memory in mice as affected by intracerebral puromycin. *Science* 141, 57–59. doi: 10.1126/science.141.3575.57

Frenkel, L., Freudenthal, R., Romano, A., Nahmod, V. E., Maldonado, H., and Delorenzi, A. (2002). Angiotensin II and the transcription factor Rel/NF-κB link environmental water shortage with memory improvement. *Neuroscience* 115, 1079–1087. doi: 10.1016/s0306-4522(02)00583-3

Freudenthal, R., Romano, A., and Routtenberg, A. (2004). Transcription factor NF-κB activation after *in vivo* perforant path LTP in mouse hippocampus. *Hippocampus* 14, 677–683. doi: 10.1002/hipo.20020

Freudenthal, R., and Romano, A. (2000). Participation of Rel/NF-κB transcription factors in long-term memory in the crab. *Brain Res.* 855, 274–281. doi: 10.1016/s0006-8993(99)02358-6

Freudenthal, R., Boccia, M. M., Acosta, G. B., Blake, M. G., Merlo, E., Baratti, C. M., et al. (2005). NF-κB transcription factor is required for inhibitory avoidance long-term memory in mice. *Eur. J. Neurosci.* 21, 2845–2852. doi: 10.1111/j.1460-9568.2005.04126.x

Freudenthal, R., Locatelli, F., Hermitte, G., Maldonado, H., Lafourcade, C., Delorenzi, A., et al. (1998). Kappa-B like DNA-binding activity is enhanced after spaced training that induces long-term memory in the crab *chasmagnathus*. *Neurosci. Lett.* 242, 143–146. doi: 10.1016/s0304-3940(98)00059-7

Goelet, P., Castellucci, V. F., Schacher, S., and Kandel, E. R. (1986). The long and the short of long-term memory--a molecular framework. *Nature* 322, 419–422. doi: 10.1038/322419a0

Guerrini, L., Blasi, F., and Denis-Donini, S. (1995). Synaptic activation of NF-kappa B by glutamate in cerebellar granule neurons *in vitro*. *Proc. Natl. Acad. Sci. U S A* 92, 9077–9081. doi: 10.1073/pnas.92.20.9077

Hayden, M. S., and Ghosh, S. (2008). Shared principles in NF-kappaB signaling. *Cell* 132, 344–362. doi: 10.1016/j.cell.2008.01.020

Heckscher, E. S., Fetter, R. D., Marek, K. W., Albin, S. D., and Davis, G. W. (2007). NF-kappaB, IkappaB and IRAK control glutamate receptor density at the *drosophila* NMJ. *Neuron* 55, 859–873. doi: 10.1016/j.neuron.2007.08.005

Jones, M. W., Errington, M. L., French, P. J., Fine, A., Bliss, T. V., Garel, S., et al. (2001). A requirement for the immediate early gene Zif268 in the expression of late LTP and long-term memories. *Nat. Neurosci.* 4, 289–296. doi: 10.1038/85138

Kaang, B. K., Kandel, E. R., and Grant, S. G. (1993). Activation of cAMP-responsive genes by stimuli that produce long-term facilitation in *aplysia* sensory neurons. *Neuron* 10, 427–435. doi: 10.1016/0896-6273(93)90331-k

Kaltschmidt, B., Ndiaye, D., Korte, M., Pothion, S., Arbibe, L., Prüllage, M., et al. (2006). NF-κB regulates spatial memory formation and synaptic plasticity through protein kinase A/CREB signaling. *Mol. Cell. Biol.* 26, 2936–2946. doi: 10.1128/mcb.26.8.2936-2946.2006

Kaltschmidt, C., Kaltschmidt, B., and Baeuerle, P. A. (1993). Brain synapses contain inducible forms of the transcription factor NF-kappa B. *Mech. Dev.* 43, 135–147. doi: 10.1016/0925-4773(93)90031-r

Kassed, C. A., Willing, A. E., Garbuzova-Davis, S., Sanberg, P. R., and Pennypacker, K. R. (2002). Lack of NF-κB p50 exacerbates degeneration of hippocampal neurons after chemical exposure and impairs learning. *Exp. Neurol.* 176, 277–288. doi: 10.1006/exnr.2002.7967

Korzus, E., Rosenfeld, M. G., and Mayford, M. (2004). CBP histone acetyltransferase activity is a critical component of memory consolidation. *Neuron* 42, 961–972. doi: 10.1016/j.neuron.2004.06.002

Krushel, L. A., Cunningham, B. A., Edelman, G. M., and Crossin, K. L. (1999). NF-κB activity is induced by neural cell adhesion molecule binding to neurons and astrocytes. *J. Biol. Chem.* 274, 2432–2439. doi: 10.1074/jbc.274.4.2432

Kundu, S., and Peterson, C. L. (2009). Role of chromatin states in transcriptional memory. *Biochim. Biophys. Acta* 1790, 445–455. doi: 10.1016/j.bbagen.2009.02.009

Levenson, J. M., Choi, S., Lee, S. Y., Cao, Y. A., Ahn, H. J., Worley, K. C., et al. (2004). A bioinformatics analysis of memory consolidation reveals involvement of the transcription factor c-rel. *J. Neurosci.* 24, 3933–3943. doi: 10.1523/jneurosci.5646-03.2004

Liu, Y. W., Chen, C. C., Wang, J. M., Chang, W. C., Huang, Y. C., Chung, S. Y., et al. (2007). Role of transcriptional factors Sp1, c-Rel and c-Jun in LPS-induced C/EBPdelta gene expression of mouse macrophages. *Cell. Mol. Life Sci.* 64, 3282–3294. doi: 10.1007/s00018-007-7375-5

Lubin, F. D., and Sweatt, J. D. (2007). The IkappaB kinase regulates chromatin structure during reconsolidation of conditioned fear memories. *Neuron* 55, 942–957. doi: 10.1016/j.neuron.2007.07.039

Lucchesi, M., Mizuno, K., and Giese, K. P. (2011). Novel insights into CaMKII function and regulation during memory formation. *Brain Res. Bull.* 85, 2–8. doi: 10.1016/j.brainresbull.2010.10.009

Marek, R., Coelho, C. M., Sullivan, R. K., Baker-Andresen, D., Li, X., Ratnu, V., et al. (2011). Paradoxical enhancement of fear extinction memory and synaptic

plasticity by inhibition of the histone acetyltransferase p300. *J. Neurosci.* 31, 7486–7491. doi: 10.1523/JNEUROSCI.0133-11.2011

Meberg, P. J., Kinney, W. R., Valcourt, E. G., and Routtenberg, A. (1996). Gene expression of the transcription factor NF-kappa B in hippocampus: regulation by synaptic activity. *Brain Res. Mol. Brain Res.* 38, 179–190. doi: 10.1016/0169-328x(95)00229-l

Meffert, M. K., Chang, J. M., Wiltgen, B. J., Fanselow, M. S., and Baltimore, D. (2003). NF-κB functions in synaptic signaling and behavior. *Nat. Neurosci.* 6, 1072–1078. doi: 10.1038/nn1110

Mehler, M. F. (2008). Epigenetic principles and mechanisms underlying nervous system functions in health and disease. *Prog. Neurobiol.* 86, 305–341. doi: 10.1016/j.pneurobio.2008.10.001

Merlo, E., Freudenthal, R., and Romano, A. (2002). The IkappaB kinase inhibitor sulfasalazine impairs long-term memory in the crab *chasmagnathus*. *Neuroscience* 112, 161–172. doi: 10.1016/s0306-4522(02)00049-0

Mikenberg, I., Widera, D., Kaus, A., Kaltschmidt, B., and Kaltschmidt, C. (2007). Transcription factor NF-κB is transported to the nucleus via cytoplasmic dynein/dynactin motor complex in hippocampal neurons. *PLoS One* 2:e589. doi: 10.1371/journal.pone.0000589

Morris, K. R., Lutz, R. D., Choi, H. S., Kamitani, T., Chmura, K., and Chan, E. D. (2003). Role of the NF-κB signaling pathway and kappaB cis-regulatory elements on the IRF-1 and iNOS promoter regions in mycobacterial lipoarabinomannan induction of nitric oxide. *Infect Immun.* 71, 1442–1452. doi: 10.1128/iai.71.3.1442-1452.2003

Ohkawa, N., Sugisaki, S., Tokunaga, E., Fujitani, K., Hayasaka, T., Setou, M., et al. (2008). N-acetyltransferase ARD1-NAT1 regulates neuronal dendritic development. *Genes Cells* 13, 1171–1183. doi: 10.1111/j.1365-2443.2008.01235.x

Oikawa, K., Odero, G. L., Platt, E., Neuendorff, M., Hatherell, A., Bernstein, M. J., et al. (2012). NF-κB p50 subunit knockout impairs late LTP and alters long term memory in the mouse hippocampus. *BMC Neurosci.* 13:45. doi: 10.1186/1471-2202-13-45

Okuno, H., and Miyashita, Y. (1996). Expression of the transcription factor Zif268 in the temporal cortex of monkeys during visual paired associate learning. *Eur. J. Neurosci.* 8, 2118–2128. doi: 10.1111/j.1460-9568.1996.tb00733.x

Oliveira, A. M., Estévez, M. A., Hawk, J. D., Grimes, S., Brindle, P. K., and Abel, T. (2011). Subregion-specific p300 conditional knock-out mice exhibit long-term memory impairments. *Learn. Mem.* 18, 161–169. doi: 10.1101/lm.1939811

Pradhan, M., Baumgarten, S. C., Bembinster, L. A., and Frasor, J. (2012). CBP mediates NF-κB-dependent histone acetylation and estrogen receptor recruitment to an estrogen response element in the BIRC3 promoter. *Mol. Cell. Biol.* 32, 569–575. doi: 10.1128/MCB.05869-11

Raisner, R. M., and Madhani, H. D. (2006). Patterning chromatin: form and function for H2A.Z variant nucleosomes. *Curr. Opin. Genet. Dev.* 16, 119–124. doi: 10.1016/j.gde.2006.02.005

Saha, R. N., Liu, X., and Pahan, K. (2006). Up-regulation of BDNF in astrocytes by TNF-alpha: a case for the neuroprotective role of cytokine. *J. Neuroimmune Pharmacol.* 1, 212–222. doi: 10.1007/s11481-006-9020-8

Salles, A., Romano, A., and Freudenthal, R. (2014). Synaptic NF-kappa B pathway in neuronal plasticity and memory. *J. Physiol. Paris* 108, 256–262. doi: 10.1016/j.jphysparis.2014.05.002

Salles, A., Boccia, M., Blake, M., Corbi, N., Passananti, C., Baratti, C. M., et al. (2015). Hippocampal dynamics of synaptic NF-kappa B during inhibitory avoidance long-term memory consolidation in mice. *Neuroscience* 291, 70–80. doi: 10.1016/j.neuroscience.2015.01.063

Schmeisser, M. J., Baumann, B., Johannsen, S., Vindedal, G. F., Jensen, V., Hvalby, Ø. C., et al. (2012). κB kinase/nuclear factor κB-dependent insulin-like growth factor 2 (Igf2) expression regulates synapse formation and spine maturation via Igf2 receptor signaling. *J. Neurosci.* 32, 5688–5703. doi: 10.1523/JNEUROSCI.0111-12.2012

Si, J., Yang, J., Xue, L., Yang, C., Luo, Y., Shi, H., et al. (2012). Activation of NF-κB in basolateral amygdala is required for memory reconsolidation in auditory fear conditioning. *PLoS One* 7:e43973. doi: 10.1371/journal.pone.0043973

Simpson, C. S., and Morris, B. J. (2000). Regulation of neuronal cell adhesion molecule expression by NF-kappa B. *J. Biol. Chem.* 275, 16879–16884. doi: 10.1074/jbc.275.22.16879

Sirri, A., Bianchi, V., Pelizzola, M., Mayhaus, M., Ricciardi-Castagnoli, P., Toniolo, D., et al. (2010). Temporal gene expression profile of the hippocampus following trace fear conditioning. *Brain Res.* 1308, 14–23. doi: 10.1016/j.brainres.2009.10.049

Song, W., and Lahiri, D. K. (1998). Molecular cloning of the promoter of the gene encoding the rhesus monkey beta-amyloid precursor protein: structural characterization and a comparative study with other species. *Gene* 217, 151–164. doi: 10.1016/s0378-1119(98)00337-0

Soulé, J., Penke, Z., Kanhema, T., Alme, M. N., Laroche, S., and Bramham, C. R. (2008). Object-place recognition learning triggers rapid induction of plasticity-related immediate early genes and synaptic proteins in the rat dentate gyrus. *Neural Plast.* 2008:12. doi: 10.1155/2008/269097

Squire, L. R., Wixted, J. T., and Clark, R. E. (2007). Recognition memory and the medial temporal lobe: a new perspective. *Nat. Rev. Neurosci.* 8, 872–883. doi: 10.1038/nrn2154

Suh, K. S., Tatunchak, T. T., Crutchley, J. M., Edwards, L. E., Marin, K. G., and Yuspa, S. H. (2003). Genomic structure and promoter analysis of PKC-delta. *Genomics* 82, 57–67. doi: 10.1016/s0888-7543(03)00072-7

Suzuki, T., Mitake, S., Okumura-Noji, K., Yang, J. P., Fujii, T., and Okamoto, T. (1997). Presence of NF-κB-like and IkappaB-like immunoreactivities in postsynaptic densities. *Neuroreport* 8, 2931–2935. doi: 10.1097/00001756-199709080-00025

Thyss, R., Virolle, V., Imbert, V., Peyron, J.-F., Aberdam, D., and Virolle, T. (2005). NF-κB/Egr-1/Gadd45 are sequentially activated upon UVB irradiation to mediate epidermal cell death. *EMBO J.* 24, 128–137. doi: 10.1038/sj.emboj.7600501

Warburton, E. C., and Brown, M. W. (2010). Findings from animals concerning when interactions between perirhinal cortex, hippocampus and medial prefrontal cortex are necessary for recognition memory. *Neuropsychologia* 48, 2262–2272. doi: 10.1016/j.neuropsychologia.2009.12.022

Wellmann, H., Kaltschmidt, B., and Kaltschmidt, C. (2001). Retrograde transport of transcription factor NF-kappa B in living neurons. *J. Biol. Chem.* 276, 11821–11829. doi: 10.1074/jbc.m009253200

Wood, M. A., Kaplan, M. P., Park, A., Blanchard, E. J., Oliveira, A. M., Lombardi, T. L., et al. (2005). Transgenic mice expressing a truncated form of CREB-binding protein (CBP) exhibit deficits in hippocampal synaptic plasticity and memory storage. *Learn. Mem.* 12, 111–119. doi: 10.1101/lm.86605

Yang, J., Yu, J., Jia, X., Zhu, W., Zhao, L., Li, S., et al. (2011). Inhibition of nuclear factor-κB impairs reconsolidation of morphine reward memory in rats. *Behav. Brain Res.* 216, 592–596. doi: 10.1016/j.bbr.2010.08.047

Yeh, S. H., Lin, C. H., and Gean, P. W. (2004). Acetylation of nuclear factor-kappaB in rat amygdala improves long-term but not short-term retention of fear memory. *Mol. Pharmacol.* 65, 1286–1292. doi: 10.1124/mol.65.5.1286

Yeh, S. H., Lin, C. H., Lee, C. F., and Gean, P. W. (2002). A requirement of nuclear factor-kappaB activation in fear-potentiated startle. *J. Biol. Chem.* 277, 46720–46729. doi: 10.1074/jbc.m206258200

Yin, J. C., Wallach, J. S., Del Vecchio, M., Wilder, E. L., Zhou, H., Quinn, W. G., et al. (1994). Induction of a dominant negative CREB transgene specifically blocks long-term memory in *drosophila*. *Cell* 79, 49–58. doi: 10.1016/0092-8674(94)90399-9

Zalcman, G., Federman, N., de la Fuente, V., and Romano, A. (2015). Nuclear factor kappa B-dependent Zif268 expression in hippocampus is required for recognition memory in mice. *Neurobiol. Learn. Mem.* 119, 10–17. doi: 10.1016/j.nlm.2014.12.013

Zhou, A., Scoggin, S., Gaynor, R. B., and Williams, N. S. (2003). Identification of NF-kappa B-regulated genes induced by TNFalpha utilizing expression profiling and RNA interference. *Oncogene* 22, 2054–2064. doi: 10.1038/sj.onc.1206262

Conflict of Interest Statement: The authors declare that the research was conducted in the absence of any commercial or financial relationships that could be construed as a potential conflict of interest.

frontiers in Molecular Neuroscience

REVIEW
published: 24 November 2015
doi: 10.3389/fnmol.2015.00069

NF-KappaB in Long-Term Memory and Structural Plasticity in the Adult Mammalian Brain

Barbara Kaltschmidt[1]* *and Christian Kaltschmidt*[2]

[1] Molecular Neurobiology, University of Bielefeld, Bielefeld, Germany, [2] Cell Biology, University of Bielefeld, Bielefeld, Germany

The transcription factor nuclear factor kappaB (NF-κB) is a well-known regulator of inflammation, stress, and immune responses as well as cell survival. In the nervous system, NF-κB is one of the crucial components in the molecular switch that converts short- to long-term memory—a process that requires *de novo* gene expression. Here, the researches published on NF-κB and downstream target genes in mammals will be reviewed, which are necessary for structural plasticity and long-term memory, both under normal and pathological conditions in the brain. Genetic evidence has revealed that NF-κB regulates neuroprotection, neuronal transmission, and long-term memory. In addition, after genetic ablation of all NF-κB subunits, a severe defect in hippocampal adult neurogenesis was observed during aging. Proliferation of neural precursors is increased; however, axon outgrowth, synaptogenesis, and tissue homeostasis of the dentate gyrus are hampered. In this process, the NF-κB target gene PKAcat and other downstream target genes such as Igf2 are critically involved. Therefore, NF-κB activity seems to be crucial in regulating structural plasticity and replenishment of granule cells within the hippocampus throughout the life. In addition to the function of NF-κB in neurons, we will discuss on a neuroinflammatory role of the transcription factor in glia. Finally, a model for NF-κB homeostasis on the molecular level is presented, in order to explain seemingly the contradictory, the friend or foe, role of NF-κB in the nervous system.

Keywords: NF-kappaB, long-term memory, transcription factors, synapse, dentate gyrus, long term potentiation

OPEN ACCESS

Edited by:
Benedict C. Albensi, University of Manitoba, Canada

Reviewed by:
Arturo Gabriel Romano, University of Buenos Aires, Argentina
Subhajit Dasgupta, Saint James School of Medicine, Anguilla

***Correspondence:**
Barbara Kaltschmidt
barbara.kaltschmidt@uni-bielefeld.de

Received: *01 June 2015*
Accepted: *30 October 2015*
Published: *24 November 2015*

Citation:
Kaltschmidt B and Kaltschmidt C (2015) NF-KappaB in Long-Term Memory and Structural Plasticity in the Adult Mammalian Brain. Front. Mol. Neurosci. 8:69. doi: 10.3389/fnmol.2015.00069

WHAT IS MEMORY?

In its simplest form, we can define memory as information that can be retrieved later when required. The frequently used definitions of memory in psychology are called declarative memory and non-declarative memory. These terms can be used to discriminate memories of tasks such as riding a bicycle (non-declarative) from other tasks such as remembering a lecture, events, or places (declarative). As one might see with this simple example, there is no easy way to describe how information from the real world (outer world) is stored within the brain. Current knowledge describes what is necessary and sufficient for long-term memory formation such as neurons, action potentials, synapses, engram cells, and neuronal networks. The term 'engram' was coined by Richard Wolfgang Semon, who was the first to call memory traces as engram (Semon, 1920). There are several hypotheses involving single synapses, such as the synaptic tagging and capture hypothesis (Redondo and Morris, 2011), or involving engram cells and their plasticity in neuronal networks (Ryan et al., 2015 and see below). It seems to be unclear that which information

of the real world is stored and how so many different memories acquired during lifetime can be stored and retrieved. A standard approach to memory research is that the observation, i.e., the information from the real world, is taken up by sensory organs, e.g., eyes, and then the information is transformed into signals, which are transmitted to other neurons in the form of ion flux, generating action potentials (neuronal activity). Long lasting storage of this neuronal activity is thought to be stored in small subnets of neurons within the brain. These neurons fire together, show correlated responses, and have strong synaptic connections, which may be used for memory storage (see Mayford et al., 2012 for review), whereas most synapses, not integrated in the investigated subnet, have only weak connections. Kandel and coworkers provided another definition for memory: "Learning is the biological process of acquiring new knowledge about the world, and memory is the process of retaining and reconstructing that knowledge over time" (Kandel et al., 2014), suggesting that memory retrieval could alter memory itself. For additional details on electrophysiology and memory, see Section Target Genes with Potential Involvement in Memory.

Pioneering work of Eric Kandel and coworkers has led to the identification of molecular pathways that translate changes of gene expression to behavior. This process involves intracellular protein phosphorylation and later on the nuclear transcription factor CREB as a target of the protein kinase A (Kandel, 2001). These findings inspired the interest of investigating transcription factors as regulators of memory traces, taking up an old concept from Richard Semon, who called memory traces engram (Semon, 1920): "Ich bezeichne diese Wirkung der Reize als ihre engraphische Wirkung, weil sie sich in die organische Substanz sozusagen eingräbt oder einschreibt. Die so bewirkte Veränderung der organsichen Substanz bezeichne ich als das Engramm des betreffenden Reizes…" Own translation to English: "I call this action of a stimulus an engraphic action, because it engraves or writes into the organic substance. This change in the organic substance is called engram of the corresponding stimulus." Recently Susumo Tonegawa and coworkers identified engram cells that retain memory even under retrograde amnesia (Ryan et al., 2015). They labeled engram cells by transcription of the activity-dependent *c-fos* promoter, driving tTA-dependent expression of either mCherry or chanelrhodopsin. Engram cells showed vast changes in synaptic plasticity on many spines. This could be fully inhibited by inhibiting protein synthesis. For an in depth discussion of the engram concept, see Ramirez et al. (2014). This work underscores the importance of transcription factors such as c-FOS for the formation of long-term memory in specific neurons (engram cells). We conclude that long-term memory could be stored in specific neurons (engram cells) and that engram cells are tagged during memory acquisition by the activation of transcription factors.

TRANSCRIPTION FACTORS AND MEMORY

As discussed previously, transcription factors might provide a way to measure memory traces in neuronal networks, which are involved in memory storage. What is the definition of a transcription factor? A recent census of human transcription factors was done by identifying proteins that bind DNA in a sequence-specific manner (Vaquerizas et al., 2009). For this analysis, DNA-binding domains and families from the Interpro database were assembled and used for database search. This led to the identification of 1391 transcription factors in the human genome. However, only 62 of these putative transcription factors have been experimentally verified for both DNA-binding and regulatory functions. The authors reported among the most-cited transcription factors such as p53, FOS, JUN, CREB, and NF-kappaB. Our own PubMed search in 2015 with MeSH entries "p53 and brain" resulted in 721 publications, whereas inclusion of "memory" in this search resulted in only 29 publications. Another PubMed search with "FOS and brain" resulted in 1399 publications, and with the additional search term "memory," 76 publications were found. About 3196 publications were found for "CREB and brain"; 796 hits were found with the addition of search term "memory." These results might underscore the importance of publications by Noble Prize winner Eric Kandel, who advanced the work on transcription and memory, especially on CREB (Kandel, 2001). Still NF-κB with MeSH term "brain" gives 1430 publications, and together with "memory," we received 108 publications. Reading of the abstracts immediately revealed that some important work was not found by these search strategies. Therefore, here, we will review the current literature on NF-κB and memory in mammalian systems. Besides NF-κB, other transcription factors activated by neuronal activity and involved in memory include cAMP response element-binding protein (CREB), CCAAT enhancer-binding protein (C/EBP), activating protein 1 (AP-1), and early growth response factor (Egr) (Alberini, 2009). Certainly there could be more.

INTRODUCTION TO NF-κB

NF-κB is a master transcription factor that is ubiquitously expressed and responds to diverse stimuli including cytokines, growth factors, and bacteria or viruses by the expression of stress response genes in many cells (Hayden and Ghosh, 2012). NF-κB (nuclear factor kappa B) was discovered in the laboratory of David Baltimore (Sen and Baltimore, 1986), as a DNA-binding factor that is specific to a 10-base pair nearly palindromic sequence: 5′-GGGACTTTCC-3, initially binding to the enhancer of the antibody kappa-light chain. Hence, this might explain its name. Cloning revealed a heterodimer composed of p50 kDa and p65 kDa (RelA) subunits. Further research identified other transcription factors with homology to the reticuloendotheliosis virus of turkeys (v-Rel). Each family member contains a Rel Homology region (RHR) near its N-terminus (**Figure 1**). The RHR contains two domains, the N-terminal domain (NTD) and the Dimerization domain (Dim), joined by flexible linker sequences. In addition, RHR contains a nuclear localization signal (NLS). Therefore, the RHR combines sequence-specific DNA-binding, dimerization, nuclear localization, and interaction with IκB proteins. IκB was purified by Patrick Baeuerle as a 60- to 70-kD inhibitory protein (called I kappa B) from a latent form of NF-κB in the cytoplasm, where latent NF-κB could be activated by treatment with mild detergent deoxycholate

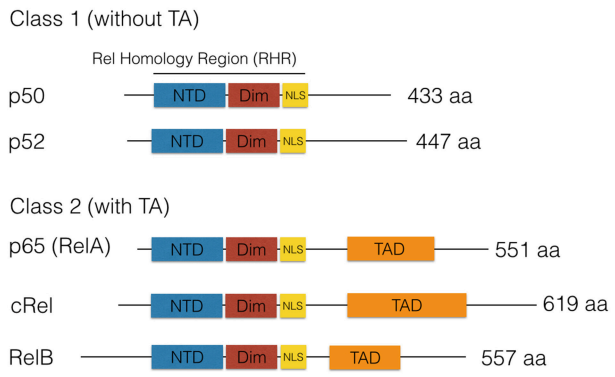

FIGURE 1 | The NF-κB family of DNA-binding proteins. Five DNA-binding subunits found in the mammalian genome, which combine as homo- or heterodimers. A frequently found dimer is composed of p50/p65. All dimers can exist in a latent form in the cytoplasm complexed by IκB family members. This leads to inhibition of NF-κB due to cytoplasmic retention. Furthermore, NF-κB subunits can be classified as Class I (without transactivation, TA) or as Class II with TA due to the presence of a transactivation domain (TAD) in the C-terminal region.

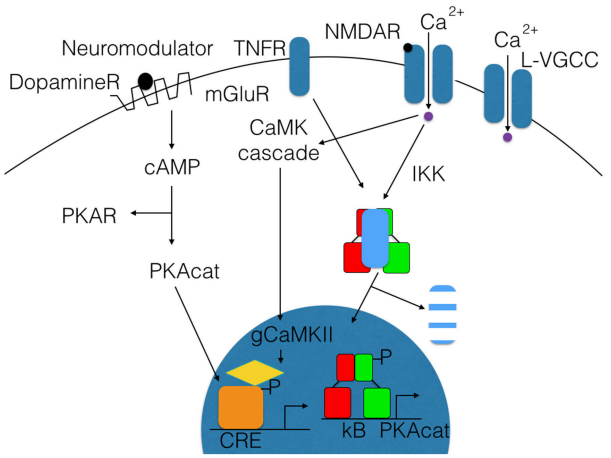

FIGURE 2 | Schematic representation for the activation of transcription factors like NF-κB and CREB by synaptic activity. Upon synaptic stimulation of the receptors for NMDA or voltage-gated calcium channels (L-VGCC), a calcium influx induces activation of IkB kinases and phosphorylation of IkB (blue). Finally, degradation within the proteasome takes place, and thereby the nuclear localization signal of NF-kB is unmasked and allows NF-κB (red/green) to enter the nucleus, where it binds to kb sites and activates the transcription of target genes like PKAcat (catalytic subunit of protein kinase A). On the left site, CREB is activated after stimulation of mGluR or dopamine receptors by dopamine, and cAMP increases activating PKA. This phosphorylates the transcription factor CREB and other proteins like MAP kinases. P-CREB (orange) is bound by CBP (yellow), which initiates the transcription of its target genes. Interestingly, activation of NF-κB and expression of its target gene PKAcat will induce a positive feed-forward loop to CREB activation without additional synaptic activation, which might explain the late phase of long-term potentiation.

(Baeuerle and Baltimore, 1988a). These data suggested a non-covalent interaction of IκB with NF-κB, which could be purified and cloned (Baeuerle and Baltimore, 1988b). Later, many different proteins with IκB function were identified (Hinz et al., 2012).

ACTIVATION OF CREB AND NF-κB IN NEURONS

NF-κB is a transcription factor composed of two DNA-binding subunits that is activated by various stimuli in the nervous system (see **Figure 2**; Kaltschmidt and Kaltschmidt, 2009). Therefore, knockout or genetic ablation has various effects within the nervous system. In contrast, only knockout of subunit RelA (p65) is embryonically lethal. Genetic evidence for a role of NF-κB in the nervous system including cognitive effects or other neurological defects are summarized in **Table 1**.

A comparison of NF-κB in the nervous system and CREB activation is shown in **Figure 2**. The CREB family contains CREB (cyclic-AMP-response element (CRE)-binding protein), CREM (CRE-modulatory protein), and ATF1 (activation transcription factor 1). Double-knockout of CREB and CREM resulted in a massive apoptotic cell death of neurons of the cortical plate and in the hippocampus and striatum, whereas neurogenesis seemed to be unaffected (Mantamadiotis et al., 2002), and no fiber defects were reported. Phosphorylation by protein kinase A at Ser133 activates CREB to promote transcription (for review, see West et al., 2002). Phosphorylation can lead to the recruitment of the transcriptional coactivator CREB-binding protein (CBP). CBP belongs to a family of histone acetyl-transferases, which catalyze hyper-acetylation of core histones, thereby leading to gene activation by loosening chromatin packing. Neuromodulators such as dopamine can activate G-protein-coupled receptors, which in turn activates membrane localized adenylate cyclase, which leads to the elevation of intracellular cAMP (**Figure 2**). Activation by cAMP frees the catalytically active protein kinase A (PKAcat) to enter the nucleus and phosphorylate CREB, which could ameliorate age-dependent memory deficits (Bach et al., 1999). Neuromodulators binding to metabotropic glutamate receptors can also activate NF-κB in neurons (O'Riordan et al., 2006). Activation of plasma membrane-localized ion channels, such as NMDA (*N*-methyl-D-aspartate) receptors (NMDARs) and L-type voltage-gated calcium channels (L-VGCCs), allow the influx of calcium (**Figure 2**). The classical view was that CREB could be activated by phosphorylation via the depolarization-activated $Ca^{(2+)}$-calmodulin-dependent protein kinases (CaM kinases) I and II (Sheng et al., 1991). Then, how the calcium signal is transmitted to the nucleus? This story was unfolded about 25 years later. Recent results suggest a CaM kinase cascade (see **Figure 2**), where the calcium signal is transmitted via calmodulin-dependent phosphorylation of gamma CaMKII. The activated γCaMKII travels to the nucleus where phosphorylation of CREB is initiated (Ma et al., 2014). Until now, there are only two transcription factors known to decode frequency of calcium oscillations: NFAT and NF-κB (Dolmetsch et al., 1998). While NF-κB is already activated by low frequency of calcium oscillations and by infrequent oscillations even at the level of its target genes IL2 and IL8 (Dolmetsch et al., 1998), nothing

TABLE 1 | Genetic mouse models interfering with NF-κB activity in the nervous system.

Genotype	Cell type afflicted	Cognitive effect	Additional phenotype	References
$p50^{-/-}$	All	Defect in novel task acquisition; decreased anxiety; reduced short-term memory; Declining L-LTP; Egr-2 not upregulated after theta burst stimulation	Reduced neuroprotection; hearing loss; reduced neurogenesis; reduced ischemic damage; impaired acute and inflammatory nociception; Premature aging	Schneider et al., 1999; Yu et al., 1999, 2000; Kassed et al., 2002; Kassed and Herkenham, 2004; Duckworth et al., 2006; Niederberger et al., 2007; Denis-Donini et al., 2008; Oikawa et al., 2012; Bernal et al., 2014; Jurk et al., 2014; Nafez et al., 2015
$P65^{-/-}$	Isolated sensory neurons	na*	Reduced neuroprotection	Middleton et al., 2000
$p65^{-/-}$	Isolated Schwann cells	na*	Reduced myelination of peripheral nerves	Nickols et al., 2003
$p65^{-/-}$Tnfrl$^{-/-}$	All	Delayed spatial learning in radial maze	No synaptic NF-kB	Meffert et al., 2003
CamKII tTA/tetO super-repressor IκB-α	Glutamatergic forebrain neurons	Impairments in spatial memory; reduced LTP and LTD; reduced spatial pattern separation; decreased synapse density (spine and presynapse); loss of mossy fibers	Reduced neuroprotection; decreased PKA expression and P-CREB; decreased neurogenesis; defects in dentate gyrus tissue homestasis	Fridmacher et al., 2003; Kaltschmidt et al., 2006; Imielski et al., 2012
Prion-tTA/tetO super-repressor IκB-α	Glutamatergic and inhibitory neurons	Enhanced spatial learning; enhanced LTD	Reduced GAD65 expression	O'Mahony et al., 2006
GFAP- super-repressor IκB-α	Glia: astrocytes	Deficits in learning only in females; delayed spatial learning, impaired cued fear memory	LTP reduced in females; LTP enhanced in males; reduction of mGluR5 in females; better recovery after spinal cord injury; reduced pain sensitivity	Brambilla et al., 2005; Bracchi-Ricard et al., 2008
c-Rel$^{-/-}$	All	Impaired late phase LTD; impaired long-term memory; impaired cued fear memory	Reduced neuroprotection; Late onset Parkinson	Pizzi et al., 2002; Levenson et al., 2004; Ahn et al., 2008; Baiguera et al., 2012
LsyM-Cre/IKK-2$^{FL/FL}$	Glia: microglia; macrophages	na*	30% reduction of neuronal death: 10-fold reduced infarct size after MCAO	Cho et al., 2008
Nestin-Cre/IKK-2$^{FL/FL}$	Precurosor and Neural (glia and neuron)	na*	25% reduction of infarct size after MCAO; amelioration of EAE	Herrmann et al., 2005; van Loo et al., 2006
Nestin-Cre/Ikk-1$^{FL/FL}$	Neural (glia and neuron)	na*	No effect on EAE	van Loo et al., 2006
Nestin-Cre/Nemo$^{FL/FL}$	Neural (glia and neuron)	na*	Amelioration of EAE	van Loo et al., 2006
NSE-SR-IκB-α	Neuronal	na*	Improved LPS-induced hypothermia and survival	Jüttler et al., 2007
CamK2a-tTA x luciferase-(tetO)7-IKK2-CA, called IKK2nCA	Neuronal	Defect in hippocampus-dependent learning and memory after 9 month measured in Morris water maze	Selective neuroinflammation; Reduction of BDNF expression; Granule cell degeneration	Maqbool et al., 2013
GFAP.tTA × (tetO)7.IKK2-CA	Astrocytes (Aldh1l1^{+})	Abnormal development of hippocampus and cerebellum; Strong upregulation of chemokines such as Ccl5, Cxcl10, and Ccl2, perhaps defect in neuronal stem cell migration	Defects could be induced during early development only: Hydrocephalus, massive increase of lateral ventricles, neuroinflammation; loss of cilia on ependymal cells in lateral ventricles	Lattke et al., 2012
Lentiviral constitutively-active IKKβ (^{CA}IKKβ)	Mediobasal hypothalamus neurons	Reduced performance in T-maze	Life span decrease, GnRH expression reduced	Zhang et al., 2013
Nestin-Cre/IKK-2$^{FL/FL}$	Precurosor and Neural (glia and neuron)	Old mice perform better than WT in Morris water maze	Increased life span	Zhang et al., 2013

na, not analyzed.*

is known about the situation in neurons. It is suggested that NF-κB could be activated by calcium in cerebellar granule cells (Lilienbaum and Israël, 2003). Further investigations might clear the mechanisms in other neuronal cell types. All NF-κB-activating stimuli culminate on the IKK complex composed from the IκB kinases IKK 1 and 2 (alpha and beta) and the third subunit NEMO (Israël, 2010). Activation of the IKK complex could involve ubiquitinylation of NEMO and upstream kinases, and the entire mechanism is not solved so far. Activation of the IKK complex leads to phosphorylation of the inhibitory subunit IκB alpha at Ser 32 and 36 followed by ubiquitinylation. This is a signal for proteolytic degradation of IκB in the proteasome. Anti-cancer drugs such as bortecomib (Velclade) are used to inhibit constitutive NF-κB activity in multiple myeloma plasmacytoma cells. In the context reviewed here, bortecimib can have serious side effects on the nervous system (see Velcade EMA/27714/2015) such as posterior reversible encephalopathy syndrome, autonomic neuropathy (damage to nerves controlling organs such as the bladder, eyes, gut, heart, and blood vessels), or more commonly peripheral neuropathy (nerve damage in hands and feet). Furthermore, inhibition of the proteasome system during consolidation blocked long-term memory both in crabs and mice (Sol Fustiñana et al., 2014). Degradation of IκB frees DNA-binding subunits to enter the nucleus by active transport (**Figure 2**), leading to the expression of target genes such as PRKACA (catalytic subunit of PKA; Kaltschmidt et al., 2006). NF-κB could be activated in neurons by depolarization, kainate, and glutamate (Kaltschmidt et al., 1995; Simpson and Morris, 1999). Stimulation in young cerebellar granule cells functions even at the concentration of 10 nM glutamate, alone or together with 10 μM glycine or 100 μM NMDA (Guerrini et al., 1995); interestingly, neurons prepared from older age depicted constitutive NF-κB activity as already reported for hippocampal and cortical neurons *in vitro* and *in vivo* (Kaltschmidt et al., 1994). This constitutive NF-κB activity could be modulated by co-cultured astrocytes, which could inhibit activation of NF-κB *in vitro* (Kaltschmidt and Kaltschmidt, 2000). Constitutive NF-κB activity is also found *in vivo* when reporter genes were analyzed. LacZ expression driven by NF-κB promoters (p105lacZ and 3 × Igk conalacZ) in brain was constitutive in various brain regions of the adult brain including cerebellar granule cells, the hippocampus and several layers as CA1, CA3 and dentate gyrus, and the cerebral cortex (Schmidt-Ullrich et al., 1996). Expression of reporter genes was only neuronal. Furthermore, forced expression of transdominant IκB alpha completely blocked constitutive expression of this lacZ NF-κB reporter gene (Fridmacher et al., 2003). Similar results were achieved with another mouse model (Bhakar et al., 2002) using a κB tandem repeat derived from HIV LTR to drive an SV40 minimal promoter lacZ gene. LacZ expression was strong in the telencephalon and along the roof plate of midbrain. Among other loci of staining, tactile hair follicles were prominently stained. Layers of the cortex cerebri are stained to a lesser extent, but strong staining was evident in hippocampal fields CA1, CA2, DG, and to a lesser extent in CA3. Forced expression of RelA protected cortical neurons against apoptosis induced by etoposide (Bhakar et al., 2002). We found that pre-conditioning neurons with tumor necrosis factor alpha (TNF) or low amounts of amyloid beta peptide (Aβ) could protect neurons against Aβ-mediated neurotoxicity (Kaltschmidt et al., 1999). In this line, it could be shown that TNF is involved in hippocampal synaptic plasticity (Albensi and Mattson, 2000). Furthermore, we have previously shown (Kaltschmidt et al., 1999) that treatment of cerebellar granule cells with TNF or low dose Aβ peptide (0.1 μM) could protect against neurotoxic amounts of Aβ (10 μM). This type of neuroprotection involves NF-κB and might be enhanced by CBP as a potential NF-κB target gene. CBP is a co-activator, which seems to be important for chromatin opening, due to its histone acetyltransferase activity (Ogryzko et al., 1996). Interestingly, several neuroprotective small molecules could be identified by a screening strategy using NF-κB activation (Manuvakhova et al., 2011). Memory decline is one of the hallmarks of Alzheimer's disease, which could be correlated to reduced NF-κB activity around Aβ containing plaques (Kaltschmidt et al., 1999). Neuroprotection against kainate was blocked by forced expression of transdominant IκB alpha (Fridmacher et al., 2003). In **Figure 2**, as an example of a target gene, the catalytic subunit of protein kinase A (PKAcat) is depicted; this gene is regulated by NF-κB in hippocampal neurons *in vivo* (Kaltschmidt et al., 2006). Forskolin-induced (cAMP-dependent) CREB phosphorylation is strongly impaired when NF-κB is repressed. These data suggest a cross-coupling of CREB and NF-κB-dependent memory pathways. However, the question which are the relevant memory target genes still remains.

TARGET GENES WITH POTENTIAL INVOLVEMENT IN MEMORY

Long-lasting long-term potentiation (L-LTP) is a well-established model for memory at the synaptic level. In this paradigm, short voltage trains are used to induce a long-lasting post-synaptic response. It was discovered by Lømo when stimulating the perforant path (input to dentate gyrus granule cells) (Bliss and Lømo, 1973). Recording of field potentials of granule cells showed a long-lasting potentiation of granule cells lasting for hours (L-LTP). The requirement of L-LTP for protein synthesis was first described by Krug et al. (1984). *In vivo* L-LTP resulted in long-lasting biphasic CREB phosphorylation (Schulz et al., 1999). NF-κB $p50^{-/-}$ animals showed only decremental LTP that faded over time, even when high frequency stimulation trains were used, which elicited L-LTP in control animals (Oikawa et al., 2012). Furthermore, LTP magnitude and LTD induction were blocked by inhibiting NF-κB DNA binding in hippocampal slices (Albensi and Mattson, 2000). In this line, expression of Egr-2 was upregulated in WT hippocampal slices preparation after theta burst stimulation but not in $p50^{-/-}$ slices (Nafez et al., 2015). Same authors identified Egr-2 as novel NF-κB target gene in brain. Knockout of c-Rel also led to decremental LTP, whereas c-Rel expression was up-regulated during novel object recognition (Ahn et al., 2008). Late-onset Parkinson's disease was reported in mice with c-Rel knockout with loss of tyrosine hydroxylase positive neurons in the substantia nigra only visible at 18 month of age (Baiguera et al., 2012). Inhibition

of all NF-κB subunits by forced IκB expression led to reduced LTP induction and longer learning phases in Morris water maze (Kaltschmidt et al., 2006). As potential mechanisms, the current models discuss the formation of novel post-synapses and NMDA receptor density increase. Previous reviews suggested that the two secreted proteins, brain-derived neurotrophic factor (BDNF) and tissue plasminogen activator (tPA), have been repeatedly implicated in L-LTP as memory-relevant CREB target genes (Kandel, 2001) or nNOS and presenilin as additional CREB targets (West et al., 2002). To analyze this question in more detail, Eric Kandel and coworkers expressed a constitutively transactivating mutant of CREB (VP16-CREB) in transgenic mice under the control of the tetracycline operator, which can be activated by CamKII promoter-driven expression of the tetracycline-dependent transactivator (Barco et al., 2005). Surprisingly, this study identified only a handful of genes that are activated by VP16-CREB-induced L-LTP, but not by increased neuronal activity alone (kainate treatment). These genes include prodynorphin, MHC Class I and JunD/cFos in CA1, and dentate gyrus (see **Figure 3**). A low amount of induction in all hippocampal subfields was detected for BDNF. Surprisingly, Arc was only induced by kainate treatment, suggesting a difference in genes activated by neuronal activity and memory-relevant gene expression. Furthermore, MHC Class II genes seemed to be induced by VP16-CREB. These data could be reproduced in part with a cellular model of cultured hippocampal neurons (Benito et al., 2011). One might be surprised by the fact that a similar set of genes were identified in a different but technically similar *in vivo* screen, involving loss of function of NF-κB (Kaltschmidt et al., 2006). Therefore, we suggest that JunD, MHC Class I, II and beta 2 microglobulin, prodynorphin, and BDNF might be a common set of genes that are regulated by CREB and NF-κB together. Indeed, MHC Class I, II and beta 2 microglobulin share common response elements including the CREB-binding site, CRE (Gobin et al., 2001). Similarly, these genes are NF-κB target genes (Israël et al., 1989) even in neurons (Kaltschmidt et al., 1995; Yang et al., 2014). However, function in neurons remained unclear. MHC Class I molecules are trimeric proteins that are composed of a transmembrane heavy chain, a soluble κ2-microglobulin (κ2-m) light chain, and a peptide bound to the heavy chain. Only recently, Carla Shatz and coworkers have suggested a synaptic glue hypothesis (Huh et al., 2000), where MHC Class I molecules might be used for adhesion of specific synapses. Surprisingly, LTP is enhanced and LTD is absent in mice without functional MHC Class I (Huh et al., 2000). Expression of MHC Class I genes H2-D and T22 could be detected in the hippocampus (Huh et al., 2000). However, other authors argue that MHC Class I has a function in pathological situations (e.g., synapses and neuron elimination by T-cells; Cebrián et al., 2014). Similarly, no memory-relevant target genes for the AP-1 complex (Fos/Jun) were presented so far. Prodynorphin was identified as a NF-κB target gene with mapped response sites (Bakalkin et al., 1994). BDNF expression might be regulated indirectly via the NF-κB target gene XIAP (Kairisalo et al., 2009). In our humble opinion, the correlation with memory formation is better for NF-κB target genes (**Figure 3** right part of the Venn diagram). The initial idea of synaptic enhancement by transcription is of a target gene that can indeed enhance post- or pre-synapse function. We think there are now, after more than 20 years of research on NF-κB in the nervous system, enough evidences on involvement of NF-κB target genes in synaptic enhancement. In this line, a recent genetic screen identified an insulin-like growth factor 2 (Igf2, see **Figure 4**) as a novel neuronal NF-κB target gene involved in spine density regulation (Schmeisser et al., 2012). Interestingly, Igf2 could rescue the spine reduction in neurons with NF-κB inhibition (Schmeisser et al., 2012). In addition, Igf2 is critically involved in memory consolidation and enhancement (Chen et al., 2011). Igf2 could ameliorate the neurodegeneration in a mouse

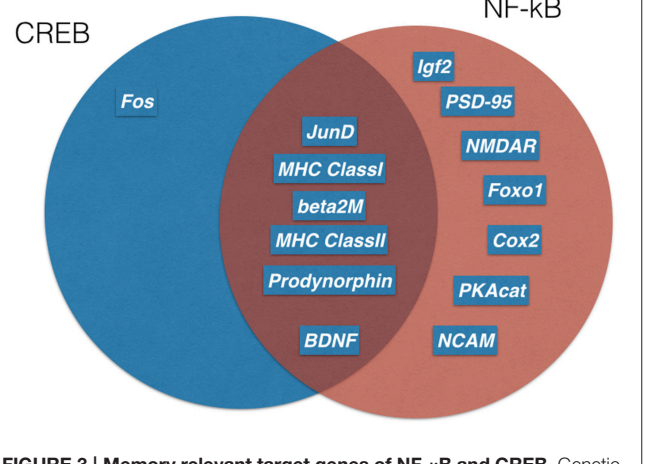

FIGURE 3 | Memory relevant target genes of NF-κB and CREB. Genetic screens in transgenic mice identified several target genes of CREB (blue) and NF-kB(red). A Venn diagram shows overlapping target genes (dark red) of both transcription factors. For references see text.

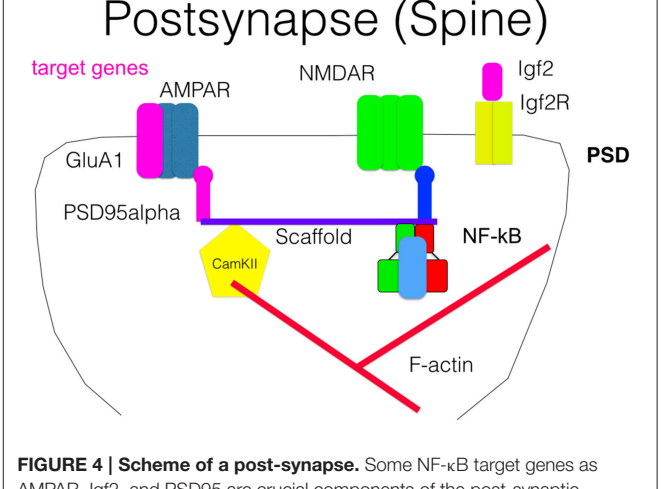

FIGURE 4 | Scheme of a post-synapse. Some NF-κB target genes as AMPAR, Igf2, and PSD95 are crucial components of the post-synaptic compartment and involved in signal transmission. Association of NF-κB with the scaffold is suggested by biochemical fractionation but was not directly proven.

model with Alzheimer's disease, and its expression is reduced in Alzheimer patients' hippocampi (Pascual-Lucas et al., 2014). Similarly, NF-κB activity was reduced in Alzheimer patients' brains (Kaltschmidt et al., 1999), suggesting that Igf2 could be a target gene of NF-κB in humans. In addition, amyloid beta peptides could activate NF-κB p65 in neurons and might activate NF-κB in the close vicinity of early plaques in Alzheimer patients' brains (Kaltschmidt et al., 1997). In this respect, it might be important to note that the activation of NF-κB by Alzheimer's disease follows a bell-shaped curve where low amounts of Aβ activate NF-κB, but high amounts repress NF-κB; for discussion, see Kaltschmidt et al. (2005). In a recent study (Schmeisser et al., 2012), a dominant negative version of the IKK2 protein was expressed in neurons using the tet system. Spine density was reduced to the half of control in CA1, especially the memory-relevant mushroom spines were reduced to about 25%. Learning was slower as with IκB over-expression. Synapses contained significantly less GluA1 and PSD95. Ultrastructure depicted a high amount of synapses with disrupted post-synaptic density. Similarly, it was shown earlier in cultured neurons that NF-κB activity positively regulated spine densitiy and glutamatergic synapse formation (Boersma et al., 2011). These data describing post-synaptic damage fit to our data reporting reduced size and number of presynaptic mossy fiber buttons (Imielski et al., 2012). In addition, we observed that axonal growth is regulated by NF-κB *in vitro* and *in vivo* in the mossy fiber pathway (Imielski et al., 2012). Taken together, NF-κB regulates post-synapse formation (see **Figure 4**) by expression of Igf2, whose receptor is post-synaptic and by additional target genes such as PSD95 (Boersma et al., 2011). Furthermore, NF-κB directs the expression of AMPA receptor components (Boersma et al., 2011; Schmeisser et al., 2012). NMDA receptor component NR1 appears to be regulated by NF-κB, and regulation of NF-κB target genes such as Cox2 (Kaltschmidt et al., 2002), PKAcat (Kaltschmidt et al., 2006), Foxo1, and NCAM (Imielski et al., 2012) were described. Localization of NF-κB in synaptosomes (Kaltschmidt et al., 1993; Meberg et al., 1996; Meffert et al., 2003; Schmeisser et al., 2012) suggests a function of NF-κB as retrograde messenger (see **Figure 5**). In this line, we and others could show that p65-GFP is traveling to the nucleus when activated by glutamate (Wellmann et al., 2001; Meffert et al., 2003). This retrograde transport is dependent on the nuclear localization signal of p65 and involves a dynein–dynactin motor protein complex traveling on microtubules (Mikenberg et al., 2007; Shrum et al., 2009). The traveling complex seems to be a signaling endosome with scaffolding proteins such as Huntingtin and/or HSC70 (Marcora and Kennedy, 2010; Klenke et al., 2013). In comparison, it might be interesting to note that CREB could be translated in axons and mediate a retrograde survival signaling in response to nerve growth factor (Cox et al., 2008).

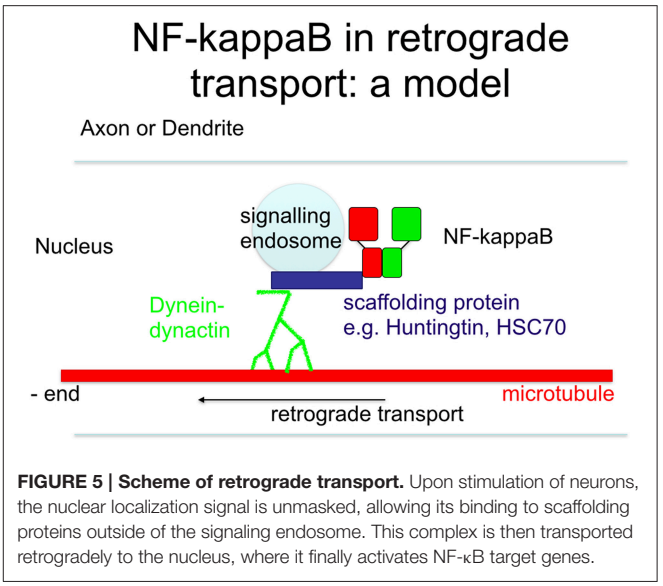

FIGURE 5 | Scheme of retrograde transport. Upon stimulation of neurons, the nuclear localization signal is unmasked, allowing its binding to scaffolding proteins outside of the signaling endosome. This complex is then transported retrogradely to the nucleus, where it finally activates NF-κB target genes.

NF-κB SIGNALING IS ESSENTIAL FOR DENTATE GYRUS TISSUE HOMEOSTASIS

Previously, we have shown that NF-κB plays an important role at three consecutive stages of neurogenesis (see **Figure 6**): proliferation/differentiation of neural progenitor cells, axon specification, and integration of young neurons and survival of mature granule cells (Imielski et al., 2012). Recently, the role of NF-κB p50 in neurogenesis was analyzed (Denis-Donini et al., 2008) in $p50^{-/-}$ mice, where the net rate of neural precursor proliferation was unchanged, but only 50% of newborn neurons survived in the DG and a defect in spatial short-term memory was observed. Because in $p50^{-/-}$ mice only one NF-κB subunit is deleted in all cell types, we used (Imielski et al., 2012) a neuronal-specific ablation of all NF-κB subunits in our study. We confirmed in part the results of Denis-Donini and coworkers for a role of NF-κB in neurogenesis and extended that findings to a function of NF-κB in tissue of the dentate gyrus homeostasis, synaptogenesis, axogenesis, and spatial pattern separation. In contrast to Denis-Donini et al., we found an increased rate of proliferating DCX-positive granule cell progenitors, presumably due to the high rate of apoptosis observed in DG after forced expression of transdominant negative IκB-alpha. Regrowing of DG after re-activation of NF-κB had a major impact on integration and survival of newborn DCX+ neurons. Similarly, neurogenesis within the subventricular zone depends on NF-κB (Zhang et al., 2012).

The regulation of adult neurogenesis by transcription factors is still a matter of debate (Chen et al., 2011), and our data show that the transcription factor NF-κB is a crucial regulator of neurogenesis, essential for axogenesis, and integration of newborn neurons. Taken together, these data indicate that NF-κB plays an important role in structural plasticity of the hippocampus.

Surprisingly, another study showed that over-activation of NF-κB in a transgenic mouse model with forced expression of ncaIKK-2 (Maqbool et al., 2013) resulted in a similar structural defect: degeneration of granule cells to about 50% of control level and massive astrocytosis. In addition, a reduction of BDNF was described but no decrease of Prkca was measured. However,

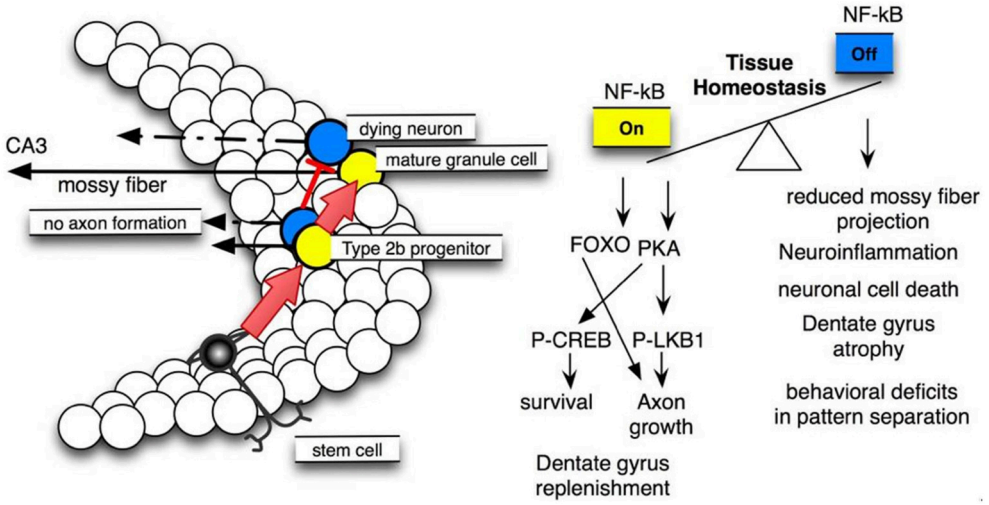

FIGURE 6 | NF-κB signaling is crucial for dentate gyrus tissue homeostasis. Left site: scheme of neural stem cell differentiation in the dentate gyrus, note that NF-κB activation is essential for type 2b progenitor (yellow) maturation to mature granule cells. **Right site:** molecular pathways involved and resulting phenotypes.

expression of the NF-κB target gene Igf2 was not elevated in this mouse model, arguing against the validity of gain of function approaches to study NF-κB target genes.

To the best of our knowledge, NF-κB is the one and only factor where ablation or over-activation showed such severe effects in structural plasticity.

The observed NF-κB-dependent structural defects resulted in a behavioral phenotype. Recently, behavioral tests (Clelland et al., 2009) were developed to measure the memory of subtle differences in spatial environment. The authors suggest that neurogenesis enhanced the recognition of weakly separated cues. In this line, we developed a special behavioral test (*SPS-BM*), which is able to measure spatial pattern separation with the advantage to analyze search strategies (Widera et al., 2014).

Interestingly, the mouse model described in Imielski et al. (2012) is a phenocopy of Alzheimer's disease (AD) in three aspects: reduced NF-κB activity as in AD brains (Kaltschmidt et al., 1999), increased proliferation of immature DCX+ neuronal precursors, and progressive cell loss (Jin et al., 2004) coupled with strong neuroinflammation. Thus, re-activation of NF-κB might be an interesting therapeutic strategy for neuroregeneration of the adult dentate gyrus in the future.

CONCLUSION

We suggest that NF-κB activation in neurons could be an interesting strategy to ameliorate memory diseases such as Alzheimer's disease. Dose–response curve of such kind of drugs might be bell shaped, too much will lead to neurodegeneration. Furthermore, constitutive activation of NF-κB in glia during aging might lead to cognitive decline. Finally, re-activation of NF-κB inhibition might lead to neuroregeneration due to stem cell action, which could be the basis for further understanding of brain repair.

ACKNOWLEDGMENTS

We thank the German Research Council (DFG), the Walcker Stiftung, Isny, Germany, and the University of Bielefeld for funding our research.

REFERENCES

Ahn, H. J., Hernandez, C. M., Levenson, J. M., Lubin, F. D., Liou, H. C., and Sweatt, J. D. (2008). C-Rel, an NF-κB family transcription factor, is required for hippocampal long-term synaptic plasticity and memory formation. *Learn. Mem.* 15, 539–549. doi: 10.1101/lm.866408

Albensi, B. C., and Mattson, M. P. (2000). Evidence for the involvement of TNF and NF-κB in hippocampal synaptic plasticity. *Synapse* 35, 151–159. doi: 10.1002/(SICI)1098-2396(200002)35:2<151::AID-SYN8>3.0.CO;2-P

Alberini, C. M. (2009). Transcription factors in long-term memory and synaptic plasticity. *Physiol. Rev.* 89, 121–145. doi: 10.1152/physrev.00017.2008

Bach, M. E., Barad, M., Son, H., Zhuo, M., Lu, Y. F., Shih, R., et al. (1999). Age-related defects in spatial memory are correlated with defects in the late phase of hippocampal long-term potentiation *in vitro* and are attenuated by drugs that enhance the cAMP signaling pathway. *Proc. Natl. Acad. Sci. U.S.A.* 96, 5280–5285. doi: 10.1073/pnas.96.9.5280

Baeuerle, P. A., and Baltimore, D. (1988a). I kappaB: a specific inhibitor of the NF-kappa B transcription factor. *Science* 242, 540–546. doi: 10.1126/science.3140380

Baeuerle, P. A., and Baltimore, D. (1988b). Activation of DNA-binding activity in an apparently cytoplasmic precursor of the NF-κB transcription factor. *Cell* 53, 211–217. doi: 10.1016/0092-8674(88)90382-0

Baiguera, C., Alghisi, M., Pinna, A., Bellucci, A., de Luca, M. A., Frau, L., et al. (2012). Late-onset Parkinsonism in NFκB/c-Rel-deficient mice. *Brain* 135, 2750–2765. doi: 10.1093/brain/aws193

Bakalkin, G., Yakovleva, T., and Terenius, L. (1994). Prodynorphin gene expression relates to NF-kappa B factors. *Brain Res. Mol. Brain Res.* 24, 301–312. doi: 10.1016/0169-328X(94)90143-0

Barco, A., Patterson, S. L., Alarcon, J. M., Gromova, P., Mata-Roig, M., Morozov, A., et al. (2005). Gene expression profiling of facilitated L-LTP in VP16-CREB mice reveals that BDNF is critical for the maintenance of LTP and its synaptic capture. *Neuron* 48, 123–137. doi: 10.1016/j.neuron.2005.09.005

Benito, E., Valor, L. M., Jimenez-Minchan, M., Huber, W., and Barco, A. (2011). cAMP response element-binding protein is a primary hub of activity-driven neuronal gene expression. *J. Neurosci.* 31, 18237–18250. doi: 10.1523/JNEUROSCI.4554-11.2011

Bernal, G. M., Wahlstrom, J. S., Crawley, C. D., Cahill, K. E., Pytel, P., Liang, H., et al. (2014). Loss of Nfkb1 leads to early onset aging. *Aging* 6, 931–942.

Bhakar, A. L., Tannis, L. L., Zeindler, C., Russo, M. P., Jobin, C., Park, D. S., et al. (2002). Constitutive nuclear factor-κB activity is required for central neuron survival. *J. Neurosci.* 22, 8466–8475.

Bliss, T. V. P., and Lømo, T. (1973). Long-lasting potentiation of synaptic transmission in the dentate area of the anaesthetized rabbit following stimulation of the perforant path. *J. Physiol.* 232, 331–356. doi: 10.1113/jphysiol.1973.sp010273

Boersma, M. C., Dresselhaus, E. C., De Biase, L. M., Mihalas, A. B., Bergles, D. E., and Meffert, M. K. (2011). A requirement for nuclear factor-kappaB in developmental and plasticity-associated synaptogenesis. *J. Neurosci.* 31, 5414–5425. doi: 10.1523/JNEUROSCI.2456-10.2011

Bracchi-Ricard, V., Brambilla, R., Levenson, J., Hu, W.-H., Bramwell, A., Sweatt, J. D., et al. (2008). Astroglial nuclear factor-κB regulates learning and memory and synaptic plasticity in female mice. *J. Neurochem.* 104, 611–623. doi: 10.1111/j.1471-4159.2007.04993.x

Brambilla, R., Bracchi-Ricard, V., Hu, W.-H., Frydel, B., Bramwell, A., Karmally, S., et al. (2005). Inhibition of astroglial nuclear factor κB reduces inflammation and improves functional recovery after spinal cord injury. *J. Exp. Med.* 202, 145–156. doi: 10.1084/jem.20041918

Cebrián, C., Loike, J. D., and Sulzer, D. (2014). Neuronal MHC-I expression and its implications in synaptic function, axonal regeneration and Parkinson's and other brain diseases. *Front. Neuroanat.* 8:114. doi: 10.3389/fnana.2014.00114

Chen, D. Y., Stern, S. A., Garcia-Osta, A., Saunier-Rebori, B., Pollonini, G., Bambah-Mukku, D., et al. (2011). A critical role for IGF-II in memory consolidation and enhancement. *Nature* 469, 491–497. doi: 10.1038/nature09667

Cho, I.-H., Hong, J., Suh, E. C., Kim, J. H., Lee, H., Lee, J. E., et al. (2008). Role of microglial IKKβ in kainic acid-induced hippocampal neuronal cell death. *Brain* 131, 3019–3033. doi: 10.1093/brain/awn230

Clelland, C. D., Choi, M., Romberg, C., Clemenson, G. D. Jr., Fragniere, A., Tyers, P., et al. (2009). A functional role for adult hippocampal neurogenesis in spatial pattern separation. *Science* 325, 210–213. doi: 10.1126/science.1173215

Cox, L. J., Hengst, U., Gurskaya, N. G., Lukyanov, K. A., and Jaffrey, S. R. (2008). Intra-axonal translation and retrograde trafficking of CREB Promotes neuronal survival. *Nat. Cell Biol.* 10, 149–159. doi: 10.1038/ncb1677

Denis-Donini, S., Dellarole, A., Crociara, P., Francese, M. T., Bortolotto, V., Quadrato, G., et al. (2008). Impaired adult neurogenesis associated with short-term memory defects in NF-κB p50-deficient mice. *J. Neurosci.* 28, 3911–3919. doi: 10.1523/JNEUROSCI.0148-08.2008

Dolmetsch, R. E., Xu, K., and Lewis, R. S. (1998). Calcium oscillations increase the efficiency and specificity of gene expression. *Nature* 392, 933–936. doi: 10.1038/31960

Duckworth, E. A. M., Butler, T., Collier, L., Collier, S., and Pennypacker, K. R. (2006). NF-κB protects neurons from ischemic injury after middle cerebral artery occlusion in mice. *Brain Res.* 1088, 167–175. doi: 10.1016/j.brainres.2006.02.103

Fridmacher, V., Kaltschmidt, B., Goudeau, B., Ndiaye, D., Rossi, F. M., Pfeiffer, J., et al. (2003). Forebrain-specific neuronal inhibition of nuclear factor-κB activity leads to loss of neuroprotection. *J. Neurosci.* 23, 9403–9408.

Gobin, S. J. P., van Zutphen, M., Westerheide, S. D., Boss, J. M., and van den Elsen, P. J. (2001). The MHC-specific enhanceosome and its role in MHC Class, I., and β2-microglobulin gene transactivation. *J. Immunol.* 167, 5175–5184. doi: 10.4049/jimmunol.167.9.5175

Guerrini, L., Blasi, F., and Denis-Donini, S. (1995). Synaptic activation of NF-Kappa B by glutamate in cerebellar granule neurons *in vitro*. *Proc. Natl. Acad. Sci. U.S.A.* 92, 9077–9081. doi: 10.1073/pnas.92.20.9077

Hayden, M. S., and Ghosh, S. (2012). NF-κB, the first quarter-century: remarkable progress and outstanding questions. *Genes Dev.* 26, 203–234. doi: 10.1101/gad.183434.111

Herrmann, O., Baumann, B., de Lorenzi, R., Muhammad, S., Zhang, W., Kleesiek, J., et al. (2005). IKK mediates ischemia-induced neuronal death. *Nat. Med.* 11, 1322–1329. doi: 10.1038/nm1323

Hinz, M., Arslan, S. Ç., and Scheidereit, C. (2012). It takes two to tango: IκBs, the multifunctional partners of NF-κB. *Immunol. Rev.* 246, 59–76. doi: 10.1111/j.1600-065X.2012.01102.x

Huh, G. S., Boulanger, L. M., Du, H., Riquelme, P. A., Brotz, T. M., and Shatz, C. J. (2000). Functional requirement for class I MHC in CNS development and plasticity. *Science* 290, 2155–2159. doi: 10.1126/science.290.5499.2155

Imielski, Y., Schwamborn, J. C., Lüningschrör, P., Heimann, P., Holzberg, M., Werner, H., et al. (2012). Regrowing the adult brain: NF-κB controls functional circuit formation and tissue homeostasis in the dentate gyrus. *PLoS ONE* 7:e30838. doi: 10.1371/journal.pone.0030838

Israël, A. (2010). The IKK complex, a central regulator of NF-κB activation. *Cold Spring Harb. Perspect. Biol.* 2:a000158. doi: 10.1101/cshperspect.a000158

Israël, A., Yano, O., Logeat, F., Kieran, M., and Kourilsky, P. (1989). Two purified factors bind to the same sequence in the enhancer of mouse MHC class I genes: one of them is a positive regulator induced upon differentiation of teratocarcinoma cells. *Nucleic Acids Res.* 17, 5245–5257. doi: 10.1093/nar/17.13.5245

Jin, K., Peel, A. L., Mao, X. O., Xie, L., Cottrell, B. A., Henshall, D. C., et al. (2004). Increased hippocampal neurogenesis in alzheimer's disease. *Proc. Natl. Acad. Sci. U.S.A.* 101, 343–347. doi: 10.1073/pnas.2634794100

Jurk, D., Wilson, C., Passos, J. F., Oakley, F., Correia-Melo, C., Greaves, L., et al. (2014). Chronic inflammation induces telomere dysfunction and accelerates ageing in mice. *Nat. Commun.* 2:4172. doi: 10.1038/ncomms5172

Jüttler, E., Inta, I., Eigler, V., Herrmann, O., Maegele, I., Maser-Gluth, C., et al. (2007). Neuronal NF-κB influences thermoregulation and survival in a sepsis model. *J. Neuroimmunol.* 189, 41–49. doi: 10.1016/j.jneuroim.2007.06.020

Kairisalo, M., Korhonen, L., Sepp, M., Pruunsild, P., Kukkonen, J. P., Kivinen, J., et al. (2009). NF-κB-dependent regulation of brain-derived neurotrophic factor in hippocampal neurons by X-linked inhibitor of apoptosis protein. *Eur. J. Neurosci.* 30, 958–966. doi: 10.1111/j.1460-9568.2009.06898.x

Kaltschmidt, B., and Kaltschmidt, C. (2000). Constitutive NF-kappa B activity is modulated via neuron-astroglia interaction. *Exp. Brain Res.* 130, 100–104. doi: 10.1007/s002210050011

Kaltschmidt, B., and Kaltschmidt, C. (2009). NF-κB in the nervous system. *Cold Spring Harb. Perspect. Biol.* 1:a001271. doi: 10.1101/cshperspect.a001271

Kaltschmidt, B., Linker, R. A., Deng, J., and Kaltschmidt, C. (2002). Cyclooxygenase-2 is a neuronal target gene of NF-κB. *BMC Mol. Biol.* 3:16. doi: 10.1186/1471-2199-3-16

Kaltschmidt, B., Ndiaye, D., Korte, M., Pothion, S., Arbibe, L., Prüllage, M., et al. (2006). NF-κB regulates spatial memory formation and synaptic plasticity through protein kinase A/CREB signaling. *Mol. Cell. Biol.* 26, 2936–2946. doi: 10.1128/MCB.26.8.2936-2946.2006

Kaltschmidt, B., Uherek, M., Volk, B., Baeuerle, P. A., and Kaltschmidt, C. (1997). Transcription factor NF-kappaB is activated in primary neurons by amyloid beta peptides and in neurons surrounding early plaques from patients with Alzheimer disease. *Proc. Natl. Acad. Sci. U.S.A.* 94, 2642–2647. doi: 10.1073/pnas.94.6.2642

Kaltschmidt, B., Uherek, M., Wellmann, H., Volk, B., and Kaltschmidt, C. (1999). Inhibition of NF-κB potentiates amyloid β-mediated neuronal apoptosis. *Proc. Natl. Acad. Sci. U.S.A.* 96, 9409–9414.

Kaltschmidt, B., Widera, D., and Kaltschmidt, C. (2005). Signaling via NF-κB in the nervous system. *Biochim. Biophys. Acta* 1745, 287–299.

Kaltschmidt, C., Kaltschmidt, B., and Baeuerle, P. A. (1993). Brain synapses contain inducible forms of the transcription factor NF-kappa, B. *Mech. Dev.* 43, 135–147.

Kaltschmidt, C., Kaltschmidt, B., and Baeuerle, P. A. (1995). Stimulation of ionotropic glutamate receptors activates transcription factor NF-kappa B in primary neurons. *Proc. Natl. Acad. Sci. U.S.A.* 92, 9618–9622. doi: 10.1073/pnas.92.21.9618

Kaltschmidt, C., Kaltschmidt, B., Neumann, H., Wekerle, H., and Baeuerle, P. A. (1994). Constitutive NF-kappa B activity in neurons. *Mol. Cell. Biol.* 14, 3981–3992. doi: 10.1128/MCB.14.6.3981

Kandel, E. R. (2001). The molecular biology of memory storage: a dialogue between genes and synapses. *Science* 294, 1030–1038. doi: 10.1126/science.1067020

Kandel, E. R., Dudai, Y., and Mayford, M. R. (2014). The molecular and systems biology of memory. *Cell* 157, 163–186. doi: 10.1016/j.cell.2014.03.001

Kassed, C. A., and Herkenham, M. (2004). NF-κB p50-deficient mice show reduced anxiety-like behaviors in tests of exploratory drive and anxiety. *Behav. Brain Res.* 154, 577–584. doi: 10.1016/j.bbr.2004.03.026

Kassed, C. A., Willing, A. E., Garbuzova-Davis, S., Sanberg, P. R., and Pennypacker, K. R. (2002). Lack of NF-κB p50 exacerbates degeneration of hippocampal neurons after chemical exposure and impairs learning. *Exp. Neurol.* 176, 277–288. doi: 10.1006/exnr.2002.7967

Klenke, C., Widera, D., Engelen, T., Müller, J., Noll, T., Niehaus, K., et al. (2013). Hsc70 is a novel interactor of NF-kappaB p65 in living hippocampal neurons. *PLoS ONE* 8:e65280. doi: 10.1371/journal.pone.0065280

Krug, M., Lössner, B., and Ott, T. (1984). Anisomycin blocks the late phase of long-term potentiation in the dentate gyrus of freely moving rats. *Brain Res. Bull.* 13, 39–42. doi: 10.1016/0361-9230(84)90005-4

Lattke, M., Magnutzki, A., Walther, P., Wirth, T., and Baumann, B. (2012). Nuclear factor κB activation impairs ependymal ciliogenesis and links neuroinflammation to hydrocephalus formation. *J. Neurosci.* 32, 11511–11523. doi: 10.1523/JNEUROSCI.0182-12.2012

Levenson, J. M., Choi, S., Lee, S.-Y., Cao, Y. A., Ahn, H. J., Worley, K. C., et al. (2004). A bioinformatics analysis of memory consolidation reveals involvement of the transcription factor c-Rel. *J. Neurosci.* 24, 3933–3943. doi: 10.1523/JNEUROSCI.5646-03.2004

Lilienbaum, A., and Israël, A. (2003). From calcium to NF-kappa B signaling pathways in neurons. *Mol. Cell. Biol.* 23, 2680–2698. doi: 10.1128/MCB.23.8.2680-2698.2003

Ma, H., Groth, R. D., Cohen, S. M., Emery, J. F., Li, B., Hoedt, E., et al. (2014). γCaMKII shuttles Ca^{2+}/CaM to the nucleus to trigger CREB phosphorylation and gene expression. *Cell* 159, 281–294. doi: 10.1016/j.cell.2014.09.019

Mantamadiotis, T., Lemberger, T., Bleckmann, S. C., Kern, H., Kretz, O., Martin Villalba, A., et al. (2002). Disruption of CREB function in brain leads to neurodegeneration. *Nat. Genet.* 31, 47–54. doi: 10.1038/ng882

Manuvakhova, M. S., Johnson, G. G., White, M. C., Ananthan, S., Sosa, M., Maddox, C., et al. (2011). Identification of novel small molecule activators of nuclear factor-κB with neuroprotective action via high-throughput screening. *J. Neurosci. Res.* 89, 58–72. doi: 10.1002/jnr.22526

Maqbool, A., Lattke, M., Wirth, T., and Baumann, B. (2013). Sustained, neuron-specific IKK/NF-κB activation generates a selective neuroinflammatory response promoting local neurodegeneration with aging. *Mol. Neurodegener.* 8:40. doi: 10.1186/1750-1326-8-40

Marcora, E., and Kennedy, M. B. (2010). The huntington's disease mutation impairs huntingtin's role in the transport of NF-κB from the synapse to the nucleus. *Hum. Mol. Genet.* 19, 4373–4384. doi: 10.1093/hmg/ddq358

Mayford, M., Siegelbaum, S. A., and Kandel, E. R. (2012). Synapses and memory storage. *Cold Spring Harb. Perspect. Biol.* 4:a005751. doi: 10.1101/cshperspect.a005751

Meberg, P. J., Kinney, W. R., Valcourt, E. G., and Routtenberg, A. (1996). Gene expression of the transcription factor NF-K B in hippocampus: regulation by synaptic activity. *Mol. Brain Res.* 38, 179–190. doi: 10.1016/0169-328X(95)00229-L

Meffert, M. K., Chang, J. M., Wiltgen, B. J., Fanselow, M. S., and Baltimore, D. (2003). NF-kappa B functions in synaptic signaling and behavior. *Nat. Neurosci.* 6, 1072–1078. doi: 10.1038/nn1110

Middleton, G., Hamanoue, M., Enokido, Y., Wyatt, S., Pennica, D., Jaffray, E., et al. (2000). Cytokine-induced nuclear factor kappa B activation promotes the survival of developing neurons. *J. Cell Biol.* 148, 325–332. doi: 10.1083/jcb.148.2.325

Mikenberg, I., Widera, D., Kaus, A., Kaltschmidt, B., and Kaltschmidt, C. (2007). Transcription factor NF-κB is transported to the nucleus via cytoplasmic dynein/dynactin motor complex in hippocampal neurons. *PLoS ONE* 2:e589. doi: 10.1371/journal.pone.0000589

Nafez, S., Oikawa, K., Odero, G. L., Sproule, M., Ge, N., Schapansky, J., et al. (2015). Early growth response 2 (Egr-2) expression is triggered by NF-κB activation. *Mol. Cell. Neurosci.* 64, 95–103. doi: 10.1016/j.mcn.2014.12.008

Nickols, J. C., Valentine, W., Kanwal, S., and Carter, B. D. (2003). Activation of the transcription factor NF-κB in Schwann cells is required for peripheral myelin formation. *Nat. Neurosci.* 6, 161–167. doi: 10.1038/nn995

Niederberger, E., Schmidtko, A., Gao, W., Kühlein, H., Ehnert, C., and Geisslinger, G. (2007). Impaired acute and inflammatory nociception in mice lacking the p50 subunit of NF-κB. *Eur. J. Pharmacol.* 559, 55–60. doi: 10.1016/j.ejphar.2006.11.074

Ogryzko, V. V., Schiltz, R. L., Russanova, V., Howard, B. H., and Nakatani, Y. (1996). The transcriptional coactivators p300 and CBP are histone acetyltransferases. *Cell* 87, 953–959. doi: 10.1016/S0092-8674(00)82001-2

Oikawa, K., Odero, G. L., Platt, E., Neuendorff, M., Hatherell, A., Bernstein, M. J., et al. (2012). NF-κB p50 subunit knockout impairs late LTP and alters long term memory in the mouse hippocampus. *BMC Neurosci.* 13:45. doi: 10.1186/1471-2202-13-45

O'Mahony, A., Raber, J., Montano, M., Foehr, E., Han, V., Lu, S., et al. (2006). NF-κB/Rel regulates inhibitory and excitatory neuronal function and synaptic plasticity. *Mol. Cell. Biol.* 26, 7283–7298. doi: 10.1128/MCB.00510-06

O'Riordan, K. J., Huang, I. C., Pizzi, M., Spano, P., Boroni, F., Egli, R., et al. (2006). Regulation of nuclear factor κB in the hippocampus by group I metabotropic glutamate receptors. *J. Neurosci.* 26, 4870–4879. doi: 10.1523/JNEUROSCI.4527-05.2006

Pascual-Lucas, M., Viana da Silva, S., Di Scala, M., Garcia-Barroso, C., González-Aseguinolaza, G., Mulle, C., et al. (2014). Insulin-like growth factor 2 reverses memory and synaptic deficits in APP transgenic mice. *EMBO Mol. Med.* 6, 1246–1262. doi: 10.15252/emmm.201404228

Pizzi, M., Goffi, F., Boroni, F., Benarese, M., Perkins, S. E., Liou, H.-C., et al. (2002). Opposing roles for NF-κB/Rel factors p65 and c-Rel in the modulation of neuron survival elicited by glutamate and interleukin-1β. *J. Biol. Chem.* 277, 20717–20723. doi: 10.1074/jbc.M201014200

Ramirez, S., Tonegawa, S., and Liu, X. (2014). Identification and optogenetic manipulation of memory engrams in the hippocampus. *Front. Behav. Neurosci.* 7:226. doi: 10.3389/fnbeh.2013.00226

Redondo, R. L., and Morris, R. G. (2011). Making memories last: the synaptic tagging and capture hypothesis. *Nat. Rev. Neurosci.* 1, 17–30. doi: 10.1038/nrn2963

Ryan, T. J., Roy, D. S., Pignatelli, M., Arons, A., and Tonegawa, S. (2015). Engram cells retain memory under retrograde amnesia. *Science* 348, 1007–1013. doi: 10.1126/science.aaa5542

Schmeisser, M. J., Baumann, B., Johannsen, S., Vindedal, G. F., Jensen, V., Hvalby, Ø. C., et al. (2012). IκB kinase/nuclear factor κB-dependent insulin-like growth factor 2 (Igf2) expression regulates synapse formation and spine maturation via Igf2 receptor signaling. *J. Neurosci.* 32, 5688–5703. doi: 10.1523/JNEUROSCI.0111-12.2012

Schmidt-Ullrich, R., Mémet, S., Lilienbaum, A., Feuillard, J., Raphaël, M., and Israel, A. (1996). NF-kappaB activity in transgenic mice: developmental regulation and tissue specificity. *Development* 122, 2117–2128.

Schneider, A., Martin-Villalba, A., Weih, F., Vogel, J., Wirth, T., and Schwaninger, M. (1999). NF-κB is activated and promotes cell death in focal cerebral ischemia. *Nat. Med.* 5, 554–559. doi: 10.1038/6458

Schulz, S., Siemer, H., Krug, M., and Höllt, V. (1999). Direct evidence for biphasic cAMP responsive element-binding protein phosphorylation during long-term potentiation in the rat dentate gyrus *in vivo*. *J. Neurosci.* 19, 5683–5692.

Semon, R. (1920). *Die Mneme*. Leipzig: Verlag von Wilhelm Engelmann. 4. und 5. Auflage.

Sen, R., and Baltimore, D. (1986). Inducibility of kappa immunoglobulin enhancer-binding protein Nf-kappa B by a posttranslational mechanism. *Cell* 47, 921–928. doi: 10.1016/0092-8674(86)90807-X

Sheng, M., Thompson, M. A., and Greenberg, M. E. (1991). CREB: a $Ca^{(2+)}$-regulated transcription factor phosphorylated by calmodulin-dependent kinases. *Science* 252, 1427–1430. doi: 10.1126/science.1646483

Shrum, C. K., Defrancisco, D., and Meffert, M. K. (2009). Stimulated nuclear translocation of NF-kappaB and shuttling differentially depend on dynein and the dynactin complex. *Proc. Natl. Acad. Sci. U.S.A.* 106, 2647–2652. doi: 10.1073/pnas.0806677106

Simpson, C. S., and Morris, B. J. (1999). Activation of nuclear factor κB by nitric oxide in rat striatal neurones. *J. Neurochem.* 73, 353–361. doi: 10.1046/j.1471-4159.1999.0730353.x

Sol Fustiñana, M., de la Fuente, V., Federman, N., Freudenthal, R., and Romano, A. (2014). Protein degradation by ubiquitin-proteasome system in formation and labilization of contextual conditioning memory. *Learn. Mem.* 21, 478–487. doi: 10.1101/lm.035998.114

van Loo, G., De Lorenzi, R., Schmidt, H., Huth, M., Mildner, A., Schmidt-Supprian, M., et al. (2006). Inhibition of transcription factor NF-κB in the central nervous system ameliorates autoimmune encephalomyelitis in mice. *Nat. Immunol.* 7, 954–961. doi: 10.1038/ni1372

Vaquerizas, J. M., Kummerfeld, S. K., Teichmann, S. A., and Luscombe, N. M. (2009). A census of human transcription factors: function, expression and evolution. *Nat. Rev. Genet.* 10, 252–263. doi: 10.1038/nrg2538

Wellmann, H., Kaltschmidt, B., and Kaltschmidt, C. (2001). Retrograde transport of transcription factor NF-κB in living neurons. *J. Biol. Chem.* 276, 11821–11829. doi: 10.1074/jbc.M009253200

West, A. E., Griffith, E. C., and Greenberg, M. E. (2002). Regulation of transcription factors by neuronal activity. *Nat. Rev. Neurosci.* 3, 921–931. doi: 10.1038/nrn987

Widera, D., Müller, J., Imielski, Y., Heimann, P., Kaltschmidt, C., and Kaltschmidt, B. (2014). Methods for the modulation and analysis of NF-κB-dependent adult neurogenesis. *J. Vis. Exp.* 84:e50870. doi: 10.3791/50870 doi: 10.3791/50870

Yang, J., Hawkins, O. E., Barham, W., Gilchuk, P., Boothby, M., Ayers, G. D., et al. (2014). Myeloid IKKβ promotes antitumor immunity by modulating CCL11 and the innate immune response. *Cancer Res.* 74, 7274–7284. doi: 10.1158/0008-5472.CAN-14-1091

Yu, Z., Zhou, D., Bruce-Keller, A. J., Kindy, M. S., and Mattson, M. P. (1999). Lack of the p50 subunit of nuclear factor-κb increases the vulnerability of hippocampal neurons to excitotoxic injury. *J. Neurosci.* 19, 8856–8865.

Yu, Z., Zhou, D., Cheng, G., and Mattson, M. P. (2000). Neuroprotective role for the p50 subunit of NF-κB in an experimental model of Huntington's disease. *J. Mol. Neurosci.* 15, 31–44. doi: 10.1385/JMN:15:1:31

Zhang, G., Li, J., Purkayastha, S., Tang, Y., Zhang, H., Yin, Y., et al. (2013). Hypothalamic programming of systemic aging involving IKKβ/NF-κB and GnRH. *Nature* 497, 211–216. doi: 10.1038/nature12143

Zhang, Y., Liu, J., Yao, S., Li, F., Xin, L., Lai, M., et al. (2012). Nuclear factor kappa B signaling initiates early differentiation of neural stem cells. *Stem Cells* 30, 510–524. doi: 10.1002/stem.1006

Conflict of Interest Statement: The authors declare that the research was conducted in the absence of any commercial or financial relationships that could be construed as a potential conflict of interest.

frontiers in Molecular Neuroscience

REVIEW
published: 26 August 2015
doi: 10.3389/fnmol.2015.00046

A new perspective on the role of the CREB family of transcription factors in memory consolidation via adult hippocampal neurogenesis

*Sylvia Ortega-Martínez**

Turku Centre for Biotechnology, Åbo Akademi University and University of Turku, Turku, Finland

Adult neurogenesis is the process by which new neurons are generated in the brains of adults. Since its discovery 50 years ago, adult neurogenesis has been widely studied in the mammalian brain and has provided a new perspective on the pathophysiology of many psychiatric and neurodegenerative disorders, some of which affect memory. In this regard, adult hippocampal neurogenesis (AHN), which occurs in the subgranular zone (SGZ) of the dentate gyrus (DG), has been suggested to play a role in the formation and consolidation of new memories. This process involves many transcription factors, of which cyclic AMP (cAMP)-responsive element-binding protein (CREB) is a well-documented one. In the developing brain, CREB regulates crucial cell stages (e.g., proliferation, differentiation, and survival), and in the adult brain, it participates in neuronal plasticity, learning, and memory. In addition, new evidence supports the hypothesis that CREB may also participate in learning and memory through its involvement in AHN. This review examines the CREB family of transcription factors, including the different members and known signaling pathways. It highlights the role of CREB as a modulator of AHN, which could underlie its function in memory consolidation mechanisms.

Keywords: adults, mammals, cyclic AMP-responsive element-binding protein, hippocampus, memory, neurogenesis, neuronal plasticity, transcription factors

OPEN ACCESS

Edited by:
Benedict C. Albensi, University of Manitoba, Canada

Reviewed by:
John Oberdick, The Ohio State University, USA
Baojin Ding, University of Massachusetts Medical School, USA

***Correspondence:**
Sylvia Ortega-Martínez, Turku Centre for Biotechnology, Åbo Akademi University and University of Turku, Tykistokatu 6, FI-20520 Turku, Finland
sylviaortegamartinez@gmail.com

Received: *16 February 2015*
Accepted: *11 August 2015*
Published: *26 August 2015*

Citation:
Ortega-Martínez S (2015) A new perspective on the role of the CREB family of transcription factors in memory consolidation via adult hippocampal neurogenesis. Front. Mol. Neurosci. 8:46. doi: 10.3389/fnmol.2015.00046

The CREB Family of Transcription Factors

Cyclic AMP (cAMP)-responsive element-binding protein (CREB) belongs to the family of leucine zipper transcription factors, which are expressed in a variety of tissues (Yamashima, 2012). In 1986, Marc Montminy and R.H. Goodman first defined cAMP response element (CRE) as a conserved DNA sequence in promoter elements that were activated by cAMP. One or several copies of CRE are present within the regulatory regions of genes. Binding of different transcription factors to CRE regulates RNA polymerase activity, thereby controlling gene expression. A year after CREB was defined, Montminy and Bilezikjian (1987) described CREB as a cellular transcription factor that binds CRE and induces transcription of the somatostatin gene.

The CREB family of transcription factors is now known to include CREB, CRE modulator (CREM), and activating transcription factor-1 (ATF-1). This family belongs to the superfamily of

Abbreviations: CREB, cAMP-responsive element-binding protein; AHN, adult hippocampal neurogenesis; DG, dentate gyrus; SGZ, subgranular zone; SVZ, subventricular zone; KID, central kinase-inducible domain.

basic region/leucine zipper (bZIP) transcriptional regulators, and all its members mediate cAMP-responsive transcription. CREB and ATF-1 are expressed ubiquitously, whereas CREM is mainly expressed in the neuroendocrine system. Each transcription factor is encoded by a single gene and contains the highly conserved leucine zipper sequence with an adjacent basic region that binds to a CRE DNA sequence. Members of the CREB family also have a regulatory central kinase-inducible domain (KID), although the Q1 and Q2 glutamine-rich regions adjacent to KID are less conserved among different family members (see review Barco et al., 2003).

Creb1 is the gene responsible for transcription of all known CREB isoforms; the α isoform is the most common, but the β and Δ isoforms are also transcribed. Several approaches have been used to clarify the roles of different CREB isoforms. One study assessed CRE-DNA binding in nuclear extracts obtained from several brain regions of wild-type and CREBΔ/α mutant mice. The results suggested that CRE-DNA–binding complexes contain both CREB and CREM proteins. However, CRE-DNA binding was abolished in the cortex, hippocampus, cerebellum, and amygdala of CREBΔ/α mutant mice. Because these transgenic animals lack CREBΔ and α isoforms, the expression of other forms of CREB, such as CREB-β and CREM, is upregulated. The findings indicate that CREM binding to CRE sites requires the presence of CREBΔ/α, and that CREB-β may not efficiently bind to CRE sites (Pandey et al., 2000). In addition, mice lacking the α and Δ CREB proteins have abnormal long-term, but not short-term memory (STM), indicating that these isoforms are essential for the role of CREB in long-term memory (LTM; Bourtchuladze et al., 1994). In contrast to previous classical studies in adult mice, some studies have focused on the effect of these isoforms on neocortical plasticity in young mice to highlight the age-dependent role of CREB in neuroplasticity. In one of these studies, the CREBα/Δ mutation did not affect plasticity in cortical layers II/III of the younger adolescent mice (1–2 months) indicating that different plasticity processes occur at this age. In the same model, CREBβ expression was upregulated in the barrel cortex of CREBα/Δ knock-out animals, suggesting that this subunit may partly compensate for the loss of the α/Δ isoforms in the young mice. Overall, the study results suggested that CREB isoforms play a role in experience-dependent plasticity in the adult neocortex (Glazewski et al., 1999).

The *Creb1* gene has a complex structure with multiple exons and introns that result in several alternatively spliced mRNAs encoding proteins with distinct transcription-activating or transcription-repressing properties. However, two structural features are present in most members of the CREB family: (a) the well-conserved bZIP domain at the C-terminus, which facilitates dimerization between different family members and participates in the recognition of and binding to CRE sites; and (b) KID (mentioned above), which encloses sites for phosphorylation by protein kinase A (PKA) and other kinases. KID is delineated by two glutamine-rich domains (Q1 and Q2), which are responsible for basal transactivation activity. Q2 connects with TAF_{II} 130 (TBP [TATA-binding protein]-associated $factor_{II}$ 130) and recruits the transcription machinery to the promoter region. Constitutive (Q2) and inducible (KID) domains work together in response to different stimuli that trigger CREB-dependent gene expression (see review Barco et al., 2003). Transcription factors of the CREB family exert their actions as homodimers or heterodimers, but the CREB-CREB homodimer is the most potent transcriptional activator (Dworkin and Mantamadiotis, 2010). CREB isoforms are widely distributed in the adult mouse brain under homeostatic conditions and remain inactive when bound to CRE elements within target gene promoters (Nichols et al., 1992).

The transcriptional activity of CREB depends on its phosphorylation status, which is determined by the opposing actions of protein kinases and phosphatases. Phosphorylation is a key mechanism in signaling and has been described to regulate several processes such as the cell cycle (Liu et al., 2014), cell death (Martin, 2010), DNA damage (Abreu et al., 2013) and neurogenesis (Faigle and Song, 2013). For example, increase in intracellular calcium (Ca^{2+}) levels through voltage- and ligand-dependent channels results in increased cAMP levels via activation of G-protein-coupled receptors. Growth factors can also activate receptor tyrosine kinases to augment cAMP levels. All these pathways affect CREB phosphorylation levels. Downstream of neuronal activity, the PKA, mitogen-activated protein kinase (RSK [p90 ribosomal protein S6 kinase]/MAPK), and CaMKIV (Ca^{2+}/calmodulin-dependent protein kinase IV) kinase pathways result in CREB phosphorylation at Ser133. PP-1 (protein phosphatase-1) and PP2-A are the major CREB phosphatases, and Ca^{2+}-dependent signals can induce intracellular events that lead to phosphorylation or dephosphorylation. The effect of stimulation depends on the nature of the stimulus and its cellular context. For example, activation of *N*-methyl-D-aspartate (NMDA) receptors leads to CREB dephosphorylation in extrasynaptic neurons, while in synaptic sites, it leads to CREB phosphorylation and CREB-dependent gene expression (Ghiani et al., 2007).

The phosphorylation of a serine residue (S133) in KID regulates CREB activity. This phosphorylation establishes an effector role for CREB, initiating the translation of extracellular stimuli into gene expression (Yamashima, 2012). Indeed, CREB phosphorylation facilitates signal transduction, and molecules responsible for its phosphorylation/dephosphorylation are, therefore, highly relevant as modulators of the target gene status. There are a number of signaling cascades upstream of CREB phosphorylation, such as the cAMP pathway (Montminy and Bilezikjian, 1987), and protein kinase pathways (e.g., PKA and CaMKII and IV; Yamashima, 2012). These cascades are activated by stress, inflammatory cytokine activity (MAPK or phosphoinositide 3-kinase (PI3)/Akt pathways; Yamashima, 2012), growth factor/receptor tyrosine kinase activity (Ras/Erk/RSK2 pathway; Ghosh et al., 1994), and phospholipase C (PLC)-PKC signaling (see **Figure 1**). All these cascades have been shown to induce CREB phosphorylation (Du and Montminy, 1998; Lonze and Ginty, 2002). For example, CREB phosphorylation is facilitated by membrane-bound NMDA receptors (Ghiani et al., 2007), the non-receptor tyrosine protein kinase

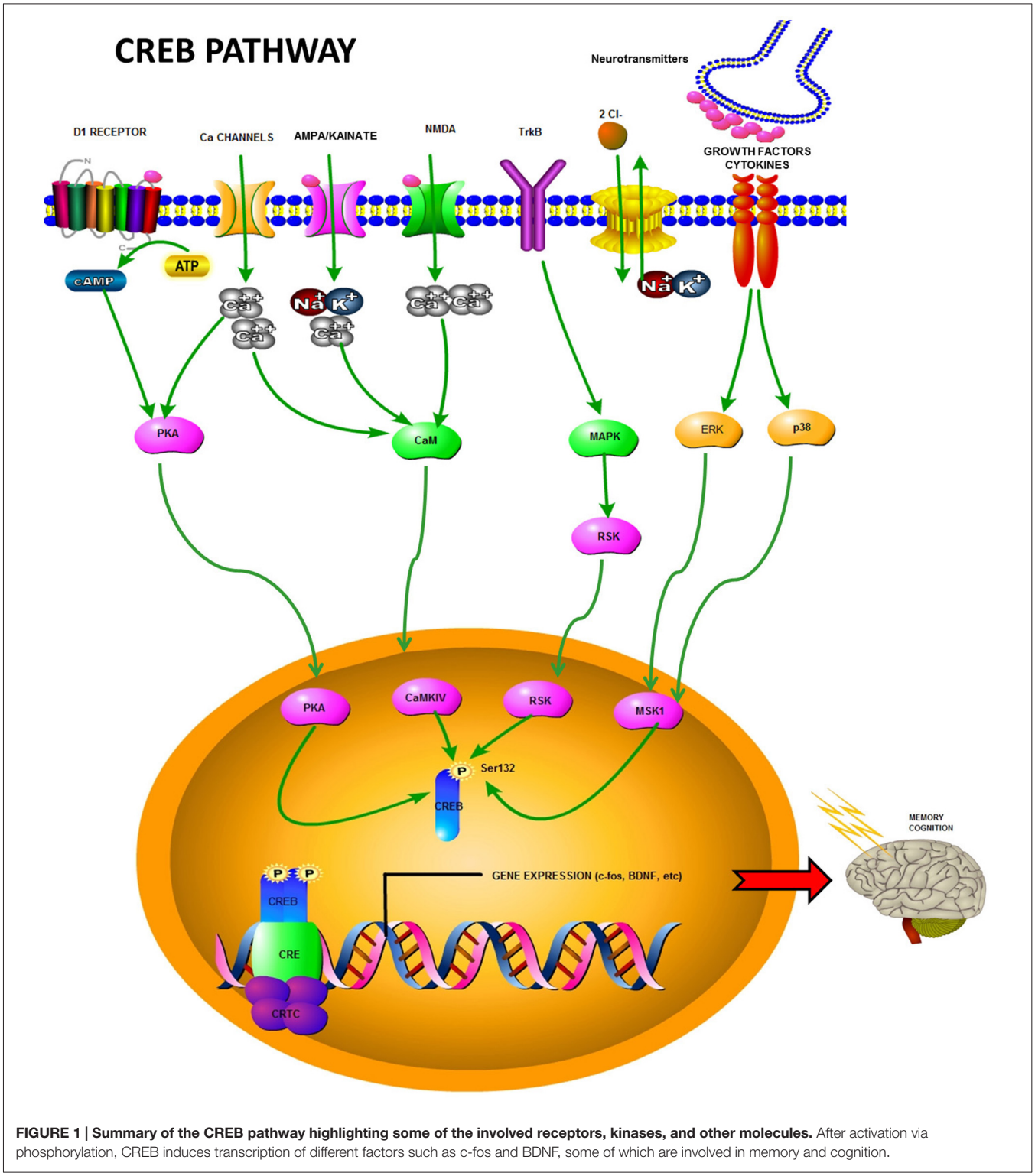

FIGURE 1 | Summary of the CREB pathway highlighting some of the involved receptors, kinases, and other molecules. After activation via phosphorylation, CREB induces transcription of different factors such as c-fos and BDNF, some of which are involved in memory and cognition.

c-Src (Zhao et al., 2003a), fibroblast growth factor receptor 1 (FGFR1; Hu et al., 2004), and estrogen receptors (Sharma et al., 2007), all of which are part of distinct intracellular cascades. The molecules involved in the modulation of CREB phosphorylation include several neurotransmitters [e.g., dopamine, glutamate, serotonin, gamma-aminobutyric acid (GABA)], growth factors (e.g., insulin-like growth factor 1 IGF-1; vascular endothelial growth factor, VEGF), and neurotrophins (brain-derived neurotrophic factor, BDNF; Yamashima, 2012). A summary of CREB pathways is depicted in **Figure 1**.

CREB-mediated transcription requires CREB phosphorylation, but the latter is not a reliable predictor of target gene activation; additional regulatory processes are required for the engagement of transcriptional promoter elements. For example, clustering of CBP (CREB-binding protein) has recently been described as crucial, and the CBP paralog p300 enhances CREB functionality. CBP and p300 are both chromatin remodelers (histone acetyltransferases) involved in unwinding promoter chromatin and providing the RNA polymerase II (Pol II) transcription machinery access to promoter DNA (Chan and La Thangue, 2001). If CBP/p300 does not cluster at a gene promoter after CREB phosphorylation, the gene remains transcriptionally silent (Merz et al., 2011). Thus, many co-factors, including some that are directly affected by neuronal activity and growth factors, influence CREB-mediated regulation at the final stage (Merz et al., 2011). This allows CREB signaling to control expression of a variety of target genes.

CREB was first isolated from undifferentiated neuron-like PC12 cells (Montminy and Bilezikjian, 1987) and from the mouse brain (Yamamoto et al., 1988). Interest in CREB's role in the nervous system has increased in the last few decades, and it has been proposed to be a key regulator of several complex processes ranging from development to plasticity (Yamashima, 2012). For example, CREB has been postulated as a regulator of cell survival, proliferation, and differentiation in the developing brain, whereas its roles in the adult brain include learning, memory, and neuronal plasticity (Yamashima, 2012). It is a key molecule involved in LTM in the majority of species (Bourtchuladze et al., 1994; Yin et al., 1994).

CREB participation in memory processes has been widely analyzed using animal models ranging from nematodes to higher mammals. The use of different CREB-mutant mice has been one of the most important approaches in elucidating CREB's role in these memory processes (see review Kida, 2012). CREB has been implicated in the regulation of embryonic and adult neurogenesis (Dworkin et al., 2009). Both neurogenesis and memory, which have been shown to be highly related, constitute an important field of research (see **Figure 2**). It is widely accepted that adult neurogenesis is involved in memory consolidation and pattern separation, and impairment of these processes has been described in various diseases associated with memory loss, including Alzheimer's disease (AD; Taupin, 2009; Braun and Jessberger, 2014; Fitzsimons et al., 2014; Cameron and Glover, 2015).

Current Understanding of CREB, Neurogenesis, and Memory

There were fewer scientific publications on CREB until the 1990s after which the number of publications on this topic have increased. This rise has been accompanied by an exponential increase in publications on learning and memory. Although memory and learning have been studied for a long time, only recent advances in molecular and cellular techniques have enabled researchers to investigate the mechanisms underlying these processes. These advances have permitted the study of complex events such as gene expression in greater detail. Considering that the DNA helix was discovered in 1953, transcription factors (e.g., CREB) are relatively new concepts. Moreover, ideas about neurogenesis have evolved since its discovery 50 years ago (**Figure 2**).

This review focuses on the most relevant and recent studies on CREB's role in memory regulation and its participation in neurogenic processes. CREB influences cognitive processes directly by affecting memory and indirectly by affecting adult hippocampal neurogenic capacity. CREB's affects memory consolidation through its regulation of adult hippocampal neurogenesis (AHN), which mainly occurs in the hippocampal subgranular zone (SGZ) of the dentate gyrus (DG). This mechanism provides a novel perspective on memory consolidation within the adult hippocampus.

Adult Neurogenesis

The existence of "adult neurogenesis" in mammals was first confirmed 50 years ago (Altman and Das, 1965). Adult neurogenesis refers to the generation of new neurons in the adult brain. Despite its importance, this emergent concept remained obscure until neurogenesis was found to occur in the brain of adult humans (Eriksson et al., 1998). Neurogenesis was traditionally understood to be mainly an embryogenetic phenomenon, but new research has shown the generation of new nerve cells in several areas of the adult brain, including the DG, subventricular zone (SVZ), olfactory bulb (OB), and other areas where it was recently observed (e.g., the cortex and hypothalamus (Gould, 2007). Adult neurogenesis involves cell proliferation, survival, and cell differentiation. AHN, which occurs for specific brain functions, involves not only new neuron formation but also integration of these new-born neurons into functional networks. From this perspective, AHN facilitates memory consolidation via formation of networks (Deng et al., 2010; Weisz and Argibay, 2012). Furthermore, AHN provides plasticity required in memory processes and allows for "pattern separation mechanisms," which is crucial for memory consolidation (Bruel-Jungerman et al., 2007; Sahay et al., 2011a; Bekinschtein et al., 2013; Yassa and Reagh, 2013). It is critical to understand this phenomenon because neurogenesis also occurs after brain injury or during brain alteration (e.g., epilepsy); however, in these cases, it is a non-functional process as it is not related with their normal brain function and does not involve wiring of new neurons into networks (Zhang et al., 2014).

AHN and Memory

In the adult brain, neural stem cells (NSCs) are found in the SGZ, a specific DG subregion (Fanselow and Dong, 2010). These NSCs give rise to new neurons, which are incorporated as new granule cells into hippocampal networks. These networks contribute to learning (Zhao et al., 2003b; Joiner, 2009; Zhang et al., 2009) and memory (van Praag et al., 1999, 2002). In contrast, the ventral DG hippocampus (ventral SGZ) has been implicated in emotion-related disorders (Fanselow and Dong, 2010), including stress, depression, and anxiety. Studies on the types of memories related to AHN have highlighted its role in trace fear conditioning, recognition, spatial memory, pattern

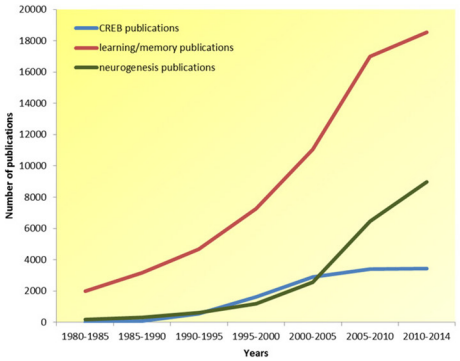

Years	CREB publications	learning/memory publications	neurogenesis publications
1980-1985	0	1979	164
1985-1990	63	3151	319
1990-1995	537	4682	617
1995-2000	1610	7275	1179
2000-2005	2909	11071	2544
2005-2010	3403	16989	6469
2010-2014	3441	18557	8962

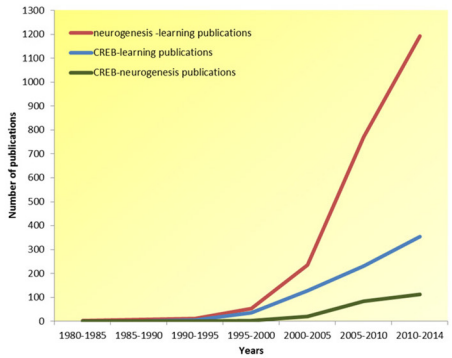

Years	neurogenesis -learning publications	CREB-learning publications	CREB-neurogenesis publications
1980-1985	2	0	0
1985-1990	7	0	0
1990-1995	12	4	0
1995-2000	53	36	3
2000-2005	236	128	21
2005-2010	770	232	85
2010-2014	1192	354	113

FIGURE 2 | Article publication trend in the last 34 years (1980–2014). In over three decades, there has been an exponential increase in the number of publications addressing all topics of interest here (i.e., CREB, learning-memory and neurogenesis), as well as publications addressing the confluence of these interrelated topics (i.e., neurogenesis-learning, CREB-learning, and CREB-neurogenesis), pointing to the scientific recognition of these topic's mutual relevance.

separation, and non-mnemonic tasks (reviewed in Cameron and Glover, 2015).

Numerous studies have focused on the relationship between AHN and BDNF. It is widely accepted that BDNF stimulates neurogenesis (Zhang et al., 2011) and is expressed solely in the hippocampus with no additional sources from the peripheral blood. Increased BDNF levels have been shown to enhance hippocampal neurogenic capacity, resulting in improvements in hippocampus-dependent memory (Hsiao et al., 2014). The effects of voluntary exercise and enriched environments on BDNF levels and adult neurogenesis have also been widely studied (Bekinschtein et al., 2011; Yu et al., 2014). IGF-1, another growth factor involved in the BDNF pathway, was also found to affect AHN. Exercise increases IGF-1 levels, which leads to increments in AHN with subsequent improvements in memory and learning. Serotonin and noradrenaline release also upregulate BDNF, explaining the high BDNF levels and neurogenesis following antidepressant treatment (Albert and Benkelfat, 2013).

In summary, adult neurogenesis is considered essential for memory consolidation. Recently, neurogenesis has been discovered to occur in more brain areas; however, memory-related neurogenesis primarily occurs in the DG of the hippocampus and OB. The adult hippocampus has been widely studied for its role in the development of numerous neurodegenerative and neuropsychiatric disorders characterized by decreased AHN. Because hippocampus-dependent memory processes are altered in such diseases, understanding the underlying molecular mechanisms is important for restoring normal brain function. Indeed, some recent drug discovery efforts have focused on increasing AHN.

AHN and Olfaction

Neurogenesis attributed to the SVZ, the largest neurogenic niche, is also responsible for generating astrocytes, oligodendrocytes, and OB interneurons (Lois and Alvarez-Buylla, 1994); which are involved in "olfactory memory" (enhanced odor differentiation; Sahay et al., 2011b). In fact, a reduction in the generation of olfactory interneurons during adulthood is associated with a decreased ability to discriminate odors (Gheusi et al., 2000). Considering that humans have poor olfactory memory, the role of AHN in olfaction in humans needs to further explored.

CREB and Adult Hippocampal Neurogenesis

AHN is a highly regulated process, and several transcription factors have been reported to be involved in this regulation (Hodge and Hevner, 2011). In this regard, the role of CREB in AHN process has been widely investigated. The

presence of phosphorylated CREB (pCREB) has been found in many new-born immature neurons in the most important neurogenic niches, including the DG in the SGZ (Nakagawa et al., 2002a,b; Jagasia et al., 2009), SVZ, and OB system (Giachino et al., 2005; Herold et al., 2011). CREB activation in the DG resulting in postnatal hippocampal neurogenesis was first reported in Young et al. (1999). Jagasia et al. (2009) found that CREB expression in the DG persists for 3–21 days after cell generation and overlaps with doublecortin (DCX) expression. DCX is a microtubule-associated protein characteristic of immature neurons and precursor cells. The expression of pCREB subsided with the emergence of mature neuronal markers such as calbindin in mature granule cells (Jagasia et al., 2009) or NeuN in the SVZ/OB neurogenic system, where pCREB presence declines along a rostral-to-caudal gradient (Giachino et al., 2005; Herold et al., 2011).

CREB signaling in adult neurogenesis has been widely studied using *in vivo* and *in vitro* approaches. Two groups used rolipram, an inhibitor of phosphodiesterase-4-enhancing CREB signaling, (Nakagawa et al., 2002b; Fujioka et al., 2004) to examine CREB function *in vivo*; they reported an increase in different parameters of adult neurogenesis in the SGZ, including a higher survival rate of new neurons, more precursor cell proliferation, and enhanced neurite outgrowth and dendritic branching (Merz et al., 2011). CREB/CREM signaling has been described as crucial for survival of adult-born neurons. The positive effects of CREB in AHN were inhibited when CREB expression was repressed. In addition, Giachino et al. (2005) reported a significant decrease in number of newborn cells in the OB of transgenic CREM-null knockout mice. Other studies have shown that rolipram's effects on the morphology of immature and mature neurons in the adult hippocampal DG were eradicated when CREB signaling was repressed by expressing a dominant-negative CREB inhibitor (Fujioka et al., 2004).

The role of CREB signaling in neuronal activation and during survival stages of neurogenesis is better understood than its effects on cell migration and proliferation (Dworkin and Mantamadiotis, 2010). In addition, the pharmacological and genetic approaches used to study the relationship between CREB and AHN do not only affect newborn neurons. Therefore, whether CREB signaling exerts its action by controlling NSCs/new neurons or altering the neurogenic context is an open question warranting further research.

Glucocorticoids are widely considered to negatively influence adult neurogenesis. For example, dexamethasone given at postnatal day 6, a crucial point in the generation of hippocampal neural precursors that survive in the adult brain (Ortega-Martinez, 2015; Ortega-Martínez and Trejo, 2015), suppresses AHN, decreases cell proliferation, and induces behavioral impairments (e.g., learning deficits and increased anxiety; Ortega-Martinez, 2015; Ortega-Martínez and Trejo, 2015). Notably, increased levels of corticosterone, which is known to decrease neural precursor cell proliferation and contribute to neuronal atrophy, were also correlated with lower pCREB levels (Yu et al., 2004).

Various studies have demonstrated that inhibition of CREB signaling with the dominant-negative CREB inhibitor A-CREB (Ahn et al., 1998; Herold et al., 2011) significantly decreases newborn cell survival (Jagasia et al., 2009). New cells showed loss of expression of DCX and Pax6 transcription factor (both of which are related to cell maturity), impairments in rostral migratory stream (RMS) migration, decreased cell proliferation and survival, and increased morphological defects in newborn OB cells (Herold et al., 2011; Merz et al., 2011). The effects of CREB-signaling suppression show that this pathway is crucial for proliferation, differentiation, survival, maturation, and functionality in adult neurogenesis sites (mainly the OB, SVZ, and DG; Merz et al., 2011).

These assumptions are also pertinent to *in vivo* experiments that have described how CREB signaling affects proliferation of NSC precursors enhancing this cellular mechanism (Kim et al., 2002; Dworkin et al., 2009; Grimm et al., 2009; Merz et al., 2011).

The epigenetic mechanisms of DNA methylation has also been shown to regulate CREB signaling. The CRE sequence contains a CpG island that can be methylated; methylation inhibits binding and restricts CREB localization to functional sites (Zhang et al., 2005). Furthermore, neuronal activity regulates DNA methylation via different enzymes such as DNA-demethylase Gadd5b, suggesting a new link between CREB signaling and neuronal activity, which may be important in adult neurogenesis (Ma et al., 2009).

Another mechanism by which CREB can regulate neurogenesis is by affecting crucial microRNAs (s). miRNAs are ncRNAs (non-coding RNAs) that generally contain 19–23 nucleotides and regulate translation through one of two mechanisms: degradation of target mRNAs or inhibition of the translation machinery (Merz et al., 2011). miRNAs are known to control both precursor cell survival and differentiation in adult neurogenesis. Notably, CREB controls the expression of both MeCP2 (Klein et al., 2007; Chahrour et al., 2008). miRNA-132, which is a member of a cluster of miRNAs enhanced by neuronal activity (Fiore et al., 2009), participates in neuronal morphogenesis, and regulates cognitive capacity (Vo et al., 2005; Hansen et al., 2013). miRNA-134 regulates CREB post-transcriptionally (Gao et al., 2010). In addition, factors known to regulate the proliferation of neural precursor cells (e.g., Wnt; Hirsch et al., 2007; Dworkin and Mantamadiotis, 2010) have been shown to enhance CREB signaling (Chen et al., 2005) in cultured cortical neurons (Vo et al., 2005).

All of the factors described above activate or inhibit CREB signaling, with or without affecting gene expression. Among the molecules related to adult neurogenesis that are also affected by CREB signaling, it is important to highlight the following: BDNF (Kida, 2012; Sable et al., 2014), prolactin (Wang et al., 2013), bcl-2 (Fujii et al., 2014), polysialylated neuronal cell adhesion molecule (PSA-NCAM; Park et al., 2004; NGF; Lim et al., 2014), and cyclin D2 (Kowalczyk et al., 2004; White et al., 2006).

One hypothesis regarding the influence of CREB on adult neurogenesis comes from a recent study that focused on polyunsaturated fatty acid (PUFA)-GPR40-CREB signaling (Yamashima, 2012). The authors showed that primate neurons

possess a PUFA-GPR40-CREB-signaling pathway that exerts its action in adult newborn neurons by enhancing the synthesis of BDNF and PSA-NCAM, both of which are implicated in adult neurogenesis (Yamashima, 2012).

A recent review discussed the functional roles of CREB as a positive regulator in the formation and enhancement of memory (Kida and Serita, 2014). Different genetic models used for the study of CREB function were analyzed. Interestingly, some of the findings are in accordance with the new perspective of CREB modulation of memory via its role in adult neurogenesis. In this regard, several transgenic lines of CREB mice such as CREB-VP16, Y134F and DIEDML, which show enhanced STM, also exhibit upregulation of hippocampal BDNF expression, which is related to higher AHN. In addition, microinfusions of BDNF or a BDNF inhibitor into the dorsal hippocampus were associated with improved or impaired STM, respectively. These findings indicate new roles for CREB in learning and memory; CREB plays a regulatory role in STM via the regulation of BDNF expression (Suzuki et al., 2011; Kida and Serita, 2014). Another similar study, Lee et al. (2013) showed that phytoceramide administration enhanced memory via the upregulation of hippocampal pCREB and BDNF expression, which resulted in increased AHN. These results suggest that phytoceramide contributes to memory enhancement and increased BDNF expression, which could lead to increased neurogenesis (Lee et al., 2013).

Finally, links between CREB signaling and neuropsychiatric diseases (e.g., depression) have been reported, and there is evidence that subjects with these diseases also have impairments in AHN (Gass and Riva, 2007). Chronic antidepressant treatment can upregulate hippocampal CREB activity, similar to CREB pathway upregulation in AHN. One study reported that CREB-deficient mice with an antidepressive phenotype also showed neurogenesis enhancement. Compared to wild-type mice, these mice responded more quickly to depression treatment.

CREB and Memory

One emergent hypothesis regarding the prevention of consolidation of STM into LTM involves the inhibition of proteins or transcription factors. This hypothesis also draws on the relationship between memory consolidation and affective and emotional depression-related circuits (Vogt et al., 2014). The translation of proteins from genes is crucial for memory consolidation (Flexner et al., 1965; Alberini and Kandel, 2015). Different pharmacological approaches have been used to block mRNA and protein synthesis, but this results in an impairment in LTM consolidation without affecting STM (Suzuki et al., 2004; Duvarci et al., 2008; Alberini and Kandel, 2015).

Brunelli et al. (1976) found that serotonin increases the level of cAMP in sensory neurons. It was one of the first reports of an association between cAMP and learning and memory (Brunelli et al., 1976). A decade later, Marc Montminy and L.M. Bilezikjian described, for first time, CREB as a cellular transcription factor that binds the CRE– thereby increasing the transcription of the somatostatin gene (Montminy and Bilezikjian, 1987). The first report of a direct role of CREB transcription factors, downstream of the cAMP pathway, in memory-related synaptic plasticity was in Dash et al. (1990). Dash et al. (1990) demonstrated that, during LTM in Aplysia neurons, PKA activates gene expression via CREB. They could selectively eliminate the long-term process by blocking the binding of CREB1 to its DNA response element. The approach used by Dash et al. (1990) was the microinjection of CRE oligonucleotides into sensory neurons co-cultured with motor neurons. These oligonucleotide bound to the CREB1 protein within the cell and inhibited CREB1. In addition, these oligonucleotide prevented CREB1 from binding to CRE sites in the regulatory regions of cAMP-responsive genes, thus blocking subsequent gene expression. The injection of this oligonucleotide selectively blocked LTM, but did not have an effect on the STM.

A number of more recent studies have demonstrated that CREB is the main element underlying the conversion of STM to LTM (Barco et al., 2003; Kim et al., 2013; Vogt et al., 2014). Several mutant mice phenotypes have been developed to investigate the roles of CREB in learning and memory formation. Walton et al. (1992) study employed a learning and memory task in which mice with a tetracycline-controlled transactivator/operator system specifically expressed a dominant-negative inhibitor of CREB activation in CaMKIIα-positive forebrain cells. It was shown that LTM but not STM was impaired. However, these mutant mice did not exhibit a contextual fear-conditioning deficit (Pittenger et al., 2002). In addition, similar results showing that the genetic loss of CREB function impaired LTM but not STM formation has been obtained by other researchers (Bourtchuladze et al., 1994; Kida et al., 2002; Kida and Serita, 2014). Kida (2012) revealed the crucial role of CREB in the consolidation of contextual fear conditioning using tamoxifen-inducible expression of a dominant-negative CREB repressor (Vogt et al., 2014). Furthermore, mutant mice with inhibited CREB activity exhibited deficits in hippocampal late long-term potentiation (L-LTP). Collectively, this evidence indicates that CREB has a central role in these processes and is necessary for both memory consolidation and LTP.

CREB exerts its action as a molecular switch for memory formation (Suzuki et al., 2011). Viral vectors-mediated gene transfer have been widely used to overexpress CREB. Research has shown that the upregulation of CREB activity promotes memory consolidation (Josselyn et al., 2001; Zhou et al., 2009; Alberini and Kandel, 2015). Even from the traditional point of view that CREB enhances LTM, it is thought that the upregulation of CREB-mediated transcription improves STM (Suzuki et al., 2011). It is established that LTM promotion occurs due to enhanced memory consolidation via upregulation of CREB transcriptional activity (Suzuki et al., 2011). In contrast, an increase in basal levels of BDNF, a CREB target gene, is related to improvements in STM. The upregulation of BDNF and CREB activity synergistically improves LTM formation (Suzuki et al., 2011). Therefore, CREB positively controls memory consolidation and is involved in controlling BDNF expression, which also affects memory processes (Suzuki et al., 2011) and is necessary for AHN.

The main CREB target-gene expression related to memory consolidation and LTP are c-fos, activity-regulated

cytoskeleton-associated protein (Arc), and BDNF (Miyamoto, 2006; Alberini and Kandel, 2015). Improvements in memory consolidation have also been attributed to overexpression of CREB or Y134F in the amygdala and hippocampus (Josselyn et al., 2001; Restivo et al., 2009; Sekeres et al., 2010). Studies that used viruses to overexpress CREB in the lateral amygdala, which is involved in the fear memory network (Han et al., 2007; Giachero et al., 2015), demonstrated that neurons in this brain area are functionally interrelated (Han et al., 2007). These neurons (i.e., those overexpressing CREB in the lateral amygdala) exhibit greater neuronal excitability (Zhou et al., 2009). These findings indicate that neurons with high levels of CREB activation may contribute to improved memory via involvement in the memory network (Kida and Serita, 2014).

In addition, some neuropsychiatric or neurodegenerative diseases such as depression (Zaninotto et al., 2015), schizophrenia (Burton and Twamley, 2015), and AD (Takeda et al., 2014) are associated with memory loss. In this regard, CREB has been postulated to change the sensitivity of the nucleus accumbens to rewarding and aversive drugs (Bilbao et al., 2014a,b). Because hippocampal CREB expression is upregulated by chronic antidepressant treatment, CREB activity appears to be involved in the pathogenesis and treatment of depression (Gass and Riva, 2007).

Taken together, these studies demonstrate that CREB plays a key role in the formation, consolidation, and enhancement of both STM and LTM. Importantly, in addition to its direct effect in memory processes, CREB may influence AHN directly or through its ability to modulate gene expression. That is, CREB modulates AHN, which affects memory consolidation. CREB mainly contributes to AHN by affecting the expression of genes such as BDNF or PSA-NCAM, and also directly participates in neurogenesis via its signaling in newborn neurons. Moreover, CREB signaling pathways are a target of drug therapies to ameliorate brain disorders associated with cognitive dysfunction (e.g., learning and memory impairments; Kida and Serita, 2014), and some of these drugs are designed to improve memory by stimulating AHN.

Concluding Remarks Regarding the Implications for CREB's Role in Memory via AHN Regulation

This review has examined how CREB regulates both adult neurogenesis and memory. With regard to the former, enhanced CREB signaling has been widely described to promote newborn neuron survival, precursor cell proliferation, and neurite outgrowth, and dendritic branching (Giachino et al., 2005; Merz et al., 2011). CREB regulation has multiple aspects, including its phosphorylation and recruitment of chromatin remodelers such as CBP and p300, which are essential for CREB gene transcription (Merz et al., 2011) This process is also regulated by multiple cofactors (Merz et al., 2011) facilitating the transcription of different genes involved in AHN mechanisms, such as the expression of BDNF, PSA-NCAM, and NGF2 (**Figure 3**). Furthermore, CREB regulates AHN directly by affecting gene expression and indirectly by influencing epigenetic mechanisms such as inhibitory DNA methylation in its CpG island (Zhang et al., 2005). Neuronal activity controlling DNA methylation patterns (Ma et al., 2009) establish interdependence between these two integrated processes (i.e., neuronal activity and CREB activation). Another mechanism by which CREB can control AHN is by mediating miRNA expression (Vo et al., 2005; Klein et al., 2007; Chahrour et al., 2008; **Figure 3**).

The relationship between CREB and memory consolidation has been widely studied since Brunelli et al. (1976). It is now accepted that CREB is the key molecule responsible for converting STM to LTM and that it plays a central role in memory consolidation (Barco et al., 2003; Kim et al., 2013; Vogt et al., 2014). It has also been established that CREB mainly affects STM by enhancing BDNF gene expression (Suzuki et al., 2011). Finally, hippocampal CREB overexpression improves memory formation (Restivo et al., 2009; Sekeres et al., 2010).

Taken together, the existing literature suggests that CREB enhances memory through several different mechanisms. Directly, it can increase expression of genes that modulate memory. The new perspective discussed here is that CREB modulates AHN, which also affect memory processes. In this regard, CREB enhances the expression of target genes such as BDNF and PSA-NCAM, which augment AHN. In addition, CREB upregulation itself promotes AHN, leading to greater neuronal survival and postnatal hippocampal neurogenesis (Cameron and Glover, 2015). CREB was also recently shown to be crucial for AHN. AHN has a central role in several cognitive processes including spatial, recognition, and fear conditioning memory (Cameron and Glover, 2015; **Figure 3**). Based on the evidence, it is reasonable to formulate the novel hypothesis referred to here as "A new perspective of memory regulation based on CREB-mediated hippocampal neurogenesis" in which CREB controls memory processes by direct regulation and effects on adult neurogenesis, which affects cognitive and memory processes.

In addition, it is important to not underscore that cognitive process attributable to CREB transcription factors are complex and difficult to study. In this regard, evidence for this hypothesis is crucial to design follow-up studies. Even though there is considerable accumulated knowledge in this domain, it is necessary to better understand how CREB works in adult neurogenesis. Many questions remain unanswered. For example, can CREB also modulate the neurogenic niche or directly affect new neurons? It would be interesting to clarify whether CREB can modify the SGZ microenvironment to facilitate AHN. Another important question is whether CREB can modulate or change the phenotype of a specific neural lineage (e.g., stem or progenitor cells instead of mature neurons). Appropriate gene expression is crucial in determining phenotype, and the transcription of different genes affects diverse mechanisms including cell quiescence, proliferation, and death. Finally, can CREB modulate adult neurogenesis through the control of other adult neurogenesis regulators such as neurotransmitters, steroid hormones, or cytokines (Ortega-Martinez, 2015)?

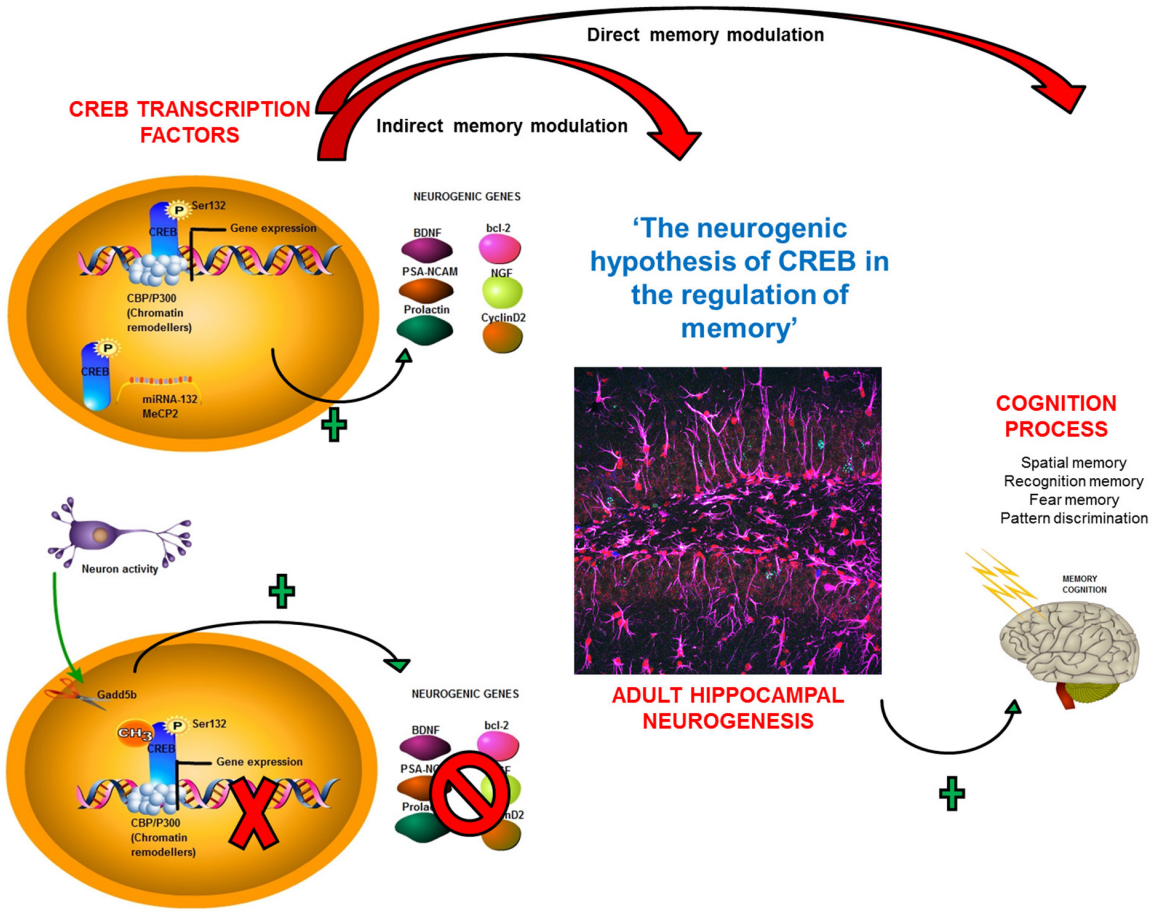

FIGURE 3 | Neurogenic hypothesis for CREB's role in the regulation of memory. A summary of how CREB can influence this cognitive process of memory formation through its direct participation in, or through its modulation of, adult hippocampal neurogenesis (AHN), constituting a new theory for CREB regulation of memory.

Importantly, due to its effect on AHN, CREB may be a strategic target in the development of therapeutic drugs for neurodegenerative and psychiatric diseases associated with cognitive impairment.

Author Contributions

SO-M is the sole author of this paper and is responsible for its content.

Acknowledgments

This work was supported by grant to Dr. Eleanor Coffey from the FP7 Marie Curie ITN r'BIRTH. The author acknowledges Marie Curie fellowship and Åbo Akademi University for supporting SO-M. The author is grateful Dr. Eleanor Coffey for the opportunity to work in her lab and for her help and support. SO-M received a postdoctoral fellowship from Marie Curie ITN r'BIRTH.

References

Abreu, C. M., Kumar, R., Hamilton, D., Dawdy, A. W., Creavin, K., Eivers, S., et al. (2013). Site-specific phosphorylation of the DNA damage response mediator rad9 by cyclin-dependent kinases regulates activation of checkpoint kinase 1. *PLoS Genet.* 9:e1003310. doi: 10.1371/journal.pgen.1003310

Ahn, S., Olive, M., Aggarwal, S., Krylov, D., Ginty, D. D., and Vinson, C. (1998). A dominant-negative inhibitor of CREB reveals that it is a general mediator of stimulus-dependent transcription of c-fos. *Mol. Cell. Biol.* 18, 967–977.

Alberini, C. M., and Kandel, E. R. (2015). The regulation of transcription in memory consolidation. *Cold Spring Harb. Perspect. Biol.* 7:a021741. doi: 10.1101/cshperspect.a021741

Albert, P. R., and Benkelfat, C. (2013). The neurobiology of depression--revisiting the serotonin hypothesis. II. Genetic, epigenetic and clinical studies. *Philos. Trans. R. Soc. Lond. B Biol. Sci.* 368:20120535. doi: 10.1098/rstb.2012.0535

Altman, J., and Das, G. D. (1965). Autoradiographic and histological evidence of postnatal hippocampal neurogenesis in rats. *J. Comp. Neurol.* 124, 319–335. doi: 10.1002/cne.901240303

Barco, A., Pittenger, C., and Kandel, E. R. (2003). CREB, memory enhancement and the treatment of memory disorders: promises, pitfalls and prospects. *Expert Opin. Ther. Targets* 7, 101–114. doi: 10.1517/eott.7.1.101.21163

Bekinschtein, P., Kent, B. A., Oomen, C. A., Clemenson, G. D., Gage, F. H., Saksida, L. M., et al. (2013). BDNF in the dentate gyrus is required for consolidation of pattern-separated memories. *Cell Rep.* 5, 759–768. doi: 10.1016/j.celrep.2013.09.027

Bekinschtein, P., Oomen, C. A., Saksida, L. M., and Bussey, T. J. (2011). Effects of environmental enrichment and voluntary exercise on neurogenesis, learning and memory and pattern separation: BDNF as a critical variable? *Semin. Cell Dev. Biol.* 22, 536–542. doi: 10.1016/j.semcdb.2011.07.002

Bilbao, A., Rieker, C., Cannella, N., Parlato, R., Golda, S., Piechota, M., et al. (2014a). CREB activity in dopamine D1 receptor expressing neurons regulates cocaine-induced behavioral effects. *Front. Behav. Neurosci.* 8:212. doi: 10.3389/fnbeh.2014.00212

Bilbao, A., Rieker, C., Cannella, N., Parlato, R., Golda, S., Piechota, M., et al. (2014b). Corrigendum: CREB activity in dopamine D1 receptor expressing neurons regulates cocaine-induced behavioral effects. *Front. Behav. Neurosci.* 8:239. doi: 10.3389/fnbeh.2014.00239

Bourtchuladze, R., Frenguelli, B., Blendy, J., Cioffi, D., Schutz, G., and Silva, A. J. (1994). Deficient long-term memory in mice with a targeted mutation of the cAMP-responsive element-binding protein. *Cell* 79, 59–68. doi: 10.1016/0092-8674(94)90400-6

Braun, S. M., and Jessberger, S. (2014). Adult neurogenesis and its role in neuropsychiatric disease, brain repair and normal brain function. *Neuropathol. Appl. Neurobiol.* 40, 3–12. doi: 10.1111/nan.12107

Bruel-Jungerman, E., Rampon, C., and Laroche, S. (2007). Adult hippocampal neurogenesis, synaptic plasticity and memory: facts and hypotheses. *Rev. Neurosci.* 18, 93–114. doi: 10.1515/revneuro.2007.18.2.93

Brunelli, M., Castellucci, V., and Kandel, E. R. (1976). Synaptic facilitation and behavioral sensitization in aplysia: possible role of serotonin and cyclic AMP. *Science* 194, 1178–1181. doi: 10.1126/science.186870

Burton, C. Z., and Twamley, E. W. (2015). Neurocognitive insight, treatment utilization and cognitive training outcomes in schizophrenia. *Schizophr. Res.* 161, 399–402. doi: 10.1016/j.schres.2014.12.002

Cameron, H. A., and Glover, L. R. (2015). Adult neurogenesis: beyond learning and memory. *Annu. Rev. Psychol.* 66, 53–81. doi: 10.1146/annurev-psych-010814-015006

Chahrour, M., Jung, S. Y., Shaw, C., Zhou, X., Wong, S. T., Qin, J., et al. (2008). MeCP2, a key contributor to neurological disease, activates and represses transcription. *Science* 320, 1224–1229. doi: 10.1126/science.1153252

Chan, H. M., and La Thangue, N. B. (2001). p300/CBP proteins: HATs for transcriptional bridges and scaffolds. *J. Cell Sci.* 114, 2363–2373.

Chen, A. E., Ginty, D. D., and Fan, C. M. (2005). Protein kinase A signaling via CREB controls myogenesis induced by Wnt proteins. *Nature* 433, 317–322. doi: 10.1038/nature03126

Dash, P. K., Hochner, B., and Kandel, E. R. (1990). Injection of the cAMP-responsive element into the nucleus of aplysia sensory neurons blocks long-term facilitation. *Nature* 345, 718–721. doi: 10.1038/345718a0

Deng, W., Aimone, J. B., and Gage, F. H. (2010). New neurons and new memories: how does adult hippocampal neurogenesis affect learning and memory? *Nat. Rev. Neurosci.* 11, 339–350. doi: 10.1038/nrn2822

Du, K., and Montminy, M. (1998). CREB is a regulatory target for the protein kinase Akt/PKB. *J. Biol. Chem.* 273, 32377–32379. doi: 10.1074/jbc.273.49.32377

Duvarci, S., Nader, K., and LeDoux, J. E. (2008). De novo mRNA synthesis is required for both consolidation and reconsolidation of fear memories in the amygdala. *Learn. Mem.* 15, 747–755. doi: 10.1101/lm.1027208

Dworkin, S., Malaterre, J., Hollande, F., Darcy, P. K., Ramsay, R. G., and Mantamadiotis, T. (2009). cAMP response element binding protein is required for mouse neural progenitor cell survival and expansion. *Stem Cells* 27, 1347–1357. doi: 10.1002/stem.56

Dworkin, S., and Mantamadiotis, T. (2010). Targeting CREB signaling in neurogenesis. *Expert Opin. Ther. Targets* 14, 869–879. doi: 10.1517/14728222.2010.501332

Eriksson, P. S., Perfilieva, E., Björk-Eriksson, T., Alborn, A. M., Nordborg, C., Peterson, D. A., et al. (1998). Neurogenesis in the adult human hippocampus. *Nat. Med.* 4, 1313–1317. doi: 10.1038/3305

Faigle, R., and Song, H. (2013). Signaling mechanisms regulating adult neural stem cells and neurogenesis. *Biochim. Biophys. Acta* 1830, 2435–2448. doi: 10.1016/j.bbagen.2012.09.002

Fanselow, M. S., and Dong, H. W. (2010). Are the dorsal and ventral hippocampus functionally distinct structures? *Neuron* 65, 7–19. doi: 10.1016/j.neuron.2009.11.031

Fiore, R., Khudayberdiev, S., Christensen, M., Siegel, G., Flavell, S. W., Kim, T. K., et al. (2009). Mef2-mediated transcription of the miR379–410 cluster regulates activity-dependent dendritogenesis by fine-tuning Pumilio2 protein levels. *EMBO J.* 28, 697–710. doi: 10.1038/emboj.2009.10

Fitzsimons, C. P., van Bodegraven, E., Schouten, M., Lardenoije, R., Kompotis, K., Kenis, G., et al. (2014). Epigenetic regulation of adult neural stem cells: implications for Alzheimer's disease. *Mol. Neurodegener.* 9:25. doi: 10.1186/1750-1326-9-25

Flexner, L. B., Flexner, J. B., and Stellar, E. (1965). Memory and cerebral protein synthesis in mice as affected by graded amounts of puromycin. *Exp. Neurol.* 13, 264–272. doi: 10.1016/0014-4886(65)90114-7

Fujii, M., Sherchan, P., Soejima, Y., Hasegawa, Y., Flores, J., Doycheva, D., et al. (2014). Cannabinoid receptor type 2 agonist attenuates apoptosis by activation of phosphorylated CREB-Bcl-2 pathway after subarachnoid hemorrhage in rats. *Exp. Neurol.* 261, 396–403. doi: 10.1016/j.expneurol.2014.07.005

Fujioka, T., Fujioka, A., and Duman, R. S. (2004). Activation of cAMP signaling facilitates the morphological maturation of newborn neurons in adult hippocampus. *J. Neurosci.* 24, 319–328. doi: 10.1523/jneurosci.1065.03.2004

Gao, J., Wang, W. Y., Mao, Y. W., Gräff, J., Guan, J. S., Pan, L., et al. (2010). A novel pathway regulates memory and plasticity via SIRT1 and miR-134. *Nature* 466, 1105–1109. doi: 10.1038/nature09271

Gass, P., and Riva, M. A. (2007). CREB, neurogenesis and depression. *Bioessays* 29, 957–961. doi: 10.1002/bies.20658

Gheusi, G., Cremer, H., McLean, H., Chazal, G., Vincent, J. D., and Lledo, P. M. (2000). Importance of newly generated neurons in the adult olfactory bulb for odor discrimination. *Proc. Natl. Acad. Sci. U S A* 97, 1823–1828. doi: 10.1073/pnas.97.4.1823

Ghiani, C. A., Beltran-Parrazal, L., Sforza, D. M., Malvar, J. S., Seksenyan, A., Cole, R., et al. (2007). Genetic program of neuronal differentiation and growth induced by specific activation of NMDA receptors. *Neurochem. Res.* 32, 363–376. doi: 10.1007/s11064-006-9213-9

Ghosh, A., Ginty, D. D., Bading, H., and Greenberg, M. E. (1994). Calcium regulation of gene expression in neuronal cells. *J. Neurobiol.* 25, 294–303. doi: 10.1002/neu.480250309

Giachero, M., Calfa, G. D., and Molina, V. A. (2015). Hippocampal dendritic spines remodeling and fear memory are modulated by GABAergic signaling within the basolateral amygdala complex. *Hippocampus* 25, 545–555. doi: 10.1002/hipo.22409

Giachino, C., De Marchis, S., Giampietro, C., Parlato, R., Perroteau, I., Schütz, G., et al. (2005). cAMP response element-binding protein regulates differentiation and survival of newborn neurons in the olfactory bulb. *J. Neurosci.* 25, 10105–10118. doi: 10.1523/jneurosci.3512-05.2005

Glazewski, S., Barth, A. L., Wallace, H., McKenna, M., Silva, A., and Fox, K. (1999). Impaired experience-dependent plasticity in barrel cortex of mice lacking the alpha and delta isoforms of CREB. *Cereb. Cortex* 9, 249–256. doi: 10.1093/cercor/9.3.249

Gould, E. (2007). How widespread is adult neurogenesis in mammals? *Nat. Rev. Neurosci.* 8, 481–488. doi: 10.1038/nrn2147

Grimm, I., Messemer, N., Stanke, M., Gachet, C., and Zimmermann, H. (2009). Coordinate pathways for nucleotide and EGF signaling in cultured adult neural progenitor cells. *J. Cell Sci.* 122, 2524–2533. doi: 10.1242/jcs.044891

Han, J. H., Kushner, S. A., Yiu, A. P., Cole, C. J., Matynia, A., Brown, R. A., et al. (2007). Neuronal competition and selection during memory formation. *Science* 316, 457–460. doi: 10.1126/science.1139438

Hansen, K. F., Karelina, K., Sakamoto, K., Wayman, G. A., Impey, S., and Obrietan, K. (2013). miRNA-132: a dynamic regulator of cognitive capacity. *Brain Struct. Funct.* 218, 817–831. doi: 10.1007/s00429-012-0431-4

Herold, S., Jagasia, R., Merz, K., Wassmer, K., and Lie, D. C. (2011). CREB signaling regulates early survival, neuronal gene expression and morphological development in adult subventricular zone neurogenesis. *Mol. Cell. Neurosci.* 46, 79–88. doi: 10.1016/j.mcn.2010.08.008

Hirsch, C., Campano, L. M., Wöhrle, S., and Hecht, A. (2007). Canonical Wnt signaling transiently stimulates proliferation and enhances neurogenesis in

neonatal neural progenitor cultures. *Exp. Cell Res.* 313, 572–587. doi: 10.1016/j.yexcr.2006.11.002

Hodge, R. D., and Hevner, R. F. (2011). Expression and actions of transcription factors in adult hippocampal neurogenesis. *Dev. Neurobiol.* 71, 680–689. doi: 10.1002/dneu.20882

Hsiao, Y. H., Hung, H. C., Chen, S. H., and Gean, P. W. (2014). Social interaction rescues memory deficit in an animal model of Alzheimer's disease by increasing BDNF-dependent hippocampal neurogenesis. *J. Neurosci.* 34, 16207–16219. doi: 10.1523/JNEUROSCI.0747-14.2014

Hu, Y., Fang, X., Dunham, S. M., Prada, C., Stachowiak, E. K., and Stachowiak, M. K. (2004). 90-kDa ribosomal S6 kinase is a direct target for the nuclear fibroblast growth factor receptor 1 (FGFR1): role in FGFR1 signaling. *J. Biol. Chem.* 279, 29325–29335. doi: 10.1074/jbc.m311144200

Jagasia, R., Steib, K., Englberger, E., Herold, S., Faus-Kessler, T., Saxe, M., et al. (2009). GABA-cAMP response element-binding protein signaling regulates maturation and survival of newly generated neurons in the adult hippocampus. *J. Neurosci.* 29, 7966–7977. doi: 10.1523/JNEUROSCI.1054-09.2009

Joiner, M. (2009). ''Quantifying cell kill and cell survival,'' in *Basic Clinical Radiobiology*, 4th Edn. eds M. C. Joiner and van A. J. der Kogel (London, UK: Hodder Arnold), 41–55.

Josselyn, S. A., Shi, C., Carlezon, W. A. Jr., Neve, R. L., Nestler, E. J., and Davis, M. (2001). Long-term memory is facilitated by cAMP response element-binding protein overexpression in the amygdala. *J. Neurosci.* 21, 2404–2412.

Kida, S. (2012). A functional role for CREB as a positive regulator of memory formation and LTP. *Exp. Neurobiol.* 21, 136–140. doi: 10.5607/en.2012.21.4.136

Kida, S., Josselyn, S. A., Peña de Ortiz, S., Kogan, J. H., Chevere, I., Masushige, S., et al. (2002). CREB required for the stability of new and reactivated fear memories. *Nat. Neurosci.* 5, 348–355. doi: 10.3410/f.1005192.61105

Kida, S., and Serita, T. (2014). Functional roles of CREB as a positive regulator in the formation and enhancement of memory. *Brain Res. Bull.* 105, 17–24. doi: 10.1016/j.brainresbull.2014.04.011

Kim, G., Choe, Y., Park, J., Cho, S., and Kim, K. (2002). Activation of protein kinase A induces neuronal differentiation of HiB5 hippocampal progenitor cells. *Brain Res. Mol. Brain Res.* 109, 134–145. doi: 10.1016/s0169-328x(02)00550-8

Kim, J., Kwon, J. T., Kim, H. S., and Han, J. H. (2013). CREB and neuronal selection for memory trace. *Front. Neural Circuits* 7:44. doi: 10.3389/fncir.2013.00044

Klein, M. E., Lioy, D. T., Ma, L., Impey, S., Mandel, G., and Goodman, R. H. (2007). Homeostatic regulation of MeCP2 expression by a CREB-induced microRNA. *Nat. Neurosci.* 10, 1513–1514. doi: 10.1038/nn2010

Kowalczyk, A., Filipkowski, R. K., Rylski, M., Wilczynski, G. M., Konopacki, F. A., Jaworski, J., et al. (2004). The critical role of cyclin D2 in adult neurogenesis. *J. Cell Biol.* 167, 209–213. doi: 10.1083/jcb.200404181

Lee, Y., Kim, J., Jang, S., and Oh, S. (2013). Administration of phytoceramide enhances memory and upregulates the expression of pCREB and BDNF in hippocampus of mice. *Biomol. Ther. (Seoul)* 21, 229–233. doi: 10.4062/biomolther.2013.002

Lim, S., Moon, M., Oh, H., Kim, H. G., Kim, S. Y., and Oh, M. S. (2014). Ginger improves cognitive function via NGF-induced ERK/CREB activation in the hippocampus of the mouse. *J. Nutr. Biochem.* 25, 1058–1065. doi: 10.1016/j.jnutbio.2014.05.009

Liu, P., Begley, M., Michowski, W., Inuzuka, H., Ginzberg, M., Gao, D., et al. (2014). Cell-cycle-regulated activation of Akt kinase by phosphorylation at its carboxyl terminus. *Nature* 508, 541–545. doi: 10.1038/nature13079

Lois, C., and Alvarez-Buylla, A. (1994). Long-distance neuronal migration in the adult mammalian brain. *Science* 264, 1145–1148. doi: 10.1126/science.8178174

Lonze, B. E., and Ginty, D. D. (2002). Function and regulation of CREB family transcription factors in the nervous system. *Neuron* 35, 605–623. doi: 10.1016/s0896-6273(02)00828-0

Ma, D. K., Jang, M. H., Guo, J. U., Kitabatake, Y., Chang, M. L., Pow-Anpongkul, N., et al. (2009). Neuronal activity-induced Gadd45b promotes epigenetic DNA demethylation and adult neurogenesis. *Science* 323, 1074–1077. doi: 10.1126/science.1166859

Martin, L. J. (2010). Mitochondrial and cell death mechanisms in neurodegenerative diseases. *Pharmaceuticals (Basel)* 3, 839–915. doi: 10.3390/ph3040839

Merz, K., Herold, S., and Lie, D. C. (2011). CREB in adult neurogenesis—master and partner in the development of adult-born neurons? *Eur. J. Neurosci.* 33, 1078–1086. doi: 10.1111/j.1460-9568.2011.07606.x

Miyamoto, E. (2006). Molecular mechanism of neuronal plasticity: induction and maintenance of long-term potentiation in the hippocampus. *J. Pharmacol. Sci.* 100, 433–442. doi: 10.1254/jphs.cpj06007x

Montminy, M. R., and Bilezikjian, L. M. (1987). Binding of a nuclear protein to the cyclic-AMP response element of the somatostatin gene. *Nature* 328, 175–178. doi: 10.1038/328175a0

Nakagawa, S., Kim, J. E., Lee, R., Chen, J., Fujioka, T., Malberg, J., et al. (2002a). Localization of phosphorylated cAMP response element-binding protein in immature neurons of adult hippocampus. *J. Neurosci.* 22, 9868–9876.

Nakagawa, S., Kim, J. E., Lee, R., Malberg, J. E., Chen, J., Steffen, C., et al. (2002b). Regulation of neurogenesis in adult mouse hippocampus by cAMP and the cAMP response element-binding protein. *J. Neurosci.* 22, 3673–3682.

Nichols, M., Weih, F., Schmid, W., DeVack, C., Kowenz-Leutz, E., Luckow, B., et al. (1992). Phosphorylation of CREB affects its binding to high and low affinity sites: implications for cAMP induced gene transcription. *EMBO J.* 11, 3337–3346.

Ortega-Martinez, S. (2015). Influences of prenatal and postnatal stress on adult hippocampal neurogenesis: the double neurogenic niche hypothesis. *Behav. Brain Res.* 281, 309–317. doi: 10.1016/j.bbr.2014.12.036

Ortega-Martínez, S., and Trejo, J. L. (2015). The postnatal origin of adult neural stem cells and the effects of glucocorticoids on their genesis. *Behav. Brain Res.* 279, 166–176. doi: 10.1016/j.bbr.2014.11.013

Pandey, S. C., Mittal, N., and Silva, A. J. (2000). Blockade of cyclic AMP-responsive element DNA binding in the brain of CREB delta/alpha mutant mice. *Neuroreport* 11, 2577–2580. doi: 10.1097/00001756-200008030-00045

Park, C., Shin, K. S., Ryu, J. H., Kang, K., Kim, J., Ahn, H., et al. (2004). The inhibition of nitric oxide synthase enhances PSA-NCAM expression and CREB phosphorylation in the rat hippocampus. *Neuroreport* 15, 231–234. doi: 10.1097/00001756-200402090-00003

Pittenger, C., Huang, Y. Y., Paletzki, R. F., Bourtchouladze, R., Scanlin, H., Vronskaya, S., et al. (2002). Reversible inhibition of CREB/ATF transcription factors in region CA1 of the dorsal hippocampus disrupts hippocampus-dependent spatial memory. *Neuron* 34, 447–462. doi: 10.1016/s0896-6273(02)00684-0

Restivo, L., Tafi, E., Ammassari-Teule, M., and Marie, H. (2009). Viral-mediated expression of a constitutively active form of CREB in hippocampal neurons increases memory. *Hippocampus* 19, 228–234. doi: 10.1002/hipo.20527

Sable, P., Kale, A., Joshi, A., and Joshi, S. (2014). Maternal micronutrient imbalance alters gene expression of BDNF, NGF, TrkB and CREB in the offspring brain at an adult age. *Int. J. Dev. Neurosci.* 34, 24–32. doi: 10.1016/j.ijdevneu.2014.01.003

Sahay, A., Scobie, K. N., Hill, A. S., O'Carroll, C. M., Kheirbek, M. A., Burghardt, N. S., et al. (2011a). Increasing adult hippocampal neurogenesis is sufficient to improve pattern separation. *Nature* 472, 466–470. doi: 10.1038/nature09817

Sahay, A., Wilson, D. A., and Hen, R. (2011b). Pattern separation: a common function for new neurons in hippocampus and olfactory bulb. *Neuron* 70, 582–588. doi: 10.1016/j.neuron.2011.05.012

Sekeres, M. J., Neve, R. L., Frankland, P. W., and Josselyn, S. A. (2010). Dorsal hippocampal CREB is both necessary and sufficient for spatial memory. *Learn. Mem.* 17, 280–283. doi: 10.1101/lm.1785510

Sharma, K., Mehra, R. D., Dhar, P., and Vij, U. (2007). Chronic exposure to estrogen and tamoxifen regulates synaptophysin and phosphorylated cAMP response element-binding (CREB) protein expression in CA1 of ovariectomized rat hippocampus. *Brain Res.* 1132, 10–19. doi: 10.1016/j.brainres.2006.11.027

Suzuki, S., al-Noori, S., Butt, S. A., and Pham, T. A. (2004). Regulation of the CREB signaling cascade in the visual cortex by visual experience and neuronal activity. *J. Comp. Neurol.* 479, 70–83. doi: 10.1002/cne.20310

Suzuki, A., Fukushima, H., Mukawa, T., Toyoda, H., Wu, L. J., Zhao, M. G., et al. (2011). Upregulation of CREB-mediated transcription enhances both short- and long-term memory. *J. Neurosci.* 31, 8786–8802. doi: 10.1523/jneurosci.3257-10.2011

Takeda, S., Sato, N., and Morishita, R. (2014). Systemic inflammation, blood-brain barrier vulnerability and cognitive/non-cognitive symptoms in alzheimer disease: relevance to pathogenesis and therapy. *Front. Aging Neurosci.* 6:171. doi: 10.3389/fnagi.2014.00171

Taupin, P. (2009). Adult neurogenesis, neural stem cells and Alzheimer's disease: developments, limitations, problems and promises. *Curr. Alzheimer Res.* 6, 461–470. doi: 10.2174/156720509790147151

van Praag, H., Kempermann, G., and Gage, F. H. (1999). Running increases cell proliferation and neurogenesis in the adult mouse dentate gyrus. *Nat. Neurosci.* 2, 266–270. doi: 10.1038/6368

van Praag, H., Schinder, A. F., Christie, B. R., Toni, N., Palmer, T. D., and Gage, F. H. (2002). Functional neurogenesis in the adult hippocampus. *Nature* 415, 1030–1034. doi: 10.1038/4151030a

Vo, N., Klein, M. E., Varlamova, O., Keller, D. M., Yamamoto, T., Goodman, R. H., et al. (2005). A cAMP-response element binding protein-induced microRNA regulates neuronal morphogenesis. *Proc. Natl. Acad. Sci. U S A* 102, 16426–16431. doi: 10.3410/f.1029191.343602

Vogt, M. A., Inta, D., Luoni, A., Elkin, H., Pfeiffer, N., Riva, M. A., et al. (2014). Inducible forebrain-specific ablation of the transcription factor creb during adulthood induces anxiety but no spatial/contextual learning deficits. *Front. Behav. Neurosci.* 8:407. doi: 10.3389/fnbeh.2014.00407

Walton, K. M., Rehfuss, R. P., Chrivia, J. C., Lochner, J. E., and Goodman, R. H. (1992). A dominant repressor of cyclic adenosine 3′,5′-monophosphate (cAMP)-regulated enhancer-binding protein activity inhibits the cAMP-mediated induction of the somatostatin promoter *in vivo*. *Mol. Endocrinol.* 6, 647–655. doi: 10.1210/me.6.4.647

Wang, J. F., Fu, S. P., Li, S. N., Hu, Z. M., Xue, W. J., Li, Z. Q., et al. (2013). Short-chain fatty acids inhibit growth hormone and prolactin gene transcription via cAMP/PKA/CREB signaling pathway in dairy cow anterior pituitary cells. *Int. J. Mol. Sci.* 14, 21474–21488. doi: 10.3390/ijms141121474

Weisz, V. I., and Argibay, P. F. (2012). Neurogenesis interferes with the retrieval of remote memories: forgetting in neurocomputational terms. *Cognition* 125, 13–25. doi: 10.1016/j.cognition.2012.07.002

White, P. C., Shore, A. M., Clement, M., McLaren, J., Soeiro, I., Lam, E. W., et al. (2006). Regulation of cyclin D2 and the cyclin D2 promoter by protein kinase A and CREB in lymphocytes. *Oncogene* 25, 2170–2180. doi: 10.1038/sj.onc.1209255

Yamamoto, K. K., Gonzalez, G. A., Biggs, W. H. 3rd, and Montminy, M. R. (1988). Phosphorylation-induced binding and transcriptional efficacy of nuclear factor CREB. *Nature* 334, 494–498. doi: 10.1038/334494a0

Yamashima, T. (2012). 'PUFA-GPR40-CREB signaling' hypothesis for the adult primate neurogenesis. *Prog. Lipid Res.* 51, 221–231. doi: 10.1016/j.plipres.2012.02.001

Yassa, M. A., and Reagh, Z. M. (2013). Competitive trace theory: a role for the hippocampus in contextual interference during retrieval. *Front. Behav. Neurosci.* 7:107. doi: 10.3389/fnbeh.2013.00107

Yin, J. C., Wallach, J. S., Del Vecchio, M., Wilder, E. L., Zhou, H., Quinn, W. G., et al. (1994). Induction of a dominant negative CREB transgene specifically blocks long-term memory in drosophila. *Cell* 79, 49–58. doi: 10.1016/0092-8674(94)90399-9

Young, D., Lawlor, P. A., Leone, P., Dragunow, M., and During, M. J. (1999). Environmental enrichment inhibits spontaneous apoptosis, prevents seizures and is neuroprotective. *Nat. Med.* 5, 448–453. doi: 10.1038/7449

Yu, J. L., Ma, L., Ma, L., and Tao, Y. Z. (2014). [Voluntary wheel running enhances cell proliferation and expression levels of BDNF, IGF1 and WNT4 in dentate gyrus of adult mice]. *Sheng Li Xue Bao* 66, 559–568. doi: 10.1016/j.bbrc.2004.03.071

Yu, I. T., Lee, S. H., Lee, Y. S., and Son, H. (2004). Differential effects of corticosterone and dexamethasone on hippocampal neurogenesis *in vitro*. *Biochem. Biophys. Res. Commun.* 317, 484–490. doi: 10.1016/j.bbrc.2004.03.071

Zaninotto, L., Guglielmo, R., Calati, R., Ioime, L., Camardese, G., Janiri, L., et al. (2015). Cognitive markers of psychotic unipolar depression: a meta-analytic study. *J. Affect. Disord.* 174, 580–588. doi: 10.1016/j.jad.2014.11.027

Zhang, Y., Allodi, S., Sandeman, D. C., and Beltz, B. S. (2009). Adult neurogenesis in the crayfish brain: proliferation, migration and possible origin of precursor cells. *Dev. Neurobiol.* 69, 415–436. doi: 10.1002/dneu.20717

Zhang, L., Hernández, V. S., Estrada, F. S., and Luján, R. (2014). Hippocampal CA field neurogenesis after pilocarpine insult: the hippocampal fissure as a neurogenic niche. *J. Chem. Neuroanat.* 56, 45–57. doi: 10.1016/j.jchemneu.2014.02.002

Zhang, Q., Liu, G., Wu, Y., Sha, H., Zhang, P., and Jia, J. (2011). BDNF promotes EGF-induced proliferation and migration of human fetal neural stem/progenitor cells via the PI3K/Akt pathway. *Molecules* 16, 10146–10156. doi: 10.3390/molecules161210146

Zhang, X., Odom, D. T., Koo, S. H., Conkright, M. D., Canettieri, G., Best, J., et al. (2005). Genome-wide analysis of cAMP-response element binding protein occupancy, phosphorylation and target gene activation in human tissues. *Proc. Natl. Acad. Sci. U S A* 102, 4459–4464. doi: 10.1073/pnas.0501076102

Zhao, W. Q., Alkon, D. L., and Ma, W. (2003a). c-Src protein tyrosine kinase activity is required for muscarinic receptor-mediated DNA synthesis and neurogenesis via ERK1/2 and c-AMP-responsive element-binding protein signaling in neural precursor cells. *J. Neurosci. Res.* 72, 334–342. doi: 10.1002/jnr.10591

Zhao, X., Ueba, T., Christie, B. R., Barkho, B., McConnell, M. J., Nakashima, K., et al. (2003b). Mice lacking methyl-CpG binding protein 1 have deficits in adult neurogenesis and hippocampal function. *Proc. Natl. Acad. Sci. U S A* 100, 6777–6782. doi: 10.3410/f.1015348.196421

Zhou, Y., Won, J., Karlsson, M. G., Zhou, M., Rogerson, T., Balaji, J., et al. (2009). CREB regulates excitability and the allocation of memory to subsets of neurons in the amygdala. *Nat. Neurosci.* 12, 1438–1443. doi: 10.1038/nn.2405

Conflict of Interest Statement: The author declares that the research was conducted in the absence of any commercial or financial relationships that could be construed as a potential conflict of interest.

frontiers in Molecular Neuroscience

ORIGINAL RESEARCH
published: 18 November 2015
doi: 10.3389/fnmol.2015.00070

Morris Water Maze Training in Mice Elevates Hippocampal Levels of Transcription Factors Nuclear Factor (Erythroid-derived 2)-like 2 and Nuclear Factor Kappa B p65

Wanda M. Snow[1,2], Payam S. Pahlavan[1,2], Jelena Djordjevic[1,2], Danielle McAllister[1], Eric E. Platt[1], Shoug Alashmali[3], Michael J. Bernstein[4], Miyoung Suh[3] and Benedict C. Albensi[1,2,5]**

[1] Division of Neurodegenerative Disorders, St. Boniface Hospital Research, Winnipeg, MB, Canada, [2] Faculty of Health Sciences, Department of Pharmacology and Therapeutics, College of Medicine, University of Manitoba, Winnipeg, MB, Canada, [3] Department of Human Nutritional Sciences, University of Manitoba, Winnipeg, MB, Canada, [4] Department of Psychological and Social Sciences, Pennsylvania State University Abington, Abington, PA, USA, [5] Faculty of Engineering, Department of Electrical and Computer Engineering, University of Manitoba, Winnipeg, MB, Canada

OPEN ACCESS

Edited by:
Nicola Maggio,
The Chaim Sheba Medical Center, Israel

Reviewed by:
Baojin Ding,
University of Massachusetts Medical School, USA
Brian Morris,
University of Glasgow, UK

***Correspondence:**
Wanda M. Snow
wsnow@sbrc.ca;
wsnow_2001@yahoo.ca;
Benedict C. Albensi
balbensi@sbrc.ca

Received: 08 September 2015
Accepted: 03 November 2015
Published: 18 November 2015

Citation:
Snow WM, Pahlavan PS, Djordjevic J, McAllister D, Platt EE, Alashmali S, Bernstein MJ, Suh M and Albensi BC (2015) Morris Water Maze Training in Mice Elevates Hippocampal Levels of Transcription Factors Nuclear Factor (Erythroid-derived 2)-like 2 and Nuclear Factor Kappa B p65. Front. Mol. Neurosci. 8:70. doi: 10.3389/fnmol.2015.00070

Research has identified several transcription factors that regulate activity-dependent plasticity and memory, with cAMP-response element binding protein (CREB) being the most well-studied. In neurons, CREB activation is influenced by the transcription factor nuclear factor kappa B (NF-κB), considered central to immunity but more recently implicated in memory. The transcription factor early growth response-2 (Egr-2), an NF-κB gene target, is also associated with learning and memory. Nuclear factor (erythroid-derived 2)-like 2 (Nrf2), an antioxidant transcription factor linked to NF-κB in pathological conditions, has not been studied in normal memory. Given that numerous transcription factors implicated in activity-dependent plasticity demonstrate connections to NF-κB, this study simultaneously evaluated protein levels of NF-κB, CREB, Egr-2, Nrf2, and actin in hippocampi from young (1 month-old) weanling CD1 mice after training in the Morris water maze, a hippocampal-dependent spatial memory task. After a 6-day acquisition period, time to locate the hidden platform decreased in the Morris water maze. Mice spent more time in the target vs. non-target quadrants of the maze, suggestive of recall of the platform location. Western blot data revealed a decrease in NF-κB p50 protein after training relative to controls, whereas NF-κB p65, Nrf2 and actin increased. Nrf2 levels were correlated with platform crosses in nearly all tested animals. These data demonstrate that training in a spatial memory task results in alterations in and associations with particular transcription factors in the hippocampus, including upregulation of NF-κB p65 and Nrf2. Training-induced increases in actin protein levels caution against its use as a loading control in immunoblot studies examining activity-dependent plasticity, learning, and memory.

Keywords: spatial memory, activity-dependent plasticity, transcription factors, Morris water maze, cAMP-response element binding protein, nuclear factor (erythroid-derived 2)-like 2, nuclear factor kappa B, early growth response-2

INTRODUCTION

The formation of various forms of memory is regulated by distinct neurobiological mechanisms. For example, the formation of long-term (across hours to days), but not short-term (across minutes), memory is associated with protein synthesis (Davis and Squire, 1984; Kandel, 2001; Alberini, 2009). Transcription factors, which can either repress or activate transcription, play a vital role in driving protein synthesis underlying synaptic plasticity and memory, whereby protein synthesis provides the necessary building blocks to accommodate structural changes at the synapse that foster memory formation (Alberini, 2009; Alberini and Kandel, 2014).

The transcription factor cAMP-response element binding protein (CREB) was among the first to be examined in a context of memory, starting with seminal work linking CREB-mediated gene expression to long-term facilitation of the gill-withdrawal reflex in the invertebrate *Aplysia* (Dash et al., 1990; Kaang et al., 1993; Bartsch et al., 1995). The importance of CREB in long-term memory (LTM) has also been demonstrated in *Drosophila melanogaster* (Yin et al., 1994) as well as mammals, including mice (Bourtchuladze et al., 1994) and rats (Josselyn et al., 2001). These data, therefore, suggest a phylogenetically conserved role for CREB in LTM formation.

The consolidation of long-term spatial memories requires protein synthesis and is generally considered to be CREB-dependent (Benito and Barco, 2010). For example, CREB knockout (KO) mice exhibit deficits in learning the location of a hidden platform based on visual cues (Bourtchuladze et al., 1994) in the Morris water maze (MWM), a behavioral paradigm to assess rodent spatial learning and memory (Morris et al., 1982). These mice also display deficits in recalling the platform location after 15 days of training. In rodents, spatial memory formation and intact MWM performance rely critically on the hippocampus (Morris et al., 1982; Bannerman et al., 1999). In rats, disruption of hippocampal CREB via antisense oligodeoxynucleotides impairs long-term spatial memory formation in the MWM (Guzowski and McGaugh, 1997). Further, hippocampal CREB levels have been shown to be strongly correlated with spatial memory capabilities in mice (Brightwell et al., 2004).

In addition to CREB, other transcription factors implicated in memory have been identified (Alberini, 2009; Alberini and Kandel, 2014), including nuclear factor kappa B (NF-κB)(Snow et al., 2014). NF-κB belongs to the Rel family, consisting of five members that form various dimers: p50, p52, p65/RelA, RelB, and c-Rel (Alberini, 2009). Only p65, c-Rel, and RelB, however, have transcriptional activation domains in the C-terminal region to induce transcription, whereas homodimers consisting of p50 and p52 suppress gene expression (Ghosh and Karin, 2002). In neurons, the most common dimers include the p50 homodimer and p65-p50 heterodimer (Meberg et al., 1996). These dimers reside in the cytoplasm in an inactive state, where they are bound to inhibitory IκB proteins. Upon stimulation, phosphorylation of the IκB subunit by IκB kinase (IKK) targets it for degradation by the proteasome, freeing the dimer to translocate to the nucleus where it regulates the expression of genes with DNA-binding sites for NF-κB (Alberini, 2009). Several activators of neuronal NF-κB have been identified, including tumor necrosis factor (Albensi and Mattson, 2000), glutamate, nerve growth factor (Meffert and Baltimore, 2005), dopamine, nitric oxide, kainite (Simpson and Morris, 1999), calcium (Cruise et al., 2000), NMDA receptor activation (Burr and Morris, 2002), and excitatory synaptic transmission via a Ca^{2+}-dependent process (Alberini, 2009). Further, the induction of long-term potentiation (LTP), a cellular correlate of learning and memory, is associated with NF-κB activation, resulting in an increase in the p65-p50 heterodimer and a decrease in IκB mRNA (Meberg et al., 1996). In the crab *Chasmagnathus, in vivo* experiments demonstrate increased activation of NF-κB in brain cell nuclei after a fear stimulus (Freudenthal et al., 1998). Further, injection of IKK blocks its activation, disrupting memory formation (Merlo et al., 2005). Inhibition of NF-κB reduces neural growth and branching in the hippocampus (O'Sullivan et al., 2010). Moreover, p50-KO mice demonstrate deficits in late-phase LTP as well as selective deficits in spatial memory assessed in the MWM (Oikawa et al., 2012). Downregulation of neuronal NF-κB results in decreased activation of CREB via alterations in protein kinase A (Kaltschmidt et al., 2006), which activates CREB by phosphorylation at Serine 133 (Walton and Dragunow, 2000).

More recently, the early growth response (Egr) family of transcription factors, consisting of Egr1-4, has been implicated in memory. The roles of these various members in memory, however, are not well-defined. For example, Egr-1 is specific to spatial navigation long-term memory consolidation (Jones et al., 2001), whereas Egr-3 is implicated in short-term acquisition (Li et al., 2007). Other studies, however, have reported improved memory in Egr-2 KO animals (Poirier et al., 2007). Egr-2 has inhibitory roles on certain cognitive functions via regulating the expression of Nab1 and Nab2 proteins (Desmazières et al., 2008) that increase transcriptional activity of other Egr family where their effect is through Nab, resulting in facilitation in some types of memory (Poirier et al., 2008). In neurons, Egr-2 is a downstream target of NF-κB (Nafez et al., 2015). As with NF-κB, studies suggest a role for Egr-2 in establishing persistent LTP (Williams et al., 1995), consistent with a role for this isoform in learning and memory.

The transcription factor nuclear factor (erythroid-derived 2)-like 2 (Nrf2) is a key regulator of antioxidant genes. Encoded by the *NFE2L2* gene, Nrf2 resides in the cytoplasm under basal conditions. Cellular stressors (i.e., oxidative, electrophilic), however, activate Nrf2, resulting in its translocation to the nucleus where it forms a heterodimer with Maf protein and initiates gene transcription through binding to DNA promoter regions (Tebay et al., 2015). Several studies report crosstalk between Nrf2 and NF-κB in pathological conditions, including cellular exposure to methamphetamine (Permpoonputtana and Govitrapong, 2013) as well as experimental models of diabetes (Agca et al., 2014), Alzheimer's disease (Ashabi et al., 2013), chronic stress (Djordjevic et al., 2015), spinal cord injury (Jin

Abbreviations: ANOVA, analysis of variance; CREB, cAMP-response element binding protein; Egr, early growth response; IKK, IκB kinase; KO, knock out; LTM, long-term memory; LTP, long-term potentiation; MW, molecular weight; MWM, Morris water maze; NF-κB, Nuclear factor kappa b; Nrf2, nuclear factor (erythroid-derived 2)-like 2; PIPES, piperazine-N,N′-bis (2-ethanesulfonic acid).

et al., 2014), and Parkinson's disease (Tobón-Velasco et al., 2013). Environmental enrichment elevates Nrf2 levels in the hippocampi of rats that have undergone experimental induction of cerebral hypoperfusion, a model of vascular dementia (Yang et al., 2015). These results suggest a role for Nrf2 in cognitive recovery after brain damage. Despite the identified role of NF-κB in synaptic plasticity, learning, and memory and its relationship to Nrf2 under several pathological conditions, alterations in Nrf2 in the context of activity-dependent plasticity, learning and memory in the typical, intact mammalian brain have not been investigated.

To further elucidate the transcriptional regulators of activity-dependent plasticity, this research investigated the effects of training in a spatial learning and memory task on transcriptional regulation in the hippocampus. We hypothesized that MWM training would alter levels of and/or be associated with NF-κB as well as transcription factors previously shown to interact (directly or indirectly) with NF-κB, specifically Nrf2, CREB (total and phosphorylated), and Egr-2, in the CD1 mouse hippocampus. Given recent technical reports questioning the use of actin as a loading control for normalization of Western blot data due to studies documenting experimentally-induced changes in actin levels (Gilda and Gomes, 2013; Li and Shen, 2013; Rivero-Gutierrez et al., 2014), we investigated putative differences in actin as a function of MWM-training in the mouse hippocampus. Here, we report several novel findings, including upregulation of Nrf2 and actin in the hippocampi of MWM-trained mice relative to untrained controls. Further, Nrf2 was highly correlated with performance in the memory retention assessment of the MWM in nearly all tested animals, suggesting a newly-identified role for Nrf2 in activity-dependent plasticity, learning, and memory outside of antioxidant regulation in the intact mammalian brain. This is the first report, to our knowledge, detailing parallel upregulation of both p65 NF-κB subunit and Nrf2 after training, in contrast to prior studies documenting opposing regulation under pathological and/or inflammatory conditions.

MATERIALS AND METHODS

Animals

Experiments were carried out in 1 month-old male CD1 mice ($N = 20$) purchased from Jackson Laboratory (Bar Harbor, ME, USA). Mice were housed in the pathogen-free animal facility at St. Boniface Research Centre and maintained on a 12-h light/12-h dark cycle at room temperature (22°C). Food and water were provided *ad libitum*. All procedures were approved by the University of Manitoba Animal Care and Use Committee, which adheres to the guidelines set forth by the Canadian Council on Animal Care. One half of the mice ($n = 10$) underwent MWM training.

MWM Training

The MWM was used to assess hippocampal-dependent spatial memory using methods previously described (Kaltschmidt et al., 2006; Kishida et al., 2006; Oikawa et al., 2012). The standard MWM consisted of a circular pool (100 cm diameter) filled with water (24–25°C) made opaque (white) with powdered milk. Visual cues were positioned equidistant above the water level, and unwanted extra-maze cues were blocked with a curtain. A non-visible escape platform (7 cm diameter) was submerged ∼5 mm below the water surface in the center of the designated target quadrant. In the acquisition phase (4 trials/day for 6 consecutive days), mice were given up to 60 s per trial to find the hidden platform and were required to remain seated on the platform for 10 s, after which the mice were returned to their home cage. Live video was recorded for each trial using the Videomex tracking system (Columbus Instruments, Columbus, OH, USA). Escape latency data (i.e., time to locate the platform) were extracted from video data during the acquisition phase. Search strategies were assigned for every trial of the acquisition phase using the classification scheme, as per Brody and Holtzman (2006). The search strategy employed by an animal in the MWM varies across training days and can indicate the formation of a spatial map (Guzowski and McGaugh, 1997; Kishida et al., 2006; Poirier et al., 2007). For example, during early training, mice will exhibit wall-hugging but tend to display a more focused search of the platform across training, representing the use of a spatial search strategy. Therefore, search strategies employed during the MWM were categorized into three main strategies, as previously described (Guzowski and McGaugh, 1997; Poirier et al., 2007): (1) repetitive looping: swimming in a circular pattern approximately equidistant from the pool wall (chaining), swimming in a circular pattern along the periphery of the pool (peripheral looping), swimming in tight circular patterns (circling), and/or thigmotaxis (wall hugging); (2) non-spatial systemic: searching the interior portion of the pool without an apparent spatial focus (scanning), searching the entire pool randomly without an apparent spatial focus (random), and/or searching a defined area of the pool in an incorrect quadrant; and (3): spatial strategies: swimming directly to the platform (spatial direct), swimming to the platform without repeated looping (spatial indirect), or swimming directly to the correct target quadrant, with continued searching of the platform confined to the target quadrant. The strategy that best described the majority of the swim path was assigned to each trial. During the retention phase, the platform was removed from the pool, and each mouse was given up to 60 s to search for the position of the missing platform (4 trials/day for 3 days). Several parameters were extracted from retention phase data, including time spent in the target quadrant, time spent in non-target quadrants, and the number of passes over the missing platform location.

Brain Tissue Collection

The day following training, mice were sacrificed by isoflurane inhalation, followed by decapitation. Brains were rapidly excised and hippocampi extracted. Hippocampi were placed in Hibernate (Gibco) and weighed. Tissues were snap-frozen in liquid nitrogen and stored at −80°C prior to Western blotting.

Protein Extraction

Hippocampal tissue was homogenized in ice-cold RIPA buffer (150 mM sodium chloride, 1.0% Triton X-100, 0.5% sodium deoxycholate, 0.1% sodium dodecyl sulfate (SDS), and 50 mM Tris, pH 8.0) supplemented with 1% protease inhibitor cocktail

(Amresco, Solon, OH, USA) and 1% phosphatase inhibitor cocktail (Sigma-Aldrich, St. Louis, MO, USA). To further solubilize intracellular proteins, samples were incubated with constant agitation for 35–40 min at 4°C. Tissue lysates were then centrifuged at 10,000 rpm for 10 min (4°C) and supernatants collected. Protein concentrations were estimated using the DC Protein Assay (Bio-Rad, Hercules, CA, USA) as described by the manufacturer. Subsequently, samples were diluted to an equal concentration with RIPA buffer.

Western Blotting

To prepare the tissue lysates for Western blotting, a 4X Laemmli buffer (16% SDS, 40% glycerol, 20% β-mercaptoethanol, 0.01% bromophenol blue, and 0.25 M Tris, pH 6.8) was added. Prior to electrophoresis, samples were denatured at 95°C for 8 min. Fifteen micrograms of protein from each sample was separated by SDS-PAGE at 200 V for approximately 45 min with 10% Criterion™ Tris-Glycine eXtended (TGX) Stain-Free™ polyacrylamide gels (Bio-Rad, Hercules, CA, USA). Stain-Free™ gels were activated by UV transillumination for 2.5 min using the ChemiDoc™ MP (Bio-Rad, Hercules, CA, USA). Proteins were transferred to nitrocellulose membranes (Bio-Rad, Hercules, CA, USA) by the Trans-Blot® Turbo™ Transfer System (Bio-Rad, Hercules, CA, USA). Transfer efficiency was visualized with the ChemiDoc™ MP. The nitrocellulose membranes were then blocked for 1 h at room temperature with 5% skim milk in 1X Tris-buffered saline with 0.1% Tween-20 (TBS-T), except those for which pCREB was detected, in which case 5% bovine serum albumin (BSA) in 1X TBS-T was used to reduce non-specific binding. After blocking, membranes were incubated overnight at 4°C with the following diluted primary antibodies: rabbit monoclonal anti-pCREB (detects CREB phosphorylated at Serine 133) (molecular weight (MW): 37 kDa; 1:1000 dilution, Abcam, Cambridge, UK, cat. no. ab32096), rabbit monoclonal anti-NF-κB p50/p105 (MW: 50 kDa/105 kDa; 1:5000 dilution, Abcam, Cambridge, UK, cat. no. ab32360), rabbit polyclonal anti-NF-κB p65 (MW: 60 kDa; 1:2000 dilution, Abcam, Cambridge, UK, cat. no. ab16502), rabbit polyclonal anti-Nrf2 (MW: 61kDa; 1:100 dilution, Santa Cruz Biotechnology, Dallas, TX, USA, sc-13032), and rabbit monoclonal anti-Egr-2 (a.k.a. krox-20, cat. no. ab108399) (MW: 53 kDa; 1:7500 dilution, Abcam, Cambridge, UK). Following incubation with primary antibodies, nitrocellulose membranes were washed with 1X TBS-T and then incubated with a peroxidase-conjugated AffiniPure goat anti-rabbit IgG (H + L) antibody (1:2000 dilution, Jackson ImmunoResearch Laboratories, West Grove, PA, USA) for 1 h at room temperature. After washing with 1X TBS-T, the relative amount of bound antibody was measured using enhanced chemiluminescence (ECL). Proteins of interest were detected using the Bio-Rad Clarity™ Western ECL Blotting Substrate (Bio-Rad, Hercules, CA, USA) and visualized by the ChemiDoc™ MP (Bio-Rad, Hercules, CA, USA) with ImageLab™ software. Membranes probed for pCREB were stripped and re-probed with the rabbit monoclonal anti-CREB (MW: 37 kDa; 1:1000 dilution, Abcam, Cambridge, UK, cat. no. ab32515) primary antibody. A subset of membranes was also stripped and re-probed with the rabbit polyclonal anti-actin primary antibody (MW: 42 kDa; 1:500 dilution, Sigma-Aldrich, St. Louis, MO, USA, cat. no. A5060). Band intensities were quantified using ImageLab™ software and normalized to the total amount of protein per lane.

Statistical Analyses

Behavioral data from the acquisition phase of the MWM were analyzed by One-way repeated-measures analysis of variance (ANOVA) across Days (6), followed by *post-hoc* comparisons using Fisher's least significant difference (LSD) tests. Analyses were conducted on the mean scores/day from the four daily trials. Search strategy data were analyzed using Chi-square tests of the proportion of trials for which a given strategy was employed. Data were analyzed using paired samples *t*-tests to compare the time spent in the target quadrant relative to the average time spent in the three non-target quadrants during the retention phase. Western blot data were analyzed using student's *t*-tests, as all variables followed a normal distribution. To investigate the relationship between transcription factor levels and memory formation in the MWM, Pearson correlations were performed on band densitometry data and retention phase parameters, including cumulative number of passes over the missing platform area and time in target quadrant. Significance was predetermined at $p < 0.05$, and all analyses were two-tailed.

RESULTS

MWM-acquisition Phase

Analysis of escape latency, the time the mouse took to find the hidden platform, revealed a significant decrease over time in the acquisition phase [repeated measures ANOVA; $p < 0.001$, $F_{(5, 45)} = 34.95$]. *Post-hoc* comparisons revealed a significant decrease in escape latency as early as Day 2 ($p < 0.01$), with continued improvements at Day 3 (vs. Day 2: $p < 0.001$; vs. Day 1: $p < 0.001$; **Figure 1**). Overall, mean latency (±SEM) decreased from 56.9 ± 4.8 s on Day 1 to a mean of 12.1 ± 1.5 s on Day 6 ($p < 0.001$), suggestive of learning the platform location. Search strategy data, analyzed using a 3 (Spatial Strategy) × 6 (Day) Chi-square analysis, revealed overall differences in the frequencies across Day and Strategy, $\chi^2_(10) = 78.78$, $p < 0.001$. Additional analyses revealed that search strategy differed at Day 1, $\chi^2_{(2)} = 27.13$, $p < 0.001$; Day 2, $\chi^2_{(2)} = 9.13$, $p = 0.01$; Day 3, $\chi^2_{(2)} = 35.38$, $p < 0.001$; Day 4, $\chi^2_{(2)} = 11.38$, $p = 0.003$; Day 5, $\chi^2_{(2)} = 27.13$, $p < 0.001$; and Day 6, $\chi^2_{(2)} = 30.88$, $p < 0.001$. For spatial strategies, a significant difference in the frequency of use occurred across days, $\chi^2_{(5)} = 44.41$, $p < 0.001$; differences also emerged for non-spatial strategies, $\chi^2_{(5)} = 19.59$, $p = 0.001$, and repetitive looping, $\chi^2_{(5)} = 15.59$, $p = 0.02$. Mice used a mixture of strategies on the first day, including spatial (12.5%), non-spatial (55%), and repetitive looping (32.5%) and then showed a progressive increase (day 2, 27.5%; day 3, 60%; day 4, 40%; day 5, 57.5%; day 6, 57.5%; in the use of spatial strategies over the rest of the 6-day acquisition phase (**Figure 2**). This increased reliance on spatial strategies to locate the platform is consistent with the formation a cognitive spatial map (Brody and Holtzman, 2006).

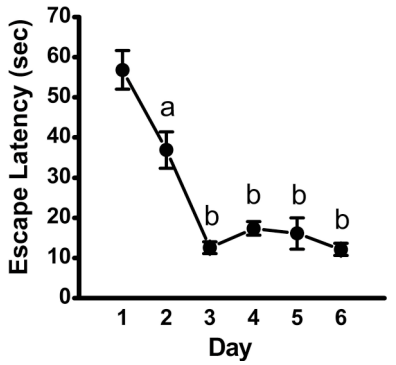

FIGURE 1 | Escape latency across training days in the acquisition phase of the MWM. Plot depicting time to locate the hidden platform (mean ± SEM; $n = 10$) across training days, as assessed using repeated-measures ANOVA, followed by Fisher's LSD *post-hoc* comparisons. a, significantly different from Day 1, $p < 0.01$; b, significantly different from Day 1 and Day 2, $p < 0.001$.

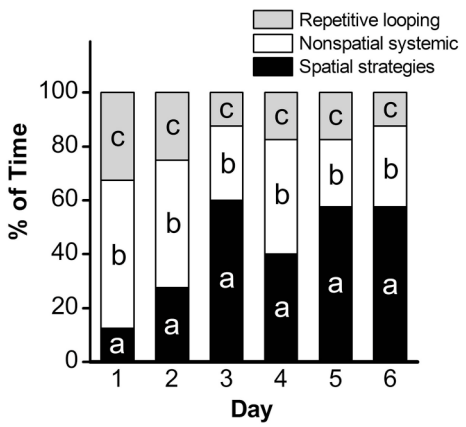

FIGURE 2 | Assessment of search strategy in the acquisition phase of the MWM. The percentage of time engaged in specific search strategies during the 60-s trial was calculated, with search strategies combined into 3 groups based on functional similarity (repetitive looping, nonspatial systemic strategies, and spatial strategies) and analyzed using Chi Square. a: $p < 0.001$; b: $p = 0.001$; c: $p = 0.02$. $n = 10$.

MWM-retention Phase

Over the 3-day retention phase in which the platform was removed, used to assess memory for the previously learned platform location, the time spent in the target quadrant was compared to the average time spent in the non-target quadrants as an indicator of the animal's recall of the platform location. Mice spent significantly more time in the target quadrant as compared to the average time spent in the non-target quadrants on Day 1 (mean ± SEM: 16.73 ± 0.82 vs. 14.07 ± 0.31 s., respectively; $p = 0.04$), suggestive of recall of the platform location. The time spent in the target quadrant was not significantly differently from the average time spent in the non-target quadrants on Day 2 (mean ± SEM: 13.33 ± 1.48 vs. 15.4 ± 0.48 s, respectively; $p > 0.05$) or Day 3 (mean ± SEM: 16.1 ± 1.35 vs. 14.63 ± 0.46 s, respectively; $p > 0.05$) of the retention phase (**Figure 3**).

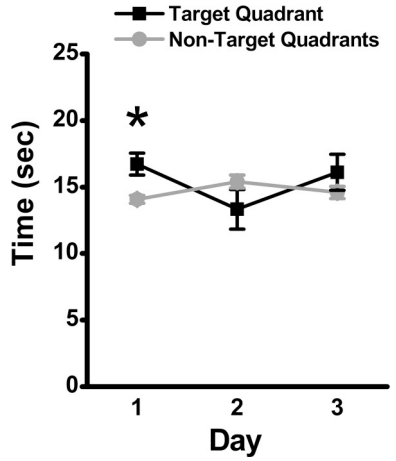

FIGURE 3 | Memory retention in the MWM assessed by time in target quadrant. During the 3-day retention phase, the platform was removed, and the time spent in the target quadrant was compared to the average time spent in the non-target quadrants. Mean ± SEM; $n = 10$; *$p < 0.05$.

Western Blot Data from the Hippocampi of MWM-trained vs. Untrained Control Mice

After MWM, brain tissue was extracted for Western blot experiments to detect transcription factor protein levels after training for comparison to levels in untrained controls. Prior to tissue freezing for Western blotting, hippocampi were weighed. No significant differences were found between untrained control (mean ± SEM: 0.054 ± 0.01) and MWM- trained mice (0.051 ± 0.01; $p = 0.8$; data not shown). Based on data normalized to total protein, hippocampal actin levels were significantly increased ($p < 0.001$; $n = 9$–10) in MWM-trained mice vs. untrained controls (**Figure 4**). This upregulation was confirmed in a repeated Western blot experiment ($p = 0.04$; $n = 9$–10; data not shown) and in an additional experiment in which group order was reversed (e.g., samples from MWM-trained mice loaded first; $p = 0.01$; $n = 5$) to rule out any systemic bias or artifact due to loading order (data not shown). Not surprisingly, no significant differences were detected in any of the transcription factors when normalized to actin levels (data not shown). Therefore, all subsequent immunoblot results were garnered with analyses based on densitometry values normalized to total protein (**Figure 4B**).

Relative to untrained controls, levels of NF-κB subunit p50 were significantly lower in the hippocampi of mice after MWM training ($p < 0.01$) relative to untrained controls, with no significant differences in its precursor subunit, p105 (**Figure 5**). In contrast, levels of hippocampal NF-κB subunit p65 were significantly higher after MWM training compared to untrained controls ($p < 0.001$), as were Nrf2 protein levels ($p < 0.05$; **Figure 5**). No such differences, however, were found in hippocampal CREB, pCREB, or Egr-2 levels as a function of training (**Figure 5**).

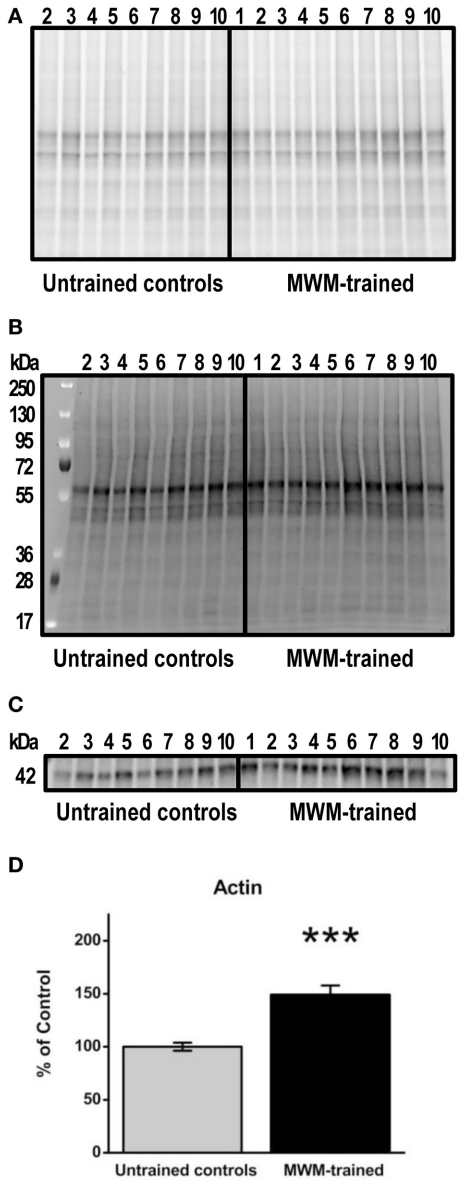

FIGURE 4 | Semi-quantification of actin protein levels in the hippocampus of MWM-trained vs. untrained control CD1 mice. (A) Gel activation image of protein from hippocampal homogenates (15 μg) using UV illumination-based stain-free technology. **(B)** Image of nitrocellulose blot after protein transfer, indicating the total amount of protein in each lane that was used for normalization. **(C)** Representative Western blot detecting total actin (1:500) in hippocampal homogenates from MWM-trained and untrained control mice ($n = 9$–10). **(D)** Bar graph of densitometry values for actin, normalized to total protein and expressed as percentage change from control mean (100%) ± SEM, from hippocampal homogenates from untrained controls and MWM-trained mice. Error bars represent standard error; $^{***}p < 0.001$.

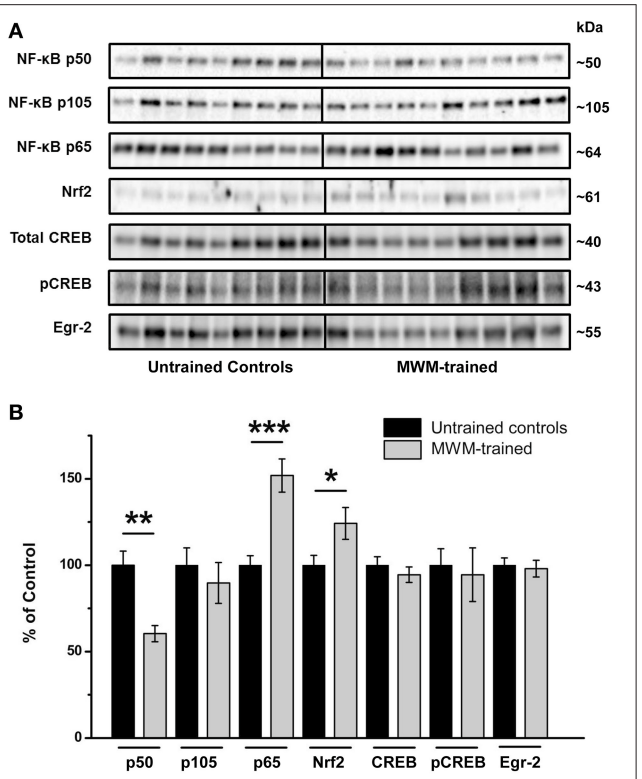

FIGURE 5 | Semi-quantification of transcription factor protein levels in the hippocampus of MWM-trained vs. untrained control CD1 mice. (A) Representative Western blots detecting NF-κB subunits (p50, p105, and p65), Nrf2, CREB (total and activated pCREB), and Egr-2. All samples ($n = 9$–10/group) were immunoblotted simultaneously using 26-well Criterion™ TGX Stain-Free™ gels (Bio-Rad). **(B)** Bar graph of densitometry values of transcription factors of interest, normalized to total protein and expressed as percentage change from control mean (100%) ± SEM, from hippocampal homogenates from untrained controls and MWM-trained mice. $^{*}p < 0.05$; $^{**}p < 0.01$; $^{***}p < 0.001$.

Associations between Performance in the Retention Phase of the MWM and Transcription Factor Levels

Correlational analyses between transcription factor densitometry values and cumulative passes over platform across the 3-day retention phase in trained mice did not reveal any significant associations (**Figure 6**). A correlation of 0.46 between Nrf2 and passes over platform, however, approached significance ($p = 0.07$). Examination of the scatterplot (**Figure 6E**) indicated the presence of a data point in which protein levels were low relative to passes over platform as compared to the trained group overall. Interestingly, a strongly positive significant correlation ($r = 0.98$; $p < 0.01$) was found between Nrf2 and passes over platform for the remaining eight animals with this inconsistent data point removed from the analysis. Therefore, in 88.8% of animals ($n = 8/9$), the relationship between Nrf2 levels and passes over platform approached near perfect linearity. Correlational analyses using time spent in the target quadrant did not yield any significant relationships with actin (**Figure 7A**) or with any of the NF-κB subunits measured (**Figures 7B–D**). As well, Nrf2 was not significantly associated with this retention phase parameter (**Figure 7E**), in contrast to the significant relationship reported with passes over platform. Densitometry values for pCREB were significantly correlated with time in target quadrant in the positive direction ($r = 0.7$; $p < 0.05$; **Figure 7G**). The positive

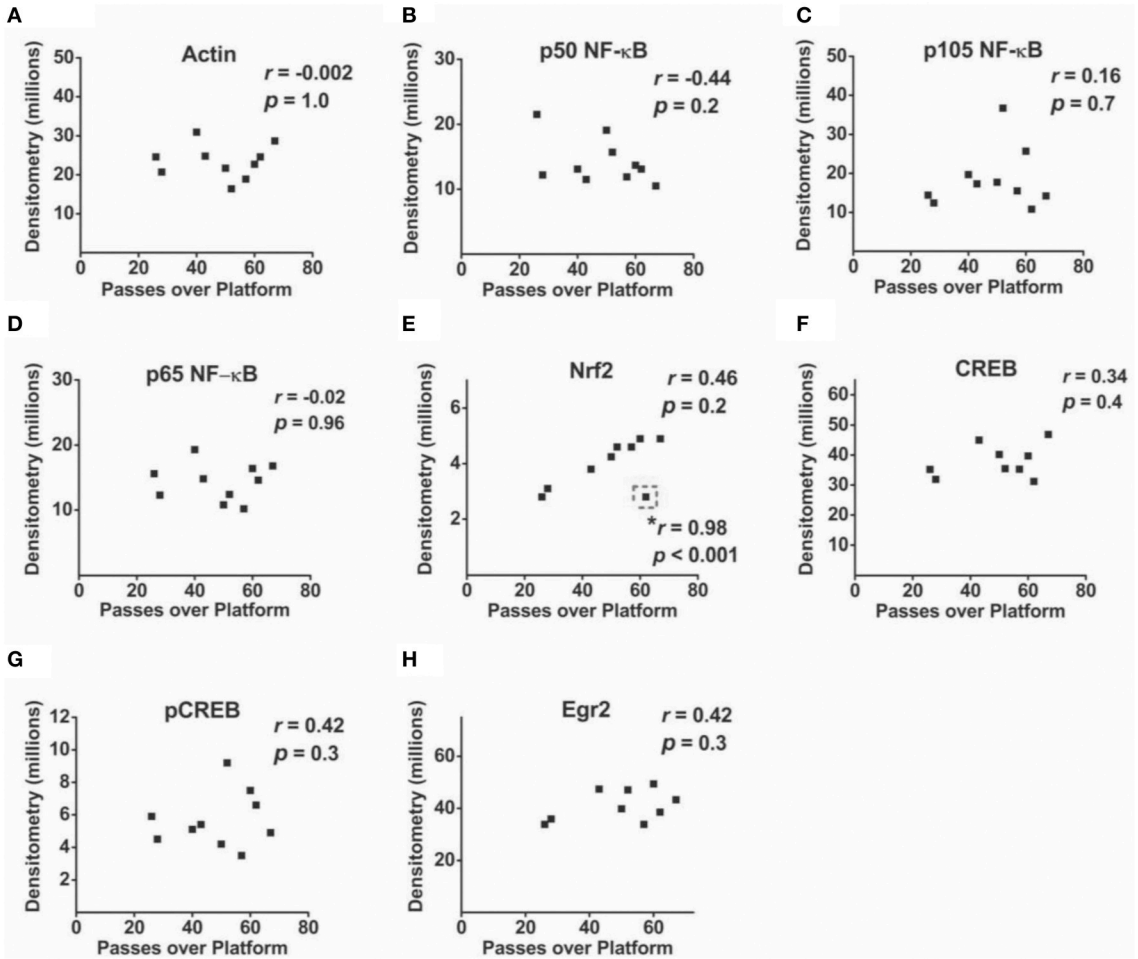

FIGURE 6 | Associations between hippocampal transcription factor protein levels and MWM-retention phase parameter passes over platform. (A–H) Scatterplots and Pearson correlation coefficients between densitometry values (normalized to total protein) from Western blot experiments and the cumulative number of passes over the platform area during the MWM retention phase ($n = 9$–10). *: highly significant positive correlation for $n = 8/9$ tested animals after removal of one inconsistent data point (outlined in dashed line).

correlation ($r = 0.58$) between time in target quadrant and CREB levels approached significance ($p < 0.1$; **Figure 7F**), as was the case for time in target quadrant and Egr-2 levels ($r = 0.65$; $p = 0.6$; **Figure 7H**).

DISCUSSION

The present study simultaneously evaluated changes associated with MWM training in levels of three transcription factors previously implicated in memory. We hypothesized that training in a task associated with spatial learning and memory would alter levels of or be associated with regulators of activity-dependent plasticity, learning and memory, including NF-κB as well as CREB, and Egr-2, both of which are influenced by NF-κB dynamics. The effects of MWM training on Nrf2 were also analyzed to investigate training-induced transcriptional modifications of this master redox regulator. We found alterations in NF-κB and Nrf2, with no effect of training on CREB or Egr-2 levels. Interestingly, we found a decrease in NF-κB p50 levels after MWM training. NF-κB has multiple roles in the central nervous system, including inflammation regulation (Vallabhapurapu and Karin, 2009), development (Mincheva-Tasheva and Soler, 2013), synaptic plasticity, and learning and memory (Snow et al., 2014). Given its diverse functions in the brain, it is not surprising that neuronal NF-κB composition is complex, consisting of various dimers that can form from its multiple isoforms. Although we found downregulation of p50 NF-κB after training, this subunit is considered inhibitory, as p50 homodimers repress downstream gene expression (Ghosh and Karin, 2002). In line with such an inhibitory role is evidence demonstrating enhanced spatial learning in the MWM but not other tests of spatial learning (e.g., Barnes maze) in NF-κB-p50 KO mice (Lehmann et al., 2010). Increased levels of p65, however, may reflect enhanced activation, given that heterodimers consisting of p50 and p65, the most common dimer composition found in neurons, initiate gene expression

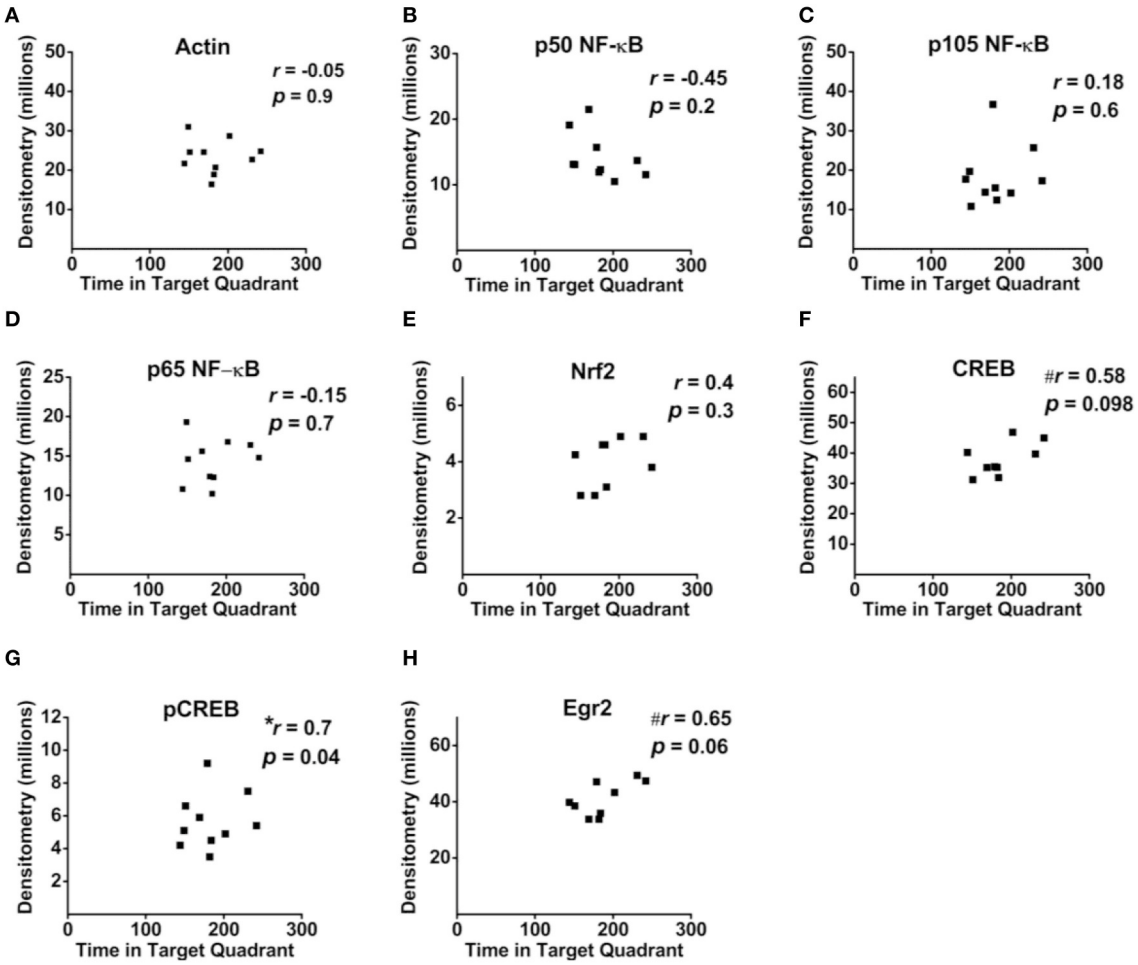

FIGURE 7 | Associations between hippocampal transcription factor protein levels and MWM-retention phase parameter time in target quadrant. (A–H) Scatterplots and Pearson correlation coefficients between densitometry values (normalized to total protein) from Western blot experiments and the time spent in the target quadrant during the MWM retention phase. $n = 9–10$.

in the nucleus (Mincheva-Tasheva and Soler, 2013). We cannot definitively state the implication of a reduction of the p50 subunit, given that its action on target genes (i.e., inhibition or activation) is a function of its associated subunit and resulting dimer composition. In addition to measures of NF-κB dimer subunits, future studies could measure levels of IκB to more accurately evaluate training-induced activation of NF-κB.

Relative to other organs, the brain has unusually high energy demands, exhibiting high oxygen consumption and robust production of reactive oxygen species (ROS). Studies have shown that formation and maintenance of LTP, a commonly studied cellular substrate for learning and memory, are ROS-dependent, including superoxide and H_2O_2 (Klann et al., 1998; Knapp and Klann, 2002). Furthermore, this regulation acts in a concentration-dependent manner (Kamsler and Segal, 2003). Therefore, ROS appear to be essential signaling components for memory formation; on the other hand, they can also impair the same neuronal networks necessary for memory function. Hence, it is logical to suggest the importance of transcriptional regulation of the redox state in memory formation. Nrf2 is a master transcriptional regulator of genes involved in antioxidant response and ROS production, and for some of these genes (SOD-1, NADPH oxidase), direct connections with hippocampus-dependent spatial memory function have already been documented (Gahtan et al., 1998; Kishida et al., 2006).

Memory improvement upon Nrf2 level modulation has been reported in aged APP/PS1 mice (Kanninen et al., 2009) and in rats with induced memory impairments (Dwivedi et al., 2013). To our knowledge, however, this is the first report to demonstrate alterations in hippocampal Nrf2 after training with a learning and memory paradigm in the typical mammalian brain. Further, we found a strong positive correlation between Nrf2 and performance in the memory retention phase of the MWM in the overwhelming majority of tested animals. Such data argue for the involvement of Nrf2 in hippocampal-mediated activity-dependent plasticity and memory.

Previous findings report opposing expression patterns between NF-κB p65 and Nrf2 (Ashabi et al., 2013;

Permpoonputtana and Govitrapong, 2013; Tobón-Velasco et al., 2013; Djordjevic et al., 2015), in contrast to our findings of training-induced increases in both NF-κB p65 and Nrf2. These reports examined this relationship in cases of pathologies and putative treatments, where oxidative stress is an accompanying phenomenon. Therefore, our results suggest a dynamic regulation of NF-κB p65 and Nrf2 that appears condition-dependent, whereby components of these two transcription factors display similar expression patterns under physiological conditions but opposing patterns under pathological conditions.

In addition to elevations in Nrf2, this is the first study of which we are aware to report increased hippocampal actin levels after Morris water maze training in mice. Several lines of research confirm a role for actin, a fundamental component of the neuronal cytoskeleton, in synaptic plasticity, learning and memory. For instance, brain-specific KO of β-actin, the major actin isoform in the mammalian central nervous system, impaired performance in the MWM in mice, particularly in the memory retention phase (Cheever et al., 2012). Morphologically, sensitivity to β-actin depletion was region-specific, despite its ubiquitous presence in the brain. For example, the hippocampus and cerebellum were particularly vulnerable to the effects of a lack of β-actin, as gross morphology was aberrant. No such abnormalities were found in the cerebral cortex (Cheever et al., 2012). Thus, the hippocampus may be especially sensitive and responsive to actin levels in the context of both learning and memory formation and development.

Actin is intricately involved in the activity-dependent modulation of dendritic spines and synaptogenesis (Hotulainen and Hoogenraad, 2010). Actin rearrangement from monomeric (G-actin) to filamentous (F-actin) states via polymerization is required for consolidation of conditioned taste aversion memory (Bi et al., 2010) and conditioned place aversion memory (Hou et al., 2009). Pharmalogical inhibition of actin polymerization within the hippocampus impairs object placement memory formation in female rats in a dose-dependent fashion (Nelson et al., 2012). Further, interventions that induce actin rearrangement improve MWM performance in mice (Fu et al., 2014) without increasing total actin, confirming actin-induced activity-dependent synaptic remodeling in a manner independent of protein synthesis. Enlargement of the actin cytoskeleton and subsequent stabilization, however, may be considered a critical determinant of memory consolidation (Rudy, 2015). Others have reported activity-dependent upregulation of actin-binding proteins in the hippocampus, including increased levels of pCofilin after object placement training (Nelson et al., 2012). Our results of increased total actin protein levels suggest an additional mechanism of actin-induced changes, perhaps through increasing the available pool of hippocampal actin that would be required to induce spine formation and synaptogenesis. Indeed, Motanis and Maroun (2012) showed distinct physiological requirements of different phases of learning and memory. Specifically, they demonstrated that acquisition of contextual fear conditioning involves both actin rearrangement and protein synthesis, whereas reacquisition of fear conditioning after extinction was dependent upon actin rearrangement; protein synthesis was not required. Given data demonstrating behavioral consequences to changes in actin and our results of increased hippocampal actin in MWM-trained mice, the use of actin as a loading control in immunoblot studies investigating proteins putatively involved in activity-dependent plasticity, learning and memory should be undertaken with caution. Moreover, recent reports indicate less variable protein loading and increased linear range of detection with total protein as the loading control (Gilda and Gomes, 2013; Li and Shen, 2013), as in the present study, as compared to normalization with actin. Immunoblot studies investigating activity-dependent plasticity and/or the molecular basis of learning and memory should confirm whether or not differences in actin levels exist as a function of the experimental condition to determine its suitability as an internal control.

The role of CREB in learning and memory has been widely studied, with the general consensus being that CREB plays a pivotal role in learning and memory, including hippocampal-dependent spatial learning (Guzowski and McGaugh, 1997). Evidence suggests a role for CREB in LTM, but not short-term memory, in MWM tests (Florian et al., 2006). CREB signaling associated with learning and memory, however, has been shown to vary in magnitude as a function of brain structure and temporal dynamics, with CREB activation following a biphasic pattern post-training (Porte et al., 2008b). Further, the duration of activation of CREB may be more important in explaining hippocampal-mediated CREB activity associated with learning than the magnitude (Porte et al., 2008b).

Although, the literature supports a role for CREB in LTM, the view that CREB is *essential* for hippocampal synaptic plasticity and memory is not unanimous. Balschun et al. (2003) found only minimal impairment in the acquisition phase of the MWM, with no deficits in the memory retention phase in transgenic mouse in which the expression of CREB isoforms in the CA1 hippocampal subregion was disrupted. Further, they found no deficit in hippocampal LTP. Disruption of all CREB isoforms brain-wide failed to alter hippocampal LTP, LTD or contextual fear conditioning. Hippocampal-independent taste aversion conditioning, however, was severely compromised in mice lacking all CREB isoforms in the brain. In another study, blockade of all CREB isoforms in the CA1 hippocampal subfield did not alter late-phase LTP, the phase associated with memory consolidation/LTM (Pittenger et al., 2002). In this study, forskolin- and dopamine-associated LTP was diminished. Although the majority of studies across various species and experimental paradigms support a pivotal role for CREB in LTM, one possible explanation for reported inconsistencies is that, in some types of memory and/or under some conditions, memory formation may be CREB-independent (Alberini, 2009).

Interestingly, although we found decreases in NF-κB p50, we saw no changes in Egr-2, a gene target of NF-κB in neurons (Nafez et al., 2015), after MWM training. In contrast to our results with Egr-2, Egr-1 levels are up-regulated during spatial memory formation in the hippocampus (Pollak et al., 2005). The Egr family of proteins plays distinct roles in particular forms of memory (Poirier et al., 2008), with previous studies showing a paradoxical role for Egr-2 in learning and memory (Poirier et al., 2007). Egr-2-deficient mice show no impairment in spatial

memory; rather, they exhibit improved performance in motor learning on rotarod tests and in object recognition memory tests (Poirier et al., 2007).

In the hippocampus, Egr-2 levels have a distinct spatial profile, with lower basal levels in the dentate gyrus relative to other subfields (Richardson et al., 1992). Other studies reveal subfield-specific differences in transcription factor levels after training. For example, although MWM-training upregulated pCREB and Egr-1, pCREB levels were highest in the CA3 region vs. CA1, whereas Egr-1 showed the reverse pattern (highest in the CA1 vs. CA3) (Zhou et al., 2013). Previous research has found no change in CREB levels after spatial learning, whereas pCREB increased (Porte et al., 2008a). Moreover, although training in the MWM induced CREB activation in the hippocampus overall, mice with the best recall of the platform location had the lowest levels of pCREB in the CA1 region (Porte et al., 2008b). The present study did not detect any differences in CREB as a function of MWM training. Performance in the memory retention phase was significantly correlated with pCREB levels but in the positive direction, unlike previous findings in the CA1 (Porte et al., 2008b). It must be noted, however, that the correlation with memory retention and pCREB levels, a finding that would not survive correction for multiple comparisons, was much weaker than that seen with Nrf2. The discrepancies in the literature regarding pCREB and memory may further be explained, in part, by the fact that we examined protein levels in homogenates from whole hippocampi, thus excluding an investigation of possible subfield-specific alterations induced by spatial learning in the MWM. Moreover, alterations in particular hippocampal transcription factors associated with memory in mice may be strain-dependent (Pollak et al., 2005). Further, not all strains of mice perform equally well in different mazes; some are better learners that others, and some perform better in specific mazes (Ammassari-Teule and De Marsanich, 1996; Crawley et al., 1997). These factors should be considered when evaluating reports of transcriptional regulation of learning and memory using mice as the model system.

Although the data presented herein demonstrate several protein alterations in the hippocampus after MWM training, indicating molecular changes associated with activity-dependent plasticity, the trained mice were exposed to significant stress, whereas the control were not. Hence, the effects of stress induced by the training paradigm on these changes cannot be ruled out. The significant correlations found for performance on the memory retention phase and Nrf2 protein levels, however, provide strong evidence implicating Nrf2 in hippocampal spatial memory formation, as do our findings of a significant association between pCREB levels and performance in the memory retention phase.

CONCLUSIONS

In summary, this study revealed modifications in the levels of transcription factors associated with MWM-training in CD1 mice, including parallel elevations in NF-κB p65 and Nrf2, unlike the expression pattern seen in the literature thus far in pathological conditions. Egr-2 levels remained unchanged after training, as did CREB levels. A measure of memory retention was significantly correlated with Nrf2 in most animals. Actin was increased in MWM-trained animals relative to controls, thereby rendering actin an ineffective loading control in the present context and arguing for the use of total protein as an internal control, as presented here. These results support the view that training and performance in a spatial memory task are associated with transcriptional changes in the hippocampus, including those related to neuronal redox regulation.

AUTHOR CONTRIBUTIONS

WS was involved in statistical analysis and interpretation of the data and writing the manuscript. PP was involved in carrying out the behavioral assays and dissections. JD was involved in experimental design of molecular data and manuscript writing. DM conducted western blot experiments and assisted with writing the manuscript. SA assisted with collecting behavioral data. EP and MB were involved in statistical analysis, interpretation, and writing the manuscript. MS assisted with editing the manuscript. BA was involved in conception and study design as well as manuscript writing.

ACKNOWLEDGMENTS

This work was funded by the National Sciences and Engineering Research Council, the St. Boniface General Hospital Research Foundation (to Dr. Albensi), and Research Manitoba (to Dr. Snow). Dr. Albensi is a Research Affiliate at the University of Manitoba's Centre on Aging, a member of the Children's Hospital Research Institute of Manitoba, and the Honorable Douglas Everett, Patricia Everett and the Royal Canadian Properties Endowment Fund Chair. Dr. Albensi is also the Manitoba Dementia Research Chair.

REFERENCES

Agca, C. A., Tuzcu, M., Hayirli, A., and Sahin, K. (2014). Taurine ameliorates neuropathy via regulating NF-kappaB and Nrf2/HO-1 signaling cascades in diabetic rats. *Food Chem. Toxicol.* 71, 116–121. doi: 10.1016/j.fct.2014.05.023

Albensi, B. C., and Mattson, M. P. (2000). Evidence for the involvement of TNF and NF-kappaB in hippocampal synaptic plasticity. *Synapse* 35, 151–159. doi: 10.1002/(SICI)1098-2396(200002)35:2<151::AID-SYN8>3.0.CO;2-P

Alberini, C. M. (2009). Transcription factors in long-term memory and synaptic plasticity. *Physiol. Rev.* 89, 121–145. doi: 10.1152/physrev.00017.2008

Alberini, C. M., and Kandel, E. R. (2014). The regulation of transcription in memory consolidation. *Cold Spring Harb. Perspect. Biol.* 7:a021741. doi: 10.1101/cshperspect.a021741

Ammassari-Teule, M., and De Marsanich, B. (1996). Spatial and visual discrimination learning in CD1 mice: partial analogy between the effect of lesions to the hippocampus and the amygdala. *Physiol. Behav.* 60, 265–271.

Ashabi, G., Alamdary, S. Z., Ramin, M., and Khodagholi, F. (2013). Reduction of hippocampal apoptosis by intracerebroventricular administration of extracellular signal-regulated protein kinase and/or p38 inhibitors in amyloid beta rat model of Alzheimer's disease: involvement of nuclear-related factor-2 and nuclear factor-kappaB. *Basic Clin. Pharmacol. Toxicol.* 112, 145–155. doi: 10.1111/bcpt.12000

Balschun, D., Wolfer, D. P., Gass, P., Mantamadiotis, T., Welzl, H., Schütz, G., et al. (2003). Does cAMP response element-binding protein have a pivotal role in hippocampal synaptic plasticity and hippocampus-dependent memory? *J. Neurosci.* 23, 6304–6314.

Bannerman, D. M., Yee, B. K., Good, M. A., Heupel, M. J., Iversen, S. D., and Rawlins, J. N. (1999). Double dissociation of function within the hippocampus: a comparison of dorsal, ventral, and complete hippocampal cytotoxic lesions. *Behav. Neurosci.* 113, 1170–1188.

Bartsch, D., Ghirardi, M., Skehel, P. A., Karl, K. A., Herder, S. P., Chen, M., et al. (1995). Aplysia CREB2 represses long-term facilitation: relief of repression converts transient facilitation into long-term functional and structural change. *Cell* 83, 979–992.

Benito, E., and Barco, A. (2010). CREB's control of intrinsic and synaptic plasticity: implications for CREB-dependent memory models. *Trends Neurosci.* 33, 230–240. doi: 10.1016/j.tins.2010.02.001

Bi, A. L., Wang, Y., Li, B. Q., Wang, Q. Q., Ma, L., Yu, H., et al. (2010). Region-specific involvement of actin rearrangement-related synaptic structure alterations in conditioned taste aversion memory. *Learn. Mem.* 17, 420–427. doi: 10.1101/lm.1772310

Bourtchuladze, R., Frenguelli, B., Blendy, J., Cioffi, D., Schutz, G., and Silva, A. J. (1994). Deficient long-term memory in mice with a targeted mutation of the cAMP-responsive element-binding protein. *Cell* 79, 59–68.

Brightwell, J. J., Gallagher, M., and Colombo, P. J. (2004). Hippocampal CREB1 but not CREB2 is decreased in aged rats with spatial memory impairments. *Neurobiol. Learn. Mem.* 81, 19–26. doi: 10.1016/j.nlm.2003.08.001

Brody, D. L., and Holtzman, D. M. (2006). Morris water maze search strategy analysis in PDAPP mice before and after experimental traumatic brain injury. *Exp. Neurol.* 197, 330–340. doi: 10.1016/j.expneurol.2005.10.020

Burr, P. B., and Morris, B. J. (2002). Involvement of NMDA receptors and a p21Ras-like guanosine triphosphatase in the constitutive activation of nuclear factor-kappa-B in cortical neurons. *Exp. Brain Res.* 147, 273–279. doi: 10.1007/s00221-002-1180-z

Cheever, T. R., Li, B., and Ervasti, J. M. (2012). Restricted morphological and behavioral abnormalities following ablation of beta-actin in the brain. *PLoS ONE* 7:e32970. doi: 10.1371/journal.pone.0032970

Crawley, J. N., Belknap, J. K., Collins, A., Crabbe, J. C., Frankel, W., Henderson, N., et al. (1997). Behavioral phenotypes of inbred mouse strains: implications and recommendations for molecular studies. *Psychopharmacology* 132, 107–124.

Cruise, L., Ho, L. K., Veitch, K., Fuller, G., and Morris, B. J. (2000). Kainate receptors activate NF-kappaB via MAP kinase in striatal neurones. *Neuroreport* 11, 395–398. doi: 10.1097/00001756-200002070-00034

Dash, P. K., Hochner, B., and Kandel, E. R. (1990). Injection of the cAMP-responsive element into the nucleus of Aplysia sensory neurons blocks long-term facilitation. *Nature* 345, 718–721.

Davis, H. P., and Squire, L. R. (1984). Protein synthesis and memory: a review. *Psychol. Bullet.* 96, 518–559.

Desmazières, A., Decker, L., Vallat, J. M., Charnay, P., and Gilardi-Hebenstreit, P. (2008). Disruption of Krox20-Nab interaction in the mouse leads to peripheral neuropathy with biphasic evolution. *J Neurosci.* 28, 5891–5900. doi: 10.1523/JNEUROSCI.5187-07.2008

Djordjevic, J., Djordjevic, A., Adzic, M., Mitic, M., Lukic, I., and Radojcic, M. B. (2015). Alterations in the Nrf2-Keap1 signaling pathway and its downstream target genes in rat brain under stress. *Brain Res.* 1602, 20–31. doi: 10.1016/j.brainres.2015.01.010

Dwivedi, S., Nagarajan, R., Hanif, K., Siddiqui, H. H., Nath, C., and Shukla, R. (2013). Standardized extract of bacopa monniera attenuates okadaic acid induced memory dysfunction in rats: effect on Nrf2 pathway. *Evid. Based Complement. Alternat. Med.* 2013:294501. doi: 10.1155/2013/294501

Florian, C., Mons, N., and Roullet, P. (2006). CREB antisense oligodeoxynucleotide administration into the dorsal hippocampal CA3 region impairs long- but not short-term spatial memory in mice. *Learn. Mem.* 13, 465–472. doi: 10.1101/lm.249306

Freudenthal, R., Locatelli, F., Hermitte, G., Maldonado, H., Lafourcade, C., Delorenzi, A., et al. (1998). Kappa-B like DNA-binding activity is enhanced after spaced training that induces long-term memory in the crab Chasmagnathus. *Neurosci. Lett.* 242, 143–146.

Fu, A., Zhou, R., and Xu, X. (2014). The synthetic thyroid hormone, levothyroxine, protects cholinergic neurons in the hippocampus of naturally aged mice. *Neural Regen. Res.* 9, 864–871. doi: 10.4103/1673-5374.131602

Gahtan, E., Auerbach, J. M., Groner, Y., and Segal, M. (1998). Reversible impairment of long-term potentiation in transgenic Cu/Zn-SOD mice. *Eur. J. Neurosci.* 10, 538–544.

Ghosh, S., and Karin, M. (2002). Missing pieces in the NF-kappaB puzzle. *Cell* 109 (Suppl.), S81–S96. doi: 10.1016/S0092-8674(02)00703-1

Gilda, J. E., and Gomes, A. V. (2013). Stain-Free total protein staining is a superior loading control to beta-actin for Western blots. *Anal. Biochem.* 440, 186–188. doi: 10.1016/j.ab.2013.05.027

Guzowski, J. F., and McGaugh, J. L. (1997). Antisense oligodeoxynucleotide-mediated disruption of hippocampal cAMP response element binding protein levels impairs consolidation of memory for water maze training. *Proc. Natl. Acad. Sci. U.S.A.* 94, 2693–2698.

Hotulainen, P., and Hoogenraad, C. C. (2010). Actin in dendritic spines: connecting dynamics to function. *J. Cell Biol.* 189, 619–629. doi: 10.1083/jcb.201003008

Hou, Y. Y., Lu, B., Li, M., Liu, Y., Chen, J., Chi, Z. Q., et al. (2009). Involvement of actin rearrangements within the amygdala and the dorsal hippocampus in aversive memories of drug withdrawal in acute morphine-dependent rats. *J. Neurosci.* 29, 12244–12254. doi: 10.1523/JNEUROSCI.1970-09.2009

Jin, W., Ni, H., Hou, X., Ming, X., Wang, J., Yuan, B., et al. (2014). Tert-butylhydroquinone protects the spinal cord against inflammatory response produced by spinal cord injury. *Ann. Clin. Lab. Sci.* 44, 151–157.

Jones, M. W., Errington, M. L., French, P. J., Fine, A., Bliss, T. V., Garel, S., et al. (2001). A requirement for the immediate early gene Zif268 in the expression of late LTP and long-term memories. *Nat. Neurosci.* 4, 289–296. doi: 10.1038/85138

Josselyn, S. A., Shi, C., Carlezon, W. A. Jr., Neve, R. L., Nestler, E. J., and Davis, M. (2001). Long-term memory is facilitated by cAMP response element-binding protein overexpression in the amygdala. *J. Neurosci.* 21, 2404–2412.

Kaang, B. K., Kandel, E. R., and Grant, S. G. (1993). Activation of cAMP-responsive genes by stimuli that produce long-term facilitation in Aplysia sensory neurons. *Neuron* 10, 427–435.

Kaltschmidt, B., Ndiaye, D., Korte, M., Pothion, S., Arbibe, L., Prüllage, M., et al. (2006). NF-kappaB regulates spatial memory formation and synaptic plasticity through protein kinase A/CREB signaling. *Mol. Cell. Biol.* 26, 2936–2946. doi: 10.1128/MCB.26.8.2936-2946.2006

Kamsler, A., and Segal, M. (2003). Hydrogen peroxide modulation of synaptic plasticity. *J. Neurosci.* 23, 269–276.

Kandel, E. R. (2001). The molecular biology of memory storage: a dialogue between genes and synapses. *Science* 294, 1030–1038. doi: 10.1126/science.1067020

Kanninen, K., Heikkinen, R., Malm, T., Rolova, T., Kuhmonen, S., Leinonen, H., et al. (2009). Intrahippocampal injection of a lentiviral vector expressing Nrf2 improves spatial learning in a mouse model of Alzheimer's disease. *Proc. Natl. Acad. Sci. U.S.A.* 106, 16505–16510. doi: 10.1073/pnas.0908397106

Kishida, K. T., Hoeffer, C. A., Hu, D., Pao, M., Holland, S. M., and Klann, E. (2006). Synaptic plasticity deficits and mild memory impairments in mouse models of chronic granulomatous disease. *Mol. Cell. Biol.* 26, 5908–5920. doi: 10.1128/MCB.00269-06

Klann, E., Roberson, E. D., Knapp, L. T., and Sweatt, J. D. (1998). A role for superoxide in protein kinase C activation and induction of long-term potentiation. *J. Biol. Chem.* 273, 4516–4522.

Knapp, L. T., and Klann, E. (2002). Role of reactive oxygen species in hippocampal long-term potentiation: contributory or inhibitory? *J. Neurosci. Res.* 70, 1–7. doi: 10.1002/jnr.10371

Lehmann, M. L., Brachman, R. A., Listwak, S. J., and Herkenham, M. (2010). NF-kappaB activity affects learning in aversive tasks: possible actions via modulation of the stress axis. *Brain Behav. Immun.* 24, 1008–1017. doi: 10.1016/j.bbi.2010.04.005

Li, L., Yun, S. H., Keblesh, J., Trommer, B. L., Xiong, H., Radulovic, J., et al. (2007). Egr3, a synaptic activity regulated transcription factor that

is essential for learning and memory. *Mol. Cell. Neurosci.* 35, 76–88. doi: 10.1016/j.mcn.2007.02.004

Li, R., and Shen, Y. (2013). An old method facing a new challenge: re-visiting housekeeping proteins as internal reference control for neuroscience research. *Life Sci.* 92, 747–751. doi: 10.1016/j.lfs.2013.02.014

Meberg, P. J., Kinney, W. R., Valcourt, E. G., and Routtenberg, A. (1996). Gene expression of the transcription factor NF-kappa B in hippocampus: regulation by synaptic activity. *Brain Res. Mol. Brain Res.* 38, 179–190.

Meffert, M. K., and Baltimore, D. (2005). Physiological functions for brain NF-kappaB. *Trends Neurosci.* 28, 37–43. doi: 10.1016/j.tins.2004.11.002

Merlo, E., Freudenthal, R., Maldonado, H., and Romano, A. (2005). Activation of the transcription factor NF-kappaB by retrieval is required for long-term memory reconsolidation. *Learn. Mem.* 12, 23–29. doi: 10.1101/lm.82705

Mincheva-Tasheva, S., and Soler, R. M. (2013). NF-kappaB signaling pathways: role in nervous system physiology and pathology. *Neuroscientist* 19, 175–194. doi: 10.1177/1073858412444007

Morris, R. G., Garrud, P., Rawlins, J. N., and O'Keefe, J. (1982). Place navigation impaired in rats with hippocampal lesions. *Nature* 297, 681–683.

Motanis, H., and Maroun, M. (2012). Differential involvement of protein synthesis and actin rearrangement in the reacquisition of contextual fear conditioning. *Hippocampus* 22, 494–500. doi: 10.1002/hipo.20915

Nafez, S., Oikawa, K., Odero, G. L., Sproule, M., Ge, N., Schapansky, J., et al. (2015). Early growth response 2 (Egr-2) expression is triggered by NF-kappaB activation. *Mol. Cell. Neurosci.* 64, 95–103. doi: 10.1016/j.mcn.2014.12.008

Nelson, B. S., Witty, C. F., Williamson, E. A., and Daniel, J. M. (2012). A role for hippocampal actin rearrangement in object placement memory in female rats. *Neurobiol. Learn. Mem.* 98, 284–290. doi: 10.1016/j.nlm.2012.09.006

Oikawa, K., Odero, G. L., Platt, E., Neuendorff, M., Hatherell, A., Bernstein, M. J., et al. (2012). NF-kappaB p50 subunit knockout impairs late LTP and alters long term memory in the mouse hippocampus. *BMC Neurosci.* 13:45. doi: 10.1186/1471-2202-13-45

O'Sullivan, N. C., Croydon, L., McGettigan, P. A., Pickering, M., and Murphy, K. J. (2010). Hippocampal region-specific regulation of NF-kappaB may contribute to learning-associated synaptic reorganisation. *Brain Res. Bull.* 81, 385–390. doi: 10.1016/j.brainresbull.2009.11.001

Permpoonputtana, K., and Govitrapong, P. (2013). The anti-inflammatory effect of melatonin on methamphetamine-induced proinflammatory mediators in human neuroblastoma dopamine SH-SY5Y cell lines. *Neurotox. Res.* 23, 189–199. doi: 10.1007/s12640-012-9350-7

Pittenger, C., Huang, Y. Y., Paletzki, R. F., Bourtchouladze, R., Scanlin, H., Vronskaya, S., et al. (2002). Reversible inhibition of CREB/ATF transcription factors in region CA1 of the dorsal hippocampus disrupts hippocampus-dependent spatial memory. *Neuron* 34, 447–462. doi: 10.1016/S0896-6273(02)00684-0

Poirier, R., Cheval, H., Mailhes, C., Charnay, P., Davis, S., and Laroche, S. (2007). Paradoxical role of an Egr transcription factor family member, Egr2/Krox20, in learning and memory. *Front. Behav. Neurosci.* 1:6. doi: 10.3389/neuro.08.006.2007

Poirier, R., Cheval, H., Mailhes, C., Garel, S., Charnay, P., Davis, S., et al. (2008). Distinct functions of egr gene family members in cognitive processes. *Front. Neurosci.* 2, 47–55. doi: 10.3389/neuro.01.002.2008

Pollak, D. D., Scharl, T., Leisch, F., Herkner, K., Villar, S. R., Hoeger, H., et al. (2005). Strain-dependent regulation of plasticity-related proteins in the mouse hippocampus. *Behav. Brain Res.* 165, 240–246. doi: 10.1016/j.bbr.2005.07.028

Porte, Y., Buhot, M. C., and Mons, N. (2008a). Alteration of CREB phosphorylation and spatial memory deficits in aged 129T2/Sv mice. *Neurobiol. Aging* 29, 1533–1546. doi: 10.1016/j.neurobiolaging.2007.03.023

Porte, Y., Buhot, M. C., and Mons, N. E. (2008b). Spatial memory in the Morris water maze and activation of cyclic AMP response element-binding (CREB) protein within the mouse hippocampus. *Learn. Mem.* 15, 885–894. doi: 10.1101/lm.1094208

Richardson, C. L., Tate, W. P., Mason, S. E., Lawlor, P. A., Dragunow, M., and Abraham, W. C. (1992). Correlation between the induction of an immediate early gene, zif/268, and long-term potentiation in the dentate gyrus. *Brain Res.* 580, 147–154.

Rivero-Gutiérrez, B., Anzola, A., Martínez-Augustin, O., and de Medina, F. S. (2014). Stain-free detection as loading control alternative to Ponceau and housekeeping protein immunodetection in Western blotting. *Anal. Biochem.* 467, 1–3. doi: 10.1016/j.ab.2014.08.027

Rudy, J. W. (2015). Variation in the persistence of memory: an interplay between actin dynamics and AMPA receptors. *Brain Res.* 1621, 29–37. doi: 10.1016/j.brainres.2014.12.009

Simpson, C. S., and Morris, B. J. (1999). Activation of nuclear factor kappaB by nitric oxide in rat striatal neurones: differential inhibition of the p50 and p65 subunits by dexamethasone. *J. Neurochem.* 73, 353–361.

Snow, W. M., Stoesz, B. M., Kelly, D. M., and Albensi, B. C. (2014). Roles for NF-kappaB and gene targets of NF-kappaB in synaptic plasticity, memory, and navigation. *Mol. Neurobiol.* 49, 757–770. doi: 10.1007/s12035-013-8555-y

Tebay, L. E., Robertson, H., Durant, S. T., Vitale, S. R., Penning, T. M., Dinkova-Kostova, A. T., et al. (2015). Mechanisms of activation of the transcription factor Nrf2 by redox stressors, nutrient cues and energy status, and pathways through which it attenuates degenerative disease. *Free Radic. Biol. Med.* 88, 108–146. doi: 10.1016/j.freeradbiomed.2015.06.021

Tobón-Velasco, J. C., Limón-Pacheco, J. H., Orozco-Ibarra, M., Macías-Silva, M., Vázquez-Victorio, G., Cuevas, E., et al. (2013). 6-OHDA-induced apoptosis and mitochondrial dysfunction are mediated by early modulation of intracellular signals and interaction of Nrf2 and NF-kappaB factors. *Toxicology* 304, 109–119. doi: 10.1016/j.tox.2012.12.011

Vallabhapurapu, S., and Karin, M. (2009). Regulation and function of NF-kappaB transcription factors in the immune system. *Annu. Rev. Immunol.* 27, 693–733. doi: 10.1146/annurev.immunol.021908.132641

Walton, M. R., and Dragunow, I. (2000). Is CREB a key to neuronal survival? *Trends Neurosci.* 23, 48–53. doi: 10.1016/S0166-2236(99)01500-3

Williams, J., Dragunow, M., Lawlor, P., Mason, S., Abraham, W. C., Leah, J., et al. (1995). Krox20 may play a key role in the stabilization of long-term potentiation. *Brain Res. Mol. Brain Res.* 28, 87–93.

Yang, Y., Zhang, J., Xiong, L., Deng, M., Wang, J., Xin, J., et al. (2015). Cognitive Improvement Induced by Environment Enrichment in Chronic Cerebral Hypoperfusion Rats: a Result of Upregulated Endogenous Neuroprotection? *J. Mol. Neurosci.* 56, 278–289. doi: 10.1007/s12031-015-0529-2

Yin, J. C., Wallach, J. S., Del Vecchio, M., Wilder, E. L., Zhou, H., Quinn, W. G., et al. (1994). Induction of a dominant negative CREB transgene specifically blocks long-term memory in Drosophila. *Cell* 79, 49–58.

Zhou, G., Xiong, W., Zhang, X., and Ge, S. (2013). Retrieval of consolidated spatial memory in the water maze is correlated with expression of pCREB and Egr1 in the hippocampus of aged mice. *Dement. Geriatr. Cogn. Dis. Extra* 3, 39–47. doi: 10.1159/000348349

Conflict of Interest Statement: The authors declare that the research was conducted in the absence of any commercial or financial relationships that could be construed as a potential conflict of interest.

frontiers in Molecular Neuroscience

ORIGINAL RESEARCH
published: 07 August 2015
doi: 10.3389/fnmol.2015.00042

Dynamical properties of gene regulatory networks involved in long-term potentiation

Gonzalo S. Nido[1,2], *Margaret M. Ryan*[2,3], *Lubica Benuskova*[1,2] *and Joanna M. Williams*[2,3]*

[1] Department of Computer Science, University of Otago, Dunedin, New Zealand, [2] Brain Health Research Centre, University of Otago, Dunedin, New Zealand, [3] Department of Anatomy, Otago School of Medical Sciences, University of Otago, Dunedin, New Zealand

The long-lasting enhancement of synaptic effectiveness known as long-term potentiation (LTP) is considered to be the cellular basis of long-term memory. LTP elicits changes at the cellular and molecular level, including temporally specific alterations in gene networks. LTP can be seen as a biological process in which a transient signal sets a new homeostatic state that is "remembered" by cellular regulatory systems. Previously, we have shown that early growth response (Egr) transcription factors are of fundamental importance to gene networks recruited early after LTP induction. From a systems perspective, we hypothesized that these networks will show less stable architecture, while networks recruited later will exhibit increased stability, being more directly related to LTP consolidation. Using random Boolean network (RBN) simulations we found that the network derived at 24 h was markedly more stable than those derived at 20 min or 5 h post-LTP. This temporal effect on the vulnerability of the networks is mirrored by what is known about the vulnerability of LTP and memory itself. Differential gene co-expression analysis further highlighted the importance of the Egr family and found a rapid enrichment in connectivity at 20 min, followed by a systematic decrease, providing a potential explanation for the down-regulation of gene expression at 24 h documented in our preceding studies. We also found that the architecture exhibited by a control and the 24 h LTP co-expression networks fit well to a scale-free distribution, known to be robust against perturbations. By contrast the 20 min and 5 h networks showed more truncated distributions. These results suggest that a new homeostatic state is achieved 24 h post-LTP. Together, these data present an integrated view of the genomic response following LTP induction by which the stability of the networks regulated at different times parallel the properties observed at the synapse.

Keywords: long-term potentiation, gene expression, maintenance, synaptic plasticity, memory, dynamic stability, co-expression analysis

OPEN ACCESS

Edited by:
Benedict C. Albensi, University of Manitoba, Canada

Reviewed by:
Utpal Das, University of California, San Diego, USA
Mohiuddin Ahmad, University of Oklahoma Health Sciences Center, USA
Philip Forsyth Copenhaver, Oregon Health & Science University, USA

***Correspondence:**
Joanna M. Williams, Department of Anatomy, Otago School of Medical Sciences, University of Otago, PO Box 913, Dunedin 9054, New Zealand
joanna.williams@otago.ac.nz

Received: *14 June 2015*
Accepted: *22 July 2015*
Published: *07 August 2015*

Citation:
Nido GS, Ryan MM, Benuskova L and Williams JM (2015) Dynamical properties of gene regulatory networks involved in long-term potentiation. Front. Mol. Neurosci. 8:42. doi: 10.3389/fnmol.2015.00042

1. Introduction

Living cells are equipped with a robust and yet plastic analog system, which allows them to respond to environmental inputs. Information sensed from the changing environment is integrated and processed by networks of interacting elements to generate an adequate response. Despite the complexity of the underlying mechanisms, some aspects of cellular behavior are of apparent

multistable nature, leading to discrete changes that can last for long periods of time. Cell cycle checkpoints, cell differentiation, and apoptosis represent phase transition of multi-component switches that generate robust (and potentially irreversible) transitions (Siegal-Gaskins et al., 2011). From a genetic control perspective, it has been postulated that attractors in the gene and protein expression dynamics, which are the more stable position to which systems tends to evolve, define the cell's character (Kauffman, 1969). Namely, if individual expression values get close enough to the attractor values, these will remain constant even if disturbed. The characterization of the structure of genetic networks from a dynamical perspective using different theoretical methods (Mestl et al., 1997) predicts two broad regimes. The *ordered* regime, robust against perturbations, and a *chaotic* regime, sensitive to perturbations. While robustness is a hallmark of homeostasis, it is reasonable to expect that transitions between cellular states require an enhanced sensitivity. In such scenario, a compromise between robustness and sensitivity could potentially be attained by a rewiring of the network or by the recruitment of different networks.

The change in synaptic efficiency known as long-term potentiation (LTP) represents the cellular correlate for long-term memory in the mammalian brain. From a systems perspective, LTP offers an attractive model of a cellular switch, whereby activation promotes movement to a new cellular state. Just as any other biological switch, LTP accommodates a compromise between robustness to genetic and environmental noise and sensitivity to discriminate meaningful signals. This characteristic is likely to be distributed at different levels of biological organization. For example, LTP requires activation and trafficking of glutamate receptors to the postsynaptic membrane, in addition to protein synthesis and *de novo* gene expression (Abraham and Williams, 2003). Indeed, specific patterns of gene expression have indeed shown to be regulated at different times following LTP induction, and are crucially involved in the maintenance of LTP (Park et al., 2006; Håvik et al., 2007; Ryan et al., 2011, 2012). Specifically, we reported that the networks derived 20 min post-LTP induction, comprised many transcription factors (TFs), including all members of the early growth response (*Egr*) family, and were associated with functions such as development, proliferation, and neurogenesis. By contrast the networks derived at 5 h contained molecules associated with calcium dynamics, dendritogenesis and neurogenesis and in the networks derived at 24 h neurotrophin-NFKB driven pathways of neuronal growth were identified. Our analysis also revealed several mechanisms controlling the temporal shifts in gene expression such as regulation of specific microRNA and histone deacetylases. Thus, the variety of functions held by the genes offers a glimpse of the potential complexity underlying the genomic response to LTP.

The involvement of complex gene networks in the maintenance of LTP suggests that a multistable switch is also present in the structure of the gene regulatory networks recruited at different times following LTP induction. From a systems perspective, we expect that the transition between the pre- and post-LTP homeostatic state is paralleled by the genomic response. We propose that while gene networks rapidly and transiently activated following LTP-inducing stimulation will show a less stable architecture, networks recruited later will exhibit an increased stability, being more directly related to LTP consolidation and post-LTP homeostatic state. Using random Boolean networks (RBN) simulations, we addressed this hypothesis by studying the dynamical stability of networks previously identified (Ryan et al., 2011, 2012). We also use the gene expression profiles provided in these studies to explore the overall co-expression network architecture. Following identification of tightly co-expressed modules, we used functional analysis to investigate the intramodular differential connectivity at different times post-LTP induction. Our results offer an integrated picture of the genomic response following LTP and support the conclusion that a new homeostatic state is achieved 24 h post-LTP.

2. Materials and Methods

2.1. Network Topologies

LTP-related gene expression profiles investigated in this study were taken from Ryan et al. (2011, 2012). Briefly, 20 min, 5 h, and 24 h following induction of LTP at perforant path synapses in the dentate gyrus in awake freely moving rats, gene expression profiling was carried out using Affymetrix RAT230.2 microarrays and the functional relationships of the differentially expressed genes ($\pm$1.15-fold change; $p < 0.05$; moderated paired t-test between the stimulated and control hemispheres) was explored using the network analysis tool Ingenuity pathway analysis, version 7 (IPA) (Ingenuity Systems, USA; https://www.analysis.ingenuity.com). In the present study we analyzed the highest scoring network from each time point ($N = 35$) alongside the yeast transcriptional network ($N = 30$) as a benchmark for RBN modeling (Lee et al., 2002). The yeast transcriptional network represents potential pathways that yeast cells can use to regulate global gene expression. It provides a useful comparison for our analysis for a number of reasons. First, it was constructed by determining experimentally the binding sites of most of the known yeast TFs. In addition to being comprehensive, the yeast network is of similar size to the LTP networks identified by IPA. Finally, it has been used previously in the literature for RBN models (Kauffman et al., 2003; Karlsson and Hörnquist, 2007; Tuğrul and Kabakçıoğlu, 2010). For a node (gene), the number of incoming connections (edges) is called the in-degree of the node and the number of outgoing connections (edges) is its out-degree. The analyses using RBNs were also applied to two different sets of null-hypothesis random networks. First, an ensemble of 100 random networks was generated for each of the 4 biological networks studied (20 min, 5 h, 24 h, and yeast) by preserving the same number of nodes and edges. In order to construct these random networks, pairs of genes are connected randomly with equal probability from the list of $N = 35$ or $N = 30$ genes until the total number of edges of the biological network has been set.

A more stringent control consisted of 4 ensembles of 100 rewired networks constructed such that each of the genes had the same in- and out-degree as the biological network. These networks are constructed by randomly choosing two edges of the biological network and swapping them so that A$\rightarrow$B and

C→D, become A→D and C→B. Swapping is prevented if either A→D or C→B exist already (Kannan et al., 1997). Hence, these sets of rewired networks preserve not only the number of genes and the total number of interactions, but also the original degree sequence and hence their local connectivity is identical to the biological network. These controls allowed us to discriminate the effects of the network's local structure from the effects of the general topology on the robustness.

2.2. Random Boolean Networks

RBNs represent one of the simplest models for gene regulatory networks (Kauffman, 1969). We assumed the expression of each gene in a network to be only "on" or "off" values (corresponding to transcriptionally active and transcriptionally inactive). If we define the state of the network as the set of values of expression of all the genes, for a network of size N, a bit vector $G(x_1, \ldots, x_N)$ with $x = 0, 1$ suffices to fully describe it. We implemented the connectivity of a given network as a matrix W of size $N \times N$ where $w_{ij} = 1$ if gene j acts upon gene i, and $w_{ij} = 0$ otherwise.

To model the gene expression dynamics of the network, we allowed the vector G to evolve across discrete time steps. We considered the value x_i of the gene i at a certain time step t to be dependent only on the values at $t - 1$ of the k_i genes that act on it. For each gene in the network, hence, a fixed Boolean function b_i mapped every possible combination of values of the k_i inputs of i to an updated value for the gene i.

On each interaction, we updated all the values of the state vector G synchronously. This means that given a set of values for the state vector $G(t)$ and a set of Boolean functions B, the dynamics of the system are deterministic and the number of possible states for G is discrete. Furthermore, it is known that using synchronous RBN dynamics leads to the expression values of the genes to converge into a number of recurring states or attractors. Crucially, these states can be regarded as different homeostatic cell states (Kauffman, 1993). The size and number of these attractors characterize the dynamical stability of a network. Note that while we allowed the values of the genes in the network to evolve over time, we kept the connectivity W and the set of Boolean functions fixed.

The choice of the synchronous Boolean approximation was guided by an optimal compromise between both conceptual simplicity and computational feasibility, while still holding the capacity to approximate a general stability characterization of a biological network (Kauffman et al., 2003). Indeed, since the gene networks studied were built based on gene expression profiles that represent averages of gene product, a choice of an asynchronous stochastic schema is difficult to justify.

The networks studied using RBN in the present work (see Section 2.1) do not convey any information on the rules for the interactions that could be used to constrain the sample space of all possible Boolean functions. However, as the present study deals with the comparison of the stability conferred by the architecture of specific networks, it suffices to construct the Boolean functions from a flat distribution. Namely, we opted not to introduce a bias in the outputs of the Boolean functions. This means that for a given Boolean function b_i the probability of the output being one of a particular combination of input values is $P(b_i = 1) = 0.5$.

2.3. Dynamical Robustness

In general, we consider a stable network one in which small perturbations are not amplified in time but rather converge into the same attractor. In this scenario, arbitrarily changing the values of few genes would not have a dramatic effect—after a few iterations, the perturbed genes would return to their original values. The opposite behavior is also possible. We consider an unstable (or chaotic) network one in which the perturbation of few genes results in a generalized change in expression values after few iterations. To simulate the effect of a perturbation in a network, we first chose a set of initial conditions $G_A(t = 0)$. We generated an additional instance of the network, with the same initial conditions but shifting some of them [a total of $H(t = 0)$ genes] to the opposite Boolean value, so that the two instances $G_A(t = 0)$ and $G_B(t = 0)$ are, in terms of gene expression, $H(t = 0)$ far apart. This measure is known as Hamming distance, and is equivalent to the size of the perturbation. We then ran RBN dynamics in parallel for both G_A and G_B, with the same Boolean functions for τ time steps. We calculated the new updated Hamming distance $H(t = \tau)$ between $G_A(t = \tau)$ and $G_B(t = \tau)$ to establish whether the perturbation converged into the same values, $H(\tau) < H(0)$, or propagated across the network, $H(\tau) > H(0)$. In the study of dynamical RBN systems, these distinct outcomes are said to fall either on the ordered or chaotic regime, respectively (Fox and Hill, 2001).

Different effects of the perturbations are expected with differing network architectures, Boolean functions or specific initial conditions. As we wanted to characterize the contribution of the topology to the stability of the network, we characterized a network by recording the effects of a perturbation over a large number of initial distances $H(0)$, initial conditions $G_A(t = 0)$ and $G_B(t = 0)$, and random Boolean functions.

In order to visually represent the average effect of perturbations in a particular network, we plotted $H(0)$ (size of the perturbation at the beginning of the parallel runs, x-axis) against $H(\tau)$ (y-axis), where τ is a small number of discrete steps. Plotting different values of $H(0)$ (sampling different perturbation sizes) results in a Derrida plot, a popular tool used in RBNs (Derrida and Weisbuch, 1986). While some network architectures tend to absorb small perturbations and the final Hamming distances $H(\tau)$ are on average smaller than the initial perturbation, some topologies tended to amplify them—few genes with different values of expression lead to dramatically different network states. Crucially, in the Derrida plots these different behaviors fall in the opposite halves of the plot, with robust architectures represented by curves underneath the diagonal, $H(0) > H(\tau)$, and sensitive architectures above, $H(0) < H(\tau)$ (Fox and Hill, 2001), and a network whose Derrida mapping appears tangent to the diagonal is said to exhibit criticality. Note that choosing small integer values for τ (shorter dynamics) captures the effects of the network's local geometry, while larger values reflect the general characteristics of the structure of the network, since information has more time to spread across the network (Aldana et al., 2003). In practice, the slope for the small $H(0)$ region reveals the average outcome of a small perturbation. Curves below the diagonal indicate a tendency toward stability (ordered regime) whereas curves above

imply instability (chaotic regime). The diagonal $H(0) = H(\tau)$ represents the transition from order to chaos.

To construct the Derrida plots, for a given network we assigned 1000 random sets of Boolean rules and for each set of randomly generated rules we ran 100 parallel simulations with random initial values, uniformly sampling different values of $H(0)$. We did not imply any structure in the Boolean rules and these were randomly generated from a flat distribution without any explicit bias.

2.4. Gene Co-expression Network Construction

Using the gene expression profiling data obtained from Ryan et al. (2011) differentially expressed genes were ranked according to the significance of their *p*-value. For computational reasons and to enhance the signal in the data, we used only the top 1700 genes of each of the temporal contrasts. The contribution to the final list of each of the different time groups was equivalent in terms of number of genes, and resulted in a set of differentially expressed genes across early and late LTP of 4804 genes with *p*-values ranging from 7.7×10^{-6} to 6.7×10^{-2}. The total number of genes used for network construction analysis is in the same order of magnitude of other co-expression studies (e.g., Ghazalpour et al., 2006).

For the formation of a gene co-expression network for each of these time points we followed the weighted gene co-expression network analysis (WGCNA) protocols (Zhang and Horvath, 2005) as implemented in the WGCNA package of R software (Langfelder and Horvath, 2008). Briefly, for every pair of genes *i*, *j* the Pearson correlation is calculated and transformed into an adjacency measure with a power function, which serves to further separate the highly co-expressed pairs from the weakly co-expressed pairs. We used the scale-free topology criterion to choose the soft threshold $p = 5$ for the adjacency measure calculation (Zhang and Horvath, 2005). As a measure of connectedness, the topological overlap (TO, Ravasz et al., 2002) was used to compute the similarity between genes, resulting in four undirected weighted networks of the same size ($N = 4804$) but with varying connectivity values of TO—control (unstimulated hemispheres), 20 min, 5 h, and 24 h. TO can be understood as a measure of "agreement" between the nearest-neighbors of two genes. It has been shown to be one of the most biologically meaningful similarity measures used in gene co-expression analysis (Ravasz et al., 2002).

2.5. Identification and Characterization of Gene Co-expression Modules

For each of the four co-expression networks, we constructed specific gene co-expression modules, clusters of densely interconnected genes. This analysis provided a summary of the networks by reducing their complexity to a small number of modules uncovering potential biological associations. For each of the four co-expression networks, we performed a hierarchical clustering using TO as a similarity measure. The branches of the resulting dendrogram were cut using the default parameters implemented in the WGCNA R package (Langfelder and Horvath, 2008). Modules were considered for further analysis if they contained at least 50 genes. Note that the intersections between the modules are not always empty since module detection was performed independently on each temporal expression dataset. As larger modules in the control and 20 min samples appear to segregate into different sets of genes, we chose to keep all the modules and not to merge overlapping modules (see Supplementary Figure S1). Intramodular functional enrichment was calculated using the topGO R package (Alexa et al., 2006) with with a significance criteria of $p < 0.01$ (Fisher's exact test).

2.6. Co-expression Network Reconfiguration

For each of the 58 modules obtained by WGCNA, we quantified the modular differential connectivity (MDC, Zhang et al., 2013), which corresponds to the ratio of the average connectivity for any pair of module-sharing genes at time T_1 compared to that of the same genes at time T_2 where w_{ij} is the TO between two genes in a given network. The statistical significance was assessed by a false discovery rate (FDR) based on permutation of the gene labels (Zhang et al., 2013). MDC > 1 indicates enhanced co-regulation between genes, whereas MDC < 1 indicates reduced co-regulation. The MDC was calculated for each of the 58 networks for each of the three temporal transitions (control $\rightarrow$ 20 min, 20 min $\rightarrow$ 5 h, 5 h $\rightarrow$ 24 h).

3. Results

3.1. Dynamic Stability of Temporal LTP Networks

3.1.1. Gene Networks Recruited Earlier Following LTP have a More Unstable Architecture

To test the hypothesis that the gene networks induced more rapidly following LTP *in vivo* show a less stable architecture when compared to the network induced later, we have drawn on data from our previously published microarray data studies Ryan et al. (2011, 2012). To understand the complexity of the gene networks regulated following the induction of LTP, we used Affymetrix DNA microarrays to identify genes differentially expressed at 20 min, 5 h, and 24 h post-LTP induction *in vivo* Ryan et al. (2011, 2012). Analysis of the gene regulatory networks derived using IPA suggested that these networks made an important contribution to the stabilization of LTP. Furthermore, not only were subsets of genes confirmed to be differentially expressed by quantitative qPCR, but also specific microRNA predicted to act as key regulatory hubs within these networks were shown to be differentially expressed in the hours following LTP induction (Ryan et al., 2013; Joilin et al., 2014). Here, we have used RBN modeling to assess the stability of the architecture of the three highest scoring networks as identified by IPA at each time point. These networks were analyzed alongside the yeast transcriptional network as a benchmark for RBN modeling (Lee et al., 2002; Kauffman et al., 2003; Karlsson and Hörnquist, 2007; Tuğrul and Kabakçıoğlu, 2010).

Consistent with our hypothesis, the output of the RBN analysis (**Figure 1**) demonstrates that the network identified 24 h following LTP induction is considerably more ordered than either of the earlier networks (20 min and 5 h) or the RBN benchmark, the yeast transcriptional network. The curve corresponding to the late (24 h) network lies underneath the

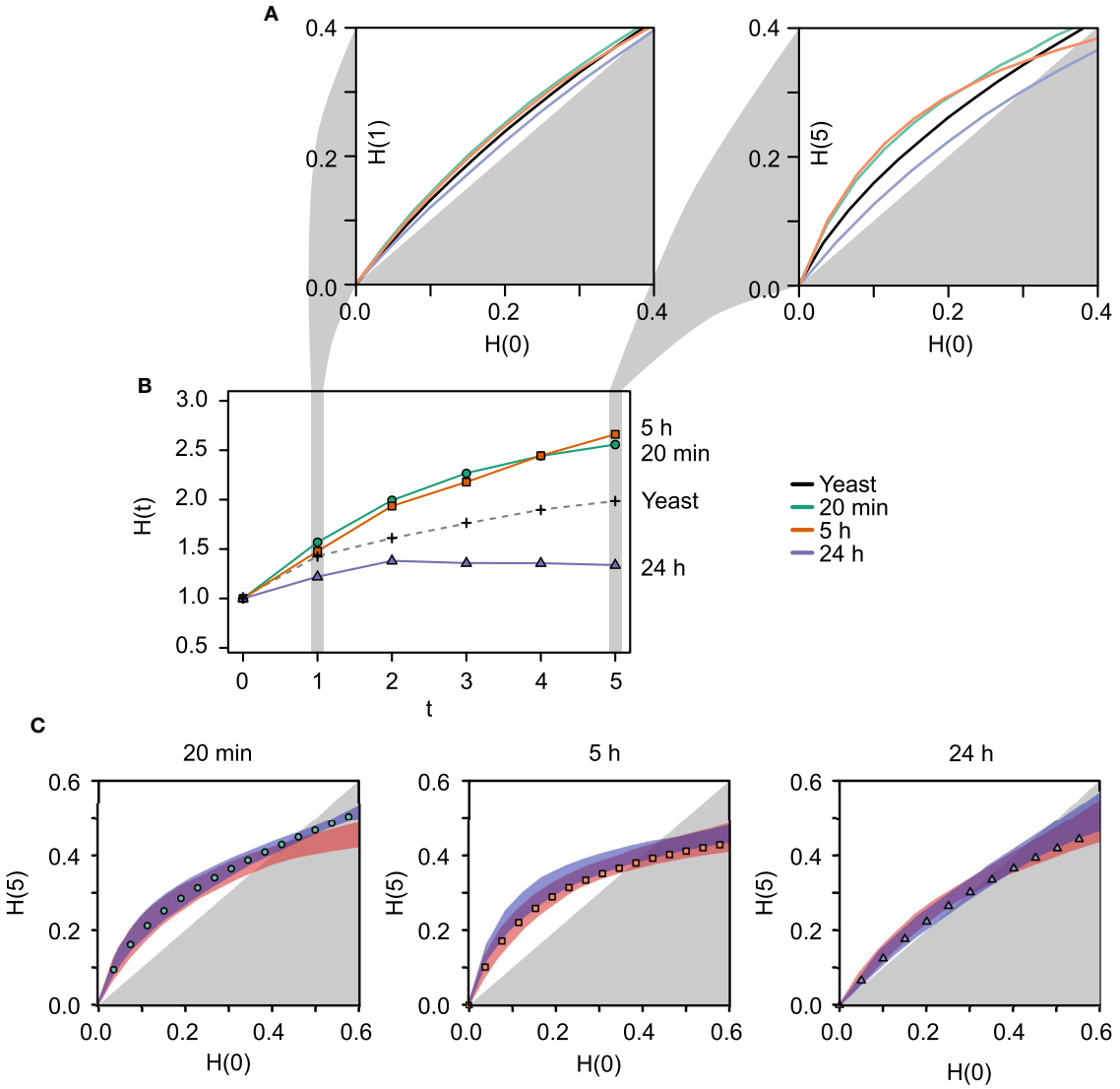

FIGURE 1 | Results of the RBN dynamical stability analysis. (A) Derrida plots for the LTP networks previously identified by Ryan et al. (2011, 2012) at different times post-LTP induction (20 min, 5 h, 24 h in green, orange, and blue, respectively) and the yeast transcriptional network (black). The left plot corresponds to the initial Hamming distance $H(0)$ plotted against the Hamming distance after 1 iteration, $H(1)$. Hence, only the nearest-neighbor interactions (local motifs) affect the dynamics. The right plot depicts $H(0)$ *vs* $H(5)$, where long-distance indirect influences between genes have an effect on the dynamics. Longer dynamics allow to reveal the influence of the overall network structure on its stability. The earlier networks (20 min and 5 h) are more unstable than the 24 h network, and the curve corresponding to the latter lies near the diagonal of the plot, which represents the border between the chaotic (white background) and the ordered regime (gray background). **(B)** Average time evolution of perturbed fixed points starting from Hamming distance $H(0) = 1$. This small difference tends to be amplified in these biological networks. The latest network recruited following LTP induction (24 h, blue), shows a less pronounced tendency to amplify the perturbation. Furthermore, from $t = 2$ to $t = 5$ the Hamming distance shows a slight decrease. The yeast transcriptional network (black dashed line) lies between the earlier LTP networks and the 24 h. **(C)** Derrida plots for each LTP network and to ensembles of random networks. The same stability profile shown in **(A)** for $H(0)$ *vs* $H(5)$ is shown separately for each of the temporal networks. The range of stability exhibited by the two ensembles of random networks (red shade: same number of nodes randomly connected by the same number of edges; blue shade: same number of nodes, same number of edges, and same in- and out-degree). These contrasts allow to isolate the effect of the specific degree sequence from the effect of the average degree (blue shade vs. red shade). In addition, it shows that if an evolutionary constraint were to act on the degree sequence, the real networks choose the less unstable option among all the possible network architectures with the same degree sequence (namely identical local motifs, blue shade). Each point in the plots is the average over 1000 random rule assignments for 100 random initial conditions (increasing these numbers has no effect on the results). Shades for random networks (red) and rewired networks (blue) correspond to the ranges observed using 100 topologies for each. Hamming distances are normalized by the number of nodes.

others, which means that the average outcomes of perturbations to the gene expression levels do not spread across the network to the same extent (**Figure 1A**; $\tau = 1$). This observation is even more apparent if the simulations are evolved for more iterations, allowing the new values for the gene expression to be used as inputs for next iteration (**Figure 1A**; $\tau = 5$) before plotting

the Hamming distances $H(0)$ *vs* $H(\tau)$. This amplification of the differences between the temporal networks with longer dynamics indicates that both local motifs and long-distance interactions contribute to the differential stability observed between the temporal networks.

The same conclusion can be drawn from the panel depicted in **Figure 1B**, where the average Hamming distance of changing one random gene [$H(0) = 1$] is plotted at each consecutive time step. In other words, the two network states differing in only one position are independently evolved over 5 time steps and the distances are monitored at each time step. The amplification of the perturbation is clearly less pronounced than the one observed for the other networks, the yeast network lies between the earlier networks (20 min and 5 h) and the more stable 24 h network.

3.1.2. Stability of Random and Rewired Versions of the Real Networks

Using a similar RBN model, Kauffman et al. (2003) compared the stability of the yeast transcriptional network with networks of the same number of nodes and edges that also preserved the degree sequence (the same sequence of in- and out-going edges); so-called "rewired" networks. The study demonstrated that the yeast network was more stable than these rewired networks, which suggested that an evolutionary pressure may be acting on the network geometry. To assess if that was the case for the temporally specific LTP-related gene networks, we conducted the same analysis by studying the stability of rewired versions of the real networks. We found that the LTP networks lean toward a more ordered regime than their rewired counterparts (**Figure 1C**), in a manner similar to the yeast transcriptional network analysis. Furthermore, we also analyzed the stability of a less constrained set of random networks that only preserve the number of nodes and the number of edges of the real network (see Section 2). This contrast isolates the effect of the specific degree sequence from the effect of the average degree. The plots indicate that the real networks lie in the less unstable margin of the possible network architectures with the same degree sequence (see **Figure 1C**). This observation is particularly marked in the cases of the 5 h and 24 h networks, and supports the idea that the stability is not only dependent on the local structural motifs but rather is distributed across the global architecture of the network (Wagner, 2005).

3.2. Co-expression Analysis

Although analysis of the IPA generated networks has provided validated and biologically meaningful data (Ryan et al., 2011, 2012; Joilin et al., 2014), some limitations are inherent to the methodology. First, potential key interactions may be excluded as the interactions of only 35 genes per network have been considered. Secondly, the architecture of each network is directly dependent upon the information contained within the IPA Knowledge base, a manually curated database, which makes these networks susceptible to false negatives. Thirdly, genes that are modestly but consistently regulated at each time point will be excluded if they do not reach the inclusion criteria at any time. Finally, the analysis is incompatible with the identification of a *control* network, allowing the characterization of a pre-LTP homeostatic state, as networks are based on differentially expressed genes. Thus, to rigorously test our findings that not only are biologically relevant groups of genes regulated following LTP, but that the resultant networks have specific architectural properties and become more stable with time, we used the WGCNA methodology (Zhang and Horvath, 2005) to construct weighted gene co-expression networks based on each of the sample classes (unstimulated hemispheres, 20 min, 5 h, and 24 h stimulated hemispheres). We next assessed the connectivity distributions within these networks.

3.2.1. Identification of Co-expression Modules

Co-expression matrices were formed using TO as a similarity measure, which represents the degree of "connectedness" between two genes (**Figure 2**). The top hubs in the co-expression networks according to their degree (TO with the other genes in the network are shown in **Table 1**). Within the TO matrices we identified a total of 58 densely connected modules through hierarchical clustering (Control: 9 modules containing between 69 and 2327 genes; 20 min: 9 modules with 64–1184 genes; 5 h: 24 modules with 31–535 genes; 24 h: 16 modules with 42–1164 genes) (see **Table 1** and Supplementary Figure S2). To explore the functional relationships of the genes within these modules, modules were tested for Gene Ontology (GO) term enrichment using the topGO R package. We present a brief summary here and a more comprehensive list in Supplementary Material.

Consistent with our previous analysis, WGCNA identified a number of transcriptional modulators as hubs in the 20 min co-expression modules. Our results stress the importance of the *Egr* family, previously reported to be expressed following LTP induction (Cole et al., 1989; Richardson et al., 1992). In particular, *Egr1* appears among the top 10 hubs of the overall 5 h co-expression network (see **Table 1**). In addition, *Wt1*, a member of the same family, appears as a key regulator in one of the co-expression modules (see Supplementary Figure S2, module brown_20). Its role as a repressor of the other *Egr* family members (Haber et al., 1991) suggests that it may play an important role in regulating *Egr* gene expression after LTP. Similarly, the *Homer* family of TFs has been implicated in LTP (Kato et al., 1997) and *Homer2* appears as a hub in a co-expression module activated at 20 min and 24 h (see Supplementary Figure S2, module turquoise_24).

A representative GO term for each module is shown in **Table 2**. Functions overrepresented in the modules identified at 20 min show "positive regulation of endocytosis," "neuron part and cytoplasmic microtubule," "axogenesis," "calmodulin-dependent kinase activity," and "transcription from RNApolI promoter" among others. At 5 h, "CNS neuron axonogenesis," "anion homeostasis and synapse assembly" are salient overrepresented functions. Regulation of gene expression is represented by the GO terms "regulation of DNA methylation" and "chromatin DNA binding," "histone H3-K27 methylation." Finally, modules identified at 24 h show "neuron projection membrane," "histone demethylation," and "response to calcium" among others.

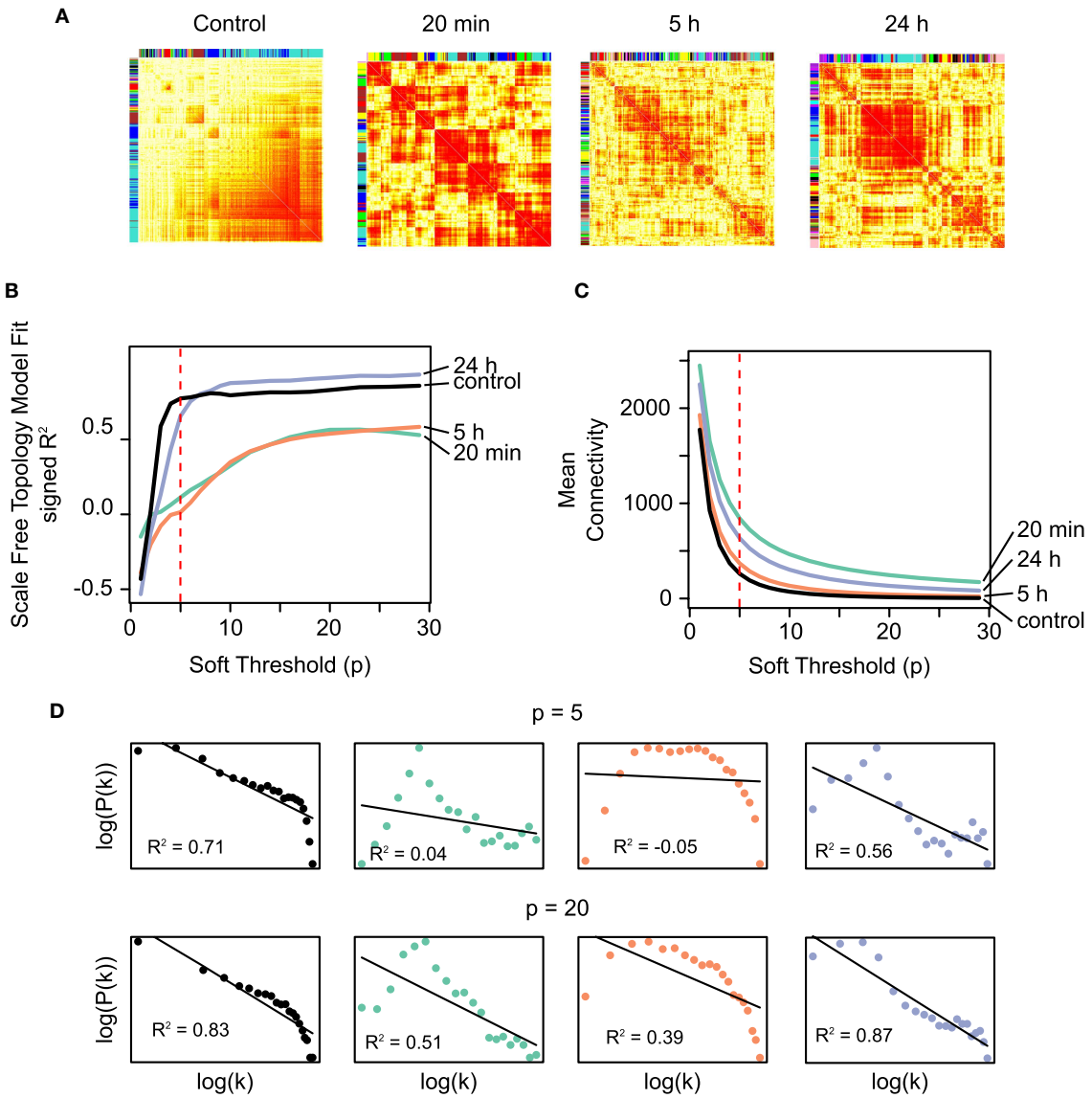

FIGURE 2 | (A) The co-expression networks ($N = 4804$) corresponding to the different temporal microarray datasets (control, 20 min, 5 h, 24 h) represented as heatmaps. The darker shade of red represents higher TO values between a pair of genes at that particular time. The TO measure represents the degree of "connectedness" between two genes, and it is based on the adjacency measure calculated from the Pearson correlation (see Section 2). **(B)** Scale-free fit index as a function of the soft-thresholding power p for the co-expression networks constructed using the time-course microarray data. The R^2 fit to a scale-free distribution of the unstimulated control and the 24 h networks (black and blue curves, respectively) are both higher and saturate at lower values of p than the earlier networks (20 min and 5 h co-expression networks, green and orange, respectively). The latter reaches a saturation only of around $R^2 = 0.5$. Scale-free networks have been shown to be more robust against small random perturbations, while at the same time are sensitive to specific directed perturbations, which confers them a high degree of sensitivity to meaningful signals. These results are in agreement with the notion drawn from the results using RBNs on the IPA networks. **(C)** Mean connectivity as a function of the soft-thresholding power p. While the temporal co-expression networks fall into two different categories according to their scale-free distribution fit, the average connectivity does not show a clear temporal-specific pattern. The dashed lines in the plots indicate the value of $p = 5$, chosen to conduct the module identification. **(D)** Fraction of nodes with degree k in the above co-expression networks using $p = 5$ and $p = 20$. These degree distributions are log-transformed both in the x- and y-axes. The black lines represent the linear model fit with the values of R^2.

3.2.2. Scale-free Distributions are Distinctive in the Pre-LTP and 24 h LTP Co-expression Networks

It is widely accepted that biological networks tend to have connectivity distributions that approximate scale-free distributions (Jeong et al., 2000), which define networks with few highly connected nodes and many sparsely connected nodes (Barabási and Albert, 1999). This structural property may be selected for in biological networks due to its robustness against

TABLE 1 | Top hubs in the co-expression networks according to their degree (TO with the other genes in the network).

Probe ID	Gene symbol	Gene title
20 MIN NETWORK		
1395900_at	Chtf8	CTF8, chromosome transmission fidelity factor 8 homolog (*S. cerevisiae*)
1385824_at	Cep350	centrosomal protein 350
1381003_at	Ikzf2	IKAROS family zinc finger 2
1386234_at	NA	NA
1391555_at	Ncoa3	nuclear receptor coactivator 3
1388079_at	Cacng8	Ca^{2+} channel, voltage-dependent, gamma subunit 8
1388684_at	Fnbp4	formin binding protein 4
1382979_at	NA	NA
1387435_at	St8sia3	ST8 alpha-N-acetyl-neuraminide alpha-2,8-sialyltransferase 3
1387795_at	Pola2	polymerase (DNA directed), alpha 2
5 H NETWORK		
1384230_at	Krtcap3	keratinocyte associated protein 3
1374827_at	Ndst2	N-deacetylase/N-sulfotransferase (heparan glucosaminyl) 2
1383540_at	NA	NA
1384860_at	Zfp84	zinc finger protein 84
1394492_at	RGD1563482	similar to hypothetical protein FLJ38663
1368005_at	Itpr3	inositol 1,4,5-triphosphate receptor, type 3
1371697_at	Pnpla2	patatin-like phospholipase domain containing 2
1368229_at	Sip1	survival of motor neuron protein interacting protein 1
1385928_at	Smad6	SMAD family member 6
1368321_at	Egr1	early growth response 1
24 H NETWORK		
1369067_at	Nr4a3	nuclear receptor subfamily 4, group A, member 3
1369398_at	Naaladl1	N-acetylated alpha-linked acidic dipeptidase-like 1
1369255_at	Il1r1	interleukin 1 receptor, type I
1384999_at	Lce1d	late cornified envelope 1D
1371003_at	Map1b	microtubule-associated protein 1B
1369237_at	Slc6a7	solute carrier family 6 (neurotransmitter transporter, L-proline), member 7
1380864_at	NA	NA
1397942_at	Cdc37l1	cell division cycle 37 homolog (*S. cerevisiae*)-like 1
1370641_s_at	Cacna1i	Ca^{2+} channel, voltage-dependent, T type, alpha 1I subunit
1377276_at	Cdk5r2	cyclin-dependent kinase 5, regulatory subunit 2 (p39)

random perturbations while retaining a high sensitivity to directed signals (Albert et al., 2000). From a perspective in which LTP is considered as a high-level switch, these characteristics are to be expected of the genetic networks associated with the pre- and post-LTP homeostatic states. On the contrary, it is plausible that transient topological rearrangements taking place during the transition exhibit architectures that depart from a scale-free architecture.

The WGCNA methodology transforms the correlation between the profiles of expression of two genes into an adjacency measure using a power function. The degree distribution of the network is hence dependent on the choice of the parameter p for the power function. To examine this dependency and characterize the temporal networks in terms of their resemblance to scale-free networks, we plotted the scale-free fit index of each temporal network (control, 20 min, 5 h, 24 h) as a function of the parameter p (**Figure 2B**). The results demonstrate that the networks reach an asymptotic maximum fit at different values of p, with the unstimulated control and the 24 h networks saturating earlier ($p \approx 5-10$) than the 20 min and 5 h networks ($p = 20$). In addition, the saturation value of the scale-free fit coefficient is higher for the control and 24 h than for the 20 min and 5 h networks. In summary, the control and the 24 h networks fit to a greater degree to a scale-free distribution, independently of the average connectivity (**Figure 2C**). Furthermore, a closer inspection to the scale-free model fit for the values of $p = 5$ and $p = 20$ reveals that the earlier networks following LTP stimulation (20 min, 5 h), have few nodes with a low degree (truncated left side of the distribution) (**Figure 2D**).

3.2.3. Changes in Connectivity Parallel Gene Up-regulation Following LTP

Interestingly, the co-expression networks corresponding to the later times (5 h and 24h) appear to be more dissociated than the earlier networks (control and 20 min), splitting up into more modules for the same power threshold (see **Table 2**).

The modular differential connectivity (MDC, Zhang et al., 2013) corresponds to the ratio of the average connectivity for any pair of module-sharing genes at time T_1 compared to that of the same genes at time T_2 where w_{ij} is the TO between two genes in a given network. We calculated the MDC in the 58 co-expression modules across each temporal transition—control → 20 min, 20 min → 5 h, and 5 h → 24 h. The findings are summarized in **Figure 3**. While the fraction of modules with a significant increase in MDC is similar along the time samples, the fraction of modules with a significant loss of connectivity increases with time (stacked bars plot, **Figure 3D**).

The rapid response elicited after LTP induction at the gene expression level corresponds to the transition observed between the control and the 20 min dataset in terms of MDC. Out of the 58 modules, 57 show a gain of connectivity (MDC > 1), of which 20 are significant with FDR < 10% (a more strict FDR < 1% gives still a total of 10 significant modules). This marked increase in the average TO connectivity takes place in combination with the documented enrichment in up-regulated genes within the set of differentially expressed genes (Ryan et al., 2011).

Our results, however, highlight a global loss of connectivity between the 20 min and 5 h networks (0.187–0.089 average TO, respectively). Yet, the proportion of modules exhibiting gain/loss/conservation of connectivity is very similar (17/17/24, respectively). More interestingly, the fraction of the modules with a significant loss of MDC corresponds to modules that showed an increase in MDC in the earliest transition. These modules subsequently undertake a loss of connectivity in the final transition to the 24 h phase.

TABLE 2 | Summary of the modules identified by WCGNA with at least 50 genes.

Module	Size	Functional category	Top genes by k_{TO}
cyan_24	97	endosome transport	Nog, Thbd, Zscan10
green_U	206	cation transmembrane transport	Camk4, St6gal1, Slc31a1
black_20	329	(+) reg. of endocytosis	Arhgap27, Kdm5b, Acrv1
brown_24	459	cofactor transporter activity	Mast2, Mlst8, Fgd2
black_24	269	epitelial polarization	Cpn1, Thoc2, Pqlc3
brown_20	730	neuron part and cytoplasmic microtubule	Ddi2, Atp5i, Rab22a
red_20	455	axogenesis	Slc10a5, Tnfrsf17, Slc4a11
yellow_U	222	BRCA1-A complex	Acap2, Dr1, Alpk3
blue_20	779	leukocyte activation	Pias2, Atp6v1b2, Pdzd3
green_20	461	response to axon injury	Igha, Tp53bp1, Tal1
pink_20	78	calmodulin-dependent kinase activity	Lmo2, Pacsin1, Hmox3
yellow_20	724	transcription from RNApoII promoter	Ndst2, Kcnj12, Ptpn7
turquoise_20	1184	oxidoreductase activity	Brpf1, Tsta3, Kdelc1
blue_24	753	reg. of endocrine process	RT1-Da, Mrpl14, Ccnd1
turquoise_24	1164	neuron projection membrane	Ak3, Cacna1i, Rbm4
black_U	145	activation of prot kinase and membrane	Znf609, Cd24, Dab2
pink_24	238	fatty-acyl-CoA binding	Gtf3c6, Ak3l1, Ap2a2
yellow_24	355	proteasomal protein catabolism	Qtrt1, Sh3glb1, Hira
magenta_U	69	integrin binding	Uba6, Samd14, Atrx
pink_U	72	mitochondrial transport and apoptosis	nod3l, Rnasen, Glce
green_24	281	histone demethylation	Gls, Junb, Fam135a
brown_U	691	synapse and reg. of secretion	Alox5, Kcnj4, Dhrs9
greenyellow_24	143	tau-protein kinase activity	Hspb3, Hist2h2be, Hiat1
magenta_24	212	proteasomal protein catabolism	Hectd1, Nans, Sec1
midnightblue_24	86	clathrin-coated endocytic vesicle	Reg3a, Dimt1l, Ctrc
red_24	278	septin complex	Crcp, Cc2d1a, Pdia6
purple_24	175	cAMP-mediated signaling	Epor, Xpnpep3, Fam120b
blue_U	836	dephosphorylation and DNA binding	Gabra5, Cdkn2c, Kl
blue_5H	521	amino acid biosynthesis	Scn11a, Abi3, Clec10a
lightyellow_5H	88	CNS neuron axonogenesis	C1qtnf3, Fbln1, St8sia3
black_5H	237	anion homeostasis and synapse assembly	Slc2a4, Pdzd4
cyan_5H	142	reg. of DNA methylation	Fmod, Fam135a, Ankrd6
magenta_5H	208	progesterone receptor signaling	Mrpl35, Prkd3, Cul5
green_5H	336	GTP-Rho binding and mitochondrion	Prelid2, Prl2b1, Abca8
lightgreen_5H	95	T cell migration	H3f3b, Cnih2, Trps1
yellow_5H	358	chromatin DNA binding	Arglu1, Mccc1, Tmem206
turquoise_5H	535	DNA catabolism	Crhr1, Kdm6b, F8
purple_5H	165	histone H3-K27 methylation	Fgf21, Adcy4, Klhl22
salmon_5H	151	oxidoreductase activity	Hs3st2, Hdac5, Ccdc115
tan_5H	158	MAPK import into nucleus	Asb1, Tpr, Pex5l
brown_5H	458	K^+ transport and Ras GTPase binding	Dhh, Cog7, Dgki
greenyellow_5H	162	response to Ca^{2+}	Flrt3, Cnga1, Adra1d
red_U	178	reg. of GTPase activity	Nppa, Cyp8b1, Igfbp2

Size, representative GO term and top genes according to their degree are reported for each module.

4. Discussion

Complex biological networks are expected to maintain a certain level of stability against environmental perturbations. Whereas some classically studied mechanisms such as gene redundancy and epistasis suggest that the dynamical properties of biological networks are restricted to small sets of genes (Sanjuán et al., 2004; Moore, 2005), other authors point in the direction of a "distributed robustness" scenario suggesting that all the regulatory interactions among genes play a role in the dynamical characterization of the network (Shmulevich et al., 2005; Wagner, 2005). These studies suggest that stable, robust attractors for genetic networks may underlie homeostatic cell states. Likewise, the capacity to generate a new phenotype by sensing specific

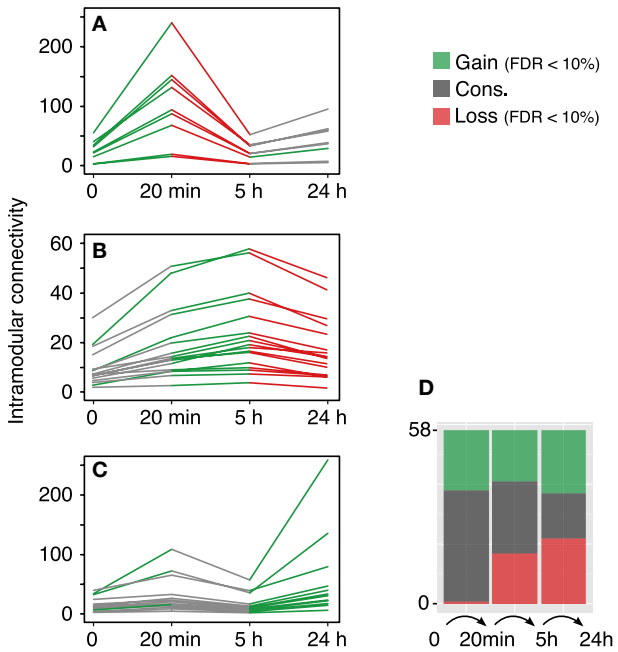

FIGURE 3 | Module reconfiguration following LTP. (A) Modules identified using the 20 min co-expression data all share a similar trend—they become tightly co-regulated at 20 min to lose the connectivity at 5 h. **(B)** Modules identified at 5 h exhibit a significant decrease in TO at 24 h. **(C)** Modules identified using the 24 h data together with two modules identified with the control data show a significant gain in intramodular connectivity at 24 h. Green lines represent significant gain of intramodular connectivity (MDC > 1, FDR < 10%) and red lines represent significant loss of modular connectivity (MDC > 1, FDR < 10%). Gray lines represent no statistical significance for the MDC. **(D)** Distribution of modules with gain, loss or conservation of intramodular connectivity.

environmental signals represents a crucial property of living organisms. The apparent antagonistic relationship between robustness and sensitivity could potentially be eased by rewiring the network architecture or by bringing other networks into operation. Network architectures recruited transiently during phenotypic transitions do not uphold a homeostatic state and conceivably they are not under a selective pressure to exhibit a stable architecture.

While some biological systems are designed to elicit a graded response to an input, other systems show behaviors that resemble multistable transitions. These systems can range from relatively simple switch-like responses to more complex multistable switches (e.g., Ferrell and Machleder, 1998; Pomerening et al., 2003; Yao et al., 2011). During LTP in particular, the cell state needs to transit from a stable point to another stable point. If this assumption holds for the gene expression profile, LTP induction can be seen as the perturbation needed to shift the gene expression equilibrium to the post-LTP attractor. The neuron has to be able to discriminate the changes eliciting LTP from the environmental noise. From this perspective, LTP represents a cellular mechanism, which operates as a switch. The essentiality of the genomic component for the maintenance of late-LTP suggests that the gene regulatory tier of information processing may have characteristics of a high-level switch. Ultimately, other tiers of regulation acting at different levels of organization (networks of neurons and nerve fiber projections between brain areas) act jointly to create, maintain, and retrieve memories.

4.1. Dynamical Stability of Temporal LTP-related Gene Networks

Previous work shows that there is a critical temporal window after LTP induction in which a rapid nuclear response takes place (Nguyen et al., 1994). This early phase is in the order of minutes, and is characterized by a rapid up-regulation of gene expression, which persists for many hours. The network identified 20 min after induction represents these early response genes. The set of genes identified 5 h post-LTP induction are not closely related to the 20 min early responding genes, as demonstrated by the expression profiles (Ryan et al., 2012). The nature of this rapid transcriptional response following LTP induction suggests that the underlying mechanisms are facilitating a switch-like response. In this line, Saha et al. (2011) documented recently the presence of stalled RNA polymerase II in LTP immediate early genes, which they interpreted as a mechanism for the rapid neuronal induction observed. However, other mechanisms may be acting jointly at different levels to complement the gene expression trigger.

The 24 h post-LTP induction represents a temporal and functionally different data set, as indicated both by the lack of overlap in gene expression (Ryan et al., 2012) as well as by the fact that mRNA-synthesis inhibitors are only effective in blocking LTP when delivered 4–6 h after stimulation (Vickers et al., 2005). We hypothesized that if the 24 h network was representative of a new homeostatic state brought about by LTP induction, its architecture should display an enhanced stability. While there seems to be an early critical time window of transcription for the induction of late-LTP (Nguyen et al., 1994; Vickers et al., 2005), the functional significance of gene expression at 24 h may be coupled to the activation and coordination of pathways related to growth and/or neurogenesis (Ryan et al., 2012). The predominant downregulation of gene expression observed at 24 h may be partly responsible for reorganizing the transcriptional layout toward homeostasis.

Using RBN modeling, we found that the networks derived in the early time points (20 min, 5 h) by the IPA software were more labile, while the most significant network derived at 24 h was markedly more stable (see **Figure 1**). Furthermore, the WGCNA showed that the degree of co-expression at the different times evidenced a contrasting distribution of the connectivity. The unstimulated control and the 24 h networks fit to a scale-free distribution fairly well while on the contrary, the co-expression networks corresponding to the 20 min and 5 h datasets displayed a truncated distribution. As higher robustness is expected of scale free distributions (Albert et al., 2000), this observation is consistent with the presence of two different homeostatic states before and after LTP induction, whereas transient topological rearrangements are characteristic of intermediate networks.

Interestingly, this temporal effect on the vulnerability of the networks is mirrored by what is known about the vulnerability of LTP and memory itself. Previous studies have shown that LTP

can be reversed within hours of induction, but then becomes resistant to reversal (e.g., Xu et al., 1998; Manahan-Vaughan et al., 2000; Woo and Nguyen, 2002). It is of particular relevance to our studies that this resistance to reversal is dependent on new protein synthesis. Thus, our new data support the conclusion that the LTP-related gene networks contribute to the stabilization of LTP.

These results reinforce the view by which the architecture of the networks is under a selective pressure. Yet the contribution of the structural properties to the overall robustness of biological circuits remains to be further clarified—this tendency toward the stable regime represents only one mechanism yielding robust behavior and does not rule out other genetic mechanisms (Wagner, 2005).

4.2. Functional Analysis of WGCNA Modules

While LTP is considered the gold standard model for the cellular mechanism underlying long-term memories, it is becoming clear that LTP encompasses a family of different processes by which neurons integrate and process the information to change their synaptic weights. For example, it has been argued recently that in the Schaffer collateral-commissural pathway at least three mechanistically different forms of synaptic plasticity co-exist, all N-methyl-D-aspartate (NMDA) receptor-dependent (Park et al., 2014). These forms can overlap partially in time, and the combination of these processes can increase their functional utility. In turn, a specific form of LTP consists of a number of mechanistically distinct phases that operate at different levels of organization and time scales. This should come as no surprise if we recognize that neurons capable of modifying the synaptic efficacy for long periods of time are to overcome the limitations imposed by protein and mRNA half-life, typically in the scale of minutes or hours. In contrast to the TFs, which act in the nucleus, some effector genes exert their functions in the distal axonal and dendritic extensions. The translocation of mRNA granules to the synaptic terminals, for example, carries a significant temporal lag between transcription and translation (Knowles et al., 1996; Steward and Schuman, 2003). The control of gene expression must act in coordination with the different time constraints posed by the different subcellular destinations. It is reasonable to assume that the genes transcribed following LTP are effectively being translated at different times and in different subcellular loci.

While understanding the genomic component underlying LTP has been the focus of recent research using differential expression analysis (Lee et al., 2005; Park et al., 2006; Ryan et al., 2011, 2012), these methods are more error-prone for genes with a large expression variation than co-expression analysis. Potentially, genes which are not detected by differential expression can be detected by co-expression if they activate other genes which change enough to be detected. Arguably, a pair of genes with a high value of co-expression are likely to be forming complexes, pathways, or participate in the same cellular circuits (Eisen et al., 1998). Using WGCNA we found that the rapid increase in gene expression observed by the differential expression analysis is complemented by the increase in intramodular connectivity. Out of the 58 modules identified by WGCNA, only one exhibits a significant decrease in average TO from the control to the 20 min time point, while a total of 20 show a significant increase. This suggests that the rapid genomic response that follows LTP induction does not only involve a marked up-regulation of gene expression, but also a tight coordination of the components that ultimately allow the transition to a new homeostatic cellular state. The transitional 5 h dataset shows a loss of intramodular connectivity that parallels the onset of a general down-regulation of gene expression, similarly to the 24 h co-expression network. We believe that the early phase following stimulation is critical in the onset of the genomic changes that are known to be essential for late-LTP. A fundamental fraction of the genes that are transcribed rapidly after LTP induction may be of crucial importance at later times (Nguyen et al., 1994).

The functional analysis confirms the central role of the *Egr* and *Homer* families in LTP consolidation and maintenance. Changes in transcription are also likely to be driven by the constitutive transcription factor NFKB in a transcription-independent manner. In fact, our results are consistent with its peaks in activity observed in learning paradigms. In agreement with previous studies, we found that the control of gene expression following LTP is, at least to a certain extent, driven by epigenetic changes. Furthermore, it appears that epigenetic control does not work in isolation, but rather in conjunction with other mechanisms (Lubin et al., 2011). Our study identifies *Akt* (protein kinase B) in the 20 min dataset even though its expression does not change significantly. The PI3K-Akt-mTOR is regulated via lipid signaling and its role in LTP may have been overlooked in previous studies (although see Sanna et al., 2002). Finally, while regulators of membrane composition are common across all the datasets, neuronal morphological changes are and the amplification of the ubiquitin-proteasome pathway are characteristic of later stages.

4.3. Conclusions

We have presented a view of LTP as a biological process in which a transient signal sets a new homeostatic state that is "remembered" by the cellular systems. Central to this process is the regulation by gene expression, in which the central role played by the *Egr* TFs early after LTP induction was highlighted by differential expression and co-expression analyses. In addition, we found a rapid enrichment in connectivity at 20 min followed by a systematic decrease. This observation provides a potential explanation for the down-regulation of gene expression at 24 h documented by previous studies. From a systems perspective, we have provided evidence that these networks will show less stable architecture, while networks recruited later will exhibit increased stability, consistent with the fact that are more directly related to LTP consolidation. The architecture exhibited by a control and the 24 h LTP co-expression networks fit well to a scale-free distribution, known to be robust against perturbations, whereas the earlier 20 min and 5 h networks showed truncated distributions. Moreover, using the RBN paradigm we have shown that the network derived at 24 h exhibited an enhanced stability when compared to those derived at earlier times post-LTP. This temporal effect on the vulnerability of the networks is mirrored by what is known about the vulnerability of LTP and memory.

Taken together, these results suggest that a new homeostatic state is achieved 24 h post-LTP, and defines an integrated view of the genomic response following LTP induction by which the stability of the networks regulated at different times parallel the properties observed at the synapse.

Supplementary Material

The Supplementary Material for this article can be found online at: http://journal.frontiersin.org/article/10.3389/fnmol.2015.00042

References

Abraham, W. C., and Williams, J., M. (2003). Properties and mechanisms of ltp maintenance. *Neuroscientist* 9, 463. doi: 10.1177/1073858403259119

Albert, R., Jeong, H., and Barabási, A.-L. (2000). Error and attack tolerance of complex networks. *Nature* 406, 378–382. doi: 10.1038/35019019

Aldana, M., Coppersmith, S., and Kadanoff, L. P. (2003). "Boolean dynamics with random couplings," in *Perspectives and Problems in Nolinear Science*, eds E. Kaplan, J. E. Marsden, and K. R. Sreenivasan (New York, NY: Springer), 23–89.

Alexa, A., Rahnenführer, J., and Lengauer, T. (2006). Improved scoring of functional groups from gene expression data by decorrelating GO graph structure. *Bioinformatics* 22, 1600–1607. doi: 10.1093/bioinformatics/btl140

Barabási, A.-L., and Albert, R. (1999). Emergence of scaling in random networks. *Science* 286, 509–512.

Cole, A. J., Saffen, D. W., Baraban, J. M., and Worley, P. F. (1989). Rapid increase of an immediate early gene messenger rna in hippocampal neurons by synaptic nmda receptor activation. *Nature* 340, 474–476.

Derrida, B., and Weisbuch, G. (1986). Evolution of overlaps between configurations in random boolean networks. *J. Phys.* 47, 1297–1303.

Eisen, M. B., Spellman, P. T., Brown, P. O., and Botstein, D. (1998). Cluster analysis and display of genome-wide expression patterns. *Proc. Natl. Acad. Sci. U.S.A.* 95, 14863–14868.

Ferrell, J. E. Jr., and Machleder, E. M. (1998). The biochemical basis of an all-or-none cell fate switch in *Xenopus oocytes*. *Science* 280, 895–898.

Fox, J. J., and Hill, C. C. (2001). From topology to dynamics in biochemical networks. *Chaos* 11, 809–815. doi: 10.1063/1.1414882

Ghazalpour, A., Doss, S., Zhang, B., Wang, S., Plaisier, C., Castellanos, R., et al. (2006). Integrating genetic and network analysis to characterize genes related to mouse weight. *PLoS Genet.* 2:e130. doi: 10.1371/journal.pgen.0020130

Haber, D. A., Sohn, R. L., Buckler, A. J., Pelletier, J., Call, K. M., and Housman, D. E. (1991). Alternative splicing and genomic structure of the wilms tumor gene wt1. *Proc. Natl. Acad. Sci. U.S.A.* 88, 9618–9622.

Håvik, B., Røkke, H., Dagyte, G., Stavrum, A., Bramham, C., and Steen, V. (2007). Synaptic activity-induced global gene expression patterns in the dentate gyrus of adult behaving rats: induction of immunity-linked genes. *Neuroscience* 148, 925–936. doi: 10.1016/j.neuroscience.2007.07.024

Jeong, H., Tombor, B., Albert, R., Oltvai, Z. N., and Barabási, A.-L. (2000). The large-scale organization of metabolic networks. *Nature* 407, 651–654. doi: 10.1038/35036627

Joilin, G., Guévremont, D., Ryan, B., Claudianos, C., Cristino, A. S., Abraham, W. C., et al. (2014). Rapid regulation of microrna following induction of long-term potentiation *in vivo*. *Front. Mol. Neurosci.* 7:98. doi: 10.3389/fnmol.2014.00098

Kannan, R., Tetali, P., and Vempala, S. (1997). "Simple markov-chain algorithms for generating bipartite graphs and tournaments," in *Proceedings of the Eighth Annual ACM-SIAM Symposium on Discrete Algorithms* (Philadelphia, PA: Society for Industrial and Applied Mathematics), 193–200.

Karlsson, F., and Hörnquist, M. (2007). Order or chaos in boolean gene networks depends on the mean fraction of canalizing functions. *Physica A* 384, 747–757. doi: 10.1016/j.physa.2007.05.050

Kato, A., Ozawa, F., Saitoh, Y., Hirai, K., and Inokuchi, K. (1997). Vesl, a gene encoding vasp/ena family related protein, is upregulated during seizure, long-term potentiation and synaptogenesis. *FEBS Lett.* 412, 183–189.

Kauffman, S. (1993). *The Origins of Order: Self-organization and Selection in Evolution*. New York, NY: Oxford University Press.

Kauffman, S., Peterson, C., Samuelsson, B., and Troein, C. (2003). Random boolean network models and the yeast transcriptional network. *Proc. Natl. Acad. Sci. U.S.A.* 100, 14796. doi: 10.1073/pnas.2036429100

Kauffman, S. A. (1969). Metabolic stability and epigenesis in randomly constructed genetic nets. *J. Theor. Biol.* 22, 437–467.

Knowles, R. B., Sabry, J. H., Martone, M. E., Deerinck, T. J., Ellisman, M. H., Bassell, G. J., et al. (1996). Translocation of rna granules in living neurons. *J. Neurosci.* 16, 7812–7820.

Langfelder, P., and Horvath, S. (2008). WGCNA: an R package for weighted correlation network analysis. *BMC Bioinformatics* 9:559. doi: 10.1186/1471-2105-9-559

Lee, P. R., Cohen, J. E., Becker, K. G., and Fields, R. R. (2005). Gene expression in the conversion of early-phase to late-phase long-term potentiation. *Ann. N. Y. Acad. Sci.* 1048, 259–271. doi: 10.1196/annals.1342.023

Lee, T., Rinaldi, N., Robert, F., Odom, D., Bar-Joseph, Z., Gerber, G., et al. (2002). Transcriptional regulatory networks in *Saccharomyces cerevisiae*. *Sci. Signal.* 298, 799. doi: 10.1126/science.1075090

Lubin, F. D., Gupta, S., Parrish, R. R., Grissom, N. M., and Davis, R. L. (2011). Epigenetic mechanisms critical contributors to long-term memory formation. *Neuroscientist* 17, 616–632. doi: 10.1177/1073858410386967

Manahan-Vaughan, D., Kulla, A., and Frey, J. U. (2000). Requirement of translation but not transcription for the maintenance of long-term depression in the ca1 region of freely moving rats. *J. Neurosci.* 20, 8572–8576.

Mestl, T., Bagley, R., and Glass, L. (1997). Common chaos in arbitrarily complex feedback networks. *Phys. Rev. Lett.* 79:653.

Moore, J. H. (2005). A global view of epistasis. *Nat. Genet.* 37, 13–14. doi: 10.1038/ng0105-13

Nguyen, P. V., Abel, T., and Kandel, E. R. (1994). Requirement of a critical period of transcription for induction of a late phase of ltp. *Science* 265:1104.

Park, C. S., Gong, R., Stuart, J., and Tang, S. J. (2006). Molecular network and chromosomal clustering of genes involved in synaptic plasticity in the hippocampus. *J. Biol. Chem.* 281, 30195. doi: 10.1074/jbc.M605876200

Park, P., Volianskis, A., Sanderson, T. M., Bortolotto, Z. A., Jane, D. E., Zhuo, M., et al. (2014). Nmda receptor-dependent long-term potentiation comprises a family of temporally overlapping forms of synaptic plasticity that are induced by different patterns of stimulation. *Philos. Trans. R. Soc. Lond. B Biol. Sci.* 369, 20130131. doi: 10.1098/rstb.2013.0131

Pomerening, J. R., Sontag, E. D., and Ferrell, J. E. (2003). Building a cell cycle oscillator: hysteresis and bistability in the activation of cdc2. *Nat. Cell Biol.* 5, 346–351. doi: 10.1038/ncb954

Ravasz, E., Somera, A. L., Mongru, D. A., Oltvai, Z. N., and Barabási, A.-L. (2002). Hierarchical organization of modularity in metabolic networks. *Science* 297, 1551–1555. doi: 10.1126/science.1073374

Richardson, C., Tate, W., Mason, S., Lawlor, P., Dragunow, M., and Abraham, W. (1992). Correlation between the induction of an immediate early gene, zif/268, and long-term potentiation in the dentate gyrus. *Brain Res.* 580, 147–154.

Ryan, M. M., Mason-Parker, S. E., Tate, W. P., Abraham, W. C., and Williams, J. M. (2011). Rapidly induced gene networks following induction of long-term potentiation at perforant path synapses *in vivo*. *Hippocampus* 21, 541–553. doi: 10.1002/hipo.20770

Ryan, M. M., Morris, G. P., Mockett, B. G., Bourne, K., Abraham, W. C., Tate, W. P., et al. (2013). Time-dependent changes in gene expression induced by secreted amyloid precursor protein-alpha in the rat hippocampus. *BMC Genomics* 14:376. doi: 10.1186/1471-2164-14-376

Ryan, M. M., Ryan, B., Kyrke-Smith, M., Logan, B., Tate, W. P., Abraham, W. C., et al. (2012). Temporal profiling of gene networks associated with the late phase of long-term potentiation *in vivo*. *PLoS ONE* 7:e40538. doi: 10.1371/journal.pone.0040538

Saha, R., Wissink, E., Bailey, E., Zhao, M., Fargo, D., Hwang, J., et al. (2011). Rapid activity-induced transcription of arc and other iegs relies on poised rna polymerase ii. *Nat. Neurosci.* 14, 848–856. doi: 10.1038/nn.2839

Sanjuán, R., Moya, A., and Elena, S. F. (2004). The contribution of epistasis to the architecture of fitness in an rna virus. *Proc. Natl. Acad. Sci. U.S.A.* 101, 15376–15379. doi: 10.1073/pnas.0404125101

Sanna, P. P., Cammalleri, M., Berton, F., Simpson, C., Lutjens, R., Bloom, F. E., et al. (2002). Phosphatidylinositol 3-kinase is required for the expression but not for the induction or the maintenance of long-term potentiation in the hippocampal ca1 region. *J. Neurosci.* 22, 3359–3365.

Shmulevich, I., Kauffman, S. A., and Aldana, M. (2005). Eukaryotic cells are dynamically ordered or critical but not chaotic. *Proc. Natl. Acad. Sci. U.S.A.* 102, 13439–13444. doi: 10.1073/pnas.0506771102

Siegal-Gaskins, D., Mejia-Guerra, M. K., Smith, G. D., and Grotewold, E. (2011). Emergence of switch-like behavior in a large family of simple biochemical networks. *PLoS Comput. Biol.* 7:e1002039. doi: 10.1371/journal.pcbi.1002039

Steward, O., and Schuman, E. M. (2003). Compartmentalized synthesis and degradation of proteins in neurons. *Neuron* 40, 347–359. doi: 10.1016/S0896-6273(03)00635-4

Tuğrul, M., and Kabakçıoğlu, A. (2010). Anomalies in the transcriptional regulatory network of the yeast *Saccharomyces cerevisiae*. *J. Theor. Biol.* 263, 328–336. doi: 10.1016/j.jtbi.2009.12.008

Vickers, C. A., Dickson, K. S., and Wyllie, D. J. (2005). Induction and maintenance of late-phase long-term potentiation in isolated dendrites of rat hippocampal ca1 pyramidal neurones. *J. Physiol.* 568, 803–813. doi: 10.1113/jphysiol.2005.092924

Wagner, A. (2005). Distributed robustness versus redundancy as causes of mutational robustness. *Bioessays* 27, 176–188. doi: 10.1002/bies.20170

Woo, N. H., and Nguyen, P. V. (2002). Silent metaplasticity of the late phase of long-term potentiation requires protein phosphatases. *Learn. Mem.* 9, 202–213. doi: 10.1101/lm.498402

Xu, L., Anwyl, R., and Rowan, M. J. (1998). Spatial exploration induces a persistent reversal of long-term potentiation in rat hippocampus. *Nature* 394, 891–894.

Yao, G., Tan, C., West, M., Nevins, J. R., and You, L. (2011). Origin of bistability underlying mammalian cell cycle entry. *Mol. Syst. Biol.* 7:485. doi: 10.1038/msb.2011.19

Zhang, B., Gaiteri, C., Bodea, L.-G., Wang, Z., McElwee, J., Podtelezhnikov, A. A., et al. (2013). Integrated systems approach identifies genetic nodes and networks in late-onset Alzheimer's disease. *Cell* 153, 707–720. doi: 10.1016/j.cell.2013.03.030

Zhang, B., and Horvath, S. (2005). A general framework for weighted gene co-expression network analysis. *Stat. Appl. Genet. Mol. Biol.* 4:1128. doi: 10.2202/1544-6115.1128

Conflict of Interest Statement: The authors declare that the research was conducted in the absence of any commercial or financial relationships that could be construed as a potential conflict of interest.

frontiers in Molecular Neuroscience

ORIGINAL RESEARCH
published: 04 September 2015
doi: 10.3389/fnmol.2015.00048

Cell biological mechanisms of activity-dependent synapse to nucleus translocation of CRTC1 in neurons

Toh Hean Ch'ng[1,2]*, *Martina DeSalvo*[3], *Peter Lin*[4], *Ajay Vashisht*[3], *James A. Wohlschlegel*[3] and *Kelsey C. Martin*[3,5]*

[1] Lee Kong Chian School of Medicine, Nanyang Technological University, Singapore, Singapore, [2] School of Biological Sciences, Nanyang Technological University, Singapore, Singapore, [3] Department of Biological Chemistry, University of California, Los Angeles, Los Angeles, CA, USA, [4] Department of Neurology and Neuroscience, Stanford University, Palo Alto, CA, USA, [5] Department of Psychiatry and Biobehavioral Sciences, University of California, Los Angeles, Los Angeles, CA, USA

OPEN ACCESS

Edited by:
Benedict C. Albensi,
University of Manitoba, Canada

Reviewed by:
Hansen Wang,
University of Toronto, Canada
Hyunsoo Shawn J. E.,
Duke-NUS Graduate Medical School, Singapore

***Correspondence:**
Toh Hean Ch'ng,
Lee Kong Chian School of Medicine, Nanyang Technological University, 61 Biopolis Drive, Proteos 04-10B, Singapore 130014, Singapore
thchng@ntu.edu.sg;
Kelsey C. Martin,
Department of Biological Sciences, 615 Charles E Young Dr. South, BSRB 354-11, Los Angeles, CA 90095, USA
kcmartin@mednet.ucla.edu

Received: 05 July 2015
Accepted: 18 August 2015
Published: 04 September 2015

Citation:
Ch'ng TH, DeSalvo M, Lin P, Vashisht A, Wohlschlegel JA and Martin KC (2015) Cell biological mechanisms of activity-dependent synapse to nucleus translocation of CRTC1 in neurons. Front. Mol. Neurosci. 8:48. doi: 10.3389/fnmol.2015.00048

Previous studies have revealed a critical role for CREB-regulated transcriptional coactivator (CRTC1) in regulating neuronal gene expression during learning and memory. CRTC1 localizes to synapses but undergoes activity-dependent nuclear translocation to regulate the transcription of CREB target genes. Here we investigate the long-distance retrograde transport of CRTC1 in hippocampal neurons. We show that local elevations in calcium, triggered by activation of glutamate receptors and L-type voltage-gated calcium channels, initiate active, dynein-mediated retrograde transport of CRTC1 along microtubules. We identify a nuclear localization signal within CRTC1, and characterize three conserved serine residues whose dephosphorylation is required for nuclear import. Domain analysis reveals that the amino-terminal third of CRTC1 contains all of the signals required for regulated nucleocytoplasmic trafficking. We fuse this region to Dendra2 to generate a reporter construct and perform live-cell imaging coupled with local uncaging of glutamate and photoconversion to characterize the dynamics of stimulus-induced retrograde transport and nuclear accumulation.

Keywords: CREB, CRTC1, learning and memory, synapse to nucleus signaling, synaptic plasticity, transcription-dependent plasticity, active transport

Introduction

Long-lasting forms of synaptic plasticity, including those underlying long-term memory, require new transcription for their persistence (Kandel, 2001; Alberini, 2009; Leslie and Nedivi, 2011). While neurons are specialized for rapid communication between compartments via electrochemical signaling, activity-dependent transcription is also regulated by the transport of soluble signaling molecules from stimulated synapses to the nucleus (Ch'ng et al., 2012; Karpova et al., 2013). Neurons are highly polarized cells that elaborate processes whose lengths can exceed that of the soma by orders of magnitude. The long-distance transport of signals from stimulated synapses to the nucleus thus requires active, regulated transport mechanisms to couple synaptic stimulation with transcription.

The regulated nuclear import of dendritically and/or synaptically localized transcriptional regulators serves as one means of directly coupling synaptic events with gene expression in the nucleus. Recent studies describe a role for the synapse to nucleus translocation of CREB-regulated transcriptional coactivator 1 (CRTC1) in regulating gene expression during long-term potentiation (LTP) of rodent hippocampal synapses (Zhou et al., 2006; Kovács et al., 2007; Ch'ng et al., 2012; Nonaka et al., 2014). CRTC1 was originally identified in an *in vitro* screen aimed at identifying proteins that enhance the transcriptional activity of CREB in non-neuronal cells (Iourgenko et al., 2003; Screaton et al., 2004). It has diverse functions in the brain including modulation of memory in rodents and flies (Zhou et al., 2006; Sekeres et al., 2012; Hirano et al., 2013; Nonaka et al., 2014), entrainment of circadian rhythms (Jagannath et al., 2013), neuroprotection during ischemia (Sasaki et al., 2011), and regulation of cocaine-induced plasticity (Hollander et al., 2010). Both Huntington's and Alzheimer's diseases have also been linked with CRTC1-mediated activation of CREB transcription of specific target genes (Jeong et al., 2012; Saura, 2012).

We previously reported that CRTC1 undergoes activity-dependent rapid translocation from distal dendrites to the nucleus during long-term plasticity of hippocampal neurons (Ch'ng et al., 2012). We showed that CRTC1 translocation required glutamate receptor activation, involved calcineurin-dependent dephosphorylation of CRTC1, and was critical to the activity-dependent expression of several CREB target genes (Ch'ng et al., 2012). These findings raised many questions about the mechanisms mediating the long-distance retrograde transport of CRTC1 from synapse to nucleus. The experiments described in this study are aimed at addressing these questions. Of note, while previous studies have examined the transport of vesicles and organelles in axons and dendrites (van den Berg and Hoogenraad, 2012; Maeder et al., 2014), much less is known about the cell biological mechanisms mediating the long-distance retrograde transport of soluble molecules in neurons. As such, our study provides insights into not only the transport of CRTC1, but also more broadly the retrograde transport of soluble molecules within dendrites.

We first examine the specific types of stimuli that trigger synapse to nuclear import of CRTC1 and find that it requires activation of glutamate receptors, calcium influx specifically though L-type but not P/Q or N-type calcium channels, and local rather than bulk elevations in intracellular calcium. We then show that CRTC1 is actively transported along microtubules by the dynein motor protein. Using protein domain analysis, we show that the N-terminal 270 amino acids of CRTC1 are sufficient for regulated nucleocytoplasmic localization, and within this region identify a non-canonical nuclear localization signal that is necessary and sufficient for CRTC1 nuclear import. We generate Ser to Ala mutations at three highly conserved Ser residues within the N-terminal third of CRTC1, and show that dephosphorylation of all three residues is necessary and sufficient for dissociation from 14-3-3ε at the synapse and for nuclear accumulation. Finally, we create a viral reporter construct consisting of the N-terminal third of CRTC1 fused to the photoconvertible fluorescent protein dendra2, and perform live cell imaging to visualize and characterize the dynamics of synapse-specific activation of CRTC1 nuclear import.

Materials and Methods

Plasmids and Antibodies

The CMV-mCherry-dynamitin expression vector was kindly shared by M. Meffert (Johns Hopkins, MD; Shrum et al., 2009) while the mCherry plasmid was a gift from R.Y. Tsien (UC San Diego, CA). The 4xGFP construct was a gift from W. Hampe (UMC Hamburg-Eppendorf, Hambug; Seibel et al., 2007). Commercial plasmids include Dendra2 (Evrogen) and CRTC1 (Open Biosystems, Huntsville, AL). Antibodies used in all these experiments include: rabbit polyclonal antibodies against CRTC1 (Bethyl, Montgomery, TX and Proteintech, Chicago, IL), pCRTC1(S151; Bethyl) Dendra2 (Evrogen, Moscow, Russia), TUJ1 (Covance, Princeton, NJ), Dynein heavy chain (Santa Cruz, Dallas, TX), and phosphoCREB-S133 (Cell Signaling); mouse monoclonal antibodies against PSD95 (Thermoscientific, Rockford, IL), synapsin1 (Millipore, Billerica, MA), CamKIIα (Millipore), HA-epitope (Sigma), GAPDH (Fitzgerald, Acton, MA), GFP (Clontech, Mt. View, CA), GAD67 (Millipore), and KPNB1 (ABR, Golden, CO); polyclonal chicken antibody against MAP2 (Phosphosolutions, Aurora, CO) and synaptotagmin (Chemicon, Temecula, CA). All secondary antibodies are conjugated to Alexa dyes (488, 546, 555, 568, and 633; Invitrogen).

Viruses and Expression Constructs

Lentiviral packaging constructs bearing the L22 (*Camk2α*) promoter were kind gifts from Pavel Osten's lab (Dittgen et al., 2004). All production of lentiviral particles is as described in Dittgen et al. (2004). Lentiviral transduction of neurons was carried out in a reduced volume for 24 h before replacement with conditioned medium. The integrated constructs were allowed to express for at least 6 d prior to experiments.

Dissociated Neuron Cultures Protocols and Pharmacological Treatments

All experiments were performed using approaches approved by the UCLA Institutional Animal Care and Use Committee. Unless otherwise stated, all experiments in this report uses mature hippocampal neurons (DIV 21–28) dissected from newborn (P0) rats and plated on poly-DL-lysine (0.5 mg/ml) coated cover slips (Carolina Biologicals, Burlington, NC). Only the siRNA knockdown of dynein heavy chain experiment utilizes cultured mouse neurons. A defined serum-free media was used to culture the neurons: Neurobasal media, (Invitrogen, Carlsbad, CA); β-mercaptoethanol (Sigma, St. Louis, MO); monosodium glutamate (Sigma); B27 (Invitrogen); GlutaMAXI (Invitrogen). For most of the experiments, unless otherwise indicated, neurons were incubated with various pharmacological agents in conditioned neuronal media, in a 37°C, 5% CO_2 incubator for the appropriate amount of time before cells were either fixed for immunocytochemistry or lysates were collected for immunoblots. For temperature-dependence experiment, neurons were maintained in parallel incubator kept at a constant

10°C. For neuronal transfection of plasmids, we employ a calcium chloride transfection protocol modified as previous described (Jiang and Chen, 2006). For receptor antagonist treatments (APV, NBQX, ifenprodil, etc.), unless otherwise stated, the cultured neurons were usually pre-treated with the antagonist for 30–60 min prior to stimulation. Unless otherwise stated, bicuculline (BIC) stimulation of neurons lasts for 15 min while AMPA or NMDA treatments lasts for 10 min followed by a washout and recovery for 5 min prior to processing for immunocytochemistry. The following pharmacological agents were used: bicuculline (BIC, 40 μM; Sigma), forskolin (FSK, 25 μM; Calbiochem, San Diego, CA), tetrodotoxin (TTX, 1 μM; Tocris, Ellisville, MO), APV (100 μM; Tocris), cyclosporin A (CsA, 5 μM; Sigma), nocodazole (NDZ, 0.1 μM or 20 μM; Tocris), BAPTA-AM (25 μM, Tocris), EGTA-AM (25 mM or 100 mM; Invitrogen), nimodipine (NIM, 10 μM; Tocris), ω-conotoxin (2 μM; Tocris), and ω-agatoxin (0.1 μM; Tocris), MNI-caged glutamate (0.2 mM; Tocris), NBQX (100 μM; Tocris); Trolox (10 nM; Tokyo Chemical Industry, Tokyo, Japan), ifenprodil (IFP, 50 μM; Tocris), MK801 (50 μM; Tocris), NMDA (20 μM; Tocris), AMPA (25 μM; Tocris), SN50 and SN50M (Enzo Lifesciences).

Immunocytochemistry

All cells were fixed at room temperature with parafomalydehyde (3.2%) for 10 min, permeabilized with 0.1% Triton-X 100 (Calbiochem) for 5 min and blocked in 10% goat-serum for 30 min. Neurons were then incubated in primary antibodies either for 4 h at room temperature or overnight at 4°C. Secondary antibodies and Hoechst nuclear dye (Invitrogen) were incubated at room temperature at 1:2000 (2 μg/ml) dilution for 2 h. All antibodies were diluted in 10% goat serum and coverslips were mounted with aqua/polymount (Polysciences, Warrington, PA).

Calcium Chelators (BAPTA-AM and EGTA-AM) and Calcium Channel Antagonists

Hippocampal neurons were pre-treated with TTX (1 μM) in the presence of DMSO, BAPTA-AM (25 mM), EGTA-AM (25 mM or 100 mM) in conditioned media. After 30 min of pretreatment, neurons were was washed with conditioned media and allowed to recover for 10 min before being stimulated in Tyrode's solution with varying concentrations of KCl (5 mM [$5K^+$] or 40 mM [$40K^+$]) for 5–7 min. Neurons were then washed and allow to recover in regular Tyrode's solution (5 mM) for another 5 min before being fixed and stained for immunocytochemistry. TTX (1 μM) was present in all media and solutions throughout pre-treatment, stimulation and recovery periods. Similarly, for calcium channel antagonists nimodipine (10 μM; NIM), ω-conotoxin (2 μM; CTX), and ω-agatoxin (0.1 μM; AGA), neurons were pre-treated for 30 min before being stimulated in Tyrode's solution containing elevated levels of KCl (40 mM) briefly for 5–7 min, washed and recovered in regular Tyrode's solution (5 mM) for another 5 min prior to fixation. TTX was present throughout the entire treatment protocol. Tyrode's solution (140 mM NaCl; 10 mM HEPES pH 7.3; 5 mM KCl; 3 mM $CaCl_2$; 1 mM $MgCl_2$; 10 mM glucose pH 7.35).

Photomanipulation and Analysis of CRTC1^{270} in Neurons

Hippocampal neurons were transduced with virus expressing either Dendra2 or CRTC1^{270}. After 1 week of expression, neurons were transferred on to a glass bottom live imaging setup containing a low Mg^{2+} Tyrode's solution (140 mM NaCl; 10 mM HEPES pH 7.3; 5 mM KCl; 3 mM $CaCl_2$; 0.1 mM $MgCl_2$; 10 mM glucose; 10 nM Trolox pH 7.35) with the appropriate reagents added as indicated for each experiment (TTX,1 μM; MNI-caged glutamate, 200 μM; DMSO). Neurons were allowed to recover on a heated stage assembly on a Zeiss LSM 700 scanning confocal microscope for approx. Ten to fifteen minutes prior to the first imaging session. Neurons with comparable levels of expression of fluorescent proteins were selected for imaging. We then selected two regions of interest (10 microns in length) in dendritic branches located roughly 100 μm away from the soma and exposed briefly to UV (405 nm) laser (dwell time: 51.2 ms) every 10th frame to photoconvert and photouncage glutamate. For each region of interest a total of 80 frames were captured per neuron. However, since the dimensions of each image capture varies slightly between neurons, the time it takes to capture 80 frames for each neuron will also have minor differences, with the average total time of image capture per neuron averaging between 13 and 15 min. To maintain consistency across the different time-lapse plots, we plotted the time elapsed in frames. Pharmacological reagents used during the experiments include APV (100 μM); NBQX (100 μM); EGTA-AM (25 μM); BAPTA-AM (25 μM); Nocodazole (0.1 μM 6 h pre-treatment prior to imaging). To analyze the data, the amount of Dendra2^{red} signal was quantified in the nucleus and the change in signal intensity over baseline was plotted over the total amount of frames acquired.

Zeiss Scanning Confocal Microscope LSM 700

Objectives: Plan Apochromat 63X 1.40 Oil DIC.
Temperature: 25 or 35°C (Zeiss Temp-control 37-2).
Media: Tyrode's solution for live imaging.
Lasers: 405, 488, 555, and 639 nm solid state lasers.
Data acquisition: Zen 2009.

Local Photoconversion and Analysis of CRTC1^{270} in Distal Dendrites

Neurons were transduced and prepared for imaging as described in the previous section "photomanipulation of CRTC1^{270} in neurons." However, we employed a Marianas spinning disc confocal system that is coupled to a Photometrics Evolve camera (Intelligent Imaging Innovations, Denver, CO) for high-speed image acquisition since this was required to capture the translocation of Dendra2-CRTC1 within the dendrite. Images were acquired within a humidified environmental chamber for regulated temperature control. A 2.25 cm^2 region of activation (ROA) was selected on a dendritic branch located approximately 50–70 μm away from the soma. Using a Vector scan module attached to the system, the selected ROA was briefly exposed to UV laser (50% intensity; 2 ms dwell; Supplemental Figure

S4). A total of 100 frames (alternating 473 and 523 nm beam excitation) were acquired per imaging session (approximately 660 ms/frame). Pharmacological reagents used in the experiment include BIC (40 μM) and forskolin (25 μM). To calculate the average intensity of dendrites flanking the ROA, a series of regions were drawn bidirectionally to highlight 40 μm of dendrites both proximal and distal to the ROA. The average intensity of these 40 μm segments were quantified over time for all neuronal samples within the same experimental group. The group data is presented as a scatter plot of the average intensity of the entire 40 μm segment either proximal or distal to the ROA over time (as indicated by the x-axis showing frames captured over time). To plot the bias index, the average intensity of the distal segment is subtracted from the proximal segment and the difference of the value is plotted on a horizontal scatter plot for all time points collected in each experimental condition. A positive bias index indicated that the proximal segment has a higher average intensity compared to the distal segment while an average index value of zero indicates the overall average intensity over time is the similar in both branches of dendrites. The cumulative bias index calculates the average bias index for all the neurons in the same experimental group and plots the cumulative total over time.

3i Marianas Spinning Disc Confocal System (CSU22 Yokugawa Scanner)

Objectives: Plan Apochromat 63X 1.40 Oil DIC.
Temperature: 35°C (Okolab temperature control chamber).
Media: Tyrode's solution for live imaging (methods and materials).
Lasers: 405, 488, and 561 nm solid state lasers.
Camera: Photometric Evolve EMCCD camera.
Data acquisition: Slidebook 5.0.

Cell Cultures, Transfections and, siRNA Treatment

All cell lines (HEK293T) were grown on Dulbecco's Modified Eagle Media (DMEM; Invitrogen) supplemented with 10% fetal bovine serum (HyClone, Logan, UT), and 1% Penicillin/Streptomycin (Invitrogen). Transfection of plasmids in cell lines was carried out with Lipofectamine 2000 (Invitrogen) using protocols recommended by the manufacturer. For siRNA treatment of human CRTC1 or GAPDH in HEK293T cells, we purchased custom designed siGENOME SMARTpool siRNA from Dharmacon (Lafeyette, CO). The SMARTpool siRNA (50 nM) was delivered into cells using Lipofectamine RNAiMAX (Invitrogen) reagent over the course of 72 h with refeeding of siRNA every 24 h and the replating and reseeding of cell after 48 h. For siRNA treatment of human importin β1 (50 nM; KPNB1; SMARTpool siRNA; Dharmacon) and GAPDH, HEK293T cells were incubated with KPNB1 siRNA for 48 h before expression plasmids bearing different 4xGFP fusion constructs were transfected into cells for another 12 h prior to immunocytochemistry or immunoblotting. For siRNA treatment of mouse neurons with Dynch1h, we purchased custom designed siGENOME SMARTpool Accell siRNA from Dharmacon. The Accell siRNA (1 μM) was delivered into neurons directly and allowed to incubate for 48–96 h. After the incubation period, cells were either fixed for immunocytochemistry or harvested in lysis buffer for analysis via Western blots.

Image Analysis and Synapse Quantification

We performed all nuclear to cytoplasmic ratio quantification using Slidebook v4.2-v5.5 (Intelligent Imaging Innovations). Briefly, raw confocal images taken using a 63X 1.4NA oil objective were imported into Slidebook. For each neuron, masks were manually drawn to highlight both the nucleus (based on Hoechst staining) and the entire cell body (based on MAP2 staining). A simple subtraction routine was performed for these two masks to obtain a separate mask for the cytoplasm. The nuclear to cytoplasmic ratio of individual neurons were calculated based on the average intensity of staining as defined by the nuclear and cytoplasmic masks for each image. All data points were then plotted using Prism Graphpad. Unless otherwise stated, all data sets are presented as mean ± SEM either as bar graphs or scatter plots and, all *p*-values were determined using One-Way analysis of variance (ANOVA) with Bonferroni's Correction *post-hoc* test. To analyze synaptic integrity, hippocampal neurons were transduced with an AAV expressing GFP being driven under the neuron-specific synapsin promoter. After 1 week of expression, neurons were incubated in NDZ (0.1 μM) for 6 h before being stimulated and processed for immunocytochemistry using antibodies against PSD95, Synapsin and MAP2. To quantify for the number of synapses, Slidebook was used to isolate only PSD95-positive and synapsin-positive puncta based on signal intensity, size exclusion, and overlapping fluorescence intensities. The stringent selection criteria to increase signal to noise for each puncta likely resulted in undersampling. To identify synapses, only PSD95 and synapsin masks that overlapped were considered as a positive score. Student's *t*-test (two-tailed, unpaired) was used as a statistical analysis.

Gene Expression in CRTC1^{270} Transduced Hippocampal Neuronal Cultures

Hippocampal cultures were transduced with lentivirus expressing CRTC1^{270} and 1 week post-transduction, neurons were pre-treated with TTX (1 μM) for another 3 h before either being continuously maintained in TTX or the TTX was withdrawn, washed and replaced with regular conditioned media. The neurons were allowed to recover for 30 min before RNA was extracted with TRIzol (Invitrogen), column purified with RNeasy kit (Qiagen, Valencia, CA), and the concentration determined via the Nanodrop (Thermo Scientific). For RT-PCR, we generated cDNA using reverse transcriptase and poly dT primers (Invtirogen). We then conducted quantitative real time PCR experiments (Stratagene Mx3000P), with SYBR Green Master Mix (Invitrogen) and specific primer pairs (Operon, Huntsville, AL) listed below. ΔΔCt values were calculated for all raw qPCR results by normalizing against mock, untreated controls and corrections for loading error we made against ΔΔCt values for HPRT1, a non-activity-dependent gene. Primer pairs

used include crtc1 (5-tggacagagtatatcgtgagcg; 5-catgcttgtctactg acaggg), arc (5-ccgtcccctcctctcttga; 5-aaggcacctcctctttgtaatcctat), hprt1 (5-agtcccagcgtcgtgattag; 5-ccatctccttcatgacatctcg), btg2 (5-tcctgaggactcggggctgc; 5-gcgatagccggagcccttgg), cfos (5-tcccagc tgcactacctatacgt; 5-tgcgcagctagggaagga), cyr61 (5-aactcggagtgc cgcctggt; 5-gccgcagtatttgggccgg), zif268 (5-attgatgtctccgctgcagat; 5-gtagttgtccatggtgggtga), and Dendra2 (5-ggaattaacctgatcaagga; 5-tggaagaagcagtcgccctc).

GST-14-3-3ε Pulldowns of CRTC1^{270} Fusion Proteins and Western Blots

Cortical neuron cultures (DIV 21–28) were transduced with lentiviruses expressing either full length or serine to alanine CRTC1^{270} mutants. After 1 week. post-transduction, neuronal lysates were collected (25 mM Tris, pH7.4; 137 mM NaCl; 1% NP40; 10% glycerol; protease and phosphatase inhibitors; Ballif et al., 2006) and subjected to pulldowns using purified GST-14-3-3 ε bound on glutathione beads. The beads were then washed extensively, resuspended in sample buffer and analyzed via immunoblots using either conventional or PhosTAG acrylamide gels. For Western blotting, all samples were loaded on 8–10% bisacrylamide minigels (Biorad) and ran on standard PAGE buffers. After appropriate amount of time, proteins bands were transferred onto PVDF (Amersham) before being incubated with antibodies for detection. All western blot images were obtained with Odyssey Imaging System (LI-COR Biosciences) and quantified using Image Studio.

Mass Spectrometry

Four confluent 10 cm dishes of Neuro-2A cells were transfected with HA-CRTC1 plasmid using Lipofectamine-2000. After 16 h, cells were washed twice in ice cold PBS and lysed cells in lysis buffer (150 mM NaCl, 50 mM Tris (pH 8.0), 1% NP40) supplemented with protease and phosphatase inhibitors (Roche). The lysates were incubated on ice for 20 min with benzonase DNase (Millipore) to reduce viscosity, then centrifuged to clarify insoluble proteins. HA-CRTC1 was immunoprecipitated using pre-equilibrated EZview Red Anti-HA Affinity Gel (Sigma) for 2 h at 4°C with constant rotation. Beads were washed 3X in ice-cold lysis buffer, and eluted using 100 μl 8M urea. Samples were mixed with loading buffer, boiled and loaded onto NuPAGE Novex 4–12% Bis-Tris gradient gel. To purify HA-CRTC1 for mass spec, the gel was stained with Simply Blue SafeStain (Invitrogen) and CRTC1 was excised from gel slices, digested with either trypsin or chymotrypsin before fractionated online using a C18 reversed phase column, and analyzed by MS/MS on a Thermofisher LTQ- Orbitrap XL as previously described (Kaiser and Wohlschlegel, 2005; Wohlschlegel, 2009). MS/MS spectra were subsequently analyzed using the ProLuCID and DTASelect algorithms (Eng et al., 1994; Tabb et al., 2002). Phosphopeptides were identified using a differential modification search that considered a mass shift of +79.9663 on serines, threonines, and tyrosines. All phosphorylated sites reported in **Figure 7** exhibit an AScore of at least 90% confidence levels.

Results

Glutamate Receptor and L-type Calcium Channel Activation Promote Nuclear Translocation of CRTC1

We previously reported that activation of NMDA receptors was required for CRTC1 synapse to nucleus transport (Ch'ng et al., 2012) but did not characterize the type of NMDA receptor involved. Here, we asked whether GluN2B-containing NMDA receptors, which are expressed at highest levels neonatally, are involved by bath applying NMDA to cultured neurons to activate NMDA receptors while selectively blocking GluN2B-containing NMDA receptors with the inhibitor ifenprodil. In control experiments, we blocked with APV, which blocks all NMDA receptors or with MK801, an open channel, usage-dependent antagonist that only blocks activated NMDA receptors (Thompson et al., 2004). Immunocytochemical analysis revealed that MK801 and APV blocked NMDA-induced nuclear accumulation of CRTC1 and phosphorylation of CREB at serine 133, but that ifenprodil did not. In fact, stimulation with NMDA in the presence of ifenprodil triggered significantly more nuclear accumulation of CRTC1 and phosphorylation of CREB at serine 133 than did NMDA alone, suggesting that activation of GluN2B-containing NMDA receptors functions to repress CRTC1 synapse to nucleus import (**Figure 1A** and Supplementary Figures S1A,B).

Next, we focused on the AMPA receptor, which plays a crucial function in various forms of learning-related neuronal plasticity (Kessels and Malinow, 2009). Inhibition of NMDA receptors with APV greatly reduced but did not completely abolish bicuculline (BIC) -induced CRTC1 translocation (Ch'ng et al., 2012), indicating that other synaptic glutamatergic receptors contribute to CRTC1 nuclear localization. Selective activation of AMPA receptors with AMPA triggered robust CRTC1 nuclear accumulation, which was significantly reduced by the AMPA receptor blocker NBQX (**Figure 1B**). The L-type voltage-gated calcium channel (VGCC) antagonist nimodipine also reduced AMPA receptor-mediated CRTC1 nuclear accumulation, suggesting that activation of synaptic AMPA receptors produces sufficient local depolarization to activate VGCCs (Macías et al., 2001; Higley and Sabatini, 2012) and that the resulting influx of calcium contributes to CRTC1 nuclear import. AMPA-induced CRTC1 nuclear accumulation was not inhibited by APV, indicating that calcium influx through AMPA and L-type VGCC is sufficient to drive CRTC1 nuclear translocation.

We next tested the hypothesis that AMPA receptor activation might enhance CRTC1 nuclear entry by activating synaptic NMDA receptors. Toward this end, we preincubated neurons with NBQX (to block AMPA receptors), TTX (to block action potentials) and ifenprodil (to block GluN2B-containing NMDA receptors) before briefly exposing neurons to low concentrations of NMDA. Under these conditions, NMDA-induced CRTC1 nuclear accumulation was significantly diminished, consistent with a role for AMPA receptors in NMDA receptor-mediated regulation of CRTC1. To explain these results, we hypothesized that bath application of NMDA triggered

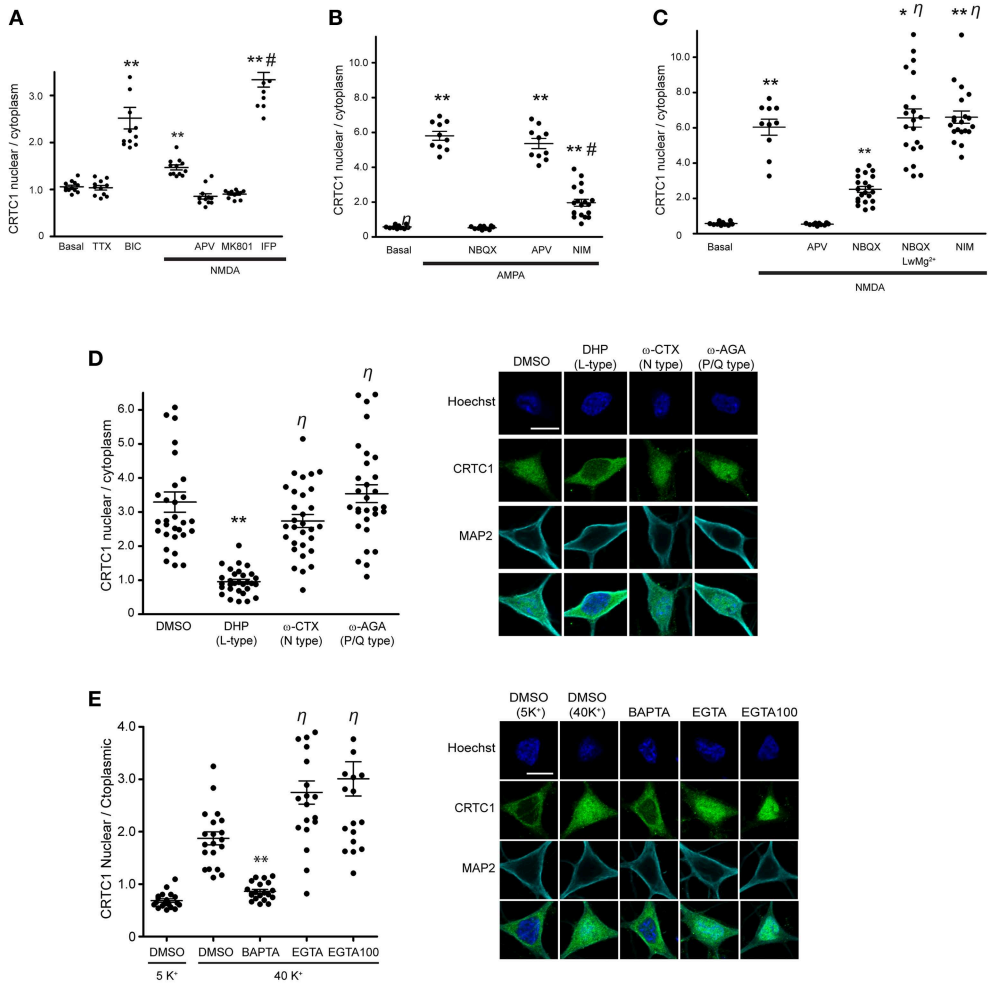

FIGURE 1 | CRTC1 nuclear translocation requires local calcium influx via glutamate receptors and L-type VGCCs. (A) Nuclear to cytoplasmic ratio of CRTC1 in cultured neurons after stimulation with NMDA in the presence of different NMDA receptor antagonists, APV, MK801 or Ifenprodil (IFP) (**$p < 0.001$ relative to basal; #$p < 0.001$ relative to NMDA). **(B,C)** Nuclear to cytoplasmic ratio of CRTC1 in cultured neurons pre-incubated with TTX and IFP, in conjunction with either NBQX, APV or nimodipine (NIM) before being stimulated with either AMPA or NMDA. Experiments were performed in either Tyrode's with regular $MgCl_2$ (1 mM) or low $MgCl_2$ (0.1 mM) (**$p < 0.001$ relative to basal; *$p < 0.001$ relative to NBQX; #$p < 0.001$ relative to AMPA; η: not significant relative to NMDA). **(D)** Confocal micrographs and nuclear to cytoplasmic ratio quantification of CRTC1 in neurons depolarized with KCl in the presence of NIM, conotoxin (ω-CTX), agatoxin (ω-AGA), or mock treated with DMSO (**$p < 0.001$ relative to DMSO; η: not significant relative to DMSO). **(E)** Membrane permeable calcium chelators BAPTA and EGTA (25 μM/100 μM) were incubated in neurons prior to depolarization with KCl ($5K^+$ 5 mM; $40K^+$ 40 mM). Nuclear to cytoplasmic ratio of CRTC1 was quantified (**$p < 0.001$ relative to DMSO $40K^+$; η: not significant relative to DMSO $40K^+$). All scale bars = 10 μm.

sufficient depolarization of neurons to enhance glutamate release, leading to AMPA receptor activation, which further depolarizes the neurons to relieve the Mg^{2+} block in NMDA receptors, thereby increasing the effect of NMDA. To test the idea that depolarization induced by AMPA receptor activation contributes to the NMDA-induced translocation by helping to relieve the voltage-dependent Mg^{2+} block of the NMDA receptor channel, we reduced the concentration of Mg^{2+} ions in the Tyrode's solution by 10-fold during NMDA stimulation and showed that CRTC1 translocation no longer required AMPA receptor function, as it was not blocked by NBQX (**Figure 1C**). These results indicate that if the post-synaptic compartment is sufficiently depolarized to relieve the Mg^{2+} block in the NMDA receptor, then calcium influx through the NMDA receptor is adequate to drive CRTC1 nuclear translocation.

In addition to inhibiting CRTC1 nuclear import induced by incubation with AMPA, we previously showed that the L-type VGCC antagonist nimodipine also blocked CRTC1 nuclear import induced by incubation with the $GABA_A$ receptor antagonist bicuculline (Ch'ng et al., 2012). To test whether the N-type or P/Q type VGCCs were also required for CRTC1 synapse to nucleus import, we depolarized neurons with KCl in the presence of conotoxin to block N-type VGCCs, agatoxin to block P/Q-type VGCCs, or nimodipine to

block L-type VGCCs. As shown in **Figure 1D**, only inhibition of L-type VGCCs with nimodipine blocked KCl-induced CRTC1 translocation. Consistent with previously published reports, we also found that only L-type VGCCs were required to trigger depolarization-induced increase in pCREB S133 immunoreactivity (Supplementary Figure S1C; Wheeler et al., 2012).

To further characterize the source of calcium entry required for stimulus-induced CRTC1 nuclear import, we assayed the effect of both high affinity, fast-acting (BAPTA) and low affinity and slower-acting (EGTA) calcium chelators. BAPTA rapidly suppresses local elevations in calcium near their source of entry at the plasma membrane while EGTA has a 100-fold slower on rate and thus blocks bulk cytosolic elevations in calcium (Neher and Almers, 1986; Deisseroth et al., 1996). We found that BAPTA, but not EGTA completely blocked the nuclear accumulation of CRTC1 and phosphorylation of CREB at Serine 133 induced by KCl depolarization (**Figure 1E** and Supplementary Figure S1D). Together, these findings indicate that the local influx of calcium produced by calcium influx through synaptic NMDA and AMPA glutamate receptors and L-type VGCCs contribute to CRTC1 nuclear translocation.

CRTC1 Synapse to Nuclear Transport Involves Active, Dynein-dependent Movement along Microtubules

In our previous experiments, the rapid nuclear accumulation of CRTC1 following synaptic stimulation suggested that soluble CRTC1 must be actively transported to the nucleus. To determine how CRTC1 is transported from distal stimulated synapses to the nucleus, we asked whether it required active transport, which, unlike passive diffusion, can be blocked at 10°C (Talcott and Moore, 1999; Wiegert et al., 2007). Stimulation of neurons with BIC at 10°C or 37°C revealed that CRTC1 nuclear accumulation was blocked at lower temperatures (**Figure 2A**), consistent with an active transport process. We then asked whether microtubules are required for the transport by depolymerizing microtubules with low concentrations of nocodazole and found that this significantly inhibited the nuclear accumulation of CRTC1 in response to BIC (**Figure 2B**) without compromising the viability, morphology or synapse density of the neurons (Supplementary Figures S2A,B).

We next asked whether CRTC1 nuclear import was mediated by the microtubule-based retrograde motor protein dynein. In initial experiments, we specifically disrupted cytoplasmic dynein function by overexpressing dynamitin, which functions as a dominant negative by triggering the disassembly of dynactin, a multiprotein complex required for dynein-based movement (Melkonian et al., 2007; Shrum et al., 2009). Dynamitin overexpression in neurons significantly decreased nuclear CRTC1 accumulation following BIC stimulation (**Figure 2C**). To complement these experiments, we used siRNA to knockdown the expression of dynein heavy chain (Supplementary Figure S2C), and found that this also significantly decreased BIC-induced CRTC1 nuclear accumulation as compared to BIC-stimulated control neurons incubated with non-targeted siRNA (**Figure 2D**). Together, these data indicate that dynein mediates the long-distance retrograde transport of CRTC1 along microtubules.

CRTC1 Encodes an Arginine-rich Nuclear Localization Signal

Having determined the source of calcium entry at the synapse that triggers CRTC1 synapse to nuclear import, and shown that CRTC1 retrograde transport is active and occurs along microtubules in a dynein-dependent manner, we next focused on the signals which regulate CRTC1 transport into the nucleus. Nuclear import of proteins larger than 40–60 kD is typically facilitated by transport proteins that recognize nuclear localization signals (NLSs), which are often comprised of short stretches of basic amino acids (Lange et al., 2007). Analysis of the CRTC1 primary amino acid sequence revealed three highly conserved clusters of basic residues near the amino-terminus of the protein (**Figure 3A**). To determine whether these amino acid clusters comprised an NLS, we fused a 57 amino-acid sequence (aa 92–148) from CRTC1 that contained all three arginine-rich clusters (CRTC1-AR) to four tandem copies of GFP (4xGFP, **Figure 3B**). While 4xGFP localized exclusively to the cytoplasm of neurons, fusion to CRTC1-AR promoted robust nuclear accumulation of 4xGFP (**Figure 3B**). The amount of nuclear accumulation was greater than the nuclear accumulation observed when 4xGFP was fused to the canonical SV40 NLS. To identify the minimal region required for nuclear translocation, we further divided CRTC1-AR into two sub-fragments, CRTC1-N1 (amino acids 103–135), which contained two clusters of arginine residues, and CRTC1-C1 (amino acids 135–147). As shown in **Figure 3B**, only CRTC1-N1 fragment was able to confer accumulation in the nucleus of neurons, although to a lesser extent than full length CRTC1-AR, while the CRTC1-C1 fragment remained cytoplasmically localized. We also tested these sequences in HEK293T cells, and found that the full length CRTC1-AR and the CRTC1-N1 fragment both promoted nuclear import of CRTC1 (Supplementary Figure S3A).

To probe the necessity of the NLS in mediating the nuclear import of CRTC1, we generated two HA epitope-tagged full-length CRTC1 alanine mutants. In the first (HA-mNLS1), we mutated four highly conserved arginines to alanines (R103A, R106A, R108A, and R110A). In the second mutant (HA-mNLS2), we mutated one proline and two arginine residues to alanine (P114A, R116A, and R117A). Neither of these mutants disrupted phosphorylation of CRTC1 at serine residue 151, a site that has been shown to regulate nucleocytoplasmic trafficking in non-neuronal cells (Supplementary Figure S3B; Screaton et al., 2004). However, neither of these mutants were efficiently imported into the nucleus upon BIC stimulation, indicating that these particular conserved residues constitute essential components of the NLS (**Figure 3C**).

To determine if the classical nuclear import pathway was involved in CRTC1 nuclear entry (Thompson et al., 2004; Jeffrey et al., 2009), we used siRNA to knock down importin β1 (KPNB1) expression to 45% of baseline values (using GAPDH siRNA knockdown as controls) in HEK293T cells (**Figure 3D** and Supplementary Figure S3C). While the knockdown blocked the nuclear import of a canonical NLS (4xGFP-SV40), it did

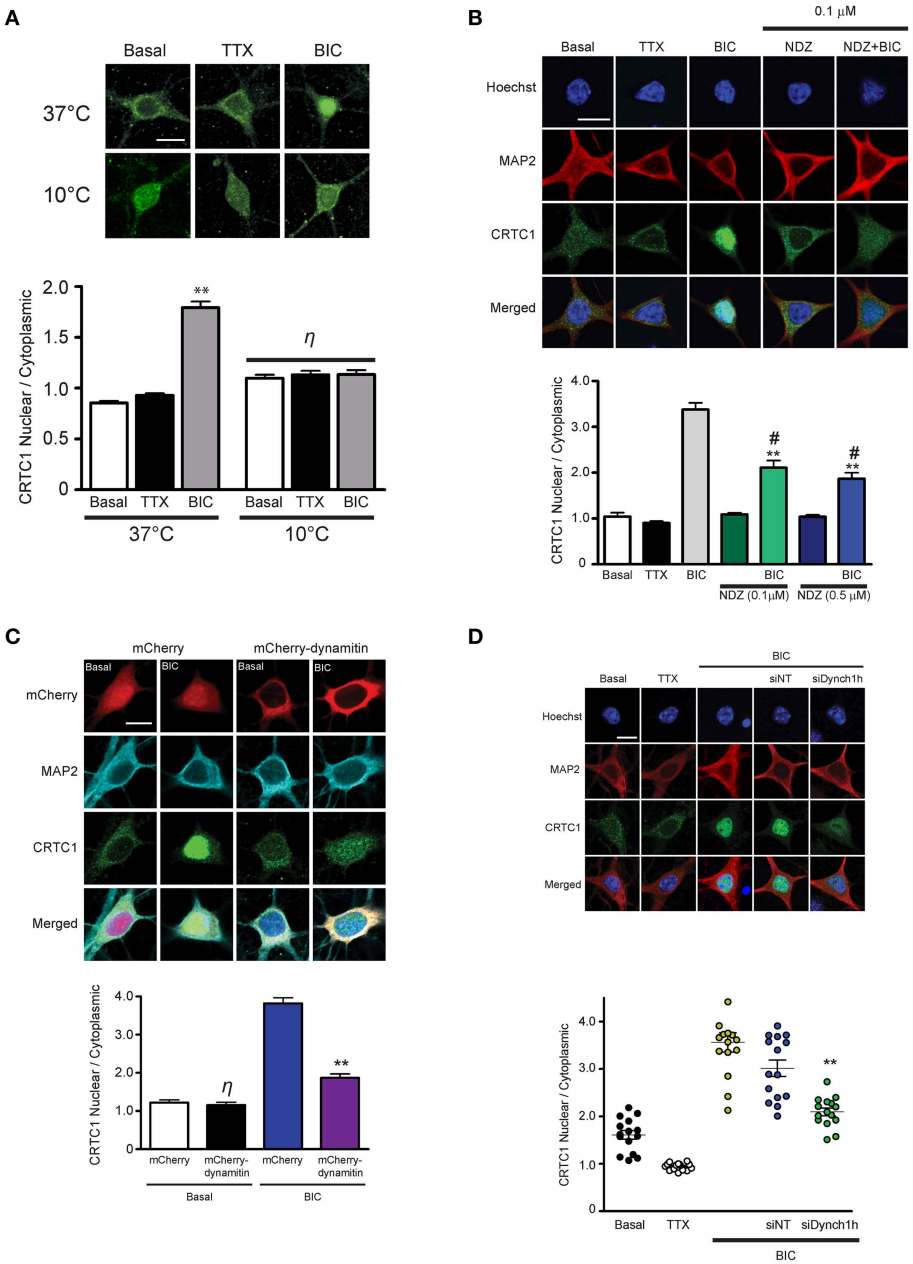

FIGURE 2 | Nuclear accumulation of CRTC1 involves active, dynein-mediated transport along microtubules. (A) Neurons were stimulated with either TTX or BIC in incubators at 37°C or 10°C. CRTC1 nuclear to cytoplasmic ratio was quantified (**$p < 0.001$ relative to basal; η: not significant). **(B)** Neurons were incubated with nocodazole (NDZ, 0.1 μM or 0.5 μM) to depolymerize microtubules prior to BIC stimulation (**$p < 0.001$ relative to non-BIC samples $^{\#}p < 0.001$ relative to BIC). **(C)** Neurons expressing either mCherry or mCherry-dynamitin were stimulated with BIC. Endogenous expression of CRTC1 in the nucleus and cytoplasm of mCherry expressing neurons were quantified (**$p < 0.001$ relative to mCherry only samples; η: not significant relative to basal mCherry). **(D)** Mouse hippocampal neurons (21–28 DIV) were incubated with dynein heavy chain siRNA (siDynch1h) or non-targeted control (siNT) followed by stimulation with TTX or BIC (**$p < 0.001$ relative to all other BIC samples). All scale bars = 10 μm.

not inhibit the nuclear translocation of 4xGFP-tagged CRTC1-AR (**Figure 3D**). We also inhibited the classical nuclear import pathway using cell-permeable inhibitor peptides that mimic the NLS of NFκB SN50 (Lai et al., 2008) and did not detect any effect on BIC-induced CRTC1 nuclear translocation (Supplementary Figure S3D). Finally, we overexpressed 4xGFP-tagged CRTC1-AR and SV40 NLS in neurons (Supplementary Figure S3E) and showed that at high expression levels, only the CRTC1 arginine-rich NLS but not the SV40 NLS was able to inhibit nuclear translocation of endogenous CRTC1. Taken together, our

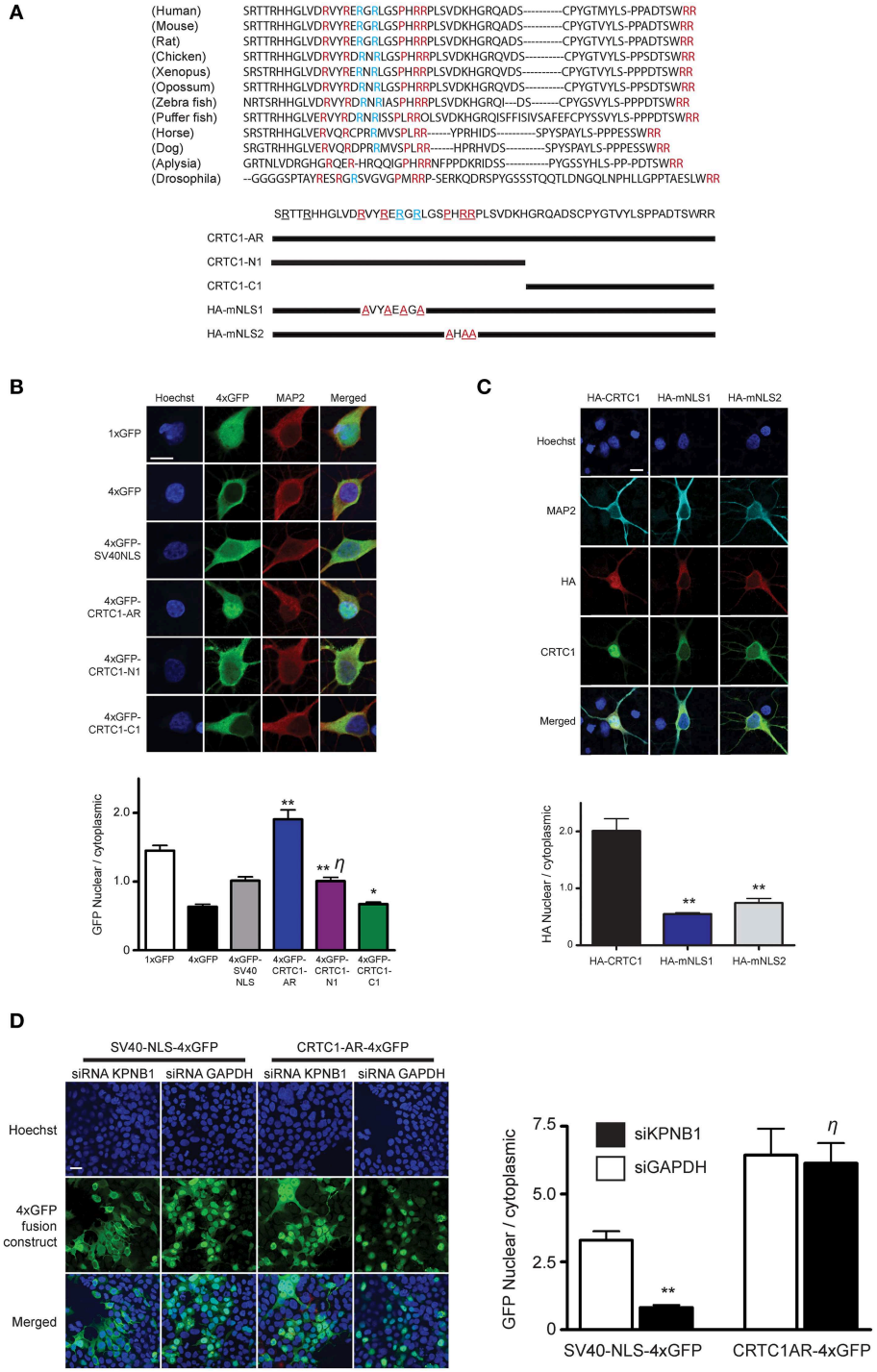

FIGURE 3 | Characterization of CRTC1's arginine-rich NLS. (A) A 57 amino acid fragment (S92-R148) in CRTC1 with sequence identity (red) and similarity (blue) across species. Expression constructs described below. **(B)** As diagramed in **(A)**, the full length arginine-rich fragment (CRTC1-AR) as well as CRTC1-N1, CRTC1-C1 and SV40NLS control fragment fused to 4xGFP were expressed in neurons. GFP signal in the nucleus and cytoplasm were quantified (**$p < 0.001$ relative to 4xGFP; * not significant relative to 4xGFP; η: not significant relative to SV40NLS). **(C)** Neurons expressing full length HA-tagged CRTC1 and alanine mutations in two arginine-rich clusters (HA-mNLS1 and HA-mNLS2, as diagramed in **A**) were stimulated with BIC and immunostained with antibodies against HA epitope (**$p < 0.001$ relative to HA-CRTC1). **(D)** HEK293T cells were treated with siRNA against KPNB1 (Importin β1) or GAPDH before being transiently transfected with SV40NLS-4xGFP or CRTC1-AR-4xGFP. The nuclear to cytoplasmic ratio of GFP was quantified (**$p < 0.001$ relative to siGAPDH; η: not significant relative to siGAPDH). Scale bars = 10 μm.

experiments indicate that CRTC1 undergoes active transport into the nucleus in a manner that is independent of the classical importin α/β1-mediated pathway.

The First 270 Amino Acids of CRTC1 Are Sufficient for Stimulus-induced Nucleocytoplasmic Shuttling

In the course of analyzing the different domains to identify the NLS in CRTC1, we observed that a fragment containing amino acids 1–270 of CRTC1 localized strongly to the nucleus of CHO cells. In contrast, the carboxy terminal fragment of CRTC1, from amino acids 271–630, localized exclusively to the cytoplasm (Supplementary Figure S4A). Further analysis in neurons show that fragment 1–270 localizes to dendrites and synapses in silenced neurons but underwent stimulus-induced translocation in a manner that was indistinguishable from full-length CRTC1 (**Figure 4B** and Supplementary Figure S4A). These findings indicated that the N-terminal 270 amino acids contained all of the signals required for regulated synaptic and nuclear localization.

We took advantage of this finding to develop a fluorescent reporter to monitor synapse to nucleus CRTC1 signaling by fusing the amino terminal fragment (aa 1–270) of CRTC1 to Dendra2, a photoconvertible fluorescent protein that switches from green (507 nm) to red (573 nm) emission following brief UV illumination. Unlike the full-length CRTC1, this fusion protein was small enough to package efficiently in a lentivirus using a *Camk2α* promoter to achieve modest levels of expression exclusively in excitatory neurons. Using this reporter, henceforth identified as $CRTC1^{270}$, we were able to photoconvert a subpopulation of CRTC1 in dendrites of cultured hippocampal neurons (21–28 DIV) and track its stimulus-induced movement and nuclear accumulation (Chudakov et al., 2010). Long-term expression (>1 week) of the fusion protein in cultured neurons did not have any visible effect on neuronal viability.

To ensure that overexpression of $CRTC1^{270}$ did not function as a dominant negative and thereby interfere with CREB-mediated activity-dependent transcription, we transfected neurons with $CRTC1^{270}$ and used qPCR to test the induction of CREB target genes following TTX withdrawal (Saha et al., 2011). As shown in **Figure 4A**, overexpression of $CRTC1^{270}$ did not alter the basal or the activity-induced expression of any CREB target genes, indicating that it did not have any dominant-negative activity.

We next set out to determine whether the dynamics of stimulus-induced synapse to nuclear import of $CRTC1^{270}$ showed any differences from that of endogenous, full-length CRTC1. Toward this end, we cultured neurons and transduced them with lentivirus to express $CRTC1^{270}$. We then stimulated with BIC, and performed immunocytochemistry with anti-dendra2 antibodies to visualize the localization of $CRTC1^{270}$. In parallel, we performed immunocytochemistry with anti-CRTC1 antibodies to visualize CRTC1 localization in neurons that were not transduced with $CRTC1^{270}$. As shown in **Figure 4B**, similar to endogenous full length CRTC1, BIC stimulated robust $CRTC1^{270}$ nuclear translocation that required calcineurin, NMDA and L-type VGCC activation. Moreover, the kinetics of nuclear export of $CRTC1^{270}$ following BIC stimulation was indistinguishable from that of full-length, endogenous CRTC1 (**Figure 4C**).

Local Uncaging of Glutamate at Synapses Drives Distally-localized CRTC1 into the Nucleus

These findings encouraged us to undertake live-cell imaging of neurons expressing $CRTC1^{270}$ (**Figure 5**). We previously showed that bath applied stimuli triggered nuclear accumulation of overexpressed CRTC1-Dendra2 (Ch'ng et al., 2012). Here we used $CRTC1^{270}$ to label and visualize in real time the nuclear accumulation of $CRTC1^{270}$ that is derived specifically from stimulated synapses. To do this, we transduced neurons with $CRTC1^{270}$, incubated neurons in low Mg^{2+} Tyrode's solution in the presence of TTX and used UV illumination to simultaneously uncage glutamate and photoconvert $CRTC1^{270}$ in a 10 μm dendritic region of activation (ROA) located approximately 100 μm away from the soma (**Figure 5** and Supplementary Figure S4D). Calcium imaging using Fluo4AM revealed that local uncaging of glutamate triggered local elevations of intracellular calcium around the region of activation, which rapidly dissipated and did not reach the soma (Supplementary Figure S4E, Video S1). We first photoconverted $CRTC1^{270}$ and uncaged glutamate in a single dendritic branch, and failed to detect nuclear accumulation of photoconverted CRTC1 (Supplementary Figure S4F). We then photoconverted $CRTC1^{270}$ and uncaged glutamate in two ROAs located on adjacent dendritic branches and observed robust nuclear accumulation of photoconverted CRTC1 (**Figure 5**). We also optimized parameters for UV illumination to ensure maximal green to red photoconversion while minimizing photobleaching. This optimized protocol was used in all subsequent live imaging experiments.

Photoconverted (red) $CRTC1^{270}$ was initially detected in the nucleus approximately 100–120 s ($t = 10$) after uncaging (**Figure 5A**), consistent with the speed of motor-driven active transport of vesicular structures in neuronal processes (0.8–1.2 μm/s; van den Berg and Hoogenraad, 2012). The nuclear accumulation of native (green) $CRTC1^{270}$ signal is not surprising given that the UV stimulation at the ROA did not completely convert all the native green Dendra2 protein to red. Following that, we performed experiments to examine if local synaptic stimulation results in nuclear translocation of $CRTC1^{270}$ and that the cell biological mechanisms underlying $CRTC1^{270}$ were identical to those mediating the nuclear import of endogenous full-length CRTC1. As shown in **Figure 5**, we found that, like full-length CRTC1, BIC-induced nuclear import of $CRTC1^{270}$ required both NMDA and AMPA receptors (**Figure 5B**), was temperature-sensitive (**Figure 5C**) and involved microtubule-dependent transport (**Figure 5D**). We also found that, like endogenous full-length CRTC1, $CRTC1^{270}$ translocation from stimulated synapses to the nucleus was blocked by BAPTA but not EGTA, indicating that, like endogenous CRTC1, its nuclear translocation was triggered by local and not bulk elevations in Ca^{2+} at the plasma membrane (**Figure 5E**). Together, these findings indicate that $CRTC1^{270}$ serves as a faithful reporter of stimulus-induced CRTC1 synapse to nuclear transport.

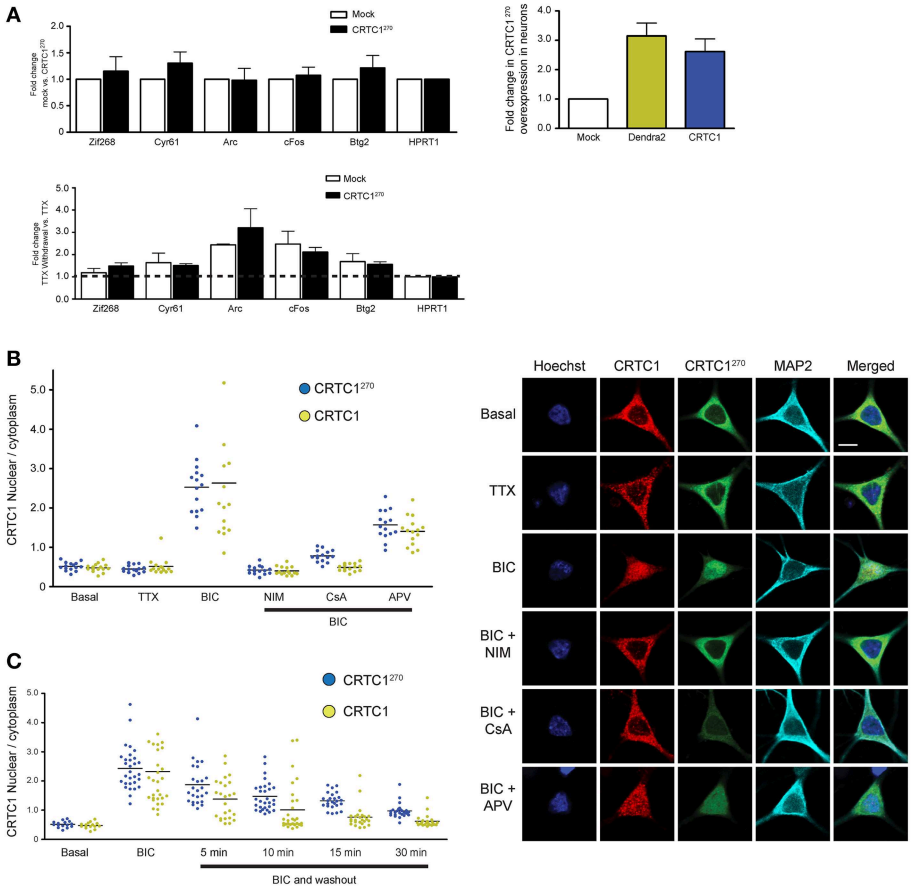

FIGURE 4 | The nuclear translocation of CRTC1^{270} is identical to endogenous full length CRTC1 and does not inhibit transcription of CREB target genes. (A) Rat neurons expressing CRTC1^{270} or mock transduced were incubated with TTX. In half the samples, TTX was withdrawn to stimulate neuronal activity while the other half of the sample remained incubated in TTX. Total RNA was extracted after treatment and CREB target genes were analyzed via qPCR ($n = 5$ basal TTX; $n = 3$ stimulation by TTX withdrawal). The expression of CRTC1^{270} in neurons was also measured via qPCR using primers against Dendra2 or mouse CRTC1. **(B,C)** Neurons transduced with CRTC1^{270} were pretreated with APV, NIM, TTX, and cyclosporinA (CsA), stimulated with BIC, and fixed immediately or at the indicated time points after BIC washout. The amount of endogenous CRTC1 and CRTC1^{270} in the nucleus and cytoplasm were quantified. All paired quantifications of nuclear to cytoplasmic ratio between endogenous CRTC1 and CRTC1^{270} were not significant. Scale bars = 10 μm.

CRTC1^{270} Movement is Biased Toward the Nucleus Following Neuronal Stimulation

As previous live-imaging studies of transport within dendrites have focused more on the movement of vesicles and organelles (Maeder et al., 2014), we set out to use the CRTC1^{270} reporter to visualize the retrograde transport of soluble molecules within dendrites. To achieve that, we visualized the transport of CRTC1 within a single dendritic branch, using spinning disc microscopy for rapid image acquisition (~100 ms/frame), which was required to detect the rapid translocation of CRTC1 within the dendrite. The signal we detected within the dendrite from local uncaging of glutamate was too weak to monitor by time lapse microscopy, and we thus combined local photoconversion of CRTC1^{270} with bath stimulation with BIC and forskolin (which promotes persistence of CRTC1 in the nucleus) to visualize the dynamics of a local population of photoconverted CRTC1, or, as a control, photoconverted Dendra2, within the dendrites of unstimulated and stimulated neurons. We tested multiple photoconversion parameters to optimize image acquisition and minimize photobleaching without compromising neuronal viability (Supplementary Figures S4G,H). In unstimulated conditions, photoconverted CRTC1^{270} underwent rapid bidirectional movement from the ROA, as did the control Dendra2 protein (**Figure 6A**). When neurons were stimulated, the movement of CRTC1^{270} became biased toward the soma (proximal), as detected by an increase in the average normalized intensity across the length of the dendrite proximal to the stimulation site over time (**Figure 6B**). We quantified the difference in normalized pixel intensity for pairwise length measurements (1.5 μm segments) along the distal and proximal lengths of the dendrite originating from the ROA and plotted a bias index. The majority of data points for stimulated CRTC1^{270} had a positive bias index, indicating a bias in movement

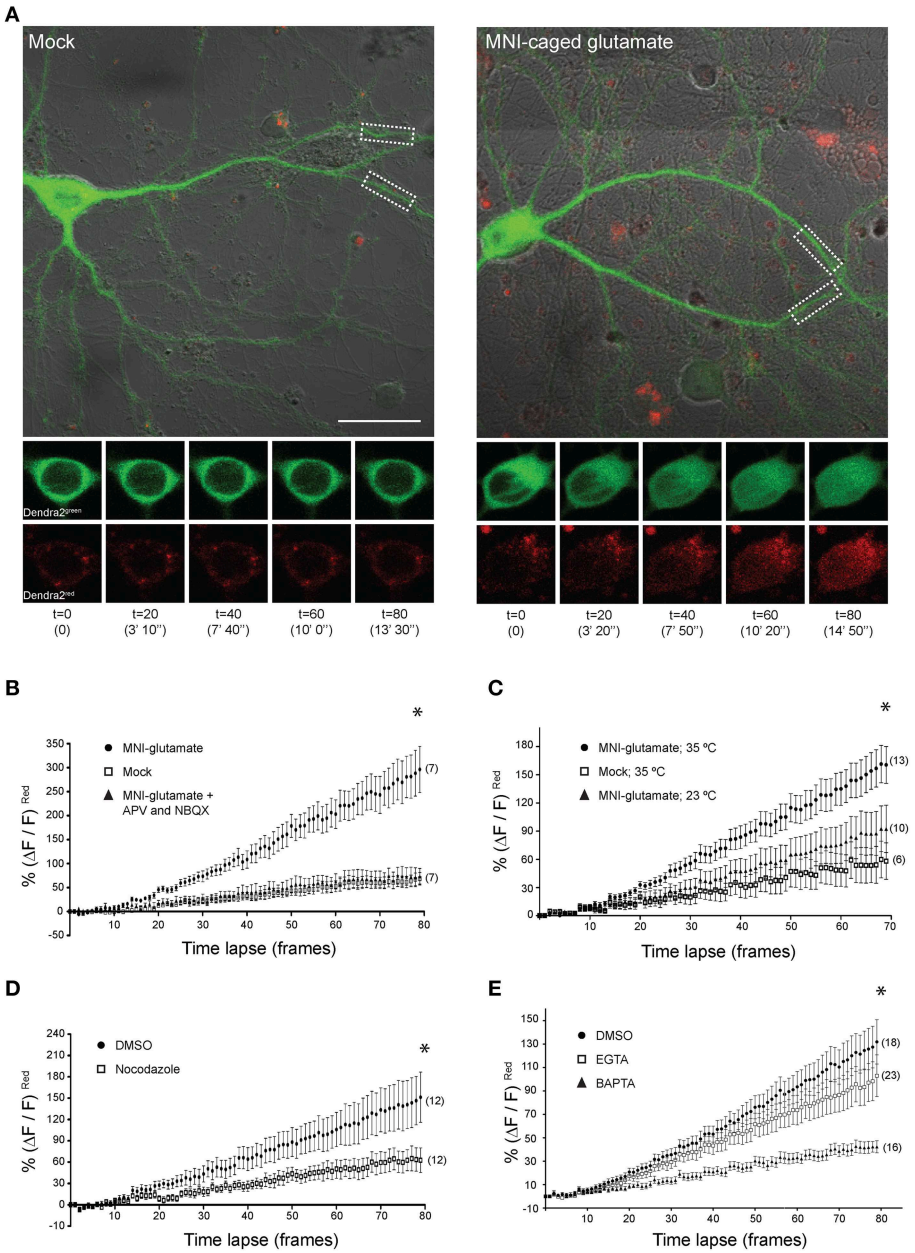

FIGURE 5 | Local uncaging of glutamate at synapses can drive distally-localized CRTC1^{270} into the nucleus. (A) Neurons expressing CRTC1^{270} were illuminated with a UV laser in the presence or absence (mock) of MNI-caged glutamate. The white dashed boxes indicate the region of activation (~10 um; ROA). Time-lapse images of the soma at every 20th frame (time stamp in parenthesis) are shown for CRTC1^{270} in both native green and photoconverted red channels. Scale bar = 20 μm. **(B–E)** Neurons expressing CRTC1^{270} were stimulated with **(B)** mock or MNI-glutamate in the presence or absence of APV and NBQX (*$p = 0.49$ mock vs. APV/NBQX; $p < 0.0001$ MNI vs. mock and APV/NBQX), **(C)** MNI-glutamate at 35°C or 23°C (*$p < 0.0001$ Mock 35°C vs. MNI 35°C, Mock 35°C vs. MNI 23°C, and MNI 35°C vs. MNI 23°C), **(D)** MNI-glutamate after incubation with NDZ (*$p < 0.0001$ DMSO vs. NDZ), or **(E)** pretreated with either BAPTA-AM or EGTA-AM prior to glutamate uncaging (*$p < 0.0001$ DMSO vs. EGTA vs. BAPTA and EGTA vs. BAPTA). Statistics were performed with linear regression analysis of the slopes for comparison of fit between data sets.

toward the soma. Conversely, the non-stimulated CRTC1^{270} control had averages closer to zero, indicating a bidirectional distribution of the photoconverted signal across the length of the dendrite (**Figures 6B,C**). To better illustrate the shift in fluorescence intensity over time, we graphed the cumulative bias of CRTC1^{270} moving toward the soma during the length of the experiment (**Figure 6C**). A positive cumulative slope indicates that activated CRTC1^{270} concentrations are much higher on the proximal branch of the dendrite throughout image acquisition.

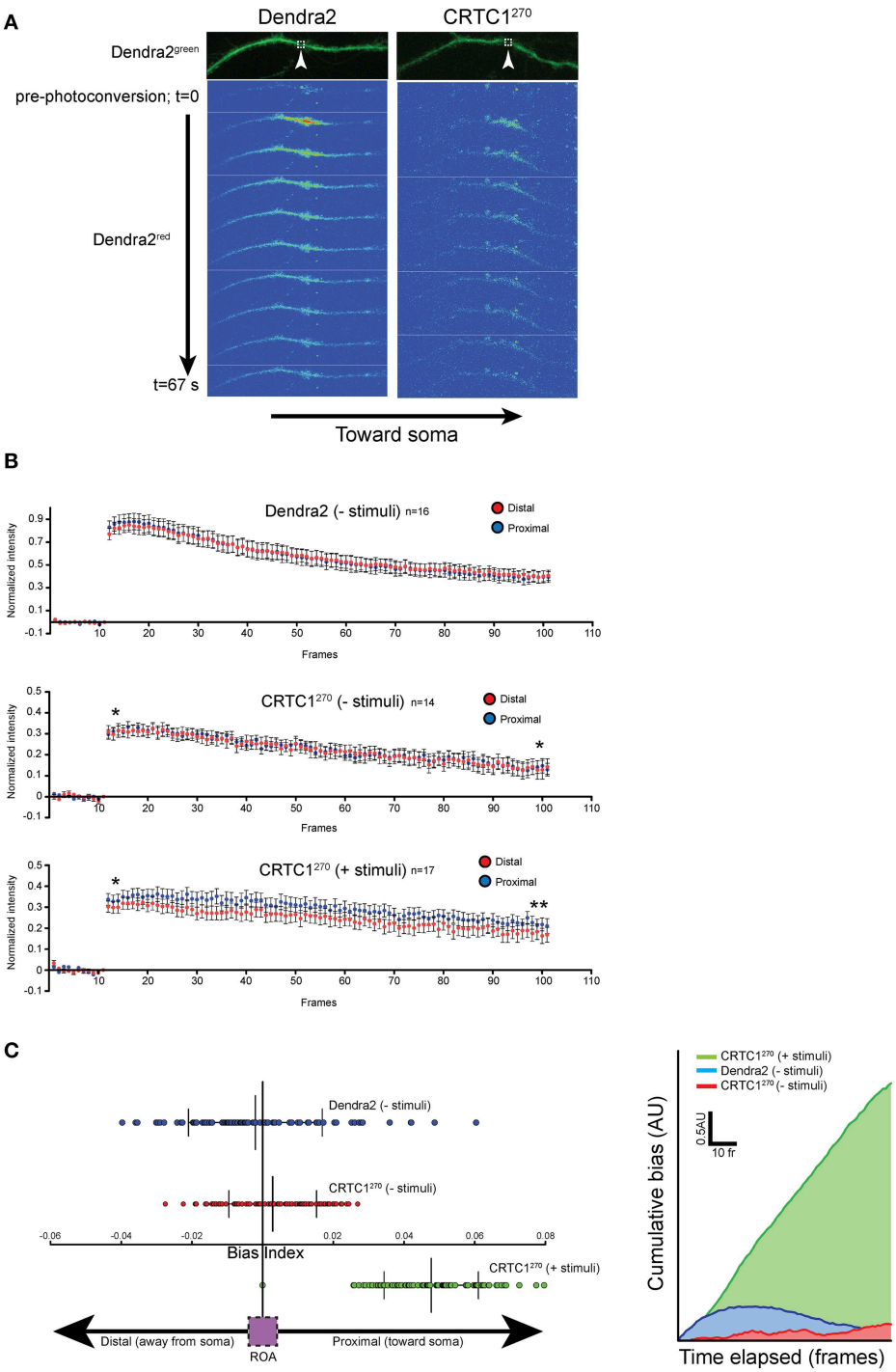

FIGURE 6 | Local CRTC1^{270} transport from dendrites is biased toward the nucleus during glutamatergic stimulation. (A,B) Neurons expressing either Dendra2 alone or CRTC1^{270} were mock treated (-stimuli) or bath stimulated (+stimuli) followed by UV activation in a (1.5 um^2) region (white box) of dendrite. The rapid movement of Dendra2^{red} was captured by spinning disc microscopy. The normalized intensity (over baseline levels) over time of Dendra2^{red} was quantified for a 40 μm segment of the dendrite either proximal (closer to the soma) or distal to the area of the photoconversion (upaired *t*-test, two-tailed $^{**}p < 0.05$ at $t = 95$–100; $^{*}p > 0.05$, not significant at $t = 11$–15). **(C)** The difference in pairwise spatial measurements of normalized Dendra2^{red} along the dendrite from the ROA was quantified as a bias index. A positive bias indicates a higher signal intensity in proximal dendrites. Data points were then plotted as a cumulative bias index over time elapsed for each stimulation paradigm (AU = arbitrary units).

Dephosphorylation at Three Conserved Serine Residues in CRTC1 Triggers Release of CRTC1 from 14-3-3ε and Synapse to Nucleus Translocation

The phosphorylation state of CRTC1 undergoes complex changes after synaptic activity in rodent hippocampal neurons (Ch'ng et al., 2012; Nonaka et al., 2014). We hypothesized that the nuclear translocation of CRTC1 involved dephosphorylation of specific residues. Analysis of the mouse CRTC1 primary amino acid sequence revealed a high conserved sequence across multiple species with significant enrichment of serine and threonine residues (**Figure 7A** and Supplementary Figure S5A). To identify the residues that are phosphorylated in CRTC1, we transiently transfected mouse Neuro-2A cell lines with full-length HA epitope-tagged CRTC1 protein, purified the protein using HA antibodies and analyzed the samples by mass spectometry. We identified candidate phosphopeptides containing 50 putative phosphoresidues (33 Ser, 14 Thr and 3 Tyr residues; **Figure 7A**; labeled in color). This is likely an underestimate of the total number of phosphorylated residues in CRTC1 since we omitted phosphopeptide hits identified with less than 90% confidence levels. Sequence homology of CRTC1 indicated that 11 of the phosphorylated residues are 100% conserved across 10 species (**Figure 7A**; labeled in red). Nine of these are located within the N-terminal 270 amino acids. To begin to dissect the role of regulated dephosphorylation in the synapse to nucleus transport of CRTC1, we generated phosphoincompetent (serine to alanine) mutations at three of these sites, S64, S151, and S245, as single, double and triple mutants within CRTC1^{270}. Dephosphorylation of S151 has been shown to be sufficient for nuclear import in non-neuronal cells (Kovács et al., 2007; Altarejos et al., 2008), while dephosphorylation of both S151 and S245 has been reported to be sufficient for significant CRTC1 nuclear accumulation in neurons (Nonaka et al., 2014). We also included S64 in our studies because, as shown in **Figure 8**, like S245, S64, shares 100% similarity across 13 species (with S64 being a T in *C. elegans*) and S64 and S245 have identical flanking amino acids (GGSLP), which are also highly conserved across species.

To elucidate the function of S64 and the conserved amino acids flanking S64, we made several substitution mutations at and surrounding S64 in CRTC1^{270}, including a double tyrosine to alanine (Y60A/Y61A) mutant and a glutamine to alanine substitution mutant (Q70A; Supplementary Figure S5B) and expressed these mutant proteins in neurons. As shown in

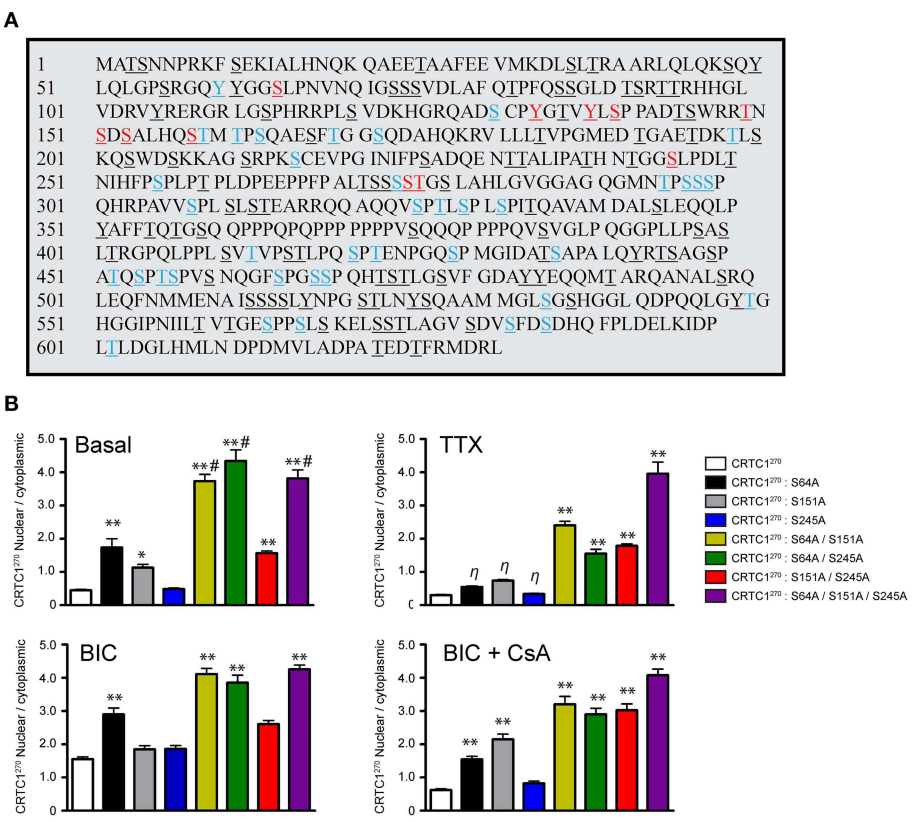

FIGURE 7 | Phosphorylation state of CRTC1. (A) HA-tagged CRTC1 was immunoprecipitated from Neuro-2A cells and analyzed by mass spectrometry. Residues in both blue and red (50/643) were identified as phosphorylation sites. Phosphorylated sites labeled in red (13/50) share 100% conservation across 10 different species. All serine, threonine and tyrosines are underlined. **(B)** Single, double or triple CRTC1^{270} serine to alanine mutations were generated (S64A, S151A, and S245A) and expressed in neurons that were silenced with TTX, stimulated with BIC or BIC and CsA (**$p < 0.001$ relative to CRTC1^{270}; *$p < 0.05$ relative to CRTC1^{270}; η: not significant relative to CRTC1^{270}; #$p < 0.001$ relative to S151A/S245A).

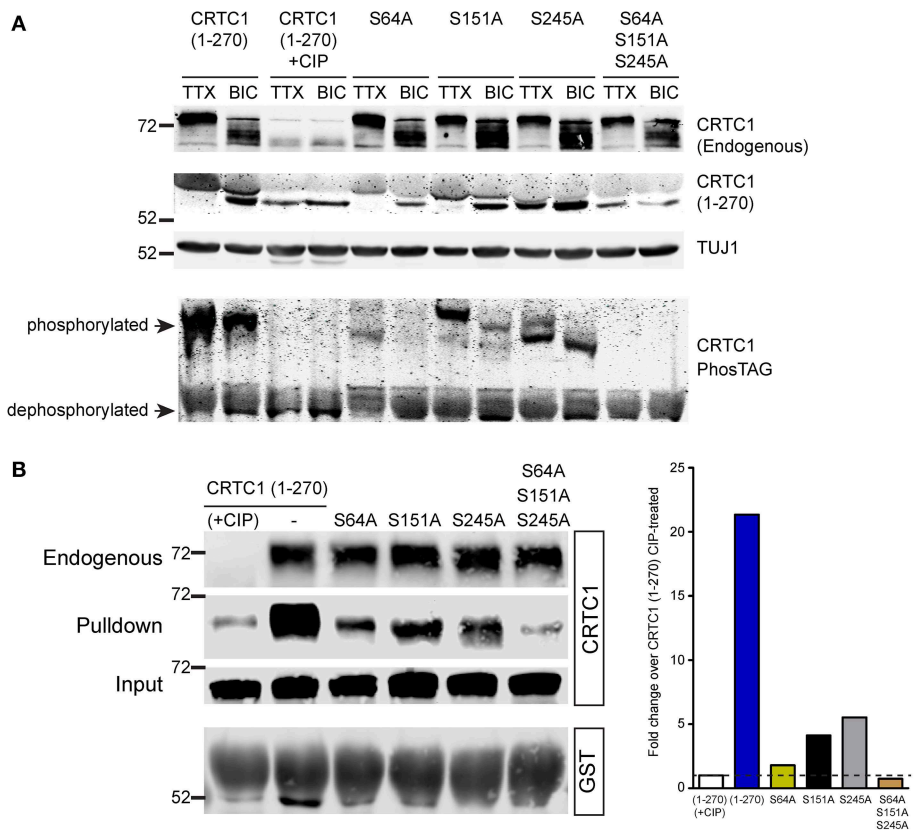

FIGURE 8 | Dephosphorylation of S64, S151 and S245 regulates interaction of CRTC1 with 14-3-3ε. (A) The single and triple alanine CRTC1^{270} mutations described in **Figure 7** were expressed in cortical neurons (21–28 DIV) and incubated with TTX or BIC. Neuronal lysates were analyzed via traditional or PhosTAG acrylamide gels and immunoblotted with antibodies against CRTC1 and TUJ1. **(B)** Cortical neuron expressing CRTC1^{270} point mutants were lysed and incubated with GST-purified 14-3-3ε and pulldowns were analyzed by immunoblotting with antibodies against GST or CRTC1. Endogenous CRTC1 binds to GST 14-3-3ε comparably across all samples while input controls indicate equivalent expression of all CRTC1^{270} proteins is neurons.

Figure 7B and Supplementary Figures S5B,D, the S64A mutant was cytoplasmically localized in TTX-silenced neurons, but exhibited enhanced nuclear accumulation compared to wildtype CRTC1^{270} in BIC-stimulated neurons and in control, unsilenced neurons (which have basal levels of action potential firing). Mutations at Y60, Y61, Q70 or at the conserved serine at 245 did not alter the localization of CRTC1^{270} as compared to wild type CRTC1^{270} in either silenced, basal or stimulated neurons.

We previously reported that unlike in non-neuronal cells (Altarejos et al., 2008), CRTC1 bearing a S151A mutation did not result in constitutive CRTC1 nuclear accumulation. We generated the S151A mutation for CRTC1^{270}, and again found that when expressed in neurons, the mutant localized to the cytoplasm in TTX-silenced neurons. Although we observed significantly more S151A-CRTC1^{270} in the nucleus in unsilenced neuronal cultures, we did not detect any enhancement of nuclear accumulation in BIC-stimulated neurons (**Figure 7**). Similarly, a single serine to alanine mutation at S245 also did not result in constitutive accumulation of CRTC1^{270} in the nucleus. These results indicate that dephosphorylation of S151 alone, similar to S64 and S245 is not sufficient to promote robust nuclear import of CRTC1.

Since none of the single serine to alanine mutations generated a constitutive nuclear localization of CRTC1^{270} in TTX-silenced neurons, we tested the possibility that dephosphorylation at combinations of the three sites was required for nuclear accumulation. To test this idea, we generated double and triple serine to alanine substitution mutants (S64A/S151A; S64A/S245A; S151A/S245A; and S64A/S151A/S245A) in CRTC1^{270}. We found that all three double mutants exhibited increased nuclear accumulation of CRTC1^{270} in TTX-silenced neurons, and enhanced nuclear accumulation in basal and BIC-stimulated neurons. The amount of CRTC1^{270} nuclear accumulation in the double mutants was less than in the triple S64A/S151A/S245A mutant under all conditions. Thus, when all three serine residues were simultaneously mutated to alanine, CRTC1^{270} was constitutively localized in the nucleus (**Figure 7** and Supplementary Figure S5B). We also constructed serine to aspartic acid or glutamic acid phosphomimetic mutations at S64, S151, and S245 individually but found that none of these mutations constitutively localized CRTC1 to the cytoplasm (Supplementary Figures S5B–D).

We used a combination of conventional and PhosTag immunoblotting to monitor the effect of these mutations on

the mobility of CRTC1^{270}. The mobility of CRTC1^{270} was higher in TTX silenced than in BIC-stimulated neurons, with phosphatase treatment of the lysates dropping the molecular weight (MW) of CRTC1^{270} similar to the MW observed in BIC-stimulated neurons (**Figure 8A**). Of the three single mutations, only the S245A mutation showed significant amounts of the lowest MW band in TTX stimulated neurons, though PhosTag gel analysis indicated that the S245 protein was not completely dephosphorylated (**Figure 8A**). One possible explanation is that S245A mutation resulted in subsequent dephosphorylation at multiple sites on CRTC1, resulting in a lower molecular weight band. All three serine to alanine mutants were responsive to BIC stimulation, as BIC increased the concentration of the lowest MW species. In contrast, the triple mutant S64A/S151A/S245A looked like the phosphatase-treated sample, with only the lowest MW band in both TTX-silenced and BIC-stimulated neurons (**Figure 8A**). As our earlier 2-D gel analyses revealed a large number of CRTC1 species, each with differential patterns of phosphorylation (Ch'ng et al., 2012), the results shown in **Figure 8A** suggest that dephosphorylation of S64, S151, and S245 may function to trigger subsequent differential dephosphorylation throughout CRTC1.

We previously demonstrated that CRTC1 binds to 14-3-3ε in an activity-dependent manner (Ch'ng et al., 2012). When neurons were silenced with TTX, phosphorylated CRTC1 bound 14-3-3ε and was sequestered in the cytoplasm; BIC triggered CRTC1 dephosphorylation and dissociation from 14-3-3ε. To assess whether S64, S151 or S245 play roles in anchoring CRTC1 to 14-3-3ε, we transduced cultured cortical neurons with lentiviral vectors expressing CRTC1^{270} harboring substitution mutations (S64A, S151A, S245A, or S64A/S151A/S245A), collected neuronal lysates and incubated with 14-3-3ε -GST. As shown in **Figure 8B**, single point mutations at S64, S151 and S245 diminished but did not abolish the interaction between CRTC1 and 14-3-3ε. Notably, the degree of interaction between the mutants and 14-3-3ε correlated inversely with their nuclear accumulation (i.e., S64A had the highest nuclear accumulation but lowest interaction with 14-3-3ε **Figure 8**). The triple S64A/S151A/S245A mutant did not bind 14-3-3ε similar to phosphatase-treated CRTC1^{270} (**Figure 8B**).

Discussion

CRTC1 undergoes robust nuclear translocation during learning-related synaptic plasticity (Zhou et al., 2006; Kovács et al., 2007; Ch'ng et al., 2012; Nonaka et al., 2014) but the mechanism for this activity-dependent translocation remains elusive. Our goal was to further characterize the cell biology of activity-dependent CRTC1 synapse to nucleus transport. Our studies revealed that local activation of synaptic glutamatergic receptors and L-type VGCCs generate the source of calcium required for the regulated nuclear import of CRTC1. We also showed that CRTC1 undergoes dynein-mediated and NLS-dependent transport along microtubules to reach the nucleus. Next, we identified the regions of CRTC1 that are critical for regulated trafficking of CRTC1, including three serine residues that undergo dephosphorylation to be released from 14-3-3ε at the synapse. Finally, we developed a reporter containing the minimal regions of CRTC1 required for regulated nuclear import fused to the photoconvertible fluorescent protein Dendra2, and used this to monitor in real time, stimulus-induced synapse to nucleus transport of CRTC1 in neurons.

CRTC1 nuclear translocation has been shown to depend on elevations in intracellular calcium resulting from synaptic activation (Zhou et al., 2006; Kovács et al., 2007; Ch'ng et al., 2012; Nonaka et al., 2014). In this report, we dissected the contributions of specific channels and receptors in generating the elevations in calcium required for CRTC1 nuclear translocation. We found that inhibition of AMPA-type receptors blocks CRTC1 synapse to nucleus translocation, but that calcium entry through AMPA receptors along with activation of L-type VGCC was sufficient to promote CRTC1 nuclear import. In other experiments, we found that calcium influx through NMDA receptors is sufficient to trigger CRTC1 nuclear translocation as long as there is sufficient depolarization to relieve the Mg^{2+} block in the receptor (**Figure 1**). Recent studies indicate that depolarization activates L-type VGCC to couple local calcium influx with transcription in the nucleus (Wheeler et al., 2012) in a manner that involves calcineurin-mediated dephosphorylation of CamKIIγ, which in turn transports calcium-calmodulin to the nucleus where it activates CamKIV, leading to the phosphorylation of CREB (Ma et al., 2014). Here we find that either activation of NMDA receptors in the absence of L-type VGCC activation, or AMPA receptor activation coupled with L-type VGCC activation is sufficient to promote CRTC1 synapse to nucleus translocation, suggesting that CRTC1-mediated transcription, like that of NFkB (Meffert et al., 2003) and Jacob (Karpova et al., 2013), tracks synaptic stimulation rather than cell-wide neuronal depolarization.

Comparison of figures magnitude of the activity-dependent nuclear accumulation of CRTC1 varied somewhat between experiments (see **Figures 2**, **5**). This can be attributed to difference in the basal network activity of cultures, since cultures with high levels of basal activity have increased concentrations of CRTC1 in the nucleus. Of relevance, we note that each set of experiments performed in this study include negative (TTX) and positive (bicuculline) controls for CRTC1 nuclear accumulation.

A paucity of cell biological studies address the long-distance retrograde transport of soluble proteins in dendrites. Theoretical evidence suggest that fast local signaling can be mediated by diffusion only under short distances (<200 nm); (Kholodenko, 2003; Howe, 2005). In this paper, we show that CRTC1 is actively transported to the nucleus in an energy-dependent manner that requires microtubules and is mediated by the motor protein dynein (**Figure 2**). While dynein is a major microtubule-based molecular motor for cargo transport from soma to dendrites (Kapitein et al., 2010), its role in synapse to nucleus signaling is not well characterized. Since microtubules have mixed polarity in dendrites (Silverman et al., 2010), our studies support a critical role for the minus-end directed motor dynein in mediating the retrograde transport of CRTC1 from synapse to nucleus.

Unlike movement of large organelles or vesicular trafficking, studying the transport of soluble proteins such as CRTC1 in dendrites poses a greater challenge since the protein moves

diffusely throughout the dendrite rather than as a punctate vesicular structure that can be tracked. By fluorescently labeling a subpopulation of CRTC1 in dendrites via photoconversion of Dendra2, we were able to track and quantify the movement of the soluble protein as a fluorescent "plume" as it propagated along dendrites and to monitor the accumulation of photoconverted Dendra2 signal in the nucleus. We detected a small but significant bias of retrograde movement of CRTC1 toward the soma following stimulation. It is likely that the small ROA coupled with the relative abundance of fluorescent CRTC1 in dendrites decreases signal to noise and thus reduced our ability to detect a larger magnitude bias in retrograde movement toward the soma. At present, it is unclear if soluble proteins in dendrites are transported as a single protein or as a macromolecular signaling complex associated with motor proteins. In axons, the hypothesis that bulk movement of soluble proteins is mainly transported as "slow" axoplasmic flow has been recently challenged by observations that soluble proteins can assemble into higher order structures that engage the active transport machinery for axonal transport (Scott et al., 2011).

We chose to study CRTC1^{270} instead of the full length protein because our goal was to identify the minimal region and the signals contained within this region that drives activity-dependent nuclear translocation and for the practical reason that tagged full-length CRTC1 was too large to package in neurotrophic viral vectors. By excluding the carboxy-terminal transcriptional activation domain of the protein, we also avoided any aberrant transcription that might occur due to overexpression of CRTC1^{270}. We systematically tested CRTC1^{270} and found it responds to stimuli and translocates to the nucleus similar to wild type protein, that it does not act as a dominant negative inhibitor of CREB-mediated transcription, and that lentiviral-mediated expression under control of the *Camk2α* promoter does not affect the long term viability of mature neurons. Our results suggest that CRTC1^{270} is a faithful reporter of neuronal activity and can be used as a tool for studying synapse to nuclear signaling in *in vivo* preparations, where its nuclear translocation may be used to rapidly identify neurons that are activated in response to specific stimuli. Moreover, our results suggest that CRTC1^{270} has the potential to serve as a useful tool for activity-dependent delivery of molecules to the nucleus. Thus, one could couple CRTC1^{270} to a chimeric transcriptional regulator, and deliver it to the nucleus only following glutamatergic activity.

CRTC1 is one of several post-synaptically localized proteins that undergo nucleocytoplasmic shuttling during various forms of neuronal plasticity (Lee et al., 2007; Lai et al., 2008; Marcora and Kennedy, 2010; Sekeres et al., 2012; Karpova et al., 2013). Many of these proteins contain strong NLSs that engages the heterodimeric importin α/β1 classical nuclear adaptor protein complex that couples to dynein-mediated microtubule transport to enter the nucleus (Perlson et al., 2005; Mikenberg et al., 2007; Shrum et al., 2009; Ben-Yaakov et al., 2012). We have identified a highly conserved and potent NLS in CRTC1 that is both necessary and sufficient to trigger nuclear entry. However, while CRTC1 is actively transported to the nucleus, its entry is not mediated by the classical nuclear import pathway. CRTC1 may enter the nucleus by binding to other NLS-bearing proteins or by non-conventional nuclear import pathways such as via a member of the importin β superfamily (Chook and Süel, 2011), direct binding to nuclear pore complex (Koike et al., 2004) or it may be escorted by other nuclear chaperone proteins (Fagotto et al., 1998).

We discovered three residues, S64, S151, and S245 that play crucial and synergistic roles in nuclear accumulation of CRTC1. While individual point mutations at these serine residues did not significantly alter the localization of CRTC1 in silenced neurons, a triple phospho-incompetent mutation resulted in constitutive nuclear localization in the absence of neuronal activity (**Figure 8**). Since the nuclear accumulation of the phosphorylation-incompetent mutants inversely correlated with the association with 14-3-3ε cytoplasmic anchoring protein, it is likely that the constitutive transport of CRTC1 into the nucleus, as opposed to defects in nuclear export, underlies the robust nuclear accumulation of the phospho-incompetent mutants.

Nonaka and colleagues recently reported that alanine scanning mutations in S151 and S245 resulted in constitutive nuclear localization of CRTC1 in cortical neurons (Nonaka et al., 2014). However, we found that a S151 and S245 double mutation showed only a slight enhancement of nuclear accumulation over the wild type protein in silenced neurons. In contrast, we provide evidence that phosphorylation at S64 is a potent regulator of CRTC1 nuclear translocation. In unstimulated neurons, a single point mutation at S64 alone led to a 2-fold increase in the nuclear to cytoplasmic ratio of CRTC1 while a double mutation of S64 paired with either S151 or S245 resulted in a 4-5-fold increase in the nuclear accumulation of CRTC1. Taken together, our results indicate that the phosphorylation state of S64 is a major contributor, together with S151 and S245, in regulating CRTC1 nucleocytoplasmic shuttling in neurons.

The fact that dephosphorylation of only 3 amino acids is sufficient to trigger nuclear import of CRTC1 raises questions about the function of the large number of remaining, highly conserved phosphorylated residues. It is unclear if dephosphorylation of any of these 3 amino acids, either individually or as a combination, also results in a coordinated dephosphorylation at other phosphorylation sites. Given that CRTC1 exists in multiple phosphorylated forms as assessed by two dimensional gel analysis (Ch'ng et al., 2012), it is plausible that the activation of distinct signaling pathways within dendrites and spines following specific types of stimulation can differentially alter the pattern of CRTC1 phosphorylation which may serve as a code that couples patterns of stimulation with specific programs of gene expression.

Taken together, the results of our experiments provide insight into the mechanisms by which soluble signals are transported from the synapse to the nucleus during transcription-dependent activity. They provide molecular insight not only into how activity regulates CRTC1 to promote its nuclear import, but also into some of the cell biological pathways mediating this long-distance transport.

Funding

The work was supported by a NARSAD Young Investigator Award (to TC) and NIH R01 MH MH077022 (to KM).

Acknowledgments

We thank T. J. O'Dell and members of the Martin lab, especially K. Olofsdotter-Otis, S. Bonanno, J. Achiro for critical reading of the manuscript. We also thank P. Osten, W. Hampe, M. Meffert, R. Y. Tsien, and B. Baliff for generously sharing reagents.

Supplementary Material

The Supplementary Material for this article can be found online at: http://journal.frontiersin.org/article/10.3389/fnmol.2015.00048

References

Alberini, C. M. (2009). Transcription factors in long-term memory and synaptic plasticity. *Physiol. Rev.* 89, 121–145. doi: 10.1152/physrev.00017.2008

Altarejos, J. Y., Goebel, N., Conkright, M. D., Inoue, H., Xie, J., Arias, C. M., et al. (2008). The Creb1 coactivator Crtc1 is required for energy balance and fertility. *Nat. Med.* 14, 1112–1117. doi: 10.1038/nm.1866

Ballif, B. A., Cao, Z., Schwartz, D., Carraway, K. L. III., and Gygi, S. P. (2006). Identification of 14-3-3epsilon substrates from embryonic murine brain. *J. Proteome Res.* 5, 2372–2379. doi: 10.1021/pr060206k

Ben-Yaakov, K., Dagan, S. Y., Segal-Ruder, Y., Shalem, O., Vuppalanchi, D., Willis, D. E., et al. (2012). Axonal transcription factors signal retrogradely in lesioned peripheral nerve. *EMBO J.* 31, 1350–1363. doi: 10.1038/emboj.2011.494

Ch'ng, T. H., Uzgil, B., Lin, P., Avliyakulov, N. K., O'Dell, T. J., and Martin, K. C. (2012). Activity-dependent transport of the transcriptional coactivator CRTC1 from synapse to nucleus. *Cell* 150, 207–221. doi: 10.1016/j.cell.2012.05.027

Chook, Y. M., and Süel, K. E. (2011). Nuclear import by karyopherin-βs: recognition and inhibition. *Biochim. Biophys. Acta* 1813, 1593–1606. doi: 10.1016/j.bbamcr.2010.10.014

Chudakov, D. M., Matz, M. V., Lukyanov, S., and Lukyanov, K. A. (2010). Fluorescent proteins and their applications in imaging living cells and tissues. *Physiol. Rev.* 90, 1103–1163. doi: 10.1152/physrev.00038.2009

Deisseroth, K., Bito, H., and Tsien, R. W. (1996). Signaling from synapse to nucleus: postsynaptic CREB phosphorylation during multiple forms of hippocampal synaptic plasticity. *Neuron* 16, 89–101. doi: 10.1016/S0896-6273(00)80026-4

Dittgen, T., Nimmerjahn, A., Komai, S., Licznerski, P., Waters, J., Margrie, T. W., et al. (2004). Lentivirus-based genetic manipulations of cortical neurons and their optical and electrophysiological monitoring *in vivo*. *Proc. Natl. Acad. Sci. U.S.A.* 101, 18206–18211. doi: 10.1073/pnas.0407976101

Eng, J. K., McCormack, A. L., and Yates, J. R. (1994). An approach to correlate tandem mass spectral data of peptides with amino acid sequences in a protein database. *J. Am. Soc. Mass Spectrom.* 5, 976–989. doi: 10.1016/1044-0305(94)80016-2

Fagotto, F., Gluck, U., and Gumbiner, B. M. (1998). Nuclear localization signal-independent and importin/karyopherin-independent nuclear import of beta-catenin. *Curr. Biol.* 8, 181–190. doi: 10.1016/S0960-9822(98)70082-X

Higley, M. J., and Sabatini, B. L. (2012). Calcium signaling in dendritic spines. *Cold Spring Harb. Perspect. Biol.* 4:a005686. doi: 10.1101/cshperspect.a005686

Hirano, Y., Masuda, T., Naganos, S., Matsuno, M., Ueno, K., Miyashita, T., et al. (2013). Fasting launches CRTC to facilitate long-term memory formation in Drosophila. *Science* 339, 443–446. doi: 10.1126/science.1227170

Hollander, J. A., Im, H. I., Amelio, A. L., Kocerha, J., Bali, P., Lu, Q., et al. (2010). Striatal microRNA controls cocaine intake through CREB signalling. *Nature* 466, 197–202. doi: 10.1038/nature09202

Howe, C. L. (2005). Modeling the signaling endosome hypothesis: why a drive to the nucleus is better than a (random) walk. *Theor. Biol. Med. Model.* 2:43. doi: 10.1186/1742-4682-2-43

Iourgenko, V., Zhang, W., Mickanin, C., Daly, I., Jiang, C., Hexham, J. M., et al. (2003). Identification of a family of cAMP response element-binding protein coactivators by genome-scale functional analysis in mammalian cells. *Proc. Natl. Acad. Sci. U.S.A.* 100, 12147–12152. doi: 10.1073/pnas.1932773100

Jagannath, A., Butler, R., Godinho, S. I., Couch, Y., Brown, L. A., Vasudevan, S. R., et al. (2013). The CRTC1-SIK1 pathway regulates entrainment of the circadian clock. *Cell* 154, 1100–1111. doi: 10.1016/j.cell.2013.08.004

Jeffrey, R. A., Ch'ng, T. H., O'Dell, T. J., and Martin, K. C. (2009). Activity-dependent anchoring of importin alpha at the synapse involves regulated binding to the cytoplasmic tail of the NR1-1a subunit of the NMDA receptor. *J. Neurosci.* 29, 15613–15620. doi: 10.1523/JNEUROSCI.3314-09.2009

Jeong, H., Cohen, D. E., Cui, L., Supinski, A., Savas, J. N., Mazzulli, J. R., et al. (2012). Sirt1 mediates neuroprotection from mutant huntingtin by activation of the TORC1 and CREB transcriptional pathway. *Nat. Med.* 18, 159–165. doi: 10.1038/nm.2559

Jiang, M., and Chen, G. (2006). High $Ca2^{+}$-phosphate transfection efficiency in low-density neuronal cultures. *Nat. Protoc.* 1, 695–700. doi: 10.1038/nprot.2006.86

Kaiser, P., and Wohlschlegel, J. (2005). Identification of ubiquitination sites and determination of ubiquitin-chain architectures by mass spectrometry. *Meth. Enzymol.* 399, 266–277. doi: 10.1016/S0076-6879(05)99018-6

Kandel, E. R. (2001). The molecular biology of memory storage: a dialogue between genes and synapses. *Science* 294, 1030–1038. doi: 10.1126/science.1067020

Kapitein, L. C., Schlager, M. A., Kuijpers, M., Wulf, P. S., van Spronsen, M., MacKintosh, F. C., et al. (2010). Mixed microtubules steer dynein-driven cargo transport into dendrites. *Curr. Biol.* 20, 290–299. doi: 10.1016/j.cub.2009.12.052

Karpova, A., Mikhaylova, M., Bera, S., Bär, J., Reddy, P. P., Behnisch, T., et al. (2013). Encoding and transducing the synaptic or extrasynaptic origin of NMDA receptor signals to the nucleus. *Cell* 152, 1119–1133. doi: 10.1016/j.cell.2013.02.002

Kessels, H. W., and Malinow, R. (2009). Synaptic AMPA receptor plasticity and behavior. *Neuron* 61, 340–350. doi: 10.1016/j.neuron.2009.01.015

Kholodenko, B. N. (2003). Four-dimensional organization of protein kinase signaling cascades: the roles of diffusion, endocytosis and molecular motors. *J. Exp. Biol.* 206, 2073–2082. doi: 10.1242/jeb.00298

Koike, M., Kose, S., Furuta, M., Taniguchi, N., Yokoya, F., Yoneda, Y., et al. (2004). beta-Catenin shows an overlapping sequence requirement but distinct molecular interactions for its bidirectional passage through nuclear pores. *J. Biol. Chem.* 279, 34038–34047. doi: 10.1074/jbc.M405821200

Kovács, K. A., Steullet, P., Steinmann, M., Do, K. Q., Magistretti, P. J., Halfon, O., et al. (2007). TORC1 is a calcium- and cAMP-sensitive coincidence detector involved in hippocampal long-term synaptic plasticity. *Proc. Natl. Acad. Sci. U.S.A.* 104, 4700–4705. doi: 10.1073/pnas.0607524104

Lai, K. O., Zhao, Y., Ch'ng, T. H., and Martin, K. C. (2008). Importin-mediated retrograde transport of CREB2 from distal processes to the nucleus in neurons. *Proc. Natl. Acad. Sci. U.S.A.* 105, 17175–17180. doi: 10.1073/pnas.0803906105

Lange, A., Mills, R. E., Lange, C. J., Stewart, M., Devine, S. E., and Corbett, A. H. (2007). Classical nuclear localization signals: definition, function, and interaction with importin alpha. *J. Biol. Chem.* 282, 5101–5105. doi: 10.1074/jbc.R600026200

Lee, S. H., Lim, C. S., Park, H., Lee, J. A., Han, J. H., Kim, H., et al. (2007). Nuclear translocation of CAM-associated protein activates transcription for long-term facilitation in Aplysia. *Cell* 129, 801–812. doi: 10.1016/j.cell.2007.03.041

Leslie, J. H., and Nedivi, E. (2011). Activity-regulated genes as mediators of neural circuit plasticity. *Prog. Neurobiol.* 94, 223–237. doi: 10.1016/j.pneurobio.2011.05.002

Ma, H., Groth, R. D., Cohen, S. M., Emery, J. F., Li, B., Hoedt, E., et al. (2014). gammaCaMKII shuttles Ca(2)(+)/CaM to the nucleus to trigger CREB phosphorylation and gene expression. *Cell* 159, 281–294. doi: 10.1016/j.cell.2014.09.019

Macías, W., Carlson, R., Rajadhyaksha, A., Barczak, A., and Konradi, C. (2001). Potassium chloride depolarization mediates CREB phosphorylation in striatal neurons in an NMDA receptor-dependent manner. *Brain Res.* 890, 222–232. doi: 10.1016/S0006-8993(00)03163-2

Maeder, C. I., Shen, K., and Hoogenraad, C. C. (2014). Axon and dendritic trafficking. *Curr. Opin. Neurobiol.* 27, 165–170. doi: 10.1016/j.conb.2014.03.015

Marcora, E., and Kennedy, M. B. (2010). The Huntington's disease mutation impairs Huntingtin's role in the transport of NF-kappaB from the synapse to the nucleus. *Hum. Mol. Genet.* 19, 4373–4384. doi: 10.1093/hmg/ddq358

Meffert, M. K., Chang, J. M., Wiltgen, B. J., Fanselow, M. S., and Baltimore, D. (2003). NF-kappa B functions in synaptic signaling and behavior. *Nat. Neurosci.* 6, 1072–1078. doi: 10.1038/nn1110

Melkonian, K. A., Maier, K. C., Godfrey, J. E., Rodgers, M., and Schroer, T. A. (2007). Mechanism of dynamitin-mediated disruption of dynactin. *J. Biol. Chem.* 282, 19355–19364. doi: 10.1074/jbc.M700003200

Mikenberg, I., Widera, D., Kaus, A., Kaltschmidt, B., and Kaltschmidt, C. (2007). Transcription factor NF-kappaB is transported to the nucleus via cytoplasmic dynein/dynactin motor complex in hippocampal neurons. *PLoS ONE* 2:e589. doi: 10.1371/journal.pone.0000589

Neher, E., and Almers, W. (1986). Patch pipettes used for loading small cells with fluorescent indicator dyes. *Adv. Exp. Med. Biol.* 211, 1–5. doi: 10.1007/978-1-4684-5314-0_1

Nonaka, M., Kim, R., Fukushima, H., Sasaki, K., Suzuki, K., Okamura, M., et al. (2014). Region-specific activation of CRTC1-CREB signaling mediates long-term fear memory. *Neuron* 84, 92–106. doi: 10.1016/j.neuron.2014.08.049

Perlson, E., Hanz, S., Ben-Yaakov, K., Segal-Ruder, Y., Seger, R., and Fainzilber, M. (2005). Vimentin-dependent spatial translocation of an activated MAP kinase in injured nerve. *Neuron* 45, 715–726. doi: 10.1016/j.neuron.2005.01.023

Saha, R. N., Wissink, E. M., Bailey, E. R., Zhao, M., Fargo, D. C., Hwang, J. Y., et al. (2011). Rapid activity-induced transcription of Arc and other IEGs relies on poised RNA polymerase II. *Nat. Neurosci.* 14, 848–856. doi: 10.1038/nn.2839

Sasaki, T., Takemori, H., Yagita, Y., Terasaki, Y., Uebi, T., Horike, N., et al. (2011). SIK2 is a key regulator for neuronal survival after ischemia via TORC1-CREB. *Neuron* 69, 106–119. doi: 10.1016/j.neuron.2010.12.004

Saura, C. A. (2012). CREB-regulated transcription coactivator 1-dependent transcription in Alzheimer's disease mice. *Neurodegener. Dis.* 10, 250–252. doi: 10.1159/000333341

Scott, D. A., Das, U., Tang, Y., and Roy, S. (2011). Mechanistic logic underlying the axonal transport of cytosolic proteins. *Neuron* 70, 441–454. doi: 10.1016/j.neuron.2011.03.022

Screaton, R. A., Conkright, M. D., Katoh, Y., Best, J. L., Canettieri, G., Jeffries, S., et al. (2004). The CREB coactivator TORC2 functions as a calcium- and cAMP-sensitive coincidence detector. *Cell* 119, 61–74. doi: 10.1016/j.cell.2004.09.015

Seibel, N. M., Eljouni, J., Nalaskowski, M. M., and Hampe, W. (2007). Nuclear localization of enhanced green fluorescent protein homomultimers. *Anal. Biochem.* 368, 95–99. doi: 10.1016/j.ab.2007.05.025

Sekeres, M. J., Mercaldo, V., Richards, B., Sargin, D., Mahadevan, V., Woodin, M. A., et al. (2012). Increasing CRTC1 function in the dentate gyrus during memory formation or reactivation increases memory strength without compromising memory quality. *J. Neurosci.* 32, 17857–17868. doi: 10.1523/JNEUROSCI.1419-12.2012

Shrum, C. K., Defrancisco, D., and Meffert, M. K. (2009). Stimulated nuclear translocation of NF-kappaB and shuttling differentially depend on dynein and the dynactin complex. *Proc. Natl. Acad. Sci. U.S.A.* 106, 2647–2652. doi: 10.1073/pnas.0806677106

Silverman, M. A., Kaech, S., Ramser, E. M., Lu, X., Lasarev, M. R., Nagalla, S., et al. (2010). Expression of kinesin superfamily genes in cultured hippocampal neurons. *Cytoskeleton* 67, 784–795. doi: 10.1002/cm.20487

Tabb, D. L., McDonald, W. H., and Yates, J. R. III. (2002). DTASelect and Contrast: tools for assembling and comparing protein identifications from shotgun proteomics. *J. Proteome Res.* 1, 21–26. doi: 10.1021/pr015504q

Talcott, B., and Moore, M. S. (1999). Getting across the nuclear pore complex. *Trends Cell Biol.* 9, 312–318. doi: 10.1016/S0962-8924(99)01608-6

Thompson, K. R., Otis, K. O., Chen, D. Y., Zhao, Y., O'Dell, T. J., and Martin, K. C. (2004). Synapse to nucleus signaling during long-term synaptic plasticity; a role for the classical active nuclear import pathway. *Neuron* 44, 997–1009. doi: 10.1016/j.neuron.2004.11.025

van den Berg, R., and Hoogenraad, C. C. (2012). Molecular motors in cargo trafficking and synapse assembly. *Adv. Exp. Med. Biol.* 970, 173–196. doi: 10.1007/978-3-7091-0932-8_8

Wheeler, D. G., Groth, R. D., Ma, H., Barrett, C. F., Owen, S. F., Safa, P., et al. (2012). Ca(V)1 and Ca(V)2 channels engage distinct modes of Ca(2+) signaling to control CREB-dependent gene expression. *Cell* 149, 1112–1124. doi: 10.1016/j.cell.2012.03.041

Wiegert, J. S., Bengtson, C. P., and Bading, H. (2007). Diffusion and not active transport underlies and limits ERK1/2 synapse-to-nucleus signaling in hippocampal neurons. *J. Biol. Chem.* 282, 29621–29633. doi: 10.1074/jbc.M701448200

Wohlschlegel, J. A. (2009). Identification of SUMO-conjugated proteins and their SUMO attachment sites using proteomic mass spectrometry. *Methods Mol. Biol.* 497, 33–49. doi: 10.1007/978-1-59745-566-4_3

Zhou, Y., Wu, H., Li, S., Chen, Q., Cheng, X. W., Zheng, J., et al. (2006). Requirement of TORC1 for late-phase long-term potentiation in the hippocampus. *PLoS ONE* 1:e16. doi: 10.1371/journal.pone.0000016

Conflict of Interest Statement: The authors declare that the research was conducted in the absence of any commercial or financial relationships that could be construed as a potential conflict of interest.

frontiers in Molecular Neuroscience

ORIGINAL RESEARCH
published: 16 September 2015
doi: 10.3389/fnmol.2015.00054

NF-κB mediates Gadd45β expression and DNA demethylation in the hippocampus during fear memory formation

*Timothy J. Jarome, Anderson A. Butler, Jessica N. Nichols, Natasha L. Pacheco and Farah D. Lubin**

Department of Neurobiology, University of Alabama at Birmingham, Birmingham, AL, USA

Gadd45-mediated DNA demethylation mechanisms have been implicated in the process of memory formation. However, the transcriptional mechanisms involved in the regulation of *Gadd45* gene expression during memory formation remain unexplored. NF-κB (nuclear factor kappa-light-chain-enhancer of activated B cells) controls transcription of genes in neurons and is a critical regulator of synaptic plasticity and memory formation. *In silico* analysis revealed several NF-κB (p65/RelA and cRel) consensus sequences within the *Gadd45β* gene promoter. Whether NF-κB activity regulates *Gadd45* expression and associated DNA demethylation in neurons during memory formation is unknown. Here, we found that learning in a fear conditioning paradigm increased *Gadd45β* gene expression and *brain-derived neurotrophic factor (BDNF)* DNA demethylation in area CA1 of the hippocampus, both of which were prevented with pharmacological inhibition of NF-κB activity. Further experiments found that conditional mutations in *p65/RelA* impaired fear memory formation but did not alter changes in *Gadd45β* expression. The learning-induced increases in *Gadd45β* mRNA levels, Gadd45β binding at the *BDNF* gene and *BDNF* DNA demethylation were blocked in area CA1 of the *c-rel* knockout mice. Additionally, local siRNA-mediated knockdown of *c-rel* in area CA1 prevented fear conditioning-induced increases in Gadd45β expression and *BDNF* DNA demethylation, suggesting that c-Rel containing NF-κB transcription factor complex is responsible for *Gadd45β* regulation during memory formation. Together, these results support a novel transcriptional role for NF-κB in regulation of Gadd45β expression and DNA demethylation in hippocampal neurons during fear memory.

Keywords: nuclear factor kappa B, hippocampus, DNA demethylation, Gadd45, memory

OPEN ACCESS

Edited by:
Benedict C. Albensi, University of Manitoba, Canada

Reviewed by:
Katja Kobow, Universitätsklinikum Erlangen, Germany
Sungjin Park, University of Utah, USA

****Correspondence:***
Farah D. Lubin, Department of Neurobiology, University of Alabama at Birmingham, Shelby Building, 1825 University Boulevard, Birmingham, AL 35294, USA
flubin@uab.edu

Received: *06 July 2015*
Accepted: *30 August 2015*
Published: *16 September 2015*

Citation:
Jarome TJ, Butler AA, Nichols JN, Pacheco NL and Lubin FD (2015) NF-κB mediates Gadd45β expression and DNA demethylation in the hippocampus during fear memory formation. Front. Mol. Neurosci. 8:54. doi: 10.3389/fnmol.2015.00054

Introduction

The formation of long-term memories requires dynamic changes in gene transcription and protein translation in neurons (Johansen et al., 2011; Jarome and Helmstetter, 2013). Over the last decade numerous studies have implicated epigenetic mechanisms, which regulate transcription without modifying the underlying gene sequence, in this memory consolidation process (Stefanko et al., 2009; Gupta et al., 2010; Gräff and Tsai, 2013; Jarome et al., 2014; Kwapis and Wood, 2014). Of the epigenetic mechanisms identified, DNA methylation

has become particularly attractive due to its potential to regulate gene expression across the lifespan (Roth et al., 2009). Active DNA methylation regulates expression of several memory-associated genes during the memory consolidation process and manipulation of DNA methyltransferase (DNMT) activity impairs memory for a variety of behavioral tasks (Miller and Sweatt, 2007; Miller et al., 2008, 2010; Feng et al., 2010; Maddox et al., 2014). In addition to the strong evidence that exists for *de novo* DNA methylation during memory formation, recent studies have indicated active DNA demethylation in the hippocampus and neocortex during memory formation and extinction (Kaas et al., 2013; Rudenko et al., 2013). This suggests that the memory consolidation process requires both gene activation and repression mediated by DNA methylation and demethylation mechanisms, respectively. However, very little is known about how DNA demethylation is regulated during the memory consolidation process.

The Growth arrest and DNA damage-inducible 45 (Gadd45) family of proteins are stress sensor genes that have been implicated in active DNA demethylation (Barreto et al., 2007; Niehrs and Schäfer, 2012). This family of proteins consists of the alpha, beta and gamma isoforms whose expression is dynamically altered as a function of learning (Leach et al., 2012). The Gadd45β isoform has been shown to mediate gene-specific DNA demethylation in the dentate gyrus following seizure and during neurogenesis (Ma et al., 2009) and one of the target genes is brain-derived neurotrophic factor (BDNF), which undergoes promoter-specific DNA demethylation in the hippocampus during memory consolidation (Lubin et al., 2008). Further, knockout of Gadd45β alters long-term potentiation and memory retention for hippocampus-dependent tasks (Leach et al., 2012; Sultan et al., 2012), supporting a role for the Gadd45 family of proteins in synaptic plasticity and memory formation (Sultan and Sweatt, 2013). However, to date, it is unknown how Gadd45 expression and its DNA demethylation activity is regulated in the hippocampus during memory consolidation.

The Nuclear Factor Kappa B (NF-κB) transcription factor exists as a homo- or hetero-dimer complex formed from a family of five proteins (p50, p52, RelA/p65, RelB, c-Rel) that share a Rel homology domain in their N-terminus and has been implicated in transcriptional regulation during activity-dependent synaptic plasticity (Meberg et al., 1996). Interestingly, while NF-κB has been implicated in the memory consolidation process (Snow et al., 2014), very little is known about how NF-κB mediates transcriptional control of genes that are necessary for proper memory formation and storage in neurons. In the present study, we examined if NF-κB signaling regulates Gadd45 expression and DNA demethylation during the memory consolidation process. Using a combination of pharmacological, genetic, biochemical and molecular approaches, we identified Gadd45β expression and its potential DNA demethylation activity as a novel target for NF-κB activity during hippocampus-dependent memory formation.

Materials and Methods

Animals

Rats

Male Sprague-Dawley rats (Harlan) weighing 250–300 g at time of arrival were used for these experiments. Animals were single housed in plastic cages, had free access to water and rat chow and were maintained on a 12:12 light:dark cycle. All procedures were approved by the University of Alabama at Birmingham Institutional Animal Care and Use Committee and done in accordance with the National Institute of Health ethical guidelines.

c-rel Knockout Mice

The *c-rel*$^{-/-}$ mice were developed as described previously (Ahn et al., 2008). Wild-type (WT) C57BL/6J littermates controls from heterozygote breeding were used as controls.

RelA$^{flox/+}$ Mice

A conditionally mutated *p65* (*relA*Δ) mouse line was developed as described previously (Algul et al., 2007). The floxed fragment of *relA* contains exons 7–10, which codes a part of the Rel homology domain and the nuclear localization site. To induce mutation of p65/relA in the CA1 region of the hippocampus, heterozygous mice were anesthetized with an intraperitoneal injection of ketamine-dexmedetomidine and received bilateral injections of Cre-containing (AAV-CMV-Cre-GFP) or empty (AAV-CMV-GFP) viral vectors (Penn Vector Core) 2 weeks prior to behavioral training using stereotaxic coordinates (AP −2.0 mm, ML ± 1.5 mm, DV −1.7 mm) relative to Bregma. The infusion was given over a 10 min period (0.1 μl per minute) for a total volume of 1 μl per side.

siRNA Delivery

Rats were anesthetized with an intraperitoneal injection of ketamine-dexmedetomidine and received bilateral injections of Accell SMARTpool siRNAs (Thermo) targeting *c-rel* (#E-085667-01-0005) or a negative control (#D-001910-10-05) into the dorsal hippocampus using stereotaxic coordinates (AP −3.6 mm, ML ± 1.7 mm, DV −3.6 mm) relative to bregma. The infusion was given over a 10 min period (0.1 μl per minute) for a total volume of 1 μl per side. Animals were allowed to recover for 5 days before behavioral testing. Fresh Accell siRNA stocks (100 μM) were resuspended in Accell siRNA resuspension buffer to a concentration of ∼4.5 μM on the day of surgery.

Behavioral Procedures

Rats were trained to a standard contextual fear conditioning paradigm in which three shock presentations (0.5 mA, 2 s, 120 s ITI) were given over a 7 min period in a novel context. For latent inhibition, animals were exposed to the training context for 2 h followed immediately by the same 7 min training session described above. In experiments using the NF-κB inhibitor sodium diethyldithiocarbamate trihydrate (DDTC; Sigma), intraperitoneal injections (200 mg/kg in 0.9% Saline) were given 2 h prior to fear conditioning. Mice were

trained to a single trial auditory plus contextual fear conditioning paradigm that consisted of a 1.5 min baseline followed a single tone (100 Hz, 30 s)—shock (0.5 mA, 2 s) pairing in a novel context. Testing to the auditory cue occurred the following day and consisted of a 1.5 min baseline followed by a 30 s nonreinforced tone presentation. Two hours after the auditory cue test, animals were placed back into the training context for 3 min to test retention for the contextual cue. Freezing behavior was scored in real-time by Med Associates software.

Collection of Area CA1

One hour after training, the whole brain was removed and placed in oxygenated (95%/5% O_2/CO_2) ice-cold cutting solution (composed of (in mM) 110 sucrose, 60 NaCl, 3 KCl, 1.25 NaH_2PO_4, 28 $NaHCO_3$, 0.5 $CaCl_2$, 7 $MgCl_2$, 5 glucose, and 0.6 Ascorbate). The CA1 region of the hippocampus was micro-dissected and flash frozen on dry ice. For the *c-rel* siRNA experiment, brains were rapidly removed and flash frozen on dry ice. The CA1 region of the dorsal hippocampus was then dissected out with the aid of a rat brain matrix (Harvard Apparatus); this was done to collect the area of CA1 targeted by the siRNA infusions. Retrosplenial cortex (RSC) tissue was collected from these animals to confirm diffusion of the siRNA. All isolated tissue was stored at −80°C for future processing.

Western Blotting

Normalized proteins (3–9 μg) were separated on 7.5% or 20% polyacrylamide gel, transferred onto an Immobilon-FL membrane using a turbo transfer system (Biorad), membranes blocked in Licor blocking buffer and probed with primary antibodies for p65 (1:200, Santa Cruz #SC-372), IκBα (1:200, Santa Cruz #SC-371), c-Rel (1:100, Santa Cruz #SC-71), Actin (1:1000, Abcam #ab1801) and Gadd45β (1:1000, Abcam #ab128920) overnight at 4°C. Secondary goat anti-rabbit 700CW antibody (1:20,000; Licor Biosciences) was used for detection of proteins using the Licor Odyssey system. All protein quantification was done using GeneTools software (Syngene).

Quantitative RT-PCR

RNA was extracted from isolated CA1 tissue using the All Prep DNA/RNA mini kit (Qiagen), converted to cDNA (iScript cDNA synthesis kit; Biorad) and RT-PCR amplified on the IQ5 or CFX1000 real-time PCR system (Biorad) as described previously (Gupta-Agarwal et al., 2014) with primer annealing temperatures of 59°C for mouse and 62.6°C for rat. Primers were as follows: rat *Gadd45α* (forward: TCATTCGTGCTTTCTGTTGC, reverse: TCCCGGCAAAA ACAAATAAG), rat *Gadd45β* (forward: GAGGGCATGAA GACCAAAAA, reverse: ATTTAGGATGGCCGGGTTAC), rat *Gadd45γ* (forward: GTCCTGAATGTGGACCCTGAC, reverse: ATGGATCTGCAGGGCTATGTC), mouse *Gadd45β* (forward: CTCTTGGGGATCTTCCGTGG, reverse: TGTCGGGGTC CACATTCATC). Quantification of *β-tubulin*-4 levels (rat forward: AGCAACATGAATGACCTGGTG, reverse: GCTTTCCCTAACCTGCTTGG; mouse forward: TAGTGGA GAACACAGACGAGA, reverse: CTGCTGTTCTTACTCTGG ATG) was used as an internal control for normalization. All data was analyzed using the comparative Ct method.

Chromatin Immunoprecipitation (ChIP)

ChIP was performed as described previously with a small scale modification (Gupta-Agarwal et al., 2014). Briefly, samples were fixed in PBS with 1% formaldehyde, chromatin was sheared using a Bioruptor on high power, lysates centrifuged and diluted in TE and RIPA buffer. Extracts were mixed with MagnaChip magnetic protein A/G beads and immunoprecipitations were carried out at 4°C overnight with primary antibody (anti-Gadd45β) or no antibody (control). Immune complexes were sequentially washed with low salt buffer, high salt buffer, LiCl immune complex buffer and TE buffer, extracted in 1 × TE containing 1% SDS and protein-DNA cross-links were reverted by heating at 65°C overnight. After proteinase K digestion (100 μg; 2 h at 37°C), DNA was extracted by phenol/chloroform/isoamyl alcohol and then ethanol-precipitated. Immunoprecipitated DNA samples were subjected to quantitative real-time PCR using primers specific to the mouse *BDNF* promoter 4 (forward: GCGCGGAATTCTGATTCTGG reverse: AAAGTGGGTGGGAGTCCA). The cumulative fluorescence for each amplicon was taken as a percentage of the input fraction, enrichment over background (no antibody control) calculated and taken as a fold change of the control group.

Direct Bisulfite Sequencing

Quantification of DNA methylation through direct bisulfite sequencing was performed as described previously (Ryley Parrish et al., 2013). Briefly, 50 μg of genomic DNA was bisulfite treated using the Qiagen Epitech Bisulfite Kit and amplified for a primer targeting 12 CpG sites in the promoter region of rat *BDNF IV* and eight CpG sites in the promoter region of mouse *BDNF IV*. Primer pairs were: rat *BDNF* promoter 4 (forward: GGTAGAGGAGGTATTATATATGATAGTTTA, reverse: TAC TCCTATTCTTCAACAAAAAAATTAAAT, product size of 250 base pairs, annealing temperature: 60°C) and mouse *BDNF* promoter 4 (forward: TTATAAAGTATGTAATGTTTTGGAA, reverse: AAATAAAAAAATAAATAAAAATCCAC, product size of 189 base pairs, annealing temperature: 59°C). PCR products were confirmed for size, cleaned using ExoSAP-IT (Affymetrix) and sequenced in duplicate using the reverse primer at the University of Alabama at Birmingham Genomics Core Facility of the Heflin Center for Human Genetics. Using Chromas software to read the electropherogram, the percent methylation of the CpG sites was then determined by the ratio between peak values of guanine (G) and adenine (A) (G/(G+A)).

Statistical Analyses

All data is presented as group average with the standard error of the mean and was analyzed using Analysis of Variance (ANOVA) with Fisher LSD *post hoc* tests or with student *t*-tests.

Results

Isoform-Specific Increases in *Gadd45* Expression in Area CA1 Following Learning

First we tested whether or not learning triggers expression changes of diverse *Gadd45* isoforms. For these experiments, animals were trained in a contextual fear conditioning paradigm and after 1 h area CA1 was isolated and we examined changes in *Gadd45α*, *Gadd45β* and *Gadd45γ* gene expression. We chose to assess *Gadd45* expression levels at 1 h following fear conditioning, as we have previously found optimal changes in DNA methylation levels in area CA1 of the hippocampus (Lubin et al., 2008). As a control for associative memory, we exposed a separate group of animals to a non-associative latent inhibition learning paradigm procedure, which involves exposure to the fear conditioning chamber only (context) followed by a delayed delivery of the aversive footshock 2 h later, preventing the subject to not associate the unconditioned stimulus (footshock) with the conditioned stimulus (context; Gupta et al., 2010). We found significant increases in Gadd45β ($F_{(2,12)}$ = 4.067, $p < 0.05$), but not *Gadd45α* ($F_{(2,12)}$ = 0.674, p = 0.527) or *Gadd45γ* ($F_{(2,11)}$ = 0.550, p = 0.591) mRNA levels in area CA1 following fear conditioning (**Figure 1A**). The increase in *Gadd45β* mRNA levels was not present in the latent inhibition group, confirming that *Gadd45β* gene expression changes were specific to context-learning along, and occurred with a moderate increase in Gadd45β protein expression ($F_{(2,10)} = 3.895$, $p = 0.056$; **Figure 1B**). Collectively, these results suggest that Gadd45β gene and protein expression are increased in area CA1 as a function of associative learning.

NF-κB Activity is Critical for Increased *Gadd45β* Expression and BDNF Promoter 4 DNA Demethylation Following Learning

Considering that NF-κB is a transcription factor that plays a critical role in memory formation (Yeh et al., 2002; Lubin and Sweatt, 2007; Federman et al., 2013), we next determined whether or not *Gadd45β* expression was being regulated by NF-κB transcriptional activity during the memory consolidation period. *In silico* analysis revealed several NF-κB consensus sequences within the *Gadd45β* gene (**Figure 2A**). We found that pharmacological inhibition of NF-κB signaling activity with diethyldithiocarbamate (DDTC) abolished the fear conditioning-induced increases in *Gadd45β* expression in area CA1 ($F_{(3,11)}$ = 34.47, $p < 0.001$; **Figure 2B**), suggesting that NF-κB signaling was critical for the increased transcription of *Gadd45β* following learning. Since *Gadd45β* regulates DNA demethylation during memory formation, we next tested if pharmacological blockade of NF-κB activity with DDTC prevented DNA demethylation of the *BDNF* gene, a well-established regulator of memory formation that undergoes dynamic activity-dependent and promoter-specific changes in DNA methylation levels (Lee et al., 2004; Bekinschtein et al., 2007; Lubin et al., 2008; Peters et al., 2010). Remarkably, we found that while fear conditioning resulted in decreased *BDNF* Promoter 4 DNA methylation, inhibiting NF-κB activity completely attenuated this effect ($F_{(2,12)}$ = 4.589, $p < 0.05$; **Figure 2C**). Together, these results suggest that NF-κB controls *Gadd45β* expression and *BDNF* DNA demethylation in the hippocampus during memory formation.

Conditional Mutation of *p65/RelA* Impairs Memory Formation but does not Alter *Gadd45β* Expression

While our pharmacological manipulation with DDTC suggests a role for NF-κB activity in regulation *Gadd45β* expression and *BDNF* DNA demethylation in the hippocampus during memory formation, our studies do not yet distinguish between the contributions of different NF-κB subunits that may have been involved. The p65/RelA and p50 heterodimer is critical for nuclear translocation and activation of the NF-κB complex, thus we tested if manipulation of p65/RelA would mimic the effects of inhibiting NF-κB signaling activity with DDTC on *Gadd45β* expression following learning. We conditionally mutated *p65/relA* using a Cre-loxP insert spanning exons 7–10 containing the Rel homology domain and nuclear translocation

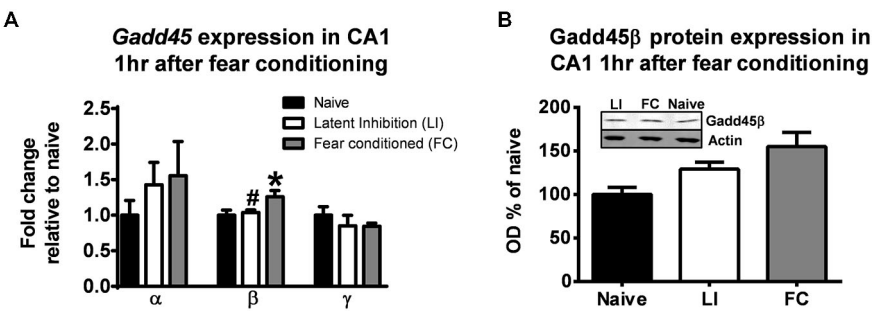

FIGURE 1 | Gadd45β expression is increased in the hippocampus following learning. (A) Animals were trained to contextual fear conditioning and area CA1 collected 1 h later (Fear conditioned). A separate group of animals was exposed to the training context for 2 h, followed by the same contextual fear conditioning procedure and area CA1 collected 1 h later (Latent Inhibition). Quantitative RT-PCR revealed an increase in *Gadd45β*, but not *Gadd45α* or *Gadd45γ*, gene expression in area CA1 following fear conditioning (n = 5–6 per group). **(B)** Western blot analysis confirmed a moderate increase in Gadd45β protein expression at 1 h in the fear conditioned, but not latent inhibition, group (n = 5–6 per group). $^{*}p < 0.05$ from Naïve. $^{\#}p < 0.05$ from FC.

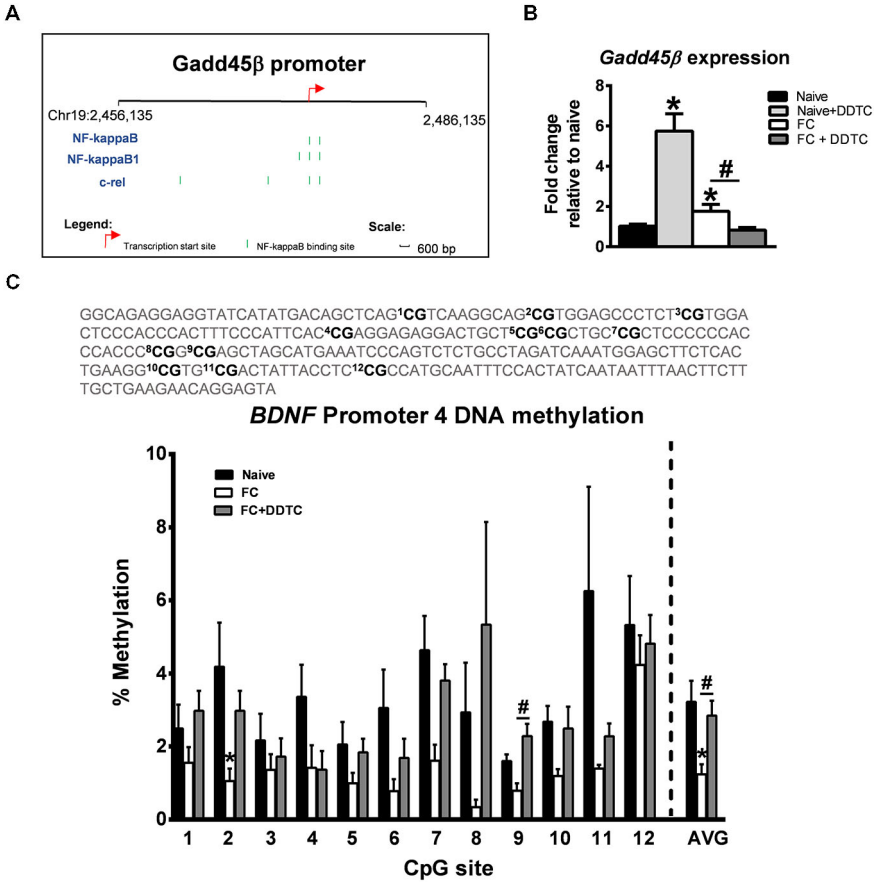

FIGURE 2 | Inhibition of NF-κB activity abolishes learning-induced changes in *Gadd45β* expression and BDNF DNA demethylation in the hippocampus. (A) *In silico* analysis revealed several NF-κB consensus sequences in the *Gadd45β* promoter. **(B)** Pharmacological inhibition of NF-κB activity with DDTC abolished fear conditioning-induced increases in *Gadd45β* expression in area CA1 (n = 3–6 per group). **(C)** Bisulfite sequencing analysis of CpG sites in the rat *BDNF* Promoter 4 region revealed that inhibition of NF-κB with DDTC completely prevented the fear conditioning-induced decreases in *BDNF* Promoter 4 DNA methylation in area CA1 (n = 4–6 per group). $^{*}p < 0.05$ from Naïve. $^{\#}p < 0.05$ from FC.

site (Algul et al., 2007). To induce the *relA*Δ mutation in area CA1 of the adult hippocampus, we infused Cre-containing (AAV-CMV-Cre-GFP) or empty (AAV-CMV-GFP) viral vectors 2 weeks prior to fear conditioning (**Figures 3A,B**). Consistent with a role for NF-κB signaling in hippocampus-dependent memory formation, we found that while $relA^{flox/+}$ mice successfully acquired the fear memory during training ($t_{(10)} = 0.9807$, $p = 0.349$), when tested 24 h later, $relA^{flox/+}$ mice had significant impairments in memory retention for contextual ($t_{(10)} = 2.182$, $p = 0.054$) but not hippocampus-independent auditory ($t_{(9)} = 1.184$, $p = 0.266$), fear memory (**Figure 3C**). This is the first evidence that local knockdown of *p65/relA* in the adult hippocampus impairs long-term memory formation. Next, we tested if mutation of *p65/relA* altered *Gadd45β* expression following learning (**Figure 3D**). Interestingly, while we confirmed that $relA^{flox/+}$ mice had reduced expression of p65 ($t_{(6)} = 3.583$, $p < 0.05$) and the NF-κB associated protein IκBα ($t_{(7)} = 2.624$, $p < 0.05$) relative to controls (**Figure 3E**), we found no effect of the *p65/relA* mutation on *Gadd45β* mRNA ($t_{(6)} = 0.214$, $p = 0.837$) or protein ($t_{(7)} = 0.427$, $p = 0.681$) levels following learning (**Figure 3F**). Thus far, our results suggest that while NF-κB signaling and p65/RelA activity in the hippocampus are critical for memory formation, p65/RelA is not responsible for the NF-κB-dependent regulation of *Gadd45β* expression during the memory consolidation process.

Manipulation of c-Rel in Area CA1 Prevents Increases in *Gadd45β* Expression and *BDNF* Promoter 4 DNA Demethylation Following Learning

In our *in silicio* analysis we found multiple c-Rel consensus sites in the *Gadd45β* promoter, suggesting that c-Rel containing NF-κB complexes may be responsible for the learning-dependent increases in *Gadd45β* expression in area CA1. To test this, we examined *Gadd45β* expression in *c-rel* knockout ($c\text{-}rel^{-/-}$) mice (**Figure 4A**), which we have previously shown to have impaired hippocampus-dependent but not hippocampus-independent fear memory (Levenson et al., 2004; O'Riordan et al., 2006; Ahn et al., 2008). First, we examined if a loss

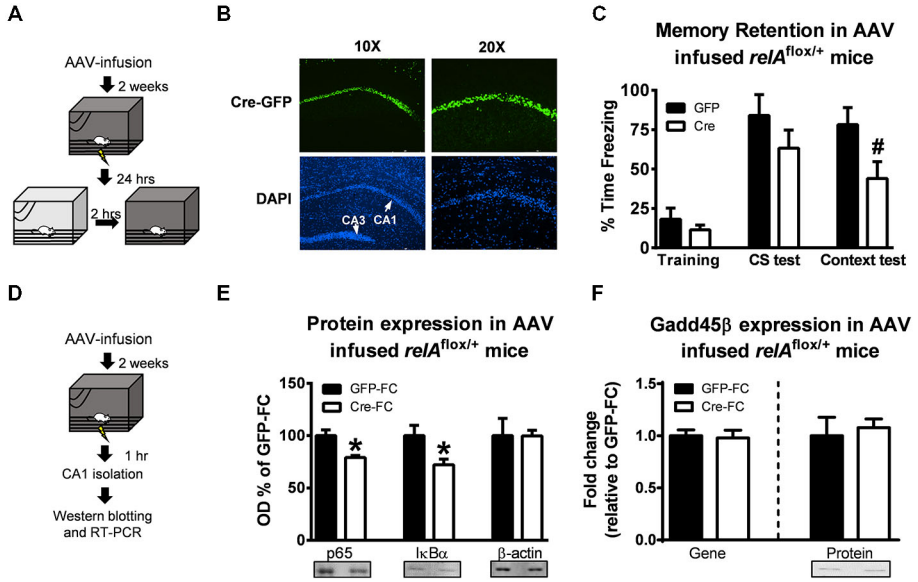

FIGURE 3 | Conditional mutation of p65/relA does not alter *Gadd45β* expression in the hippocampus following learning. (A) Floxed *p65/relA* mice (*relA*$^{flox/+}$) were injected with Cre-containing (AAV-CMV-Cre-GFP) or empty (AAV-CMV-GFP) adenoviruses 2 weeks prior to fear conditioning to induce mutation in the *p65/relA* gene. The day after training, mice were tested to the auditory cue followed by the context 2 h later. **(B)** Immunohistochemistry showing GFP expression in the hippocampus. DAPI was used to visualization the different hippocampus sub-regions. **(C)** While there were no differences between group during training or testing to the auditory cue, *relA*$^{flox/+}$ mice receiving Cre injections had impaired contextual fear memory relative to controls (n = 5–7 per group). **(D)** *relA*$^{flox/+}$ were injected with Cre-containing (AAV-CMV-Cre-GFP) or empty (AAV-CMV-GFP) adenoviruses 2 weeks prior to fear conditioning and area CA1 collected 1 h later. **(E)** Western blot analysis confirmed knockdown of p65 and IκBα expression in the Cre-infused mice (n = 4–5 per group). **(F)** There were no differences in Gadd45β gene or protein expression following Cre-infusion relative to GFP-infused controls (n = 4–5 per group). $^{*}p < 0.05$ from GFP. $^{\#}p = 0.054$ from GFP.

of *c-rel* during development resulted in long-term changes in *Gadd45β* expression. However, we did not observe altered basal levels of *Gadd45β* expression in area CA1 ($t_{(7)}$ = 0.022, p = 0.982; **Figure 4B**) of *c-rel*$^{-/-}$ mice, suggesting normal *Gadd45β* expression in the hippocampus. Next, we tested if *c-rel*$^{-/-}$ mice have altered *Gadd45β* expression in the hippocampus in response to learning. We found an increase in *Gadd45β* expression in fear conditioned WT mice relative to naïve controls ($t_{(14)}$ = 2.256, $p < 0.05$). Surprisingly, this increase in *Gadd45β* mRNA levels were not present in *c-rel*$^{-/-}$ mice ($t_{(14)}$ = 0.177, p = 0.862), suggesting that c-Rel containing NF-κB complexes were critical for the NF-κB-dependent regulation of *Gadd45β* expression following learning (**Figure 4C**). Since Gadd45β regulates DNA demethylation and we found that pharmacological inhibition of NF-κB signaling activity with DDTC prevented learning-induced DNA demethylation of *BDNF* Promoter 4, we next tested if *BDNF* Promoter 4 DNA demethylation was altered in *c-rel*$^{-/-}$ mice. Using chromatin immunoprecipitation, we found an increase in Gadd45β protein levels at *BDNF* Promoter 4 in area CA1 following fear conditioning that was abolished in *c-rel*$^{-/-}$ mice ($F_{(2,9)}$ = 4.543, $p < 0.05$; **Figure 4D**) associated with *BDNF* Promoter 4 DNA demethylation ($F_{(2,7)}$ = 4.504, p = 0.055), suggesting that there is a loss of learning-dependent Gadd45β accumulation at the *BDNF* gene in the hippocampus of *c-rel* knockout mice. Remarkably, we found that while fear conditioning resulted in decreased *BDNF* Promoter 4 DNA methylation relative to controls ($t_{(4)}$ = 3.039, $p < 0.05$), this did not occur in *c-rel*$^{-/-}$ mice ($t_{(5)}$ = 0.454, p = 0.668; **Figure 4E**). This suggests that c-Rel is likely responsible for the NF-κB-dependent regulation of *Gadd45β* expression and *BDNF* Promoter 4 DNA demethylation during memory formation.

An alternative explanation for the effects described above is that the alterations in *Gadd45β* expression and *BDNF* DNA demethylation in area CA1 of *c-rel*$^{-/-}$ mice are due to the loss of *c-rel* in multiple brain regions simultaneously, which could result in wide-scale epigenetic changes across the neural circuit. To test this possibility, we locally knocked-down *c-rel* in area CA1 of the hippocampus in adult animals using siRNA technology and examined changes in *Gadd45β* expression and *BDNF* Promoter 4 DNA demethylation following learning (**Figure 5A**). First, we confirmed the effectiveness of our siRNA by examining c-Rel protein expression in area CA1 and the surrounding cortical region following fear conditioning (**Figure 5B**). In area CA1, we found that fear conditioning increased c-Rel expression, which was attenuated in *c-rel* siRNA infused animals ($F_{(2,10)}$ = 4.150, $p < 0.05$). However, in the RSC, which requires *de novo* protein synthesis for the consolidation of contextual fear memories (Kwapis et al., 2015), we found a learning-induced increase in c-Rel expression that was unaffected by infusion of the *c-rel* siRNA into the hippocampus ($F_{(2,10)}$ = 3.838, p = 0.058). These results suggest that our siRNA effectively targeted *c-rel* in the hippocampus and supports previous studies that found increased expression of NF-κB proteins during enhanced

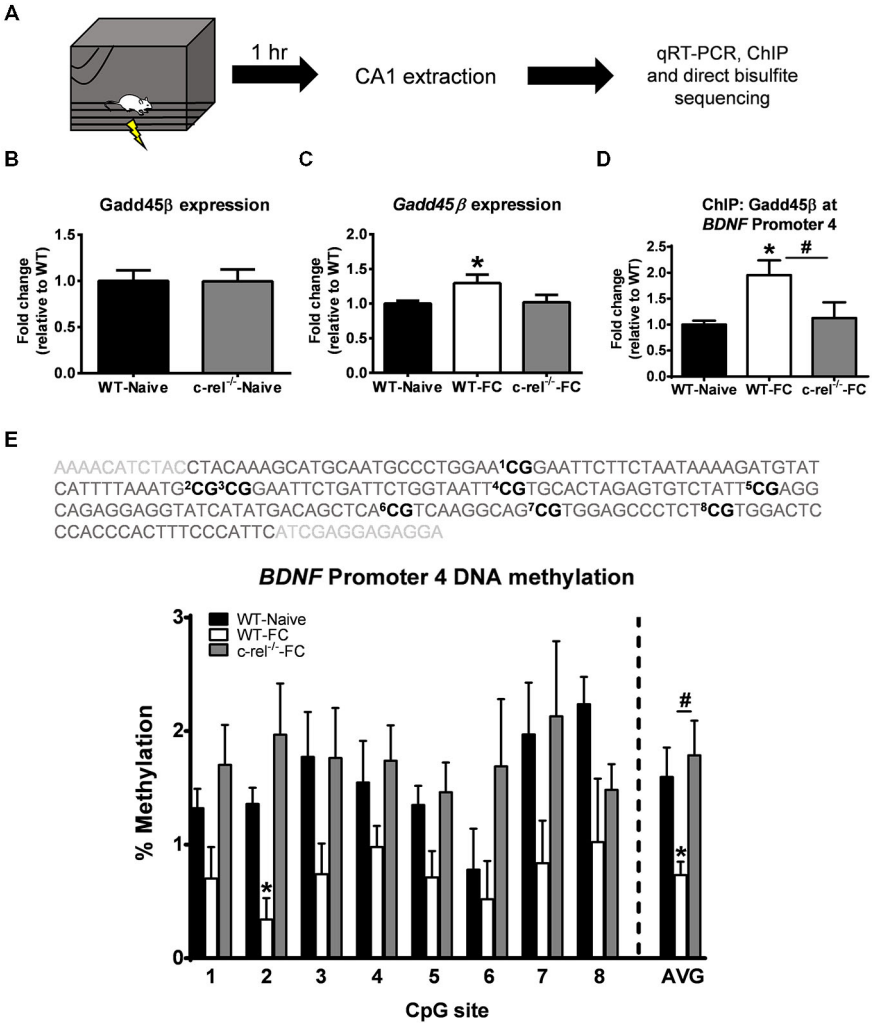

FIGURE 4 | Knockout of *c-rel* prevents fear conditioning-induced changes in *Gadd45β* expression and BDNF DNA methylation in the hippocampus. **(A)** Wild-type (WT) or *c-rel* knockout (*c-rel*$^{-/-}$) mice were fear conditioned and area CA1 collected 1 h later. **(B)** Basal expression of *Gadd45β* was not altered in *c-rel*$^{-/-}$ mice (n = 4–5 per group). **(C)** *Gadd45β* expression was increased in WT, but not *c-rel*$^{-/-}$, mice following fear conditioning (n = 8 per group). **(D)** Chromatin immunoprecipitation revealed an increase in Gadd45β binding at *BDNF* Promoter 4 following fear conditioning, which was lost in *c-rel*$^{-/-}$ mice (n = 4 per group). **(E)** Bisulfite sequencing analysis of CpG sites in the mouse *BDNF* Promoter 4 region revealed a fear conditioning-induced decrease in *BDNF* Promoter 4 DNA methylation in area CA1 that was prevented in *c-rel*$^{-/-}$ mice (n = 3–4 per group). $^{*}p < 0.05$ from WT. $^{\#}p < 0.05$ from WT-FC.

synaptic activity (Meberg et al., 1996). Next, we examined what effect *c-rel* knockdown had on Gadd45β expression and DNA demethylation following fear conditioning. We found that siRNA-mediated knockdown of *c-rel* in adulthood completely abolished the learning-induced increases in *Gadd45β* gene ($F_{(2,7)}$ = 8.760, $p < 0.05$) and largely reduced the increases in protein expression ($F_{(2,12)}$ = 3.762, p = 0.053) in area CA1 (**Figure 5C**), confirming what we observed in *c-rel*$^{-/-}$ mice. Additionally, *c-rel* siRNA knockdown abolished the learning-induced decreases in *BDNF* Promoter 4 DNA methylation ($F_{(2,6)}$ = 6.786, $p < 0.05$; **Figure 5D**). In combination with our *c-rel*$^{-/-}$ mice data, these results strongly suggest that c-Rel regulates *Gadd45β* expression and *BDNF* Promoter 4 DNA demethylation in the hippocampus during memory consolidation.

Discussion

Several studies have implicated DNA demethylation mechanisms in the memory consolidation process (Kaas et al., 2013; Rudenko et al., 2013; Li et al., 2014), however, the mechanisms regulating this process have remained equivocal. In the present study, we found that learning in an associative fear conditioning paradigm dynamically regulates the expression of *Gadd45β* in the hippocampus, which is known to regulate DNA demethylation changes that are critical for various forms of synaptic plasticity. Importantly, for the first time we identified the NF-κB transcription pathways as a key regulator of *Gadd45β* expression and DNA demethylation during the memory consolidation process. Remarkably, the loss of *Gadd45β* expression and DNA demethylation in the hippocampus observed following

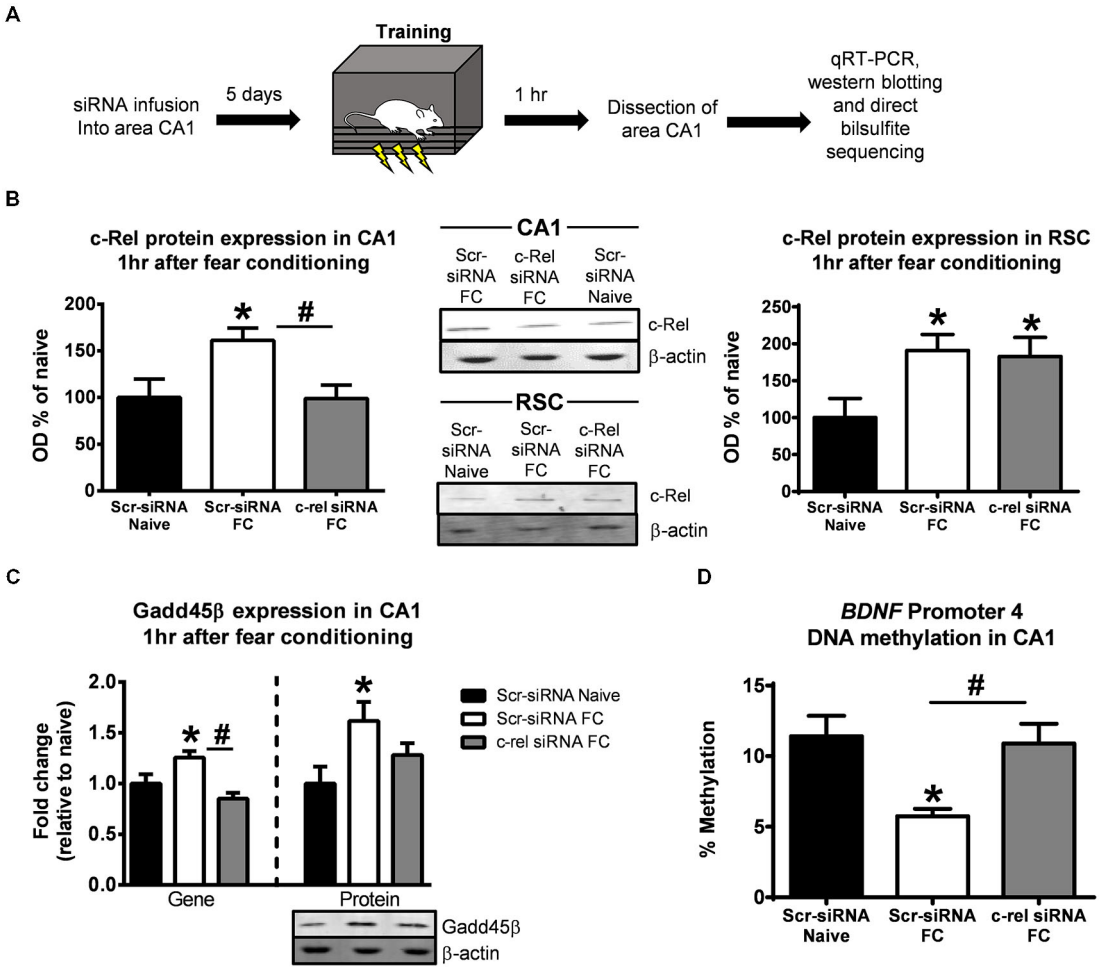

FIGURE 5 | Local knockdown of *c-rel* in the hippocampus prevents fear conditioning-induced changes in *Gadd45β* expression and *BDNF* DNA methylation. (A) Rats were infused Accell siRNAs against *c-rel* or a negative control (Scr-siRNA) 5 days prior to fear conditioning and area CA1 collected 1 h later. **(B)** Fear conditioning increased c-Rel protein expression in the hippocampus which was blocked by the *c-rel* siRNA, confirming effective gene knockdown by the siRNA infusion (left). Fear conditioning-induced increases in c-Rel protein expression in the retrosplenial cortex (RSC) were not altered by the *c-rel* siRNA when infused in the hippocampus, confirming that the siRNA did not diffuse up the injection tract (right). **(C)** Knockdown of *c-rel* prevented the fear conditioning induced increases in Gadd45β gene (n = 3–4 per group) and protein expression (n = 5 per group) in the hippocampus. **(D)** Knockdown of *c-rel* prevented the fear conditioning induced decreases in rat *BDNF* Promoter 4 DNA methylation in the hippocampus (n = 3 per group). $^{*}p < 0.05$ Scr-siRNA Naïve. $^{\#}p < 0.05$ from Scr-siRNA FC.

pharmacological inhibition of NF-κB prior to fear conditioning could be completely mimicked by knockout or knockdown of *c-rel*, but not *relA/p65*, expression. Collectively, these findings suggest that c-Rel may be a critical regulator of Gadd45β-mediated DNA demethylation during the memory consolidation process and strongly support a novel epigenetic role for NF-κB signaling in DNA demethylation mechanisms during memory formation in the hippocampus.

The NF-κB transcription factor has been widely implicated in synaptic plasticity and memory formation in neurons (Snow et al., 2014). In terms of its role in memory formation, numerous studies have reported memory impairments following global or region-specific inhibition of NF-κB activity in a diverse group of organisms and transcription of several genes has been shown to be dependent on NF-κB activation, such as *zif268/egr1* and *Arc* (O'Mahony et al., 2006; Zalcman et al., 2015), which have well described roles in the memory consolidation process (Guzowski et al., 2001; Hall et al., 2001; Ploski et al., 2008). Additionally, several studies have identified epigenetic functions of NF-κB activity in memory formation, particularly in the regulation of histone acetylation processes (Lubin and Sweatt, 2007; Si et al., 2012; Federman et al., 2013). In the present study, we add to this growing number of transcriptional processes regulated by NF-κB by demonstrating a role for it in activity-dependent DNA demethylation. However, unlike the other transcriptional processes described above which are generally transient, this DNA methylation function of NF-κB has the potential to be a long-term mechanism for gene regulation since DNA methylation can persistent across the lifespan and between generations (Roth et al., 2009; Dias and Ressler, 2014). Thus, NF-κB-dependent regulation of *Gadd45β* expression and DNA demethylation may represent a

mechanism for both memory formation and maintenance in the hippocampus.

While it has been known for several years that NF-κB activity is critical for synaptic plasticity and memory formation, few studies have examined the specific contribution of individual NF-κB subunits to transcriptional regulation during the memory consolidation process. The most studied subunit has been p50 since the p65/relA and p50 heterodimer is critical for nuclear translocation and activation of the NF-κB complex. In general, a loss of the p50 subunit impairs hippocampus-dependent synaptic plasticity and memory formation, though the results have been mixed (Kassed et al., 2002; Kassed and Herkenham, 2004; Denis-Donini et al., 2008; Lehmann et al., 2010; Oikawa et al., 2012). Additionally, it has previously been shown that a loss of the c-rel subunit impairs hippocampal LTP and memory formation (Levenson et al., 2004; O'Riordan et al., 2006; Ahn et al., 2008), suggesting that the c-Rel subunit is a critical regulator of learning-dependent synaptic plasticity (O'Riordan et al., 2006). However, no study, to date, has directly compared the contribution of individual NF-κB subunits to the regulation of a specific transcriptional process critical for synaptic plasticity and memory formation. Thus, our result that c-Rel, but not RelA/p65, regulates Gadd45 expression and DNA demethylation is the first evidence to implicate unique transcriptional functions of the NF-κB subunits during the memory consolidation process. Future studies should aim to examine the contribution of the different NF-κB subunits to other learning-dependent transcriptional processes.

DNA demethylation mechanisms have been implicated in synaptic plasticity and memory formation (Kaas et al., 2013; Rudenko et al., 2013; Li et al., 2014; Feng et al., 2015), however, little is known about how this process is regulated following learning. *Gadd45β* is one mechanism controlling activity-dependent DNA demethylation in neurons (Barreto et al., 2007; Ma et al., 2009; Niehrs and Schäfer, 2012), though how *Gadd45β* expression is regulated during memory formation remains unknown. In the present study, we identified NF-κB as the first regulator of *Gadd45β* transcription in the hippocampus during the memory consolidation process, though we do not know if c-Rel directly regulates Gadd45 expression or if it does so indirectly through other signaling pathways. However, a loss of NF-κB signaling also prevented learning-dependent DNA demethylation, revealing a novel epigenetic role for NF-κB signaling in memory formation. Interestingly, this is the second identified epigenetic function of NF-κB during memory formation, as previous studies from our group and others have suggested that NF-κB regulates histone acetylation during the memory storage process (Lubin and Sweatt, 2007; Si et al., 2012; Federman et al., 2013). Considering that very little is currently known about how different epigenetic mechanisms are regulated during memory formation and storage (Jarome and Lubin, 2014), these studies collectively suggest that NF-κB might be a critical regulator of different epigenetic marks during memory consolidation, however, at this point its role is exclusively in gene activation rather than repression. Future studies should focus on identification of other potential epigenetic functions of NF-κB during the memory consolidation process.

In summary, we found that NF-κB activity is a critical regulator of *Gadd45β* expression and active *BDNF* DNA demethylation in the hippocampus during the memory consolidation process. Importantly, the NF-κB-dependent regulation of *Gadd45β* and DNA demethylation were controlled by the c-Rel, but not RelA/p65, subunit of the NF-κB complex, suggesting that c-Rel was critical for learning-dependent DNA demethylation at least at the *BDNF* gene in the hippocampus. These findings identify a novel role for NF-κB/c-Rel in activity-dependent synaptic plasticity and suggest that DNA demethylation may be largely controlled through NF-κB-dependent signaling during the memory consolidation process.

Acknowledgments

We thank Jasmyne Thomas, Robin Davis and Rosemary Puckett for technical assistance. This work was supported by National Institutes of Health (NIH) grants MH097909 and MH082106 (FDL).

References

Ahn, H. J., Hernandez, C. M., Levenson, J. M., Lubin, F. D., Liou, H. C., and Sweatt, J. D. (2008). c-Rel, an NF-kappaB family transcription factor, is required for hippocampal long-term synaptic plasticity and memory formation. *Learn. Mem.* 15, 539–549. doi: 10.1101/lm.866408

Algul, H., Treiber, M., Lesina, M., Nakhai, H., Saur, D., Geisler, F., et al. (2007). Pancreas-specific RelA/p65 truncation increases susceptibility of acini to inflammation-associated cell death following cerulein pancreatitis. *J. Clin. Invest.* 117, 1490–1501. doi: 10.1172/jci29882

Barreto, G., Schäfer, A., Marhold, J., Stach, D., Swaminathan, S. K., Handa, V., et al. (2007). Gadd45a promotes epigenetic gene activation by repair-mediated DNA demethylation. *Nature* 445, 671–675. doi: 10.1038/nature05515

Bekinschtein, P., Cammarota, M., Igaz, L. M., Bevilaqua, L. R., Izquierdo, I., and Medina, J. H. (2007). Persistence of long-term memory storage requires a late protein synthesis- and BDNF- dependent phase in the hippocampus. *Neuron* 53, 261–277. doi: 10.1016/j.neuron.2006.11.025

Denis-Donini, S., Dellarole, A., Crociara, P., Francese, M. T., Bortolotto, V., Quadrato, G., et al. (2008). Impaired adult neurogenesis associated with short-term memory defects in NF-kappa B p50-deficient mice. *J. Neurosci.* 28, 3911–3919. doi: 10.1523/JNEUROSCI.0148-08.2008

Dias, B. G., and Ressler, K. J. (2014). Parental olfactory experience influences behavior and neural structure in subsequent generations. *Nat. Neurosci.* 17, 89–96. doi: 10.1038/nn.3594

Federman, N., de la Fuente, V., Zalcman, G., Corbi, N., Onori, A., Passananti, C., et al. (2013). Nuclear factor kappaB-dependent histone acetylation is specifically involved in persistent forms of memory. *J. Neurosci.* 33, 7603–7614. doi: 10.1523/JNEUROSCI.4181-12.2013

Feng, J., Shao, N., Szulwach, K. E., Vialou, V., Huynh, J., Zhong, C., et al. (2015). Role of Tet1 and 5-hydroxymethylcytosine in cocaine action. *Nat. Neurosci.* 18, 536–544. doi: 10.1038/nn.3976

Feng, J., Zhou, Y., Campbell, S. L., Le, T., Li, E., Sweatt, J. D., et al. (2010). Dnmt1 and Dnmt3a maintain DNA methylation and regulate synaptic function in adult forebrain neurons. *Nat. Neurosci.* 13, 423–430. doi: 10.1038/nn.2514

Gräff, J., and Tsai, L. H. (2013). Histone acetylation: molecular mnemonics on the chromatin. *Nat. Rev. Neurosci.* 14, 97–111. doi: 10.1038/nrn3427

Gupta, S., Kim, S. Y., Artis, S., Molfese, D. L., Schumacher, A., Sweatt, J. D., et al. (2010). Histone methylation regulates memory formation. *J. Neurosci.* 30, 3589–3599. doi: 10.1523/JNEUROSCI.3732-09.2010

Gupta-Agarwal, S., Jarome, T. J., Fernandez, J., and Lubin, F. D. (2014). NMDA receptor- and ERK-dependent histone methylation changes in the lateral amygdala bidirectionally regulate fear memory formation. *Learn. Mem.* 21, 351–362. doi: 10.1101/lm.035105.114

Guzowski, J. F., Setlow, B., Wagner, E. K., and McGaugh, J. L. (2001). Experience-dependent gene expression in the rat hippocampus after spatial learning: a comparison of the immediate-early genes Arc, c-fos and zif268. *J. Neurosci.* 21, 5089–5098.

Hall, J., Thomas, K. L., and Everitt, B. J. (2001). Cellular imaging of zif268 expression in the hippocampus and amygdala during contextual and cued fear memory retrieval: selective activation of hippocampal CA1 neurons during the recall of contextual memories. *J. Neurosci.* 21, 2186–2193.

Jarome, T. J., and Helmstetter, F. J. (2013). The ubiquitin-proteasome system as a critical regulator of synaptic plasticity and long-term memory formation. *Neurobiol. Learn. Mem.* 105, 107–116. doi: 10.1016/j.nlm.2013.03.009

Jarome, T. J., and Lubin, F. D. (2014). Epigenetic mechanisms of memory formation and reconsolidation. *Neurobiol. Learn. Mem.* 115, 116–127. doi: 10.1016/j.nlm.2014.08.002

Jarome, T. J., Thomas, J. S., and Lubin, F. D. (2014). The epigenetic basis of memory formation and storage. *Prog. Mol. Biol. Transl. Sci.* 128, 1–27. doi: 10.1016/b978-0-12-800977-2.00001-2

Johansen, J. P., Cain, C. K., Ostroff, L. E., and LeDoux, J. E. (2011). Molecular mechanisms of fear learning and memory. *Cell* 147, 509–524. doi: 10.1016/j.cell.2011.10.009

Kaas, G. A., Zhong, C., Eason, D. E., Ross, D. L., Vachhani, R. V., Ming, G. L., et al. (2013). TET1 controls CNS 5-methylcytosine hydroxylation, active DNA demethylation, gene transcription and memory formation. *Neuron* 79, 1086–1093. doi: 10.1016/j.neuron.2013.08.032

Kassed, C. A., and Herkenham, M. (2004). NF-kappaB p50-deficient mice show reduced anxiety-like behaviors in tests of exploratory drive and anxiety. *Behav. Brain Res.* 154, 577–584. doi: 10.1016/j.bbr.2004.03.026

Kassed, C. A., Willing, A. E., Garbuzova-Davis, S., Sanberg, P. R., and Pennypacker, K. R. (2002). Lack of NF-kappaB p50 exacerbates degeneration of hippocampal neurons after chemical exposure and impairs learning. *Exp. Neurol* 176, 277–288. doi: 10.1006/exnr.2002.7967

Kwapis, J. L., and Wood, M. A. (2014). Epigenetic mechanisms in fear conditioning: implications for treating post-traumatic stress disorder. *Trends Neurosci.* 37, 706–720. doi: 10.1016/j.tins.2014.08.005

Kwapis, J. L., Jarome, T. J., Lee, J. L., and Helmstetter, F. J. (2015). The retrosplenial cortex is involved in the formation of memory for context and trace fear conditioning. *Neurobiol. Learn. Mem.* 123, 110–116. doi: 10.1016/j.nlm.2015.06.007

Leach, P. T., Poplawski, S. G., Kenney, J. W., Hoffman, B., Liebermann, D. A., Abel, T., et al. (2012). Gadd45b knockout mice exhibit selective deficits in hippocampus-dependent long-term memory. *Learn. Mem.* 19, 319–324. doi: 10.1101/lm.024984.111

Lee, J. L., Everitt, B. J., and Thomas, K. L. (2004). Independent cellular processes for hippocampal memory consolidation and reconsolidation. *Science* 304, 839–843. doi: 10.1126/science.1095760

Lehmann, M. L., Brachman, R. A., Listwak, S. J., and Herkenham, M. (2010). NF-kappaB activity affects learning in aversive tasks: possible actions via modulation of the stress axis. *Brain Behav. Immun.* 24, 1008–1017. doi: 10.1016/j.bbi.2010.04.005

Levenson, J. M., Choi, S., Lee, S. Y., Cao, Y. A., Ahn, H. J., Worley, K. C., et al. (2004). A bioinformatics analysis of memory consolidation reveals involvement of the transcription factor c-rel. *J. Neurosci.* 24, 3933–3943. doi: 10.1523/jneurosci.5646-03.2004

Li, X., Wei, W., Zhao, Q. Y., Widagdo, J., Baker-Andresen, D., Flavell, C. R., et al. (2014). Neocortical Tet3-mediated accumulation of 5-hydroxymethylcytosine promotes rapid behavioral adaptation. *Proc. Natl. Acad. Sci. U S A* 111, 7120–7125. doi: 10.1073/pnas.1318906111

Lubin, F. D., and Sweatt, J. D. (2007). The IkappaB kinase regulates chromatin structure during reconsolidation of conditioned fear memories. *Neuron* 55, 942–957. doi: 10.1016/j.neuron.2007.07.039

Lubin, F. D., Roth, T. L., and Sweatt, J. D. (2008). Epigenetic regulation of BDNF gene transcription in the consolidation of fear memory. *J. Neurosci.* 28, 10576–10586. doi: 10.1523/JNEUROSCI.1786-08.2008

Ma, D. K., Jang, M. H., Guo, J. U., Kitabatake, Y., Chang, M. L., Pow-Anpongkul, N., et al. (2009). Neuronal activity-induced Gadd45b promotes epigenetic DNA demethylation and adult neurogenesis. *Science* 323, 1074–1077. doi: 10.1126/science.1166859

Maddox, S. A., Watts, C. S., and Schafe, G. E. (2014). DNA methyltransferase activity is required for memory-related neural plasticity in the lateral amygdala. *Neurobiol. Learn. Mem.* 107, 93–100. doi: 10.1016/j.nlm.2013.11.008

Meberg, P. J., Kinney, W. R., Valcourt, E. G., and Routtenberg, A. (1996). Gene expression of the transcription factor NF-kappa B in hippocampus: regulation by synaptic activity. *Brain Res. Mol. Brain Res.* 38, 179–190. doi: 10.1016/0169-328x(95)00229-l

Miller, C. A., Campbell, S. L., and Sweatt, J. D. (2008). DNA methylation and histone acetylation work in concert to regulate memory formation and synaptic plasticity. *Neurobiol. Learn. Mem.* 89, 599–603. doi: 10.1016/j.nlm.2007.07.016

Miller, C. A., Gavin, C. F., White, J. A., Parrish, R. R., Honasoge, A., Yancey, C. R., et al. (2010). Cortical DNA methylation maintains remote memory. *Nat. Neurosci.* 13, 664–666. doi: 10.1038/nn.2560

Miller, C. A., and Sweatt, J. D. (2007). Covalent modification of DNA regulates memory formation. *Neuron* 53, 857–869. doi: 10.1016/j.neuron.2007.02.022

Niehrs, C., and Schäfer, A. (2012). Active DNA demethylation by Gadd45 and DNA repair. *Trends Cell Biol.* 22, 220–227. doi: 10.1016/j.tcb.2012.01.002

Oikawa, K., Odero, G. L., Platt, E., Neuendorff, M., Hatherell, A., Bernstein, M. J., et al. (2012). NF-kappaB p50 subunit knockout impairs late LTP and alters long term memory in the mouse hippocampus. *BMC Neurosci.* 13:45. doi: 10.1186/1471-2202-13-45

O'Mahony, A., Raber, J., Montano, M., Foehr, E., Han, V., Lu, S. M., et al. (2006). NF-kappaB/Rel regulates inhibitory and excitatory neuronal function and synaptic plasticity. *Mol. Cell. Biol.* 26, 7283–7298. doi: 10.1128/mcb.00510-06

O'Riordan, K. J., Huang, I. C., Pizzi, M., Spano, P., Boroni, F., Egli, R., et al. (2006). Regulation of nuclear factor kappaB in the hippocampus by group I metabotropic glutamate receptors. *J. Neurosci.* 26, 4870–4879. doi: 10.1523/jneurosci.4527-05.2006

Peters, J., Dieppa-Perea, L. M., Melendez, L. M., and Quirk, G. J. (2010). Induction of fear extinction with hippocampal-infralimbic BDNF. *Science* 328, 1288–1290. doi: 10.1126/science.1186909

Ploski, J. E., Pierre, V. J., Smucny, J., Park, K., Monsey, M. S., Overeem, K. A., et al. (2008). The activity-regulated cytoskeletal-associated protein (Arc/Arg3.1) is required for memory consolidation of pavlovian fear conditioning in the lateral amygdala. *J. Neurosci.* 28, 12383–12395. doi: 10.1523/jneurosci.1662-08.2008

Roth, T. L., Lubin, F. D., Funk, A. J., and Sweatt, J. D. (2009). Lasting epigenetic influence of early-life adversity on the BDNF gene. *Biol. Psychiatry* 65, 760–769. doi: 10.1016/j.biopsych.2008.11.028

Rudenko, A., Dawlaty, M. M., Seo, J., Cheng, A. W., Meng, J., Le, T., et al. (2013). Tet1 is critical for neuronal activity-regulated gene expression and memory extinction. *Neuron* 79, 1109–1122. doi: 10.1016/j.neuron.2013.08.003

Ryley Parrish, R., Albertson, A. J., Buckingham, S. C., Hablitz, J. J., Mascia, K. L., Davis Haselden, W., et al. (2013). Status epilepticus triggers early and late alterations in brain-derived neurotrophic factor and NMDA glutamate receptor Grin2b DNA methylation levels in the hippocampus. *Neuroscience* 248, 602–619. doi: 10.1016/j.neuroscience.2013.06.029

Si, J., Yang, J., Xue, L., Yang, C., Luo, Y., Shi, H., et al. (2012). Activation of NF-kappaB in basolateral amygdala is required for memory reconsolidation in auditory fear conditioning. *PLoS One* 7:e43973. doi: 10.1371/journal.pone.0043973

Snow, W. M., Stoesz, B. M., Kelly, D. M., and Albensi, B. C. (2014). Roles for NF-kappaB and gene targets of NF-kappaB in synaptic plasticity, memory and navigation. *Mol. Neurobiol.* 49, 757–770. doi: 10.1007/s12035-013-8555-y

Stefanko, D. P., Barrett, R. M., Ly, A. R., Reolon, G. K., and Wood, M. A. (2009). Modulation of long-term memory for object recognition via HDAC inhibition. *Proc. Natl. Acad. Sci. U S A* 106, 9447–9452. doi: 10.1073/pnas.0903964106

Sultan, F. A., and Sweatt, J. D. (2013). The role of the Gadd45 family in the nervous system: a focus on neurodevelopment, neuronal injury and cognitive neuroepigenetics. *Adv. Exp. Med. Biol.* 793, 81–119. doi: 10.1007/978-1-4614-8289-5_6

Sultan, F. A., Wang, J., Tront, J., Liebermann, D. A., and Sweatt, J. D. (2012). Genetic deletion of Gadd45b, a regulator of active DNA demethylation, enhances long-term memory and synaptic plasticity. *J. Neurosci.* 32, 17059–17066. doi: 10.1523/jneurosci.1747-12.2012

Yeh, S. H., Lin, C. H., Lee, C. F., and Gean, P. W. (2002). A requirement of nuclear factor-kappaB activation in fear-potentiated startle. *J. Biol. Chem.* 277, 46720–46729. doi: 10.1074/jbc.m206258200

Zalcman, G., Federman, N., de la Fuente, V., and Romano, A. (2015). Nuclear factor kappa B-dependent Zif268 expression in hippocampus is required for recognition memory in mice. *Neurobiol. Learn. Mem.* 119, 10–17. doi: 10.1016/j.nlm.2014.12.013

Conflict of Interest Statement: The authors declare that the research was conducted in the absence of any commercial or financial relationships that could be construed as a potential conflict of interest.

frontiers in Molecular Neuroscience

ORIGINAL RESEARCH
published: 23 September 2015
doi: 10.3389/fnmol.2015.00052

Suberoylanilide hydroxamic acid, a histone deacetylase inhibitor, attenuates postoperative cognitive dysfunction in aging mice

Min Jia[1], Wen-Xue Liu[1], He-Liang Sun[1], Yan-Qing Chang[2], Jiao-Jiao Yang[1,3,4], Mu-Huo Ji[1], Jian-Jun Yang[1,3,4] and Chen-Zhuo Feng[2]**

[1] Department of Anesthesiology, Jinling Hospital, School of Medicine, Nanjing University, Nanjing, China, [2] Institute of Aging Research, School of Medicine, Hangzhou Normal University, Hangzhou, China, [3] Jiangsu Province Key Laboratory of Anesthesiology, Xuzhou Medical College, Xuzhou, China, [4] Jiangsu Province Key Laboratory of Anesthesia and Analgesia Application Technology, Xuzhou, China

OPEN ACCESS

Edited by:
Benedict C. Albensi,
University of Manitoba, Canada

Reviewed by:
Mary M. Torregrossa,
University of Pittsburgh, USA
Mauro Costa-Mattioli,
Baylor College of Medicine, USA

***Correspondence:**
Jian-Jun Yang,
Department of Anesthesiology,
Jinling Hospital, School of Medicine,
Nanjing University,
305 East Zhongshan Road,
Nanjing 210002, China
yjyangjj@126.com;
Chen-Zhuo Feng,
Institute of Aging Research,
School of Medicine,
Hangzhou Normal University,
58 Haishu Road, Yuhang District,
Hangzhou 311121, China
fengchenzhuo@hotmail.com

Received: 25 June 2015
Accepted: 28 August 2015
Published: 23 September 2015

Citation:
Jia M, Liu W-X, Sun H-L, Chang Y-Q, Yang J-J, Ji M-H, Yang J-J and Feng C-Z (2015) Suberoylanilide hydroxamic acid, a histone deacetylase inhibitor, attenuates postoperative cognitive dysfunction in aging mice.
Front. Mol. Neurosci. 8:52.
doi: 10.3389/fnmol.2015.00052

Postoperative cognitive dysfunction (POCD) is a recognized clinical entity characterized with cognitive deficits after anesthesia and surgery, especially in aged patients. Previous studies have shown that histone acetylation plays a key role in hippocampal synaptic plasticity and memory formation. However, its role in POCD remains to be determined. Here, we show that suberoylanilide hydroxamic acid (SAHA), a histone deacetylase inhibitor, attenuates POCD in aging Mice. After exposed to the laparotomy, a surgical procedure involving an incision into abdominal walls to examine the abdominal organs, 16- but not 3-month old male C57BL/6 mice developed obvious cognitive impairments in the test of long-term contextual fear conditioning. Intracerebroventricular (i.c.v.) injection of SAHA at the dose of (20 μg/2 μl) 3 h before and daily after the laparotomy restored the laparotomy-induced reduction of hippocampal acetyl-H3 and acetyl-H4 levels and significantly attenuated the hippocampus-dependent long-term memory (LTM) impairments in 16-month old mice. SAHA also reduced the expression of cleaved caspase-3, inducible nitric oxide synthase (iNOS) and N-methyl-D-aspartate (NMDA) receptor-calcium/calmodulin dependent kinase II (CaMKII) pathway, and increased the expression of brain-derived neurotrophic factor (BDNF), synapsin 1, and postsynaptic density 95 (PSD95). Taken together, our data suggest that the decrease of histone acetylation contributes to POCD and may serve as a target to improve the neurological outcome of POCD.

Keywords: postoperative cognitive dysfunction, aging, histone acetylation, neuroapoptosis, synaptic plasticity

Abbreviations: POCD, postoperative cognitive dysfunction; HATs, histone acetyltransferases; HDACs, histone deacetylases; SAHA, suberoylanilide hydroxamic acid; DMSO, dimethylsulfoxide; iNOS, inducible nitric oxide synthase; BDNF, brain-derived neurotrophic factor; PSD95, postsynaptic density 95; NMDA, N-methyl-D-aspartate; CaMKII, calcium/calmodulin dependent kinase II; HE staining, Hematoxylin-eosin staining; PBS, phosphate-buffered saline; PFA, phosphate-buffered paraformaldehyde; STM, short-term memory; LTM, long-term memory; TBST, Tris-Buffered Saline Tween; Ac-H3K9, histone H3(acetyl K9); Ac-H3K14, histone H3(acetyl K14); Ac-H4K5, histone H4 (acetyl K5); Ac-H4K12, histone H4 (acetyl K12); Ac-H3, acetyl histone H3; Ac-H4, acetyl histone H4 (Lys5/8/12/16); GAPDH, genes glyceraldehyde-3-phosphate dehydrogenase; real-time PCR, real-time polymerase chain reaction; AD, Alzheimer's disease; LTD, long-term depression; LTP, long-term potentiation.

Introduction

Postoperative cognitive dysfunction (POCD) is a cognitive progressive deterioration in memory and concentration following exposure to anesthesia and surgery (Amar et al., 1998; Terrando et al., 2011; Hovens et al., 2012). These cognitive deficits result in prolonged hospitalization and decreased quality of life (Moller et al., 1998). Tissue damage induced neuro-inflammation and altered reactivity of the immune system after operation are considered to play a major role in the development of POCD, which elicits neuron damages, affects synaptic function, and thereby induces cognitive impairments (Wan et al., 2007; Fidalgo et al., 2011). However, the molecular mechanisms underlying POCD remain largely to be determined.

Epigenetic dysregulation on the expression of key genes is widely involved in the etiology of brain disorders, including Alzheimer's disease (AD), Huntington's disease, Parkinson's disease, and Rubinstein-Taybi syndrome (Petrij et al., 1995; Kazantsev and Thompson, 2008; Chuang et al., 2009; Francis et al., 2009; Peleg et al., 2010; Gräff and Tsai, 2013). Histone acetylation is one of the most common forms of epigenetic modification, which is controlled by the balance between histone acetyltransferases (HATs) and histone deacetylases (HDACs; Fischer et al., 2010; Haggarty and Tsai, 2011; McQuown et al., 2011). In general, histone acetylation facilitates gene transcription, whereas histone deacetylation results in gene silencing (Fischer et al., 2010; Haggarty and Tsai, 2011; McQuown et al., 2011). A substantial body of evidence suggests that the dysregulation of histone acetylation contributes to the pathogenesis of neurodegenerative diseases, and targeted restoration of histone acetylation by HDAC inhibitors shows neuroprotective effects on neurodegenerative diseases (Petrij et al., 1995; Dash et al., 2010; Kilgore et al., 2010; Haettig et al., 2011; Ji et al., 2014).

The similar clinical symptoms has been revealed between POCD and neurodegenerative disorders (Wang et al., 2013; Luo et al., 2014; Xu et al., 2014). However, comparing with the studies of neurodegenerative diseases, the potential function of histone acetylation in POCD remains primarily unknown. Therefore, based on the pre-clinical animal mode of the laparotomy-induced cognitive deficits (Rosczyk et al., 2008; Barrientos et al., 2012; Hovens et al., 2014), which surgical procedure involving an incision into the abdominal wall to examine the abdominal organs, we investigated the role of histone acetylation and potential therapeutic effect of an HDAC inhibitor, suberoylanilide hydroxamic acid (SAHA), on POCD.

Materials and Methods

Animals

All animal experiments were carried out in accordance with the National Institutes of Health Guide for the Care and Use of Laboratory Animals, USA. The study protocol was approved by the Institutional Animal Care and Use Ethics Committee, Jinling Hospital, Nanjing University, Nanjing, China. The mice were purchased from The Animal Center of Jinling Hospital, Nanjing, China and efforts were made to minimize the number of animals used and their suffering. The mice were housed under specific pathogen-free conditions in a temperature-controlled room of 23 ± 1°C on a 12-h light-dark cycle, with *ad libitum* access to food and water. Mice were allowed 7 days to acclimate to the laboratory conditions before experiments.

Study Groups of Animals

In the first set of experiments, the 3- and 16-month old male C57BL/6 mice were used. Thirty-two 3-month old mice weighing 25–32 g and thirty-two 16-month old mice weighing 33–40 g were randomly assigned to receiving laparotomy or sham surgery ($n = 16$ for each group). The experimental protocol was presented in **Figure 1A**.

In the second set of experiments with SAHA (a histone deacetylase inhibitor) treatment, sixty-four 16-month old male mice weighing 33–40 g were randomly assigned to the following four groups: Sham + Vehicle group, mice received vehicle treatment and sham surgery; Sham + SAHA group, mice received SAHA treatment and sham surgery; Laparotomy + Vehicle group, mice received vehicle treatment and laparotomy; and Laparotomy + SAHA group, mice received SAHA treatment and laparotomy ($n = 16$ for each group). The experimental protocol was presented in **Figure 1B**.

Surgery

The Laparotomy or sham surgery was performed as previously described (Rosczyk et al., 2008; Barrientos et al., 2012; Hovens et al., 2014). Anesthesia was induced with 1.5% isoflurane in 100% oxygen in mice and was still maintained with 1.5% isoflurane by mice anesthesia mask during the surgery procedure. After the abdominal region of mice was shaved and cleaned with iodophor disinfectant, a 1.5 cm vertical incision, approximately 0.5 cm below the lower right rib, was created. The viscera and musculature were vigorously manipulated by inserting a sterile probe into the body cavity and stretching the musculature. Intestine was then exteriorized and manipulated between the surgeon's thumb and forefinger. The intestines were then placed back into the peritoneal cavity. The surgeries were lasted for approximately 15 min. After that, the peritoneal lining, muscle wall and the skin were closed with three dissolvable sutures and four silk thread sutures, respectively. The exterior wounds were dressed with polysporin to prevent potential infection. To eliminate the effect of hypoxia and acidosis to the experiment, both hypoxia and acidosis were analyzed by using arterial blood gas as we described before Li et al. (2014). Isoflurne anesthesia was stopped immediately for all groups of mice once the suture was in place. After recovery from anesthesia, the mice were placed back into their home cages with *ad libitum* access to food and water. For the sham surgery, mice were anesthetized, shaved, cleaned and the incision was sutured under isoflurane anesthesia for the same duration as those that the laparotomy surgical mice spent. Without manipulation of the viscera or musculature, the incision was closed and treated as described above.

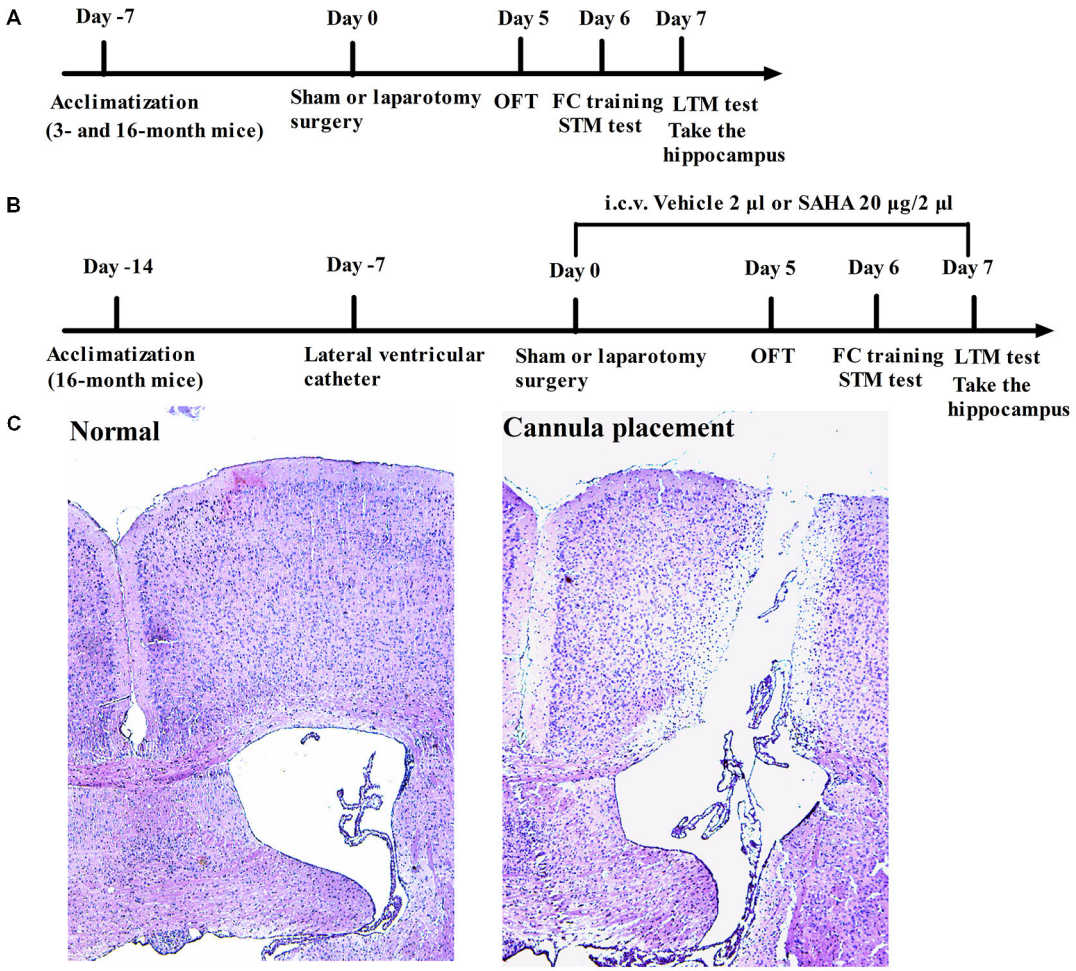

FIGURE 1 | Diagrammatic presentation of the experimental protocol (A,B) and the position of intracerebroventricular (i.c.v.) cannulation confirmed by the hematoxylin-eosin (HE) staining in the 16-month old mice (C).

Cannula Placement and SAHA Treatment

Cannula placement was performed 7 days before the surgery (**Figure 1C**). In the second set of experiments, each mouse was stereotaxically implanted with 24-gauge, stainless steel guide cannula (RWD Life Science Co., Ltd, Shenzhen, China) under anesthesia with intraperitoneal injection of 50 mg/kg 2% pentobarbital sodium. The position of guide cannula was in the left lateral ventricle, which is 0.45 mm posterior to bregma, 1.08 mm lateral to bregma, and 2.50 mm deep to dura. Once the guide cannula was placed, it was fixed to skull with glass ionomer cement (Dental Materials Factory of Shanghai Medical instrument Co., Ltd, Shanghai, China). The cannula placements were verified by postmortem dissections of brain tissue, followed by hippocampus collections.

The dose and time point for SAHA treatment (S1047, Selleckchem, TX, USA) were designed according to the previous study, in which it was showed that the hippocampal histone acetylation levels peaked 3-h after the intracerebroventricular (i.c.v.) injection of SAHA in mice (Alarcón et al., 2004). SAHA was dissolved in 40% of dimethylsulfoxide (DMSO) diluted with saline. In the group of mice treated with SAHA, the dose of 20 μg in 2 μl was used through i.c.v. injection once daily for 7 days. The first dose was given at the time of 3-h before the laparotomy or sham surgery. For the vehicle controls, the same amount of 40% DMSO was used.

Hematoxylin-Eosin (HE) Staining

In our preliminary experiment, to ensure the fixed position of left lateral ventricle, 7 days after cannula placement, mice were anesthetized deeply with intraperitoneal injection of 50 mg/kg 2% pentobarbital sodium, and then perfused transcardially with 0.1 M phosphate-buffered saline (PBS, pH 7.4), followed by 4% phosphate-buffered paraformaldehyde (PFA) for tissue fixation. The brain was removed, post-fixed in the same PFA solution for 12 h and sequentially immersed in 30% sucrose-phosphate-buffer solution for 24 h at 4°C. Coronal 5-μm-thick

cryostat sections were cut for the routine hematoxylin-eosin (HE) staining.

Each section was stained in Harris's hematoxylin solution for 8 min, differentiated in 1% acid alcohol for 30 s. After rinsing in 95% alcohol, the slides were counterstained in eosin-phloxine B solution for 45 s. After being dehydrated in a graded series of ethanol and cleared in xylene solutions, the sections were mounted for observation under a light microscope (Olympus BX53F, Tokyo, Japan).

Open Field Test

All behavioral procedures were performed during the light phase of the cycle between 10:00 A.M. and 4:00 P.M. in a sound-isolated room. Five days after the laparotomy, the mice were subjected to the open field test. The open field apparatus was positioned in a dimly lit room and consisted of a white Plexiglas chamber (40 cm × 40 cm with walls 40 cm high). Each mouse was placed at the center of the arena and left to explore the whole field for 5 min of recording by using the video tracking system (XR-XZ301, Shanghai Softmaze Information Technology Co. Ltd, Shanghai, China). The total distance traveled and the time spent in the center was measured as the parameter of anxiolytic behavior. Between each test, the surface of the arena was thoroughly cleaned with 75% alcohol to avoid the presence of olfactory cues. Tests were recorded by a person who was blinded to the grouping of mice.

Fear Conditioning Test

On the sixth day after the laparotomy, mice were subjected to fear conditioning test by using the fear conditioning paradigm (XR-XC404, Shanghai Softmaze Information Technology Co. Ltd, Shanghai, China). A mouse was placed in a conditioning training chamber (30 cm × 30 cm with walls 45 cm high) enclosed by a soundproof box with a camera fixed on top. After a 3 min baseline exploratory period in the chamber, mice received one tone (30 s, 70 dB, 3 kHz)-foot-shock (2 s, 0.75 mA) pairing. The foot-shock was carried out at the last 2 s of tone stimulation. Afterward, the mice were left in the conditioning box for additional 30 s before being returned to their home cage. Two hours after the training session, one batch of mice was place again in the training chamber and subjected to the short-term memory (STM) test. During a period of 5 min in the absence of tone and foot shock to test contextual fear conditioning to evaluate hippocampus-dependent memory, the freezing behavior of each mouse was scored every 5 s. Two hours after the contextual fear conditioning test, the mice were placed to a novel chamber for the cued (tone) fear conditioning test to evaluate amygdala-dependent memory. After a 3 min exploratory period in the new chamber, a training tone (30 s, 70 dB, 3 kHz) was applied for another 3 min and freezing behavior was scored during this tone period. The long-term memory (LTM) was performed at the time 24-h after training session and another batch of mice were used. Between each test, the chamber was thoroughly cleaned with 75% alcohol to avoid the presence of olfactory cues. The fear conditioning was administered and evaluated by a person blinded to the group assignment of mice.

Preparation of Protein Extracts

Two hours after the LTM test, mice were sacrificed and the hippocampus was harvested. The samples for measuring histone acetylation were prepared as described before Kilgore et al. (2010). Briefly, each sample was homogenized in the buffer containing 50 mM Tris-HCl, pH 7.5, 25 mM KCl, 250 mM sucrose, 2 mM sodium butyrate, 1 mM sodium orthovanadate, 0.5 mM PMSF and 1× protease inhibitor cocktail (sigma, MO, USA). After centrifuge at 7700 × g for 1 min at 4°C to pellet nuclei, 0.4 N H_2SO_4 was added to the pellet used for separating the histones. Then trichloroacetic acid with 10 mM sodium deoxycholate was added to supernatant to precipitate histone and incubate on ice for 30 min. After centrifuge at 14000 × g for 30 min at 4°C, the pellet of histone was washed once by acidified acetone and then resuspended in 10 mM Tris-HCl, pH 8.0.

For measuring the proteins of inducible nitric oxide synthase (iNOS), brain-derived neurotrophic factor (BNDF), synapsin 1, PSD-95, NR2A, NR2B, calcium/calmodulin dependent kinase II (CaMKIIα), and CaMKIIβ, Radio-Immunoprecipitation Assay (RIPA) buffer containing 1 × protease inhibitor cocktail was used. Homogenates were centrifuged at 13000 × g at 4°C for 10 min and the supernatants were collected for western blot.

Western Blot

Approximately 1 μg of histone protein or 50 μg of total protein per lane was separately by polyacrylamide gels and then transferred to a polyvinylidene difluoride membrane. After being incubated in blocking buffer of 5% non-fat milk in Tris-Buffered Saline Tween (TBST), membranes were incubated overnight in each primary antibody at 4°C. The primary antibodies used were anti-histone H3 (1:900; Cell Signaling, MA, USA), anti-histone H4 (1:900; Cell Signaling, MA, USA), anti-acetyl histone H3 (1:800; Merck Millipore, Darmstadt, Germany), anti-acetyl histone H4 (Lys5/8/12/16; 1:800; Merck Millipore, Darmstadt, Germany), anti-histone H3 (acetyl K9; 1:800; Abcam, MA, UK), anti-histone H3 (acetyl K14; 1:800; Merck Millipore, Darmstadt, Germany), anti-histone H4 (acetyl K5; 1:800; Abcam, MA, UK), anti-histone H4 (acetyl K12; 1:900; Abcam, MA, UK), anti-Cleaved Caspase-3 (1:900; Cell Signaling, MA, USA), anti-iNOS (1:2000; ANBO, CA, USA), anti-BDNF (1:1500; Santa Cru, CA, USA), anti-Synapsin 1 (1:2500; Merck Millipore, Darmstadt, Germany), anti-postsynaptic density 95 (PSD95) (1:1500; Abcam, MA, UK), anti-NMDAR2A (1:1000; Abcam, MA, UK), anti-NMDAR2B (1:1000; Abcam, MA, UK), anti-CaMKIIα (1:1000; Abcam, MA, UK), anti-CaMKIIβ (1:1000; Abcam, MA, UK). Membranes were washed with TBST and incubated with appropriate secondary antibodies (goat anti-rabbit or goat anti-mouse; Santa Cru, CA, USA). Protein bands were visualized by using enhanced chemiluminescence method and quantitatively analyzed with Image J Quant Software (NIH, Bethesda, MD, USA). The densities of histone acetylation bands were normalized to those of histone from the same

sample. The results from various experimental conditions were normalized to the data of mice in the Sham + Vehicle group.

Real-Time PCR

Real-time polymerase chain reaction (Real-time PCR) was performed as described previously (Feng et al., 2011). Total RNA was extracted from hippocampus of mouse using RNeasy micro kit (Qiagen, Valencia, CA, USA). Primers for real-time PCR were designed based on the reported sequence of mouse gene iNOS, BDNF, synapsin 1, PSD95, NR2A, NR2B, CaMKIIα, and CaMKIIβ and designed by OligoPerfect Designer. The primers in conserved coding region were preferred, if the gene has various transcripts. The sequences of the primers were detailed in **Table 1**. Quantitative PCRs were carried out in triplicate using each cDNA sample that was equivalent to 50 ng of stating total RNA. SYBR Green Quantitative PCR protocol was performed by using iQ SYBR Green Supermix (Bio-rad, CA, USA) in the Bio-Rad CFX96 real-time detection system (Bio-rad, CA, USA). To account for the possible differences in staring cDNA, quantitative PCR of the housekeeping genes glyceraldehyde-3-phosphate dehydrogenase (GAPDH) was also carried out for each sample. After PCR reaction, samples were subjected to a temperature ramp (from 70–95°C, 2°C/s) with continuous fluorescence monitoring for melting curve analysis. For each PCR product, a single narrow peak was obtained by melting curve analysis at the specific temperature. The relative amount of mRNA in each sample was determined using the comparative threshold cycle method and then normalized those of housekeeping gene GAPDH.

Statistical Analysis

Data are presented as the mean ± S.E.M. and analyzed by the Statistical Product for Social Sciences (SPSS; version 17.0, IL, USA). The difference among groups was determined by two-way analysis of variance followed by Bonferroni's *post hoc* test. Age and surgery type, or surgery type and drug treatment, were considered as two independent factors. The P values of age, surgery type, drug and interaction of factors were presented by P_{age}, P_{surg}, P_{drug} and P_{int} respectively. A P value < 0.05 was regarded as statistical significance.

Results

Laparotomy Induced the Hippocampus-Dependent Long-Term Cognitive Impairments and Down-Regulation of Hippocampal Acetyl-H3 and Acetyl -H4 Levels in the 16- but not the 3-Month Old Mice

To investigate the difference of POCD between adult and aging mice, laparotomy or sham surgery was performed on the 3- and 16-month old mice. Neither the 3- nor the 16-month old mice had significant difference in the total distance traveled (P_{age} = 0.804, $F_{age(1,28)}$ = 0.0626; P_{surg} = 0.982, $F_{surg(1,28)}$ = 0.00053; P_{int} = 0.913, $F_{int(1,28)}$ = 0.00761) or time spent in the center (P_{age} = 0.855, $F_{age(1,28)}$ = 0.0338; P_{surg} = 0.839, $F_{surg(1,28)}$ = 0.0421; P_{int} = 0.913, $F_{int(1,28)}$ = 0.0122) after the laparotomy or sham surgery (**Figures 2A,B**). Then we used fear conditioning test to determine the associative memory. The laparotomy did not induce the acquirement of associative memory during the training session of pre-stimulation (P_{age} = 0.957, $F_{age(1,28)}$ = 0.00295; P_{surg} = 0.985, $F_{surg(1,28)}$ = 0.000353; P_{int} = 0.843, $F_{int(1,28)}$ = 0.0398) or post-stimulation (P_{age} = 0.825, $F_{age(1,28)}$ = 0.0498; P_{surg} = 0.990, $F_{surg(1,28)}$ = 0.000176; P_{int} = 0.948, $F_{int(1,28)}$ = 0.00432; **Figure 2C**). In the STM test, no significant difference was found in the context (P_{age} = 0.506, $F_{age(1,28)}$ = 0.454; P_{surg} = 0.920, $F_{surg(1,28)}$ = 0.0103; P_{int} = 0.994, $F_{int(1,28)}$ = 0.0000547) or tone test (P_{age} = 0.593, $F_{age(1,28)}$ = 0.293; P_{surg} = 0.925, $F_{surg(1,28)}$ = 0.00893; P_{int} = 0.916, $F_{int(1,28)}$ = 0.0113) among the four groups (**Figure 2D**). However, in the LTM test, the laparotomy led to a shorter freezing time in the context (P_{age} = 0.003, $F_{age(1,28)}$ = 10.750; P_{surg} = 0.017, $F_{surg(1,28)}$ = 6.396; P_{int} = 0.025, $F_{int(1,28)}$ = 5.583) but not in the tone test (P_{age} = 0.301, $F_{age(1,28)}$ = 1.113; P_{surg} = 0.737, $F_{surg(1,28)}$ = 0.115; P_{int} = 0.736, $F_{int(1,28)}$ = 0.116) compared with the sham surgery in 16-month, but not 3-month old mice (**Figure 2E**).

We next examined the levels of acetyl-H3 and acetyl-H4 that are deeply involved in neurodegeneration diseases (Guan et al., 2009; Ricobaraza et al., 2009; Castellano et al., 2012). We found that the cognitive impairments in the 16-month old mice was accompanied with a decreased level of hippocampal acetyl-H3 (P_{age} = 0.034, $F_{age(1,8)}$ = 6.485; P_{surg} = 0.007, $F_{surg(1,8)}$ = 12.971; P_{int} = 0.013, $F_{int(1,8)}$ = 10.043) and acetyl-H4 (P_{age} = 0.020, $F_{age(1,8)}$ = 8.301; P_{surg} = 0.047, $F_{surg(1,8)}$ = 5.499; P_{int} = 0.049,

TABLE 1 | The sequence of primers for real-time PCR analysis.

Genes	Forward primers (5′-3′)	Reverse primers (5′-3′)	Accession number
iNOS	GGATTGTCCTACACCACACCAA	ATCTCTGCCTATCCGTCTCGTC	NM_010927
BDNF	AGCTGAGCGTGTGTGACAGT	ACCCATGGGATTACACTTGG	NM_007540
Synapsin1	GCTGGAATCCCCAGTGTAAA	AGTTCCACGATGAGCTGCTT	NM_013680
PSD95	CCCCAACATGGACTGTCTCT	ACTCCATCTCCCCCTCTGTT	NM_007864
NR2A	CTCTGATAATCCTTTCCTCCAC	GACCGAAGATAGCTGTCATTTACT	NM_008170
NR2B	TCCATCAGCAGAGGTATCTACAG	CCGTTGACTCCAGACAGGTT	NM_008171
CaMKIIα	GCCTCAGTCCTCCTGTGAAG	ACTCCTCTTCCCACCCACTT	NM_009792
CaMKIIβ	ATCGCCACCGCCATGGCCAC	GGTGATCTCTGGCCGACAGCT	NM_001174053
GAPDH	ACCCAGAAGACTGTGGATGG	CACATTGGGGGTAGGAACAC	NM_001289726

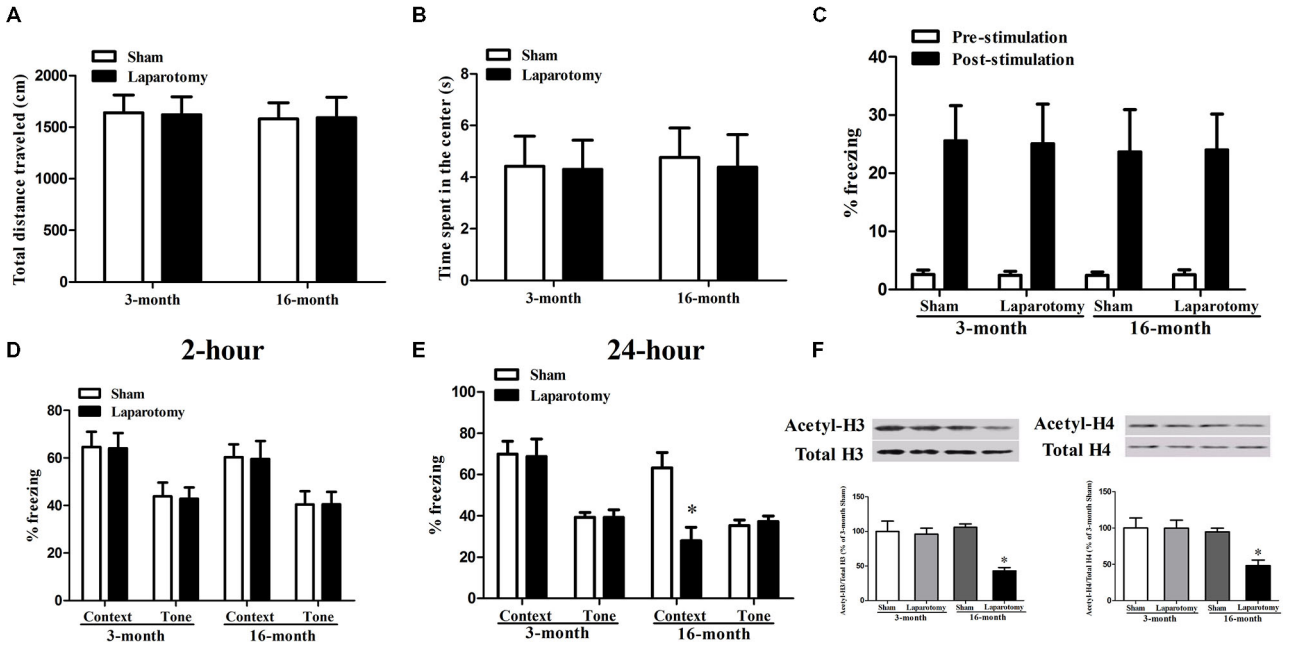

FIGURE 2 | Impact of the cognition and histone acetylation in the 3- and 16-month old mice after surgery. (A,B) Performance of total distance traveled and time spent in the center during the open field test. Data are presented as the mean ± S.E.M. (n = 16). **(C)** Performance of freezing time during the fear conditioning training session. Data are presented as the mean ± S.E.M. (n = 16). **(D,E)** Performance during fear conditioning tests 2- or 24-h after laparotomy. Data are presented as the mean ± S.E.M. (n = 8). **(F)** The acetylation level of histone H3 and H4 in the 3- or 16-month-old mice after laparotomy. Results are mean ± S.E.M. (n = 3). *$p < 0.05$ compared with the 16-month old mice subjected to sham surgery.

$F_{int(1,8)}$ = 5.359), whereas the 3-month old mice whose memory were not damaged did not show such a reduction (**Figure 2F**).

SAHA Ameliorated the Hippocampus-Dependent Long-Term Cognitive Impairments in the 16-Month Old Mice Exposed to the Laparotomy

The poor hippocampus-dependent LTM with histone acetylation down-regulation in the 16-month old mice exposed to the surgery guided us to further investigate the effect of SAHA on these mice. The results didn't showed any significant differences in the total distance traveled (P_{surg} = 0.984, $F_{surg(1,60)}$ = 0.000388; P_{drug} = 0.955, $F_{drug(1,60)}$ = 0.00318; P_{int} = 0.847, $F_{int(1,60)}$ = 0.0375), time spent in the center (P_{surg} = 0.676, $F_{surg(1,60)}$ = 0.177; P_{drug} = 0.904, $F_{drug(1,60)}$ = 0.0148; P_{int} = 0.899, $F_{int(1,60)}$ = 0.0163), or ability of memory acquirement when calculating the freezing time in the pre-stimulation (P_{surg} = 0.984, $F_{surg(1,60)}$ = 0.000388; P_{drug} = 0.955, $F_{drug(1,60)}$ = 0.00318; P_{int} = 0.847, $F_{int(1,60)}$ = 0.0375) and post-stimulation (P_{surg} = 0.774, $F_{surg(1,60)}$ = 0.0833; P_{drug} = 0.866, $F_{drug(1,60)}$ = 0.0287; P_{int} = 0.812, $F_{int(1,60)}$ = 0.0573) among the four groups (**Figures 3A–C**). In the STM test, no significant difference was found in the context (P_{surg} = 0.620, $F_{surg(1,28)}$ = 0.251; P_{drug} = 0.905, $F_{drug(1,28)}$ = 0.0146; P_{int} = 0.816, $F_{int(1,28)}$ = 0.0554) or tone test (P_{surg} = 0.872, $F_{surg(1,28)}$ = 0.0265; P_{drug} = 0.837, $F_{drug(1,28)}$ = 0.0429; P_{int} = 0.403, $F_{int(1,28)}$ = 0.721) among the four groups (**Figure 3D**). In the LTM test, the percent of freezing time in the context test decreased in the Laparotomy + Vehicle group compared with the Sham + Vehicle group, whereas SAHA diminished the decrease in the Laparotomy + SAHA group compared with the Laparotomy + Vehicle group (P_{surg} = 0.014, $F_{surg(1,28)}$ = 6.802; P_{drug} = 0.049, $F_{drug(1,28)}$ = 4.254; P_{int} = 0.021, $F_{int(1,28)}$ = 5.991; **Figure 3E**). No significant difference was observed in the tone test of LTM test among the four groups (P_{surg} = 0.803, $F_{surg(1,28)}$ = 0.0632; P_{drug} = 0.701, $F_{drug(1,28)}$ = 0.150; P_{int} = 0.898, $F_{int(1,28)}$ = 0.0167; **Figure 3E**).

SAHA Restored the Down-Regulation of Hippocampal Histone Acetylation in the 16-Month Old Mice Exposed to the Laparotomy

The hippocampal levels of acetyl-H3 (P_{surg} = 0.003, $F_{surg(1,8)}$ = 18.703; P_{drug} = 0.010, $F_{drug(1,8)}$ = 11.213; P_{int} = 0.018, $F_{int(1,8)}$ = 8.799) and acetyl-H4 ($P_{surg} < 0.001$, $F_{surg(1,8)}$ = 38.201; $P_{drug} < 0.001$, $F_{drug(1,8)}$ = 44.448; $P_{int} < 0.001$, $F_{int(1,8)}$ = 28.585) decreased in the Laparotomy + Vehicle group than those in the Sham + Vehicle group, whereas SAHA abolished the decrease in the Laparotomy + SAHA group compared with the Laparotomy + Vehicle group (**Figures 4A,B**). Four associated acetylation sites including acetyl-H3K9, acetyl-H3K14, acetyl-H4K5, and acetyl-H4K12 were analyzed. The hippocampal acetylation levels of H3K9 (P_{surg} = 0.005, $F_{surg(1,8)}$ = 14.682; P_{drug} = 0.007, $F_{drug(1,8)}$ = 12.972; P_{int} = 0.006, $F_{int(1,8)}$ = 13.898), H4K5 ($P_{surg} < 0.001$, $F_{surg(1,8)}$ = 29.653; P_{drug} = 0.003, $F_{drug(1,8)}$ = 17.851; P_{int} = 0.002, $F_{int(1,8)}$ = 20.698), and H4K12 ($P_{surg} < 0.001$, $F_{surg(1,8)}$ = 40.116; P_{drug} = 0.002,

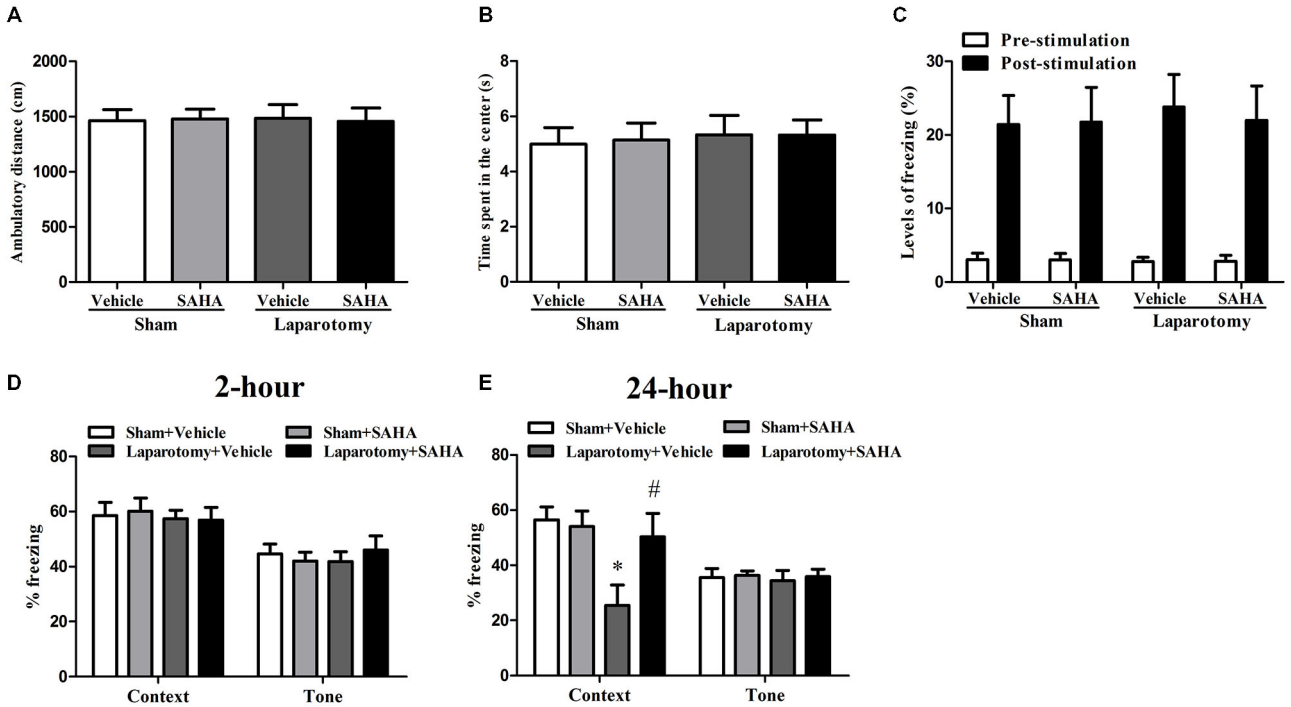

FIGURE 3 | Impact of suberoylanilide hydroxamic acid (SAHA) treatment on the cognitive performance in the 16-month old mice after surgery. **(A,B)** Performance of total distance traveled and time spent in the center during the open field test. Data are presented as the mean ± S.E.M. (n = 16). **(C)** Performance of freezing time during the fear conditioning training session. Data are presented as the mean ± S.E.M. (n = 16). **(D,E)** Performance during the fear conditioning tests 2- or 24-h after laparotomy. Data are presented as the mean ± S.E.M. (n = 8). $^{*}p < 0.05$ compared with the Sham + Vehicle group; $^{\#}p < 0.05$ compared with the Laparotomy + Vehicle group.

$F_{drug(1,8)}$ = 19.008; $P_{int} < 0.001$, $F_{int(1,8)}$ = 26.543) decreased in the Laparotomy + Vehicle group compared with the Sham + Vehicle group, whereas SAHA blocked the decreases in the Laparotomy + SAHA group compared with the Laparotomy + Vehicle group (**Figures 4A,B**). No significant difference was observed in the level of acetyl-H3K14 among the four groups (P_{surg} = 0.169, $F_{surg(1,8)}$ = 2.288; P_{drug} = 0.588, $F_{drug(1,8)}$ = 0.319; P_{int} = 0.829, $F_{int(1,8)}$ = 0.0501; **Figures 4A,B**).

SAHA Prevented the Dysregulation of Hippocampal Neuroapoptosis- and Synaptic Plasticity-Related Proteins in the 16-Month Old Mice Exposed to the Laparotomy

The hippocampal protein levels of cleaved caspase-3 ($P_{surg} < 0.001$, $F_{surg(1,8)}$ = 49.285; $P_{drug} < 0.001$, $F_{drug(1,8)}$ = 37.549; $P_{int} < 0.001$, $F_{int(1,8)}$ = 38.197) and iNOS (P_{surg} = 0.038, $F_{surg(1,8)}$ = 6.139; P_{drug} = 0.036, $F_{drug(1,8)}$ = 6.356; P_{int} = 0.015, $F_{int(1,8)}$ = 9.508) increased in the Laparotomy + Vehicle group compared with the Sham + Vehicle group, whereas SAHA eliminated the increases in the Laparotomy + SAHA group compared with the Laparotomy + Vehicle group (**Figure 5A**). The hippocampal protein levels of BDNF (P_{surg} = 0.010, $F_{surg(1,8)}$ = 11.409; P_{drug} = 0.007, $F_{drug(1,8)}$ = 13.191; P_{int} = 0.006, $F_{int(1,8)}$ = 13.434), synapsin 1 (P_{surg} = 0.039, $F_{surg(1,8)}$ = 6.070; P_{drug} = 0.049, $F_{drug(1,8)}$ = 5.387; P_{int} = 0.035, $F_{int(1,8)}$ = 6.418), and PSD95 (P_{surg} = 0.024, $F_{surg(1,8)}$ = 7.708; P_{drug} = 0.060, $F_{drug(1,8)}$ = 4.786; P_{int} = 0.069, $F_{int(1,8)}$ = 4.401) decreased in the Laparotomy + Vehicle group compared with the Sham + Vehicle group, whereas SAHA reversed the decreases in the Laparotomy + SAHA group compared with the Laparotomy + Vehicle group (**Figure 5B**).

The hippocampal NR2A (P_{surg} = 0.007, $F_{surg(1,8)}$ = 12.823; P_{drug} = 0.048, $F_{drug(1,8)}$ = 5.428; P_{int} = 0.029, $F_{int(1,8)}$ = 7.055), NR2B ($P_{surg} < 0.001$, $F_{surg(1,8)}$ = 26.202; P_{drug} = 0.025, $F_{drug(1,8)}$ = 7.533; P_{int} = 0.037, $F_{int(1,8)}$ = 6.217), CaMKIIα ($P_{surg} < 0.001$, $F_{surg(1,8)}$ = 28.352; P_{drug} = 0.007, $F_{drug(1,8)}$ = 12.744; $P_{int} < 0.001$, $F_{int(1,8)}$ = 27.711), and CaMKIIβ (P_{surg} = 0.037, $F_{surg(1,8)}$ = 6.203; P_{drug} = 0.020, $F_{drug(1,8)}$ = 8.463; P_{int} = 0.029, $F_{int(1,8)}$ = 7.001) were up-regulated in the Laparotomy +Vehicle group compared with the Sham + Vehicle group, whereas SAHA inhibited the up-regulation in the Laparotomy + SAHA group compared with the Laparotomy + Vehicle group (**Figure 6**). The gene expression level changes at the protein level measured by western blot were consistent to those at mRNA level measured by RT-real time PCR (**Figure 7**). The statistical results were as follows: iNOS ($P_{surg} < 0.001$, $F_{surg(1,8)}$ = 89.695; $P_{drug} < 0.001$, $F_{drug(1,8)}$ = 50.714; $P_{int} < 0.001$, $F_{int(1,8)}$ = 39.864), BDBF (P_{surg} = 0.019, $F_{surg(1,8)}$ = 8.523; P_{drug} = 0.256, $F_{drug(1,8)}$ = 1.499; P_{int} = 0.019, $F_{int(1,8)}$ = 8.523), synapsin 1 (P_{surg} = 0.013, $F_{surg(1,8)}$ = 10.257; P_{drug} = 0.030, $F_{drug(1,8)}$ = 6.956; P_{int} = 0.021, $F_{int(1,8)}$ = 8.254),

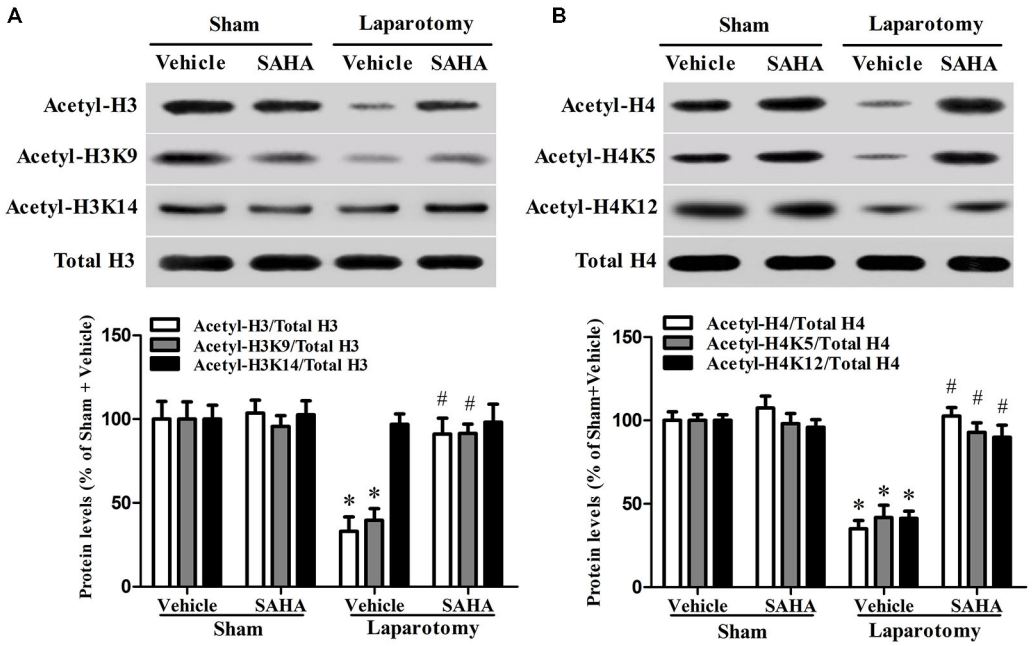

FIGURE 4 | Impact of SAHA treatment on the level of histone acetylation in the 16-month old mice after surgery. (A) The representative blot of histone H3 acetylation is shown at the top of the panel and the corresponding quantitative result is shown at the bottom. Data are presented as the mean ± S.E.M. ($n = 3$). **(B)** The representative blot of histone H4 acetylation is shown at the top of the panel and the corresponding quantitative result is shown at the bottom. Data are presented as the mean ± S.E.M. ($n = 3$). $^{*}p < 0.05$ compared with the Sham + Vehicle group; $^{\#}p < 0.05$ compared with the Laparotomy + Vehicle group.

PSD95 ($P_{surg} = 0.003$, $F_{surg(1,8)} = 16.908$; $P_{drug} = 0.004$, $F_{drug(1,8)} = 15.535$; $P_{int} = 0.033$, $F_{int(1,8)} = 6.646$), CaMKIIβ ($P_{surg} = 0.037$, $F_{surg(1,8)} = 6.203$; $P_{drug} = 0.020$, $F_{drug(1,8)} = 8.463$; $P_{int} = 0.029$, $F_{int(1,8)} = 7.001$), NR2A ($P_{surg} < 0.001$, $F_{surg(1,8)} = 27.121$; $P_{drug} = 0.021$, $F_{drug(1,8)} = 8.224$; $P_{int} = 0.037$, $F_{int(1,8)} = 6.253$), NR2B ($P_{surg} < 0.001$,$F_{surg(1,8)} = 43.819$; $P_{drug} = 0.002$, $F_{drug(1,8)} = 21.952$; $P_{int} = 0.002$, $F_{int(1,8)} = 20.371$), CaMKIIα ($P_{surg} < 0.001$, $F_{surg(1,8)} = 64.159$; $P_{drug} < 0.001$, $F_{drug(1,8)} = 31.208$; $P_{int} < 0.001$, $F_{int(1,8)} = 47.622$), and CaMKIIβ ($P_{surg} < 0.001$, $F_{surg(1,8)} = 65.655$; $P_{drug} < 0.001$, $F_{drug(1,8)} = 25.505$; $P_{int} < 0.001$, $F_{int(1,8)} = 39.780$).

Discussion

In the present study, we found that the laparotomy-induced hippocampus-dependent LTM impairments were accompanied by the decreased acetylation levels of hippocampal histone H3 and H4 in 16- but not 3-month old mice. Treatment with SAHA rescued the histone acetylation levels and ameliorated the hippocampus-dependent LTM impairments in 16-month old mice exposed to the laparotomy.

Studies have revealed many risk factors, including advanced age, poor education, duration of anesthesia, respiratory complications, severity of coexisting illness, and psychoactive drugs, contributing to the development of POCD (Moller et al., 1998; Wan et al., 2007). Of these, advanced age is regarded as the prominent risk factor for the occurrence and development of POCD (Moller et al., 1998; Wan et al., 2007; Fidalgo et al., 2011). Therefore, aging animals were used to establish the relevant POCD models (Rosczyk et al., 2008; Li et al., 2014). We showed that 3-month old mice exposed to the laparotomy had no cognitive deficits, but 16-month old mice had the hippocampal LTM impairments, suggesting that the laparotomy can induce age-related behavioral impairments. Moreover, the context-dependent associative memory serves as an indicative of hippocampus-dependent associative memory and the tone-dependent associative memory requires proper function of amygdala (Barrientos et al., 2012). Thus, the impaired hippocampal LTM in 16- but not 3-month old mice indicated that the deteriorating effects of the laparotomy on the cognitive function are age-related. Similar to previous studies (Rosczyk et al., 2008; Li et al., 2014), we also did not observe an impaired STM in the 3- or 16-month old mice, which indicated that the model of POCD used in this study unaffected the intact STM.

Epigenetics have been shown to be deeply involved in the learning and memory deficits in neurodegenerative diseases (Govindarajan et al., 2011; Haettig et al., 2011; Haberman et al., 2012), whose phenotypes and pathogenesis are similar to POCD (Wang et al., 2013; Luo et al., 2014; Xu et al., 2014). However, the role of epigenetics in the development of POCD remains to be investigated. In our study, the decreased levels of hippocampal histone H3 and H4 acetylation and the impaired cognition in the 16-month old mice exposed to the laparotomy were prevented by the SAHA treatment, which suggested that the down-regulation of hippocampal acetyl-H3 and acetyl-H4 contributes to the pathogenesis of POCD. Moreover, SAHA did not up-regulate the histone acetyl-H3 and acetyl-H4 in the mice exposed to the sham surgery compared with those exposed to the laparotomy,

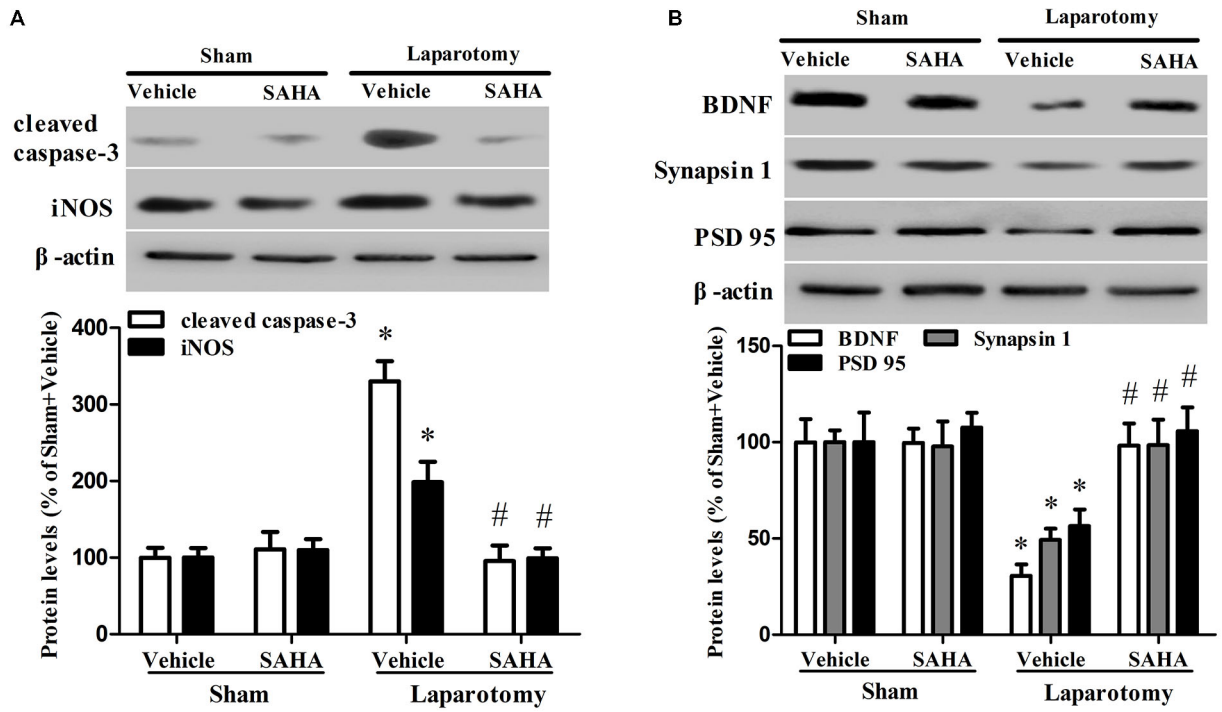

FIGURE 5 | Impact of SAHA treatment on protein expressions of cleaved caspase-3, iNOS, BDNF, synapsin 1 and PSD95 in the 16-month old mice after surgery. (A) The protein levels of cleaved caspase-3 and iNOS were determined by western blot. Representative image is at the top and quantitative result is at the bottom. Data are presented as the mean ± S.E.M. ($n = 3$). **(B)** The result of western blot for BDNF, synapsin 1, and PSD95. Representative image is shown at the top and quantitation is at the bottom. Data are presented as the mean ± S.E.M. ($n = 3$). $^{*}p < 0.05$ compared with the Sham + Vehicle group; $^{\#}p < 0.05$ compared with the Laparotomy + Vehicle group.

which indicated that the over activity of HDAC makes it more sensitive to SAHA. Previous studies have revealed that not all lysines in histone proteins are affected in the development of neurodegenerative disorders (Miao et al., 2014; Zhong et al., 2014) and different diseases induce histone acetylation level changes at different sites (Guan et al., 2009; Itzhak et al., 2013). Our results showed that the laparotomy induced histone acetylation level changes at the sites of H3K9, H4K5, and H4K12, but not H3K14, which suggested that investigating these specific acetylation sites would be helpful to further understand the potential pathogenesis of POCD.

To clarify how the altered histone acetylation leads to the laparotomy-induced cognitive deficits, we investigated the expression of proteins related to cognition performance in 16-month old mice. Studies have linked the increased histone acetylation in the hippocampus to memory permissive for the transcription of learning-related plasticity genes (Ravi and Kannan, 2013) and attributed neuron damages and synaptic plasticity changes to the development of POCD (Bozon et al., 2002; Jungwirth et al., 2009; Cibelli et al., 2010; Lin and Zuo, 2011). We observed that neuroapoptosis-related proteins cleaved caspase-3 and iNOS were up-regulated, and synaptic plasticity-related proteins BDNF, synapsin 1, and PSD95 were down-regulated in the 16-month old mice after the laparotomy.

NMDAR and CaMKII proteins mainly locate at hippocampus and prefrontal cortex and play critical roles in learning and memory (Coultrap et al., 2014). Both the aged rats after the isoflurane/nitrous oxide anesthesia and the AD-like rats exhibit cognitive deficits and neuroapoptosis associated with an over-expression of hippocampal NR2B (Liu et al., 2012; Mawhinney et al., 2012). In aged mice, a higher expression of NMDAR2 was associated with poorer memory (Zhao et al., 2009). Therefore, our finding that the activation of NMDAR2-CaMKII pathway was observed in the hippocampus of 16-month old mice exposed to the laparotomy might correspond to their memory deficits. It was well studied that extra-synaptic NMDARs interfered with the BDNF expression, shut off cell survival pathway, induced mitochondrial dysfunction and activated pro-death molecules (Hardingham et al., 2002). Our results of reduced BDNF and increased cleaved caspase-3 and iNOS suggested that cell death might be triggered in our aging mice with POCD. Since SAHA alleviated the up-regulation of NR2, CaMKII, cleaved caspase-3 and iNOS, it was conceivable that the pathological high expression of these molecules contributed to the development of POCD possibly by histone acetylation.

Increased histone acetylation is generally associated with a chromatin structure that is more permissive for gene transcript.

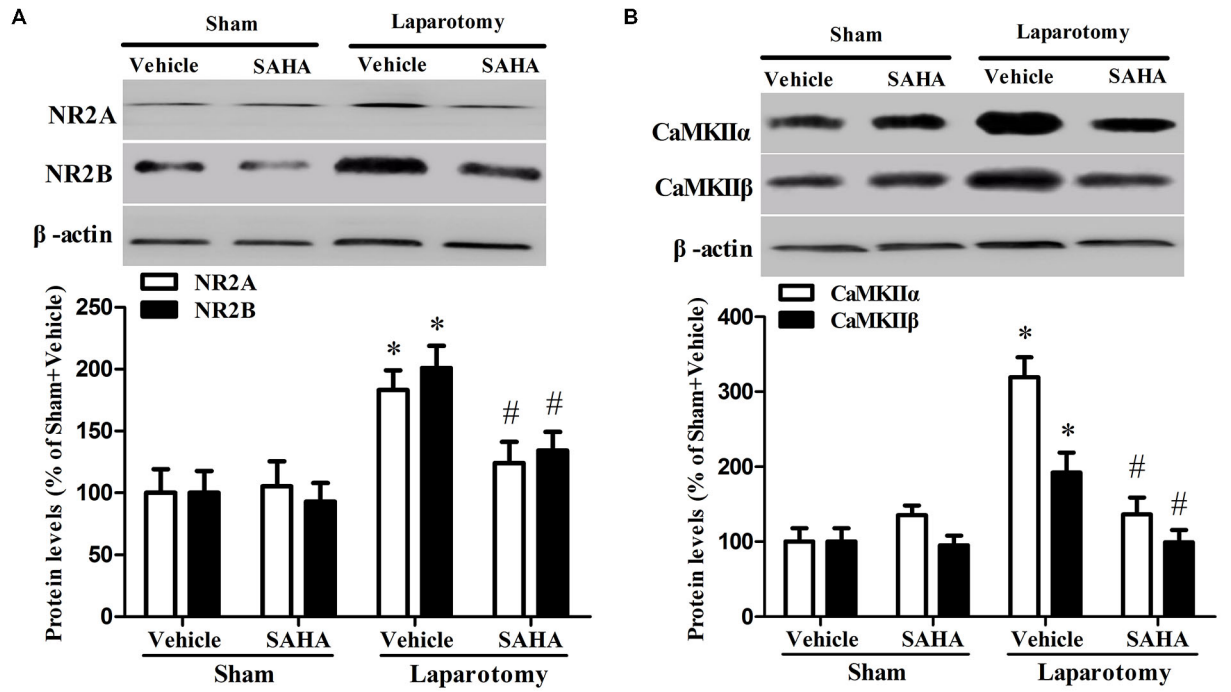

FIGURE 6 | Impact of SAHA treatment on protein expressions of NR2A, NR2B, CaMKIIα, and CaMKIIβ in the 16-month old mice after surgery. (A) The protein levels of NR2A, NR2B were determined by western blot. Representative image is shown at the top and quantitative result at the bottom. Data are presented as the mean ± S.E.M. (n = 3). **(B)** The protein levels of CaMKIIα and CaMKIIβ. Representative image is shown at the top and quantitative result at the bottom. Data are presented as the mean ± S.E.M. (n = 3). *$p < 0.05$ compared with the Sham + Vehicle group; #$p < 0.05$ compared with the Laparotomy + Vehicle group.

Our finding of the up-regulations of iNOS, NR2A, NR2B and CaMKII in the laparotomy with lower acetylation indicated that the expressions of these genes might not be regulated directly through histone acetylation on their promoters. It might have other regulation mechanisms following histone acetylation underlying these genes. While the down-regulation of BDNF, synapsin 1 and PSD 95 corresponding to the down-regulation of histone acetylation indicated that the promoters of these genes might be deacetylated by HDAC in our POCD model. Further studies on the promoters of these genes by chromatin immunoprecipitation are needed to investigate the dynamic state of histone acetylation associated with these changes of gene expressions.

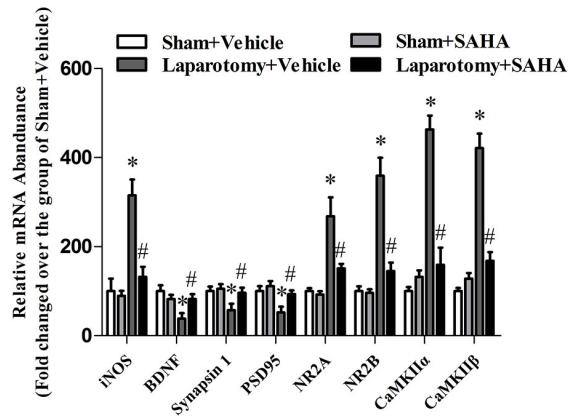

FIGURE 7 | Impact of SAHA treatment on mRNA abundances of iNOS, BDNF, synapsin 1, PSD95, NR2A, NR2B, CaMKIIα, and CaMKIIβ in the 16-month old mice after surgery. The real-time PCR results were normalized by those of genes glyceraldehyde-3-phosphate dehydrogenase (GAPDH). The results from each group were then normalized by those from the group of vehicle-treated mice subjected to sham surgery. Data are presented as the mean ± S.E.M. (n = 3). *$p < 0.05$ compared with the Sham + Vehicle group; #$p < 0.05$ compared with the Laparotomy + Vehicle group.

It is clear that not only cardiac surgeries, but also abdominal orthopedic can also produce POCD (Martin et al., 2005). The possible reason is that immune challenge induced by the laparotomy results in an exaggerated inflammatory response in the hippocampus, a region of the brain that contains a large number of pro-inflammatory cytokine receptors, through the communication between the peripheral immune system and the brain (Parnet et al., 1994). The neuroinflammatory response in turn affect the expression of other important genes to cause cognitive dysfunction, which is associated with epigenetic changes such as histone acetylation or deacetylation. At an advanced age, the long lasting neuroinflammatory response likely plays an important role to cause hippocampal-dependent memory deficits (Maier, 2003; Barrientos et al., 2009). That explains the facts that age is the strongest risk factor for the development of POCD, and that anti-inflammatory is considered as a viable strategy to prevent POCD. Noticeably,

if inflammation does not subside, it can contribute to the pathogenesis of disease (Vacas et al., 2013). Our findings of decreased histone acetylation in POCD provide novel insight into the pathology of POCD and important preclinical evidences supporting that SAHA may serve as a potential therapeutic agent for POCD.

Acknowledgments

This work was supported by National Natural Science Foundation of China (Nos. 81271216, 81300946, 81300262, and 81471105) and Natural Science Foundation of Jiangsu Province (No. BK2012778).

References

Alarcón, J. M., Malleret, G., Touzani, K., Vronskaya, S., Ishii, S., Kandel, E. R., et al. (2004). Chromatin acetylation, memory and LTP are impaired in CBP$^{+/-}$ mice: a model for the cognitive deficit in rubinstein-taybi syndrome and its amelioration. *Neuron* 42, 947–959. doi: 10.1016/j.neuron.2004.05.021

Amar, D., Fleisher, M., Pantuck, C. B., Shamoon, H., Zhang, H., Roistacher, N., et al. (1998). Persistent alterations of the autonomic nervous system after noncardiac surgery. *Anesthesiology* 89, 30–42. doi: 10.1097/00000542-199807000-00008

Barrientos, R. M., Frank, M. G., Hein, A. M., Higgins, E. A., Watkins, L. R., Rudy, J. W., et al. (2009). Time course of hippocampal IL-1 beta and memory consolidation impairments in aging rats following peripheral infection. *Brain Behav. Immun.* 23, 46–54. doi: 10.1016/j.bbi.2008.07.002

Barrientos, R. M., Hein, A. M., Frank, M. G., Watkins, L. R., and Maier, S. F. (2012). Intracisternal interleukin-1 receptor antagonist prevents postoperative cognitive decline and neuroinflammatory response in aged rats. *J. Neurosci.* 32, 14641–14648. doi: 10.1523/jneurosci.2173-12.2012

Bozon, B., Davis, S., and Laroche, S. (2002). Regulated transcription of the immediate-early gene Zif268: mechanisms and gene dosage-dependent function in synaptic plasticity and memory formation. *Hippocampus* 12, 570–577. doi: 10.1002/hipo.10100

Castellano, J. F., Fletcher, B. R., Kelley-Bell, B., Kim, D. H., Gallagher, M., and Rapp, P. R. (2012). Age-related memory impairment is associated with disrupted multivariate epigenetic coordination in the hippocampus. *PLoS One* 7:e33249. doi: 10.1371/journal.pone.0033249

Chuang, D. M., Leng, Y., Marinova, Z., Kim, H. J., and Chiu, C. T. (2009). Multiple roles of HDAC inhibition in neurodegenerative conditions. *Trends Neurosci.* 32, 591–601. doi: 10.1016/j.tins.2009.06.002

Cibelli, M., Fidalgo, A. R., Terrando, N., Ma, D., Monaco, C., Feldmann, M., et al. (2010). Role of interleukin-1beta in postoperative cognitive dysfunction. *Ann. Neurol.* 68, 360–368. doi: 10.1002/ana.22082

Coultrap, S. J., Freund, R. K., O'Leary, H., Sanderson, J. L., Roche, K. W., Dell'Acqua, M. L., et al. (2014). Autonomous CaMKII mediates both LTP and LTD using a mechanism for differential substrate site selection. *Cell Rep.* 6, 431–437. doi: 10.1016/j.celrep.2014.01.005

Dash, P. K., Orsi, S. A., Zhang, M., Grill, R. J., Pati, S., Zhao, J., et al. (2010). Valproate administered after traumatic brain injury provides neuroprotection and improves cognitive function in rats. *PLoS One* 5:e11383. doi: 10.1371/journal.pone.0011383

Feng, C., Cao, L., and Zuo, Z. (2011). RNA interference-produced autoregulation of inducible nitric oxide synthase expression. *FEBS Lett.* 585, 2488–2492. doi: 10.1016/j.febslet.2011.06.032

Fidalgo, A. R., Cibelli, M., White, J. P., Nagy, I., Maze, M., and Ma, D. (2011). Systemic inflammation enhances laparotomy surgery-induced cognitive dysfunction in mice. *Neurosci. Lett.* 498, 63–66. doi: 10.1016/j.neulet.2011.04.063

Fischer, A., Sananbenesi, F., Mungenast, A., and Tsai, L. H. (2010). Targeting the correct HDAC (s) to treat cognitive disorders. *Trends Pharmacol. Sci.* 31, 605–617. doi: 10.1016/j.tips.2010.09.003

Francis, Y. I., Fà, M., Ashraf, H., Zhang, H., Staniszewski, A., Latchman, D. S., et al. (2009). Dysregulation of histone acetylation in the APP/PS1 mouse model of Alzheimer's disease. *J. Alzheimers Dis.* 18, 131–139. doi: 10.3233/JAD-2009-1134

Govindarajan, N., Agis-Balboa, R. C., Walter, J., Sananbenesi, F., and Fischer, A. (2011). Sodium butyrate improves memory function in an Alzheimer's disease mouse model when administered at an advanced stage of disease progression. *J. Alzheimers Dis.* 26, 187–197. doi: 10.3233/JAD-2011-110080

Gräff, J., and Tsai, L. H. (2013). The potential of HDAC inhibitors as cognitive enhancers. *Annu. Rev. Pharmacol. Toxicol.* 53, 311–330. doi: 10.1146/annurev-pharmtox-011112-140216

Guan, J. S., Haggarty, S. J., Giacometti, E., Dannenberg, J. H., Joseph, N., Gao, J., et al. (2009). HDAC2 negatively regulates memory formation and synaptic plasticity. *Nature* 459, 55–60. doi: 10.1038/nature07925

Haberman, R. P., Quigley, C. K., and Gallagher, M. (2012). Characterization of CpG island DNA methylation of impairment-related genes in a rat model of cognitive aging. *Epigenetics* 7, 1008–1009. doi: 10.4161/epi.21291

Haettig, J., Stefanko, D. P., Multani, M. L., Figueroa, D. X., McQuown, S. C., and Wood, M. A. (2011). HDAC inhibition modulates hippocampus-dependent long-term memory for object location in a CBP-dependent manner. *Learn. Mem.* 18, 71–79. doi: 10.1101/lm.1986911

Haggarty, S. J., and Tsai, L. H. (2011). Probing the role of HDACs and mechanisms of chromatin-mediated neuroplasticity. *Neurobiol. Learn. Mem.* 96, 41–52. doi: 10.1016/j.nlm.2011.04.009

Hardingham, G. E., Fukunaga, Y., and Bading, H. (2002). Extrasynaptic NMDARs oppose synaptic NMDARs by triggering CREB shut-off and cell death pathways. *Nat. Neurosci.* 5, 405–414. doi: 10.1038/nn835

Hovens, I. B., Schoemaker, R. G., van der Zee, E. A., Heineman, E., Izaks, G. J., and van Leeuwen, B. L. (2012). Thinking through postoperative cognitive dysfunction: how to bridge the gap between clinical and pre-clinical perspectives. *Brain Behav. Immun.* 26, 1169–1179. doi: 10.1016/j.bbi.2012.06.004

Hovens, I. B., van Leeuwen, B. L., Nyakas, C., Heineman, E., van der Zee, E. A., and Schoemaker, R. G. (2014). Postoperative cognitive dysfunction and microglial activation in associated brain regions in old rats. *Neurobiol. Learn. Mem.* 118, 74–79. doi: 10.1016/j.nlm.2014.11.009

Itzhak, Y., Liddie, S., and Anderson, K. L. (2013). Sodium butyrate-induced histone acetylation strengthens the expression of cocaine-associated contextual memory. *Neurobiol. Learn. Mem.* 102, 34–42. doi: 10.1016/j.nlm.2013.03.007

Ji, M., Dong, L., Jia, M., Liu, W., Zhang, M., Ju, L., et al. (2014). Epigenetic enhancement of brain-derived neurotrophic factor signaling pathway improves cognitive impairments induced by isoflurane exposure in aged rats. *Mol. Neurobiol.* 50, 937–944. doi: 10.1007/s12035-014-8659-z

Jungwirth, B., Zieglgänsberger, W., Kochs, E., and Rammes, G. (2009). Anesthesia and postoperative cognitive dysfunction (POCD). *Mini. Rev. Med. Chem.* 9, 1568–1579. doi: 10.2174/138955709791012229

Kazantsev, A. G., and Thompson, L. M. (2008). Therapeutic application of histone deacetylase inhibitors for central nervous system disorders. *Nat. Rev. Drug. Discov.* 7, 854–868. doi: 10.1038/nrd2681

Kilgore, M., Miller, C. A., Fass, D. M., Hennig, K. M., Haggarty, S. J., Sweatt, J. D., et al. (2010). Inhibitors of class 1 histone deacetylases reverse contextual memory deficits in a mouse model of Alzheimer's disease. *Neuropsychopharmacology* 35, 870–880. doi: 10.1038/npp.2009.197

Lin, D., and Zuo, Z. (2011). Isoflurane induces hippocampal cell injury and cognitive impairments in adult rats. *Neuropharmacology* 61, 1354–1359. doi: 10.1016/j.neuropharm.2011.08.011

Liu, Z., Lv, C., Zhao, W., Song, Y., Pei, D., and Xu, T. (2012). NR2B-containing NMDA receptors expression and their relationship to apoptosis in hippocampus of Alzheimer's disease-like rats. *Neurochem. Res.* 37, 1420–1427. doi: 10.1007/s11064-012-0726-0

Li, X. M., Zhou, M. T., Wang, X. M., Ji, M. H., Zhou, Z. Q., and Yang, J. J. (2014). Resveratrol pretreatment attenuates the isoflurane-induced cognitive impairment through its anti-inflammation and -apoptosis actions in aged mice. *J. Mol. Neurosci.* 52, 286–293. doi: 10.1007/s12031-013-0141-2

Luo, X., Yang, L., Chen, X., and Li, S. (2014). Tau hyperphosphorylation: a downstream effector of isoflurane-induced neuroinflammation in aged rodents. *Med. Hypotheses* 82, 94–96. doi: 10.1016/j.mehy.2013.11.015

Maier, S. F. (2003). Bi-directional immune-brain communication: implications for understanding stress, pain, and cognition. *Brain Behav. Immun.* 17, 69–85. doi: 10.1016/s0889-1591(03)00032-1

Martin, T. J., Kahn, W. R., and Eisenach, J. C. (2005). Abdominal surgery decreases food-reinforced operant responding in rats: relevance of incisional pain. *Anesthesiology* 103, 629–637. doi: 10.1097/00000542-200509000-00028

Mawhinney, L. J., de Rivero Vaccari, J. P., Alonso, O. F., Jimenez, C. A., Furones, C., Moreno, W. J., et al. (2012). Isoflurane/nitrous oxide anesthesia induces increases in NMDA receptor subunit NR2B protein expression in the aged rat brain. *Brain Res.* 1431, 23–34. doi: 10.1016/j.brainres.2011.11.004

McQuown, S. C., Barrett, R. M., Matheos, D. P., Post, R. J., Rogge, G. A., Alenghat, T., et al. (2011). HDAC3 is a critical negative regulator of long-term memory formation. *J. Neurosci.* 31, 764–774. doi: 10.1523/JNEUROSCI.5052-10.2011

Miao, F., Chen, Z., Genuth, S., Paterson, A., Zhang, L., Wu, X., et al. (2014). Evaluating the role of epigenetic histone modifications in the metabolic memory of type 1 diabetes. *Diabetes* 63, 1748–1762. doi: 10.2337/db13-1251

Moller, J. T., Cluitmans, P., Rasmussen, L. S., Houx, P., Rasmussen, H., Canet, J., et al. (1998). Long-term postoperative cognitive dysfunction in the elderly: ISPOCD1 study. *Lancet* 351, 857–861. doi: 10.1016/s0140-6736(97)07382-0

Parnet, P., Amindari, S., Wu, C., Brunke-Reese, D., Goujon, E., Weyhenmeyer, J. A., et al. (1994). Expression of type I and type II interleukin-1 receptors in mouse brain. *Brain Res. Mol. Brain Res.* 27, 63–70. doi: 10.1016/0169-328x(94)90185-6

Peleg, S., Sananbenesi, F., Zovoilis, A., Burkhardt, S., Bahari-Javan, S., Agis-Balboa, R. C., et al. (2010). Altered histone acetylation is associated with age-dependent memory impairment in mice. *Science* 328, 753–756. doi: 10.1126/science.1186088

Petrij, F., Giles, R. H., Dauwerse, H. G., Saris, J. J., Hennekam, R. C., Masuno, M., et al. (1995). Rubinstein-Taybi syndrome caused by mutations in the transcriptional co-activator CBP. *Nature* 376, 348–351. doi: 10.1038/376348a0

Ravi, B., and Kannan, M. (2013). Epigenetics in the nervous system: an overview of its essential role. *Indian J. Hum. Genet.* 19, 383–391. doi: 10.4103/0971-6866.124357

Ricobaraza, A., Cuadrado-Tejedor, M., Pérez-Mediavilla, A., Frechilla, D., Del Río, J., and García-Osta, A. (2009). Phenylbutyrate ameliorates cognitive deficit and reduces tau pathology in an Alzheimer's disease mouse model. *Neuropsychopharmacology* 34, 1721–1732. doi: 10.1038/npp.2008.229

Rosczyk, H. A., Sparkman, N. L., and Johnson, R. W. (2008). Neuroinflammation and cognitive function in aged mice following minor surgery. *Exp. Gerontol.* 43, 840–846. doi: 10.1016/j.exger.2008.06.004

Terrando, N., Brzezinski, M., Degos, V., Eriksson, L. I., Kramer, J. H., Leung, J. M., et al. (2011). Perioperative cognitive decline in the aging population. *Mayo Clin. Proc.* 86, 885–893. doi: 10.4065/mcp.2011.0332

Vacas, S., Degos, V., Feng, X., and Maze, M. (2013). The neuroinflammatory response of postoperative cognitive decline. *Br. Med. Bull.* 106, 161–178. doi: 10.1093/bmb/ldt006

Wan, Y., Xu, J., Ma, D., Zeng, Y., Cibelli, M., and Maze, M. (2007). Postoperative impairment of cognitive function in rats: a possible role for cytokine-mediated inflammation in the hippocampus. *Anesthesiology* 106, 436–443. doi: 10.1097/00000542-200703000-00007

Wang, Y., Chen, Z., Zhao, Y., Shi, R., Wang, Y., Xu, J., et al. (2013). Epigenetics as a new therapeutic target for postoperative cognitive dysfunction. *Med. Hypotheses* 80, 249–251. doi: 10.1016/j.mehy.2012.11.041

Xu, Z., Dong, Y., Wang, H., Culley, D. J., Marcantonio, E. R., Crosby, G., et al. (2014). Age-dependent postoperative cognitive impairment and Alzheimer-related neuropathology in mice. *Sci. Rep.* 4:3766. doi: 10.1038/srep03766

Zhao, X., Rosenke, R., Kronemann, D., Brim, B., Das, S. R., Dunah, A. W., et al. (2009). The effects of aging on N-methyl-D-aspartate receptor subunits in the synaptic membrane and relationships to long-term spatial memory. *Neuroscience* 162, 933–945. doi: 10.1016/j.neuroscience.2009.05.018

Zhong, T., Qing, Q. J., Yang, Y., Zou, W. Y., Ye, Z., Yan, J. Q., et al. (2014). Repression of contexual fear memory induced by isoflurane is accompanied by reduction in histone acetylation and rescued by sodium butyrate. *Br. J. Anaesth.* 113, 634–643. doi: 10.1093/bja/aeu184

Conflict of Interest Statement: The authors declare that the research was conducted in the absence of any commercial or financial relationships that could be construed as a potential conflict of interest.

frontiers in Molecular Neuroscience

ORIGINAL RESEARCH
published: 09 February 2016
doi: 10.3389/fnmol.2016.00011

Characterization of a Novel Chromatin Sorting Tool Reveals Importance of Histone Variant H3.3 in Contextual Fear Memory and Motor Learning

*Anna G. McNally[1†], Shane G. Poplawski[1†], Brittany A. Mayweather[2], Kyle M. White[2] and Ted Abel[2]**

[1] Pharmacology Graduate Group, University of Pennsylvania, Philadelphia, PA, USA, [2] Department of Biology, University of Pennsylvania, Philadelphia, PA, USA

The consolidation of short-term labile memories for long-term storage requires transcription and there is growing interest in defining the epigenetic mechanisms regulating these transcriptional events. In particular, it has been hypothesized that combinations of histone post-translational modifications (PTMs) have the potential to store memory by dynamically defining the transcriptional status of any given gene loci. Studying epigenetic phenomena during long-term memory consolidation, however, is complicated by the complex cellular heterogeneity of the brain, in which epigenetic signal from memory-relevant cells can be obscured or diluted by the surrounding milieu. To address this issue, we have developed a transgenic mouse line expressing a tetO-regulated, hemagglutinin (HA)-tagged histone H3.3 exclusively in excitatory neurons of the forebrain. Unlike canonical histones, histone H3.3 is incorporated at promoter regions of transcriptionally active genes in a DNA replication-independent manner, stably "barcoding" active regions of the genome in post-mitotic cells. Immunoprecipitating H3.3-HA containing nucleosomes from the hippocampus will therefore enrich for memory-relevant chromatin by isolating actively transcribed regions of the excitatory neuron genome. To evaluate the validity of using H3.3 "barcoding" to sort chromatin, we performed a molecular and behavioral characterization of the H3.3-HA transgenic mouse line. Expectedly, we find that H3.3-HA is incorporated preferentially at promoter regions of actively-transcribed neuronal genes and that expression can be effectively regulated by doxycycline. Additionally, H3.3-HA overexpression does not adversely affect exploratory or anxiety-related behaviors, nor does it affect spatial memory. Transgenic animals do, however, exhibit deficits in contextual memory and motor learning, revealing the importance of this histone isoform in the brain. Future studies in the H3.3-HA transgenic mouse line will define the combinatorial histone PTM landscape during spatial memory consolidation and will investigate the important contributions of histone H3.3 to the normal functioning of the brain.

Keywords: histone variant, epigenetics, excitatory neuron, hippocampus, memory consolidation

OPEN ACCESS

Edited by:
Benedict C. Albensi, University of Manitoba, Canada

Reviewed by:
John J. Woodward, Medical University of South Carolina, USA
Hyunsoo S. Je, Duke-National University of Singapore Graduate Medical School, Singapore

****Correspondence:***
Ted Abel
abele@sas.upenn.edu

[†]These authors have contributed equally to this work.

Received: *09 December 2015*
Accepted: *25 January 2016*
Published: *09 February 2016*

Citation:
McNally AG, Poplawski SG, Mayweather BA, White KM and Abel T (2016) Characterization of a Novel Chromatin Sorting Tool Reveals Importance of Histone Variant H3.3 in Contextual Fear Memory and Motor Learning. Front. Mol. Neurosci. 9:11. doi: 10.3389/fnmol.2016.00011

INTRODUCTION

It is a fundamental goal in neuroscience to understand the mechanisms that regulate the formation of long-term memory. Short-term labile memories are consolidated for long-term storage through a transcription-dependent process known as memory consolidation (Agranoff et al., 1967; Nguyen et al., 1994). Although the requirement for transcription to stabilize short-term memories was demonstrated decades ago, the epigenetic processes regulating this transcription are only beginning to be uncovered. Histone post-translational modifications, or PTMs, are one such epigenetic phenomenon thought to be critical to the regulation of gene expression during long-term memory consolidation. Indeed, many modifications correlate with transcriptional level (Wang et al., 2008). Notably, histone acetylation contributes to an active transcriptional state and is critical for both long-term memory and pharmacological memory enhancement (Levenson et al., 2004; Vecsey et al., 2007; Bousiges et al., 2010; Peleg et al., 2010; Park et al., 2013; Dagnas et al., 2015).

While significant advances have been made in understanding the contributions of individual histone PTMs to long-term memory, current models postulate that histone acetylation and other PTMs function in a combinatorial fashion to dynamically regulate gene expression through alterations in chromatin accessibility and guiding the association of chromatin-binding proteins to specific genetic loci (Jenuwein and Allis, 2001; Berger, 2007). Identifying changes in the histone PTM landscape within the brain, however, is complicated by the presence of a complex cellular milieu. Long-term memory is thought to depend critically on transcriptional changes within excitatory neurons, yet epigenetic signal occurring within these cells will likely be obscured or diluted by surrounding cell types (Kauer et al., 1988; Tocco et al., 1991). Currently, few tools exist to study chromatin from within specific cellular populations. Fluorescence-activated cell sorting (FACS) is perhaps the most widely used sorting approach, but this technique is labor-intensive and has the potential to disrupt chromatin dynamics and gene expression (Jiang et al., 2008). There is therefore a substantial need for a simple approach which can be adapted to multiple cell types.

For these reasons, we have developed a transgenic mouse line expressing a tetO-regulated hemagglutinin (HA)-tagged histone variant, known as H3.3, specifically within excitatory neurons of the forebrain. Unlike canonical histones, histone H3.3 is incorporated at promoters of transcriptionally active genes in a DNA replication-independent manner, effectively "barcoding" active regions of the genome (Ahmad and Henikoff, 2002; Chow et al., 2005; Mito et al., 2005; Daury et al., 2006; Hake and Allis, 2006). By combining the tetO-regulated tagged histone with the tetracycline transactivator system, we can control both the temporal and spatial regulation of transgene expression. Here, we employ the CaMKIIα-tTA driver line to express the tagged histone H3.3 specifically in excitatory forebrain neurons, and limit its expression to adulthood by administering doxycycline in the diet (Mayford et al., 1996). Chromatin immunoprecipitation (ChIP) for the HA tag can then isolate nucleosomes bound to active regions of the excitatory neuron genome, greatly enriching for those regions most likely to be altered during long-term memory consolidation. Mass spectrometry could then be employed to define the histone PTM landscape occurring in response to learning (Young et al., 2009; Britton et al., 2011). In the current study, we perform a molecular and behavioral characterization of the H3.3-HA transgenic mouse line to evaluate the validity of this chromatin sorting approach.

MATERIALS AND METHODS

Subjects

To create tetO-H3.3-HA mice, a mouse-codon optimized N-terminal tagged H3.3-HA sequence from GeneArt (Thermo Fisher Scientific) was cloned into the MM400 plasmid containing the tetO tetracycline-regulatable enhancer element, as previously described (Hawk et al., 2012). The plasmid was digested using Not1 (New England Biolabs #R0189S) and the 2.5-kb tetO-H3.3-HA transgene fragment was sequenced to ensure complete sequence accuracy. The gel-purified transgene was submitted to the Transgenic and Chimeric Mouse Facility at the University of Pennsylvania, where it was injected into C57BL/6J pronuclei. Mice were genotyped by Southern Blotting using transgene-specific primers (F: GCGTCCATCTGGTCAGAAA, R: TGGAATCTCAGGTCGGTCTT). Four founder lines were generated and crossed with C57BL/6J mice expressing the CaMKIIα-tTA transgene (Mayford et al., 1996). Double-transgenic males (CaMKIIα-tTA+; tetO-H3.3-HA+) from the highest expressing line were chosen for active breeding to C57BL/6J females (The Jackson Laboratory). Non-transgenic and single-transgenic littermates served as wildtype controls. Mice were bred and raised on doxycycline chow until weaning (unless otherwise noted) to restrict transgene expression to adulthood.

Adult transgenic and control mice were group housed on a 12:12 light:dark cycle, with food and water access *ad libitum*. Behavioral experiments were conducted during the light cycle between 7 and 10 am. All experiments were approved by the Institution of Animal Care and Use Committee of the University of Pennsylvania and conducted in accordance with the National Institutes of Health guidelines.

Immunostaining

Anesthetized double-transgenic and wildtype littermates were transcardially perfused with 4% PFA using a peristaltic perfusion pump (Rainin Instruments). Thirty micrometer (30 μM) coronal sections were then collected in PBS, permeabilized in 0.1% Triton X-100 for 5 min, quenched in 1% H_2O_2 for 15 min, and blocked in 8% normal goat serum (NGS) containing 0.3% Triton X-100 for 50 min at RT. The following incubation steps were then performed with intervening PBS washes (3 × 5 min each): HA antibody (1:500, Roche Clone 3F10) in 2% NGS and 0.3% Triton X-100 overnight at 4°C, biotinylated goat anti-rat antibody (1:1000, Jackson ImmunoResearch #112-065-003) in PBST for

2 h at RT, Vectastain ABC solution (Vector Laboratories #PK-4000) for 1.5 h at RT, DAB solution (0.2 mg/ml) containing 0.005% H_2O_2 for 20 min at RT. Sections were then washed in PBS containing 0.01% sodium azide and mounted in 0.7% gelatin. Mounted sections were counterstained with 0.1% cresyl violet acetate (where indicated), coverslipped, and visualized through a light microscope.

For immunofluorescence staining, 30 μM sections were permeabilized and blocked as before and then incubated at 4°C overnight using the following primary antibodies: HA (1:500, Roche Clone 3F10), CaMKIIα (1:1000, Santa Cruz #sc-32288), Gfap alexafluor 488-conjugated (1:1000, Millipore #MAB3402X), and Pvalb (1:1000, Abcam #ab11427). Sections were then washed in PBS followed by the addition of DAPI (Thermo Fisher Scientific #R37605) and the respective secondary antibody: goat anti-rat Alexa Fluor 555 for HA (1:1000, Invitrogen #A-21434), goat anti-mouse Alexa Fluor 488 for CaMKIIα (1:000, Invitrogen #A-11001), and goat anti-rabbit Alexa Fluor 488 for Pvalb (1:1000, Invitrogen #A-11034). Sections were incubated in the dark for 2 h at RT, washed in PBS, mounted, dried overnight at 4°C, and coverslipped using PermaFluor Mounting Medium (Thermo Fisher Scientific #TA-030-FM). Images were collected using a Leica Widefield Microscope.

Chromatin Immunoprecipitation (ChIP)

Hippocampi were dissected from double- and single- transgenic mice and finely cut using a razor blade. Fragments were incubated in 2% PFA for 10 min at RT, followed by the addition of 100 μl 1M glycine to quench the reaction. ChIP was performed as previously described (Vecsey et al., 2007). Briefly, tissue was dounce homogenized and the nuclei lysed. Chromatin was then sheared using a Bioruptor (Diagenode) with two 15-min cycles of 1 min on and 1.5 min off. IP samples were incubated with 2 μg HA antibody (Roche Clone 3F10) at 4°C overnight. The following day, samples were incubated in a 50% slurry of Protein G Agarose beads (Pierce #20398) for 2 h at 4°C. Beads were washed in low salt buffer, high salt buffer, LiCl buffer, and twice in 1X TE buffer. DNA was then eluted at RT in 200 μl ChIP elution buffer (1% SDS/0.1M $NaHCO_3$). IP and input control samples were reverse-crosslinked at 65°C overnight in 200 mM NaCl, followed by treatment with proteinase K for 1 h at 55°C. DNA was purified using the Qiagen Qiaquick PCR Purification Kit and eluted in 200 μl water.

Quantitative RT-PCR (qPCR)

Reactions were performed in 384 well plates using the Viia7 Real Time PCR System (Applied Biosystems). Reactions consisted of 2.5 μl Fast SYBR Green Master Mix (Thermo Fisher Scientific #4385614), 0.25 μl 5 μM primer mix, and 2.25 μl ChIP or input DNA, performed in quadruplicate. The following primers were used (5′ to 3′): *Nr4a1* (F: GGAGCCTAGTGGGTCTGGAAGC, R: GGAGCGCGGATTGTTTGATCT), *Nr4a2* (F: GGGCTTGG GGGCGATGGTTC, R: AGGATCCGGCAACAGGTGCG), *Nr4a3* (F: GAGGGAGGAGGAGGGTGACGTA, R: CATAGAG TGCCTGGAATGCGAGA), *Snap25* (F: AGCCCCGGGCAA ACAACTCG, R: TTGGGTTTGCAGGGCTAGGGC), *Gfap* (F: GCTGTTCCCTCGGCCCTCTCT, R: CACCAGCCTGGCTT CGCCAT), *Olig2* (F: AGGGAGTGGGGGCCTTCTGC, R: CC TCCTGTTTCCCGCTGCCG), *Apcs* (F: AGACCCAGCTGCA GAATGGAGA, R: TGCTGGGAAGGGAAGAGCTGC), *Fgb* (F: ACGAGACCTCCGAGACAGGGC, R: TGTGGACACAGG GGGTTCCTCG), *Line1* (F: AACGAGGAGTTGGTTCTTTG AG, R: TTTGTCCCTGTGCCCTTTAGTGA), *Snap25 5′ UTR* (F: CAGCAGCCTCCATGCCCCAC, R: CTGAGCTCCCGC CATCGCAC), *Snap25 3′ UTR* (F: ACGCATGCTCAGTATTGG GACACT, R: ACACAGCTGCAGGTTTTGCTGGT), *Snap25 TES* (F: TCACACCAGAAAACACAGTCTGCAT, R: ACCA AGCCAAAGTGTCCATTGTCAT), *Nr4a1 Exon1* (F: TCTG GACGCACCCGTGACCT, R: CCCTCGCTGCCACCTGAA GC), *Nr4a1 TES* (F: GGACAGCGGCTAACCCAGGGA. R: ACCTGAGACCCAAGGCCAGGTC). Data were normalized as percent input and to repeat element *Line1*. Fold change of double- to single-transgenic mice was determined and fold changes were compared using unpaired *t*-tests, with two-tailed *p* values reported.

Behavioral Procedures

Two cohorts of double-transgenic and wildtype male mice (aged 3–4 months) were used for behavioral testing, with two additional cohorts kept continuously on doxycycline (Bio-Serv, 40 mg/kg) for behavioral rescue experiments. Wildtype mice included both single-transgenic and non-transgenic littermates. The behavioral tasks were performed in the following order with at least 1 week recovery between tasks: Rotarod, open field, object location memory (OLM), and contextual fear conditioning. Weights were recorded in male mice prior to the rotarod task. Mice were group housed until 1 week prior to contextual fear training, at which point animals were housed individually. Female mice (aged 3–4 months) were evaluated in rotarod, open field, and contextual fear conditioning.

Rotarod

The rotarod apparatus contains a rotating rod (3 cm diameter) raised 16 cm above a platform, divided into five sections. The rotarod task was performed as previously described (Oliveira et al., 2006). Briefly, on habituation day, mice were placed on the rod rotating at 4 RPM for 30 s. The following three consecutive days consisted of testing trials, where mice underwent three 5 min trials per day, with an inter-trial interval of 1 h. During testing trials, the rotarod gradually accelerated from 4 to 40 RPM over the course of 5 min. Latency to fail was recorded, with failure defined as falling off or passively gripping onto the rod. A repeated measures ANOVA was used to compare latencies to fail across testing sessions. Bonferroni correction was used to adjust for multiple comparisons.

Open Field

Locomotor activity was measured for 30 min in a 41 × 41 cm Open Field (San Diego Instruments). The box was equipped with a 16 × 16 photobeam configuration, spaced every 2.54 cm. Total ambulation and preference for the periphery vs. the center of the

open field were measured by number of beam breaks (Stein et al., 2006) and group means were compared across genotypes using unpaired *t*-tests, with two-tailed *p* values reported.

Object Location Memory (OLM)

Mice were handled in the experimental setting for five consecutive days (5 min/mouse) prior to OLM training. Training and testing were performed as previously described (Havekes et al., 2014) and both began at lights on (7 am). On training day, mice were placed individually into the training arena which contained an internal visual cue on one of the four walls. Mice underwent a total of four 6 min sessions, with an intersession interval of 3 min in the home cage. The first session consisted of habituation to the empty arena, while the following three sessions contained three distinct objects (a glass bottle, metal tower, and plastic cylinder). Arenas and objects were wiped down between all sessions with 70% ethanol. Twenty-four hours following training, mice were re-exposed to the arena for 6 min, with one object displaced to a novel spatial location. Training and testing sessions were video monitored and object exploration times were scored off-line by an experimenter blind to genotype. OLM was assessed by calculating the percent preference for the displaced object relative to all objects (DO/(DO + NDO) during testing. A two-way ANOVA was used to compare training and testing means, with Tukey's *post hoc* analysis performed where indicated. A repeated measures ANOVA was used to compare exploration time across the three training sessions. Bonferroni correction was used to adjust for multiple comparisons.

Contextual Fear Conditioning

Individually housed double-transgenic and wildtype mice were handled for three consecutive days (1 min/mouse) prior to contextual fear training. Handling occurred in the same experimental setting without context exposure. Training and testing were performed as previously described (Wood et al., 2006; Vecsey et al., 2007; Hawk et al., 2012). The training session entailed a single 2 s, 1.5 mA foot shock, terminating 2.5 min after placement of the mouse in the chamber (Med-Associates, 31.8 × 25.4 × 26.7 cm). The mouse remained in the chamber for an additional 30 s and was then returned to the homecage. A 5 min test session was conducted 24 h following training where the mouse was re-exposed to the context in the absence of a footshock. Freezing behavior was measured during all sessions using automated scoring software (Clever Systems). Multiple unpaired *t*-tests were used to compare pre-shock and 24 h test freezing levels between genotypes, with multiple comparison adjustments made using the Holm-Sidak method.

Statistical Analyses

All data are presented as mean ± SEM and analyzed using GraphPad Prism 6 software. Comparisons were made using unpaired *t*-tests, two-way ANOVA, or two-way repeated measures ANOVA, as indicated. *Post hoc* tests were used where appropriate. For all statistical tests, $p < 0.05$ was considered significant.

RESULTS

Novel Sorting Strategy for the Isolation of Active Chromatin from Excitatory Neurons

In this study, founder lines expressing a tetO-regulated HA-tagged histone H3.3 in C57BL/6J mice were generated and crossed with an excitatory neuron-specific tetracycline transactivator (tTA) line, CaMKIIα-tTA (Mayford et al., 1996) to produce double-transgenic mice (**Figure 1A**). Histone variant H3.3 was selected because it is known to incorporate at promoters of transcriptionally active genes in a DNA replication-independent manner, effectively "barcoding" active regions of the genome (Hake and Allis, 2006). By combining tagged H3.3 with the tetracycline-transactivator system, standard chromatin immunoprecipitation methodologies can be employed to enrich for active regions of the excitatory neuron genome in the mouse hippocampus during behavioral tasks.

H3.3-HA Expression is Restricted to Excitatory Neurons of the Forebrain

The first step in validating the feasibility of this approach was to demonstrate the expected expression patterns of H3.3-HA. As anticipated, immunostaining for the HA tag in double-transgenic and wildtype littermates revealed pronounced expression of H3.3-HA in areas of the forebrain, including the hippocampus, striatum, and cortex, with no expression observed in the cerebellum (**Figure 1B**). Exploiting one of the key advantages of the tetracycline transactivator system, we next wanted to determine if transgene expression could be controlled through the administration of doxycycline in the diet (Bio-Serv, 40 mg/kg). Indeed, mice removed from doxycycline at weaning (postnatal day 28) showed marked H3.3-HA expression at postnatal day 60, particularly in the dentate gyrus (**Figure 1C**). In contrast, mice that remained on a doxycycline diet showed no transgene expression. Restricting transgene expression to adulthood in this way avoided potentially confounding effects of H3.3-HA overexpression on development.

Finally, we wanted to demonstrate that H3.3-HA expression was specific to excitatory neurons expressing CaMKIIα in the hippocampus. Using immunofluorescent staining to compare the overlay of the HA tag and DAPI counterstain with CaMKIIα, Gfap (astrocyte marker), and Pvalb (inhibitory neuron marker), we found that H3.3-HA colocalized exclusively with excitatory neurons, and was not expressed in glia or inhibitory neurons (**Figure 1D**). Colocalization was nearly complete in the dentate gyrus, particularly within the subgranular zone (**Figure 1D**). Together, these findings suggest that ChIP of the HA tag from hippocampal tissue should selectively isolate only chromatin from excitatory neurons.

Chromatin Immunoprecipitation of H3.3-HA Isolates Active Regions of the Excitatory Neuron Genome

Based on the known incorporation of histone variant H3.3 into regions of active transcription, we expected that ChIP of

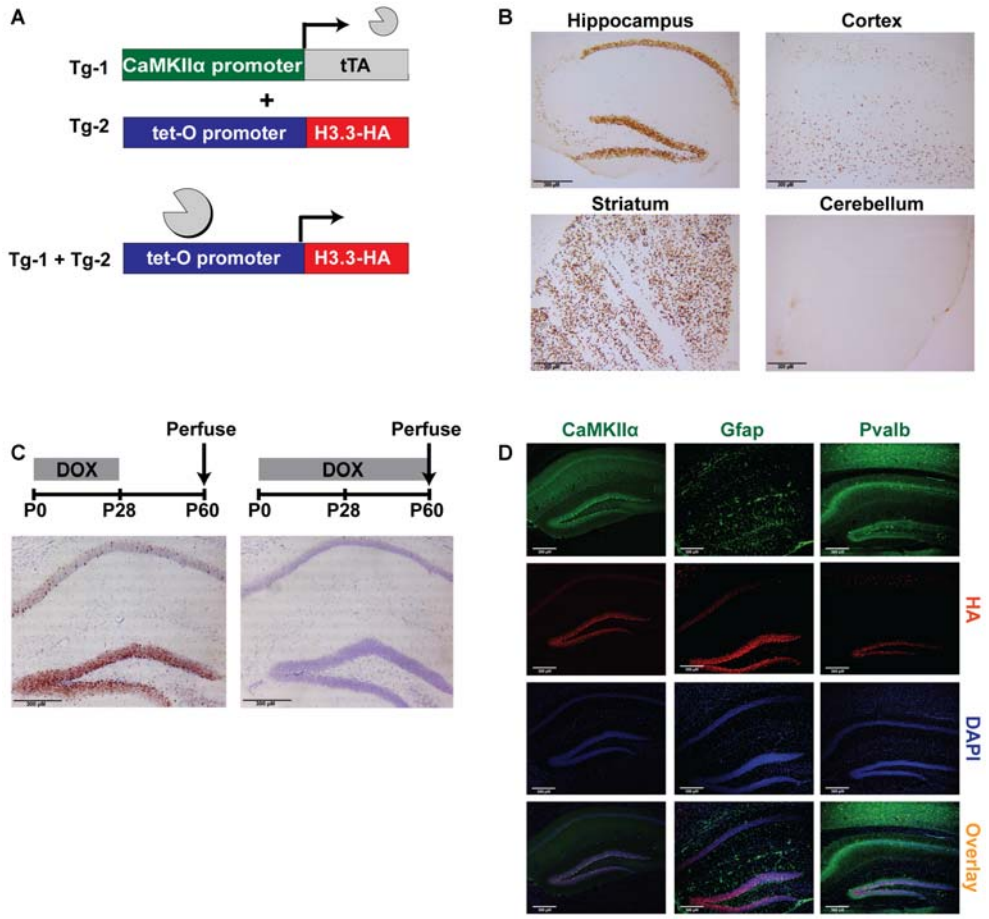

FIGURE 1 | Tagging histone H3.3 in excitatory neurons of the forebrain as a novel epigenetic tool to sort chromatin. (A) CaMKIIα-tTA transgene was used to drive expression of the tetO-regulated HA-tagged histone H3.3 exclusively in excitatory neurons of the forebrain. **(B)** In double-transgenic mice, DAB staining for the HA tag revealed robust expression of H3.3-HA in the hippocampus, striatum, and cortex, but not in the cerebellum. **(C)** Double-transgenic mice removed from a doxycycline diet at weaning displayed high expression of H3.3-HA (brown), while mice receiving continuous doxycycline showed no expression. Cresyl violet was used as a counterstain. **(D)** Hippocampal immunofluorescent staining divided into green channel (1st panel), red channel (2nd panel), blue channel (3rd panel) and overlay (4th panel). H3.3-HA colocalizes exclusively with excitatory neuron marker CaMKIIα, and not astrocyte marker Gfap, or inhibitory neuron marker Pvalb. (CaMKIIα = Ca^{2+}/calmodulin-dependent protein kinase II; Gfap = glial fibrillary acidic protein; Pvalb = parvalbumin).

the HA tag would enrich for genomic regions that are actively transcribed in excitatory neurons. Indeed, immunoprecipitating chromatin containing H3.3-HA from whole hippocampi showed enrichment for promoters of genes expressed in excitatory neurons (*Nr4a1, Nr4a2, Nr4a3, Snap25*), over genes expressed specifically in glial (*Gfap, Olig2*) or liver cells (*Apcs, Fgb*; **Figure 2A**). The nuclear receptor 4a (*nr4a*) family of transcription factors are activity-dependent CREB target genes that are critical effectors of long-term memory (Bridi and Abel, 2013). Synaptosomal-associated protein 25 (*snap25*) is a neuron-specific SNARE protein that mediates synaptic vesicle membrane docking and fusion (Oyler et al., 1989). Enrichment at non-neuronal genes was evaluated using astrocyte-specific gene, glial fribrillary acidic protein (*gfap*), a key mediator of astrocyte-neuron interactions, and oligodendrocyte-specific gene, oligodendrocyte lineage transcription factor 2 (*olig2*), a transcription factor required for oligodendrocyte determination (Weinstein et al., 1991; Brenner et al., 1994; Takebayashi et al., 2002). Two liver-specific genes were used as controls, serum amyloid P component (*apcs*) and fibrinogen beta chain (*fgb*), as these genes are not expressed in the brain (Peixoto et al., 2015).

Additionally, because H3.3 has exhibited promoter bias in other systems (Chow et al., 2005), we next wanted to test if H3.3-HA was preferentially incorporated at promoters of neuronally-expressed genes as compared to gene bodies. Using primers specific to these regions in two neuronally expressed genes, we found that gene promoters had the highest proportion of H3.3-HA incorporation (**Figure 2B**). These data suggest that this sorting strategy will enrich for promoters of genes specifically expressed in excitatory neurons. This tool could therefore be useful not only for isolating active regions of the excitatory neuron genome, but also for studying the incorporation of H3.3 throughout the genome during

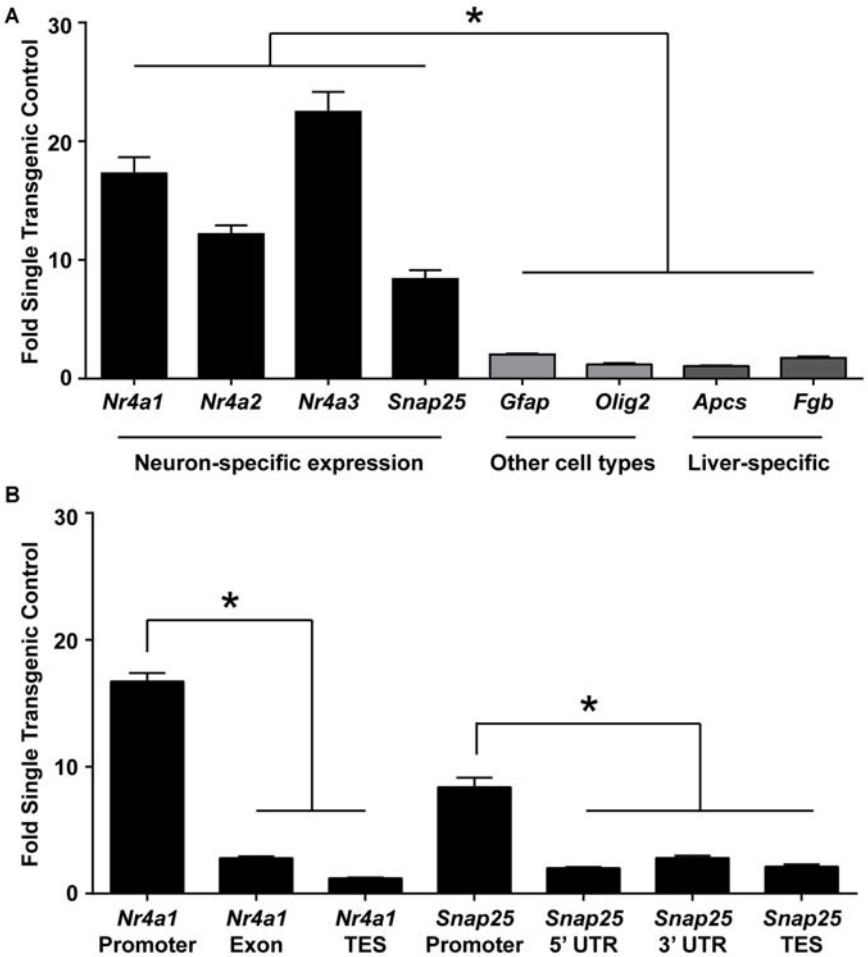

FIGURE 2 | ChIP for H3.3-HA enriches for promoters of genes active in excitatory neurons. (A) ChIP was performed for the HA tag of H3.3-HA from whole hippocampi and primers against promoters of neuron-, astrocyte-, oligodendrocyte-, and liver- specific genes were evaluated. Neuronally-expressed genes were significantly more enriched over genes expressed in other cell types. **(B)** Primers were selected throughout two neuronally expressed genes. Enrichment was biased toward the promoter of both genes tested as compared to transcription end sites (TES) and untranslated regions (UTR). Data are presented as mean fold enrichment over single-transgenic controls ± SEM (n = 3 per group). *$p < 0.05$. (*nr4a* = nuclear receptor 4a; *snap25* = synaptosomal-associated protein 25 kda; *olig2* = oligodendrocyte transcription factor 2; *apcs* = amyloid P component, serum; *fgb* = fibrinogen beta chain).

learning; a currently nascent area of research (Maze et al., 2015).

Overexpression of H3.3-HA in Excitatory Neurons of the Forebrain does not Affect Exploration, Anxiety-Related Behavior, or Spatial Memory

An important next step in the characterization of this novel tool was to test the performance of these animals in a battery of behavioral tasks, as abnormalities in specific behaviors have been observed in other overexpressing tagged histones (Ito et al., 2014). In the open field paradigm, mice are allowed to explore a novel, enclosed open field for 30 min, with locomotor activity assessed through the automatic scoring of beam breaks (Stein et al., 2006). No difference in total ambulation was detected between transgenic mice and their wildtype littermates (p = 0.195), indicating that exploratory behavior is unaffected by H3.3-HA overexpression (**Figure 3A**). This result was corroborated in female mice (p = 0.667). In comparing preference for the periphery of the open field vs. the center, both genotypes displayed a marked preference for the periphery of the open field, as expected, with no difference in percent center activity between genotypes (p = 0.494; **Figure 3B**). Percent center activity was similarly comparable between genotypes in female mice (p = 0.924). This indicates an absence of gross anxiety-related deficits in the double-transgenic animals.

This sorting tool was developed to study the epigenetic changes occurring in active regions of the excitatory neuron genome during long-term memory consolidation. Accordingly, we wanted to evaluate the performance of these animals in memory tasks. In the OLM task (OLM), mice explore an arena containing three distinct objects arranged in a specific

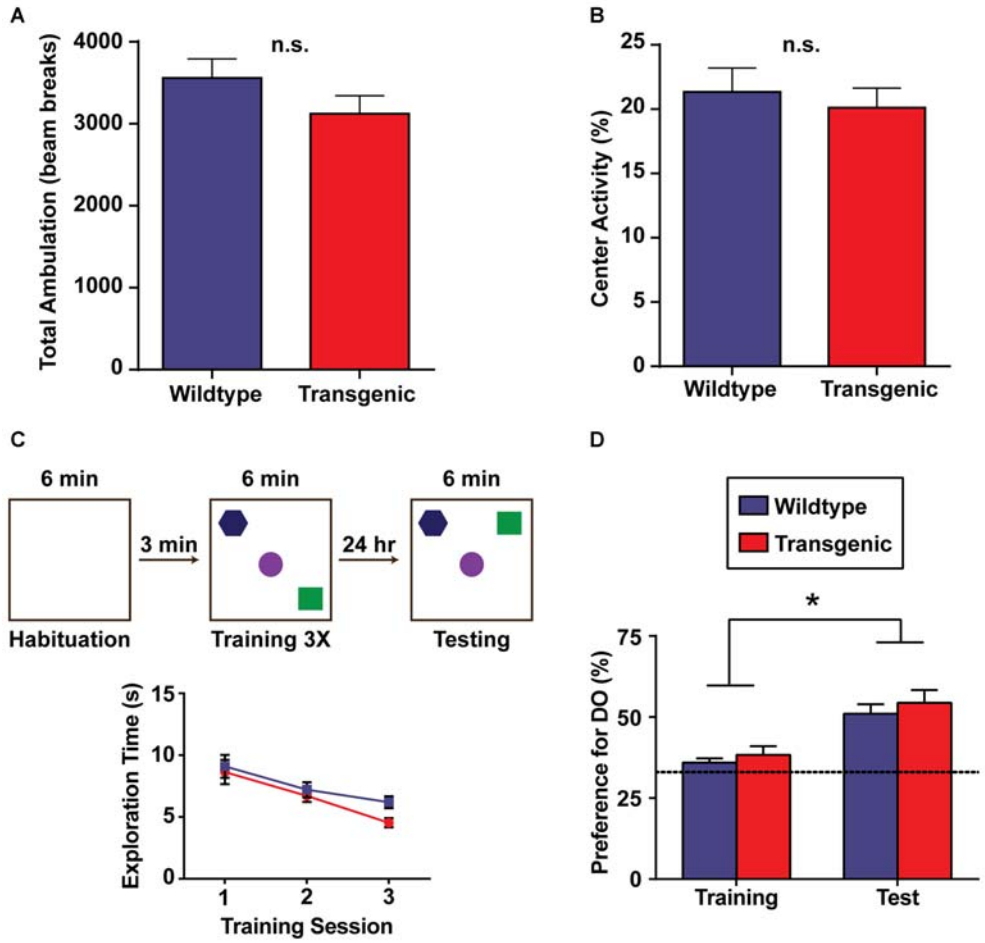

FIGURE 3 | Overexpression of H3.3-HA in excitatory neurons of the forebrain does not affect exploration, anxiety-related behavior, or spatial memory. **(A)** There was no difference in total ambulation (as measured by beam breaks) between genotypes across 30 min of exploration in an open field. **(B)** Double-transgenic and wildtype mice exhibited a comparable preference for the periphery of an open field vs. the center (n = 9–11 per group). **(C)** Schematic diagram illustrating the object-location memory (OLM) task during habituation (left), training (middle) and testing (right). Testing was performed 24 h after training. Both genotypes showed a decrease in total object exploration time during the three consecutive training sessions, as expected. **(D)** Double-transgenic and wildtype mice exhibited a comparable and significant preference for the displaced object during testing as compared to training, signifying long-term object-location memory. Preference for the displaced object was calculated as the percentage of object exploration time dedicated to this object as compared to all objects (DO/(DO + NDO). Dotted line indicates chance performance. Data are presented as group means ± SEM (n = 18 per group). *$p < 0.05$.

spatial orientation. The following day, mice are re-exposed to the same arena, but with one object displaced to a novel spatial location. Long-term spatial memory is then assessed by measuring the preference for the displaced object as compared to all objects at testing (Havekes et al., 2014). Across all three training sessions, both double-transgenic mice and their wildtype littermates showed a comparable decrease in total object exploration time ($F_{(2,68)}$ = 22.13, $p < 0.0001$), with no effect of genotype ($F_{(1,34)}$ = 1.36, $p = 0.25$) or a training session × genotype interaction observed ($F_{(2,68)}$ = 0.84, $p = 0.44$; **Figure 3C**). Both genotypes also displayed a significant preference for the displaced object during testing ($F_{(1,68)}$ = 29.64, $p < 0.0001$) as compared to training, indicating intact long-term spatial memory (**Figure 3D**). No effect of genotype ($F_{(1,68)}$ = 0.988, $p = 0.32$) or a session × genotype interaction was observed ($F_{(1,68)}$ = 0.031, $p = 0.86$).

Double-Transgenic Mice have Deficits in Contextual Fear Memory and Motor Learning

In contrast to OLM, the contextual fear conditioning task has the advantage of allowing for the precise temporal resolution of the molecular events occurring in the hippocampus during a learning event, as only a single training session is required to develop a robust contextual memory (Bourtchouladze et al., 1998). For this reason, contextual fear conditioning would be the preferred paradigm to use in conjunction with this novel chromatin sorting tool. In this task, long-term retention of a

context-shock association is evaluated by measuring freezing behavior (Wood et al., 2006; Vecsey et al., 2007; Hawk et al., 2012). Interestingly, while both double-transgenic and wildtype mice displayed a significant increase in freezing behavior at the 24 h test as compared to pre-shock freezing levels (t = 3.51, p = 0.001; t = 8.67, $p < 0.0001$, respectively), demonstrating the capacity for contextual learning, double-transgenic mice froze at significantly lower levels than their wildtype littermates at the 24 h test (t = 2.86, p = 0.007; **Figure 4A**). Similarly in females, both genotypes showed increased freezing behavior at the 24 h test as compared to pre-shock levels (t = 2.99, p = 0.008; t = 4.48, p = 0.002), with double-transgenic mice freezing at significantly lower levels than their wildtype littermates at the 24 h test (t = 3.83, p = 0.002).

In addition to memory tasks, we also wanted to evaluate motor learning using the rotarod task. In this task, mice are placed on a slowly-accelerating rod and latencies to fail are measured across three testing session (Oliveira et al., 2006). Prior to rotarod testing, body weights were evaluated. No difference was observed between double-transgenic and wildtype mice (p = 0.12). Both double-transgenic and wildtype mice exhibited a significant improvement in time spent on the rotating rod across testing sessions ($F_{(2,38)}$ = 28.34, $p < 0.0001$). Despite comparable latencies to fail on test day 1, double-transgenic mice had significantly lower latencies to fail on testing days 2 and 3 than their wildtype littermates ($F_{(1,19)}$ = 12.66, p = 0.0021), indicating deficits in motor learning. No effect of genotype × trial day interaction was observed ($F_{(2,38)}$ = 0.96, p = 0.39; **Figure 4B**). In female mice, both genotypes significantly improved in time spent on the rotating rod across trials (effect of trial $F_{(2,24)}$ = 16.46, $p < 0.0001$). In contrast to male mice, female double-transgenic mice had significantly lower latencies to fail only on testing day 1 (effect of genotype $F_{(1,12)}$ = 5.76, p = 0.0335. This may suggest deficits in motor coordination, as opposed to motor learning. No effect of genotype × trial interaction ($F_{(2,24)}$ = 2.39, p = NS) was observed.

Doxycycline Rescues Deficits in Contextual Fear Conditioning and Rotarod

To determine if the observed behavioral deficits were a direct result of H3.3-HA overexpression, or were simply an effect of transgene insertion, two cohorts of male double-transgenic and wildtype mice were kept continuously on doxycycline to suppress H3.3-HA expression. Despite the double-transgenic animals having significantly higher pre-shock freezing levels (t = 2.35, p = 0.027), both genotypes displayed significant increases in percent freezing at the 24 h test as compared to pre-shock levels (t = 6.35, $p < 0.0001$; t = 6.13, $p < 0.0001$, respectively), indicating a learned association between context and shock. Importantly, doxycycline fully rescued the deficits in freezing levels observed in the transgenic animals at the 24 h test (t = 1.31, p = 0.20), implicating H3.3-HA overexpression as driving impairments in contextual fear memory (**Figure 5A**).

We next wanted to test whether this rescue effect could be extended to the rotarod task. Indeed, across testing days, both genotypes exhibited a significant improvement in time spent on the rotating rod ($F_{(2,24)}$ = 10.28, p = 0.0006) with no effect of genotype ($F_{(1,12)}$ = 0.48, p = 0.50) or a genotype × trial day interaction ($F_{(2,24)}$ = 0.21, p = 0.81) observed (**Figure 5B**).

DISCUSSION

Despite significant advances in the field of neuroepigenetics, studying epigenetic phenomenon is complicated by the complex cellular heterogeneity of the brain. Currently, few tools exist to examine epigenetic regulation in specific cellular populations. Prior attempts to perform epigenetic analysis in a cell-type specific manner have used FACS, but this technique relies on

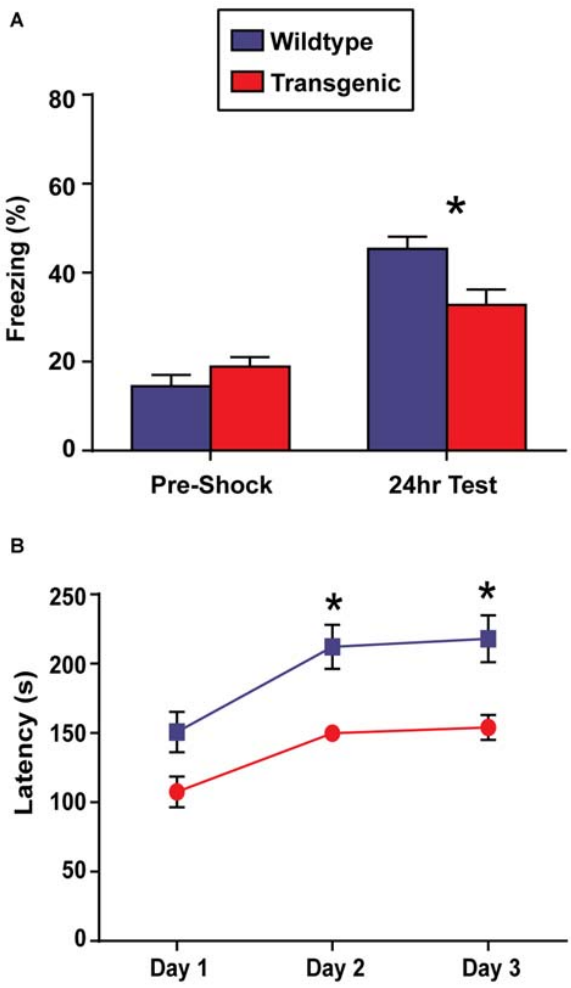

FIGURE 4 | Overexpression of H3.3-HA in excitatory neurons of the forebrain induces deficits in contextual fear memory and motor learning. (A) While both genotypes displayed significant increases in percent freezing at the 24 h test as compared to pre-shock levels, double-transgenic mice froze at significantly lower levels than their wildtype littermates at the 24 h test (n = 17–18 per group). **(B)** Across testing days, there was a significant improvement in time spent on the rotating rod for both genotypes. Despite comparable latencies to fail on testing day 1, double-transgenic mice displayed significantly lower latencies to fail on testing days 2 and 3, indicating deficits in motor learning. Data are presented as group means ± SEM (n = 10–11 per group). *$p < 0.05$.

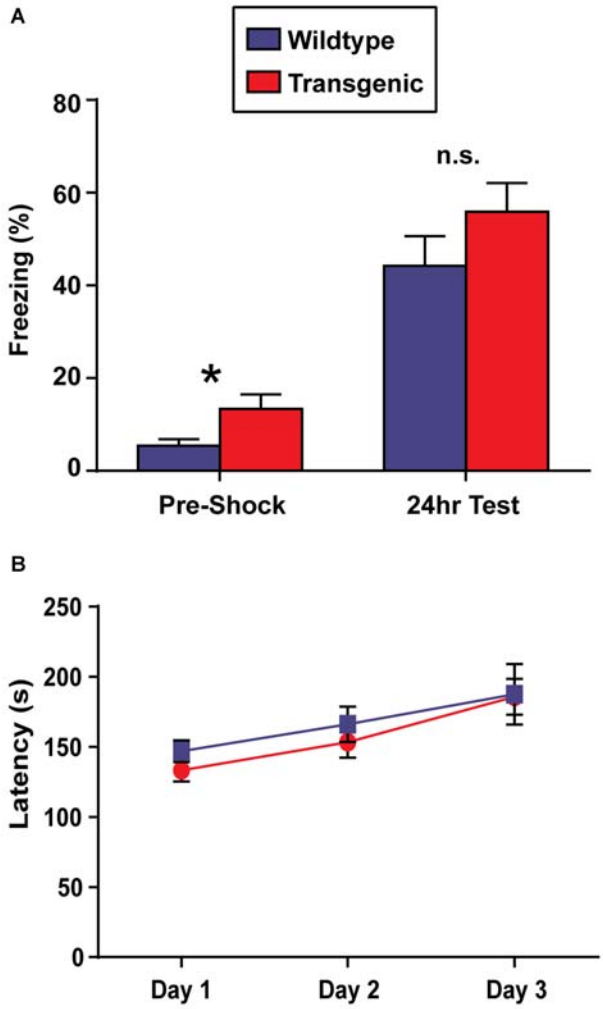

FIGURE 5 | Doxycycline rescues deficits in contextual fear memory and motor learning. (A) Both genotypes exhibited significant increases in percent freezing at the 24 h test as compared to pre-shock levels. There was no statistical difference in percent freezing at the 24 h test between genotypes (n = 13 per group). **(B)** Across testing days, both genotypes exhibited a significant improvement in time spent on the rotating rod, and performance was comparable on all days (n = 6–8 per group). Data are presented as group means ± SEM. *$p < 0.05$.

harsh separating techniques that have the potential to alter the epigenome (Jiang et al., 2008). In the present study, we employ a novel tool based on histone H3.3 "barcoding" to isolate actively transcribed regions of the excitatory neuron genome using standard ChIP protocols (Hake and Allis, 2006). We create transgenic mice that express the tagged histone exclusively in excitatory neurons of the forebrain in a doxycycline-regulatable manner. Importantly, we find that ChIP for H3.3-HA isolates promoters of genes active in excitatory neurons over genes expressed in other cell types, demonstrating that H3.3-HA is effectively marking active regions of the genome. In addition to a molecular characterization, we also evaluated the performance of the transgenic animals in several behavioral tasks, as genetic alterations in the brain have the potential to alter behavior (Leach et al., 2012; Cao et al., 2014; Ito et al., 2014). We find that H3.3-HA overexpression does not alter exploratory or anxiety-related phenotypes and does not interfere with long-term spatial memory. Transgene expression does, however, cause deficits in contextual memory and motor learning; effects that can be rescued by the continuous administration of doxycycline in the diet. Collectively, these findings establish the validity of employing histone "barcoding" to sort active regions of the excitatory neuron genome. We anticipate that this technique will be useful in studying the epigenome during spatial memory consolidation.

One often overlooked aspect in the characterization of new transgenic mouse lines is the effect of transgene expression on behavior. Indeed, there are many examples of unexpected consequences of transgene overexpression in the brain (Gong et al., 2011; Ito et al., 2014). By using behavioral tasks with known neural correlates, we can start to delineate which brain regions are most sensitive to H3.3-HA overexpression. Contextual fear conditioning is known to require both the amygdala and the hippocampus, while OLM is dependent on the hippocampus (Phillips and LeDoux, 1992; Haettig et al., 2011). The deficits observed in contextual fear conditioning, but not OLM, might therefore suggest impairments in amygdala functioning. This possibility could be evaluated by performing cued-fear conditioning, a memory task requiring the amygdala that is independent of the hippocampus (Phillips and LeDoux, 1992). Although previous work using a similar CaMKIIα–tTA driver line demonstrates robust transgene expression levels in both the hippocampus and the amygdala, an important future direction would be to confirm amygdala expression of H3.3-HA in the tetO-H3.3-HA animals (Mayford et al., 1996). In addition to deficits in contextual fear memory, these animals also displayed deficits in motor learning. The rotarod task is linked to cortical and striatal function, and future studies should thoroughly evaluate H3.3-HA expression in these regions as well (Costa et al., 2004; Dang et al., 2006). A possible strategy to mitigate behavioral deficits would be to restrict transgene expression to a shorter window by altering the timing of doxycycline treatment, as is done with the fos-tTA driver line (Reijmers et al., 2007). Alternatively, we could instead utilize the Cre-dependent, double-floxed inverted orientation system combined with CaMKIIα-Cre mice, to virally express H3.3-HA selectively in excitatory neurons (Schnütgen et al., 2003). This would allow for more precise spatial specificity, as virus injections can be restricted to the hippocampus, and would allow for a shorter duration of transgene expression (Havekes et al., 2014).

The tagged H3.3 transgenic line is the second example of a tagged histone overexpression system developed in mice (Ito et al., 2014). Previous work has employed the tetracycline transactivator system to express a GFP-tagged histone H2B specifically in excitatory neurons of the forebrain (Ito et al., 2014). The overexpression of H2B-GFP was shown to produce marked consequences on chromatin architecture, perhaps through the steric interference of compacted heterochromatin structures (Ito et al., 2014). These structural changes were associated with alterations in gene expression at specific genomic

loci as well as behavioral effects including hyperlocomotion, reduced nociception, and deficits in spatial memory and contextual- and cued-conditioning (Ito et al., 2014). Although it is unlikely that the nine amino acid HA tag would cause steric hindrance in a way that would dramatically alter chromatin architecture, it is possible that overexpression of H3.3-HA may cause chaperone dysregulation or alterations in baseline and activity-induced gene expression, both of which could contribute to the behavioral abnormalities observed here. These possibilities can be tested in future experiments using immunohistochemistry and qPCR-based methodologies.

There is growing interest in understanding the role of histone variant exchange in the brain and recently, the dynamic exchange of two histone variants in particular has been shown to contribute to long-term memory (Zovkic et al., 2014; Maze et al., 2015). Notably, histone variant H3.3 is dynamically deposited into the nucleosome in an activity-dependent fashion, helping to drive changes in gene expression required for synaptic connectivity and long-term memory (Michod et al., 2012; Maze et al., 2015). Because H3.3 is deposited in an activity-dependent fashion, this begs the question of whether a learning task may alter the localization of the tagged H3.3 in the genome. If this is the case, comparing changes in histone PTMs following learning may be confounded by differing genomic associations. This could be addressed by comparing ChIP-seq in transgenic animals after learning with control animals to define H3.3-HA localization across the genome. Additionally, ChIP-qPCR could be used in these mice to demonstrate "barcoding" of active regions of the genome following a learning event.

In summary, the tagged H3.3 transgenic mouse line provides a simple, adaptable tool to address the issue of cellular heterogeneity in neuroepigenetics. While excitatory neurons are a logical starting point for evaluating epigenetic changes during long-term memory consolidation, an advantage of using the tetracycline transactivator system is that it allows for substantial flexibility in terms of cellular specificity, as many cell-type specific tTA driver lines are available. Indeed, the tetO-H3.3-HA line could be combined with GFAP-tTA or fos-tTA lines to drive expression in astrocytes or recently-activated cells, respectively (Reijmers et al., 2007; Florian et al., 2011). In addition to its usefulness across cell types, we anticipate that this line could be employed to study the epigenome during spatial memory consolidation using the OLM task. Defining the changes in histone PTMs following learning is critical to understanding transcriptional regulation during long-term memory consolidation and may help to uncover novel epigenetic targets for future therapeutic benefit.

AUTHOR CONTRIBUTIONS

Transgenic mouse design by SGP and TA. Molecular characterization by AGM, SGP, and BAM. Behavioral studies conducted by AGM. Scoring of behavioral video by KMW. Data analysis and interpretation by AGM. Manuscript preparation by AM with editing by SGP, BAM, KMW, and TA.

FUNDING

This research was supported by NIH R21 MH102679 to TA. AGM and SGP acknowledge funding from the Pharmacology Graduate Group Training Grant T32 GM008076.

ACKNOWLEDGMENTS

We thank the UPenn Trangenic and Chimeric Mouse Facility for developing H3.3-overexpressing founder lines.

REFERENCES

Agranoff, B. W., Davis, R. E., Casola, L., and Lim, R. (1967). Actinomycin D blocks formation of memory of shock-avoidance in goldfish. *Science* 158, 1600–1601. doi: 10.1126/science.158.3808.1600

Ahmad, K., and Henikoff, S. (2002). The histone variant H3.3 marks active chromatin by replication-independent nucleosome assembly. *Mol. Cell* 9, 1191–1200. doi: 10.1016/s1097-2765(02)00542-7

Berger, S. (2007). The complex language of chromatin regulation during transcription. *Nature* 447, 407–412. doi: 10.1038/nature05915

Bourtchouladze, R., Abel, T., Berman, N., Gordon, R., Lapidus, K., and Kandel, E. R. (1998). Different training procedures recruit either one or two critical periods for contextual memory consolidation, each of which requires protein synthesis and PKA. *Learn. Mem.* 5, 365–374.

Bousiges, O., Vasconcelos, A. P., Neidl, R., Cosquer, B., Herbeaux, K., Panteleeva, I., et al. (2010). Spatial memory consolidation is associated with induction of several lysine-acetyltransferase (histone acetyltransferase) expression levels and H2B/H4 acetylation-dependent transcriptional events in the rat hippocampus. *Neuropsychopharmacology* 35, 2521–2537. doi: 10.1038/npp.2010.117

Brenner, M., Kisseberth, W. C., Su, Y., Besnard, F., and Messing, A. (1994). GFAP promoter directs astrocyte-specific expression in transgenic mice. *J. Neurosci.* 14, 1030–1037.

Bridi, M. S., and Abel, T. (2013). The NR4A orphan nuclear receptors mediate transcription-dependent hippocampal synaptic plasticity. *Neurobiol. Learn. Mem.* 105, 151–158. doi: 10.1016/j.nlm.2013.06.020

Britton, L. M., Gonzales-Cope, M., Zee, B. M., and Garcia, B. A. (2011). Breaking the histone code with quantitative mass spectrometry. *Expert Rev. Proteomics* 8, 631–643. doi: 10.1586/epr.11.47

Cao, L., Molina, J., Abad, C., Carmona-Mora, P., Cárdenas Oyarzo, A., Young, J. I., et al. (2014). Correct developmental expression level of Rai1 in forebrain neurons is required for control of body weight, activity levels and learning and memory. *Hum. Mol. Genet.* 23, 1771–1782. doi: 10.1093/hmg/ddt568

Chow, C. M., Georgiou, A., Szutorisz, H., Maia e Silva, A., Pombo, A., Barahona, I., et al. (2005). Variant histone H3.3 marks promoters of transcriptionally active genes during mammalian cell division. *EMBO Rep.* 6, 354–360. doi: 10.1038/sj.embor.7400366

Costa, R. M., Cohen, D., and Nicolelis, M. A. L. (2004). Differential corticostriatal plasticity during fast and slow motor skill learning in mice. *Curr. Biol.* 14, 1124–1134. doi: 10.1016/j.cub.2004.06.053

Dagnas, M., Micheau, J., Decorte, L., Beracochea, D., and Mons, N. (2015). Post-training, intrahippocampal HDAC inhibition differentially impacts neural circuits underlying spatial memory in adult and aged mice. *Hippocampus* 25, 827–837. doi: 10.1002/hipo.22406

Dang, M. T., Yokoi, F., Yin, H. H., Lovinger, D. M., Wang, Y., and Li, Y. (2006). Disrupted motor learning and long-term synaptic plasticity in mice lacking *NMDAR1* in the striatum. *Proc. Natl. Acad. Sci. U S A* 103, 15254–15259. doi: 10.1073/pnas.0601758103

Daury, L., Chailleux, C., Bonvallet, J., and Trouche, D. (2006). Histone H3.3 deposition at E2F-regulated genes is linked to transcription. *EMBO Rep.* 7, 66–71. doi: 10.1038/sj.embor.7400561

Florian, C., Vecsey, C. G., Halassa, M. M., Haydon, P. G., and Abel, T. (2011). Astrocyte-derived adenosine and A1 receptor activity contribute to sleep loss-induced deficits in hippocampal synaptic plasticity and memory in mice. *J. Neurosci.* 31, 6956–6962. doi: 10.1523/JNEUROSCI.5761-10.2011

Gong, P., Roseman, J., Fernandez, C. G., Vetrivel, K. S., Bindokas, V. P., Zitzow, L. A., et al. (2011). Transgenic neuronal overexpression reveals that stringently regulated p23 expression is critical for coordinated movement in mice. *Mol. Neurodegener.* 6:87. doi: 10.1186/1750-1326-6-87

Haettig, J., Stefanko, D. P., Multani, M. L., Figueroa, D. X., McQuown, S. C., and Wood, M. A. (2011). HDAC inhibition modulates hippocampus-dependent long-term memory for object location in a CBP-dependent manner. *Learn. Mem.* 18, 71–79. doi: 10.1101/lm.1986911

Hake, S. B., and Allis, C. D. (2006). Histone H3 variants and their potential role in indexing mammalian genomes: the "H3 barcode hypothesis". *Proc. Natl. Acad. Sci. U S A* 103, 6428–6435. doi: 10.1073/pnas.0600803103

Havekes, R., Bruinenberg, V. M., Tudor, J. C., Ferri, S. L., Baumann, A., Meerlo, P., et al. (2014). Transiently increasing cAMP levels selectively in hippocampal excitatory neurons during sleep deprivation prevents memory deficits caused by sleep loss. *J. Neurosci.* 34, 15715–15721. doi: 10.1523/JNEUROSCI.2403-14.2014

Hawk, J. D., Bookout, A. L., Poplawski, S. G., Bridi, M., Rao, A. J., Sulewski, M. E., et al. (2012). NR4A nuclear receptors support memory enhancement by histone deacetylase inhibitors. *J. Clin. Invest.* 122, 3593–3602. doi: 10.1172/JCI64145

Ito, S., Magalska, A., Alcaraz-Iborra, M., Lopez-Atalaya, J., Rovira, V., Contreras-Moreira, B., et al. (2014). Loss of neuronal 3D chromatin organization causes transcriptional and behavioural deficits related to serotonergic dysfunction. *Nat. Comm.* 5:4450. doi: 10.1038/ncomms5450

Jenuwein, T., and Allis, C. D. (2001). Translating the histone code. *Science* 293, 1074–1080. doi: 10.1126/science.1063127

Jiang, Y., Matevossian, A., Huang, H.-S., Straubhaar, J., and Akbarian, S. (2008). Isolation of neuronal chromatin from brain tissue. *BMC Neurosci.* 9:42. doi: 10.1186/1471-2202-9-42

Kauer, J. A., Malenka, R. C., and Nicoll, R. A. (1988). NMDA application potentiates synaptic transmission in the hippocampus. *Nature* 334, 250–252. doi: 10.1038/334250a0

Leach, P. T., Poplawski, S. G., Kenney, J. W., Hoffman, B., Lieberman, D. C., Abel, T., et al. (2012). Gadd45b knockout mice exhibit selective deficits in hippocampus-dependent long-term memory. *Learn. Mem.* 19, 319–324. doi: 10.1101/lm.024984.111

Levenson, J. M., O'Riordan, K. J., Brown, K. D., Trinh, M. A., Molfese, D. L., and Sweatt, J. D. (2004). Regulation of histone acetylation during memory formation in the hipocampus. *J. Biol. Chem.* 279, 40545–40559. doi: 10.1074/jbc.m402229200

Mayford, M., Bach, M. E., Huang, Y.-Y., Wang, L., Hawkins, R. D., and Kandel, E. R. (1996). Control of memory formation through regulated expression of a CaMKII transgene. *Science* 274, 1178–1683. doi: 10.1126/science.274.5293.1678

Maze, I., Wenderski, W., Noh, K.-M., Bagot, R. C., Tzavaras, N., Purushothaman, I., et al. (2015). Critical role of histone turnover in neuronal transcription and plasticity. *Neuron* 87, 77–94. doi: 10.1016/j.neuron.2015.06.014

Michod, D., Bartesaghi, S., Khelifi, A., Bellodi, C., Berliocchi, L., Nicotera, P., et al. (2012). Calcium-dependent dephosphoyrlation of the histone chaperone DAXX regulates H3.3 loading and transcription upon neuronal activation. *Neuron* 74, 122–135. doi: 10.1016/j.neuron.2012.02.021

Mito, Y., Henikoff, J., and Henikoff, S. (2005). Genome-scale profiling of histone H3.3 replacement patterns. *Nat. Genet.* 37, 1090–1097. doi: 10.1038/ng1637

Nguyen, P. V., Abel, T., and Kandel, E. R. (1994). Requirement of a critical period of transcription for induction of a late phase of LTP. *Science* 265, 1104–1107. doi: 10.1126/science.8066450

Oliveira, A. M. M., Abel, T., Brindle, P., and Wood, M. A. (2006). Differential role for CBP and p300 CREB-binding domain in motor skill learning. *Behav. Neurosci.* 120, 724–729. doi: 10.1037/0735-7044.120.3.724

Oyler, G. A., Higgins, G. A., Hart, R. A., Battenberg, E., Billingsley, M., Bloom, F. E., et al. (1989). The identification of a novel synaptosomal-associated protein, SNAP-25, differentially expressed by neuronal subpopulations. *J. Cell Biol.* 109, 3039–3052. doi: 10.1083/jcb.109.6.3039

Park, C. S., Rehrauer, H., and Mansuy, I. M. (2013). Genome-wide analysis of H4K5 acetylation associated with fear memory in mice. *BMC Genomics* 14:539. doi: 10.1186/1471-2164-14-539

Peixoto, L., Risso, D., Poplawski, S. G., Wimmer, M. E., Speed, T. P., Wood, M. A., et al. (2015). How data analysis affects power, reproducibility and biological insight of RNA-seq studies in complex datasets. *Nucleic Acids Res.* 43, 7664–7674. doi: 10.1093/nar/gkv736

Peleg, S., Sananbenesi, F., Zovoilis, A., Burkhardt, S., Bahari-Javan, S., Agis-Balboa, R. C., et al. (2010). Altered histone acetylation is associated with age-dependent memory impairment in mice. *Science* 328, 753–756. doi: 10.1126/science.1186088

Phillips, R. G., and LeDoux, J. E. (1992). Differential contribution of amygdala and hippocampus to cued and contextual fear conditioning. *Behav. Neurosci.* 106, 274–285. doi: 10.1037/0735-7044.106.2.274

Reijmers, L. G., Perkins, B. L., Matsuo, N., and Mayford, M. (2007). Localization of a stable neural correlate of associative memory. *Science* 317, 1230–1233. doi: 10.1126/science.1143839

Schnütgen, F., Doerflinger, N., Calléja, C., Wendling, O., Chambon, P., and Ghyselinck, N. B. (2003). A directional strategy for monitoring cre-mediated recombination at the cellular level in the mouse. *Nat. Biotechnol.* 21, 562–565. doi: 10.1038/nbt811

Stein, J. M., Bergman, W., Fang, Y., Davison, L., Brensinger, C., Robinson, M. B., et al. (2006). Behavioral and neurochemical alterations in mice lacking the RNA-binding protein translin. *J. Neurosci.* 28, 2184–2196. doi: 10.1523/jneurosci.4437-05.2006

Takebayashi, H., Nabeshima, Y., Yoshida, S., Chisaka, O., Ikenaka, K., and Nabeshima, Y. (2002). The basic helix-loop-helix factor olig2 is essential for the development of motorneuron and oligodendrocyte lineages. *Curr. Biol.* 12, 1157–1163. doi: 10.1016/s0960-9822(02)00926-0

Tocco, G., Devgan, K. K., Hauge, S. A., Weiss, C., Baudry, M., and Thompson, R. F. (1991). Classical conditioning selectively increases AMPA receptor binding in rabbit hippocampus. *Brain Res.* 559, 331–336. doi: 10.1016/0006-8993(91)90020-v

Vecsey, C. G., Hawk, J. D., Lattal, K. M., Stein, J. M., Fabian, S. A., Attner, M. A., et al. (2007). Histone deacetylation inhibitors enhance memory and synaptic plasticity via CREB:CBP-dependent transcriptional activation. *J. Neurosci.* 27, 6128–6140. doi: 10.1523/jneurosci.0296-07.2007

Wang, Z., Zang, C., Rosenfeld, J. A., Schones, D. E., Barski, A., Cuddapah, S., et al. (2008). Combinatorial patterns of histone acetylations and methylations in the human genome. *Nat. Genet.* 40, 897–903. doi: 10.1038/ng.154

Weinstein, D. E., Shelanski, M. L., and Liem, R. K. (1991). Suppression by antisense mRNA demonstrates a requirement for the glial fibrillary acidic protein in the formation of stable astrocytic processes in response to neurons. *J. Cell Biol.* 112, 1205–1213. doi: 10.1083/jcb.112.6.1205

Wood, M. A., Attner, M. A., Oliveira, A. M. M., Brindle, P. K., and Abel, T. (2006). A transcription factor-binding domain of the coactivator CBP is essential for long-term memory and the expression of specific target genes. *Learn. Mem.* 13, 609–617. doi: 10.1101/lm.213906

Young, N. L., DiMaggio, P. A., Plazas-Mayorca, M. D., Baliban, R. C., Floudas, C. A., and Garcia, B. A. (2009). High throughput characterization of combinatorial histone codes. *Mol. Cell. Proteomics* 8, 2266–2284. doi: 10.1074/mcp.M900238-MCP200

Zovkic, I. B., Paulukaitis, B. S., Day, J. J., Etikala, D. M., and Sweatt, D. J. (2014). Histone H2A.Z subunit exchange controls consolidation of recent and remote memory. *Nature* 515, 582–586. doi: 10.1038/nature13707

Conflict of Interest Statement: The authors declare that the research was conducted in the absence of any commercial or financial relationships that could be construed as a potential conflict of interest.

Advantages of publishing in Frontiers

OPEN ACCESS
Articles are free to read, for greatest visibility

COLLABORATIVE PEER-REVIEW
Designed to be rigorous – yet also collaborative, fair and constructive

FAST PUBLICATION
Average 85 days from submission to publication (across all journals)

COPYRIGHT TO AUTHORS
No limit to article distribution and re-use

TRANSPARENT
Editors and reviewers acknowledged by name on published articles

SUPPORT
By our Swiss-based editorial team

IMPACT METRICS
Advanced metrics track your article's impact

GLOBAL SPREAD
5'100'000+ monthly article views and downloads

LOOP RESEARCH NETWORK
Our network increases readership for your article

Frontiers
EPFL Innovation Park, Building I • 1015 Lausanne • Switzerland
Tel +41 21 510 17 00 • Fax +41 21 510 17 01 • info@frontiersin.org
www.frontiersin.org

Find us on